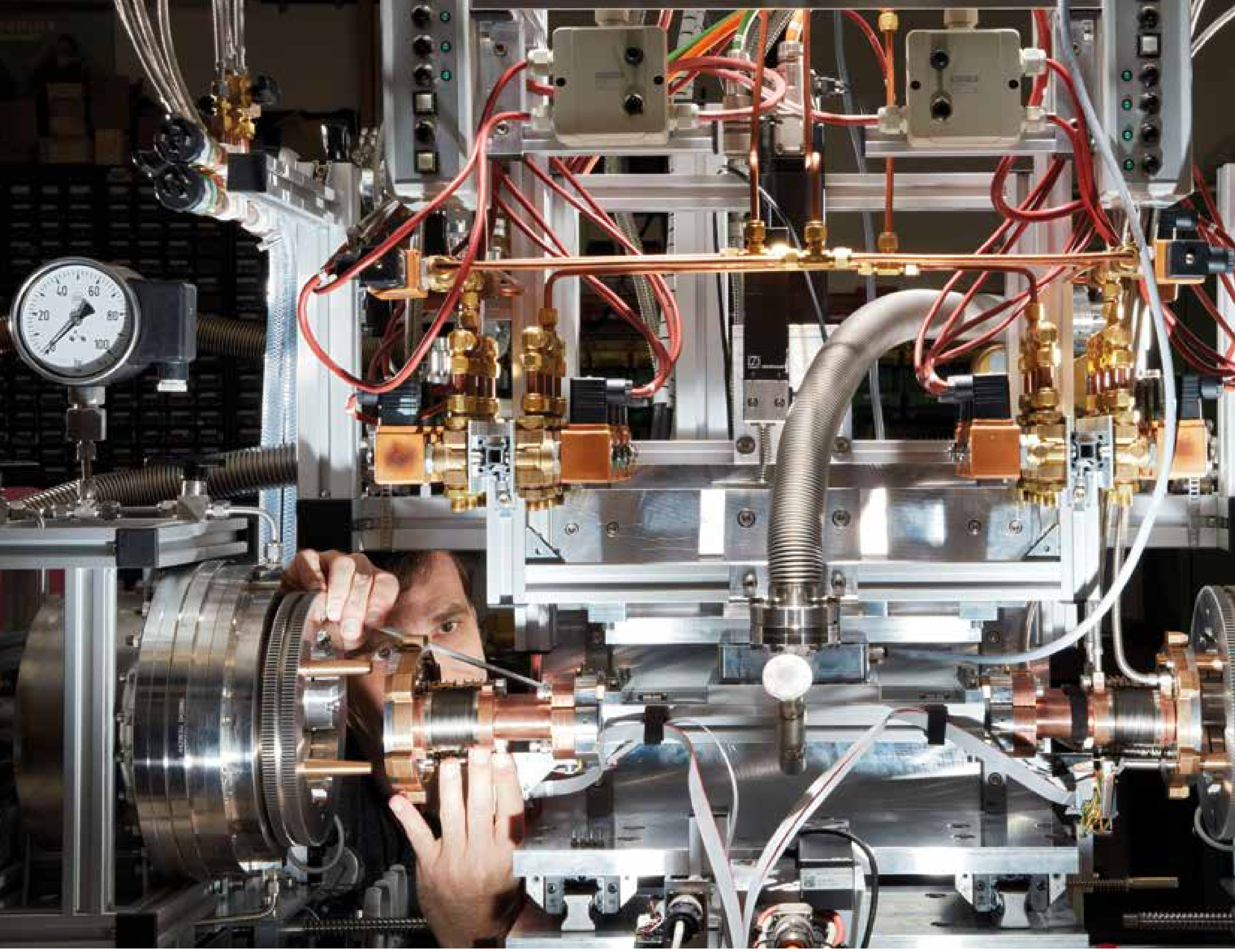

PARTICLE PHYSICS 2017.

Highlights and Annual Report

Accelerators | Photon Science | Particle Physics

Deutsches Elektronen-Synchrotron
A Research Centre of the Helmholtz Association

Cover

A sophisticated vacuum connection system developed at DESY links the beam tube and the high-tech detector Belle II at the SuperKEKB collider at the Japanese national particle physics laboratory KEK.

PARTICLE PHYSICS 2017.

Highlights and
Annual Report

Contents.

The year 2017 at DESY.

Chairman's foreword

Dear Colleagues and Friends of DESY,

It would be almost tautological to say that 2017 was – again! – a very busy year at DESY, with several exciting developments initiated across our campus and throughout our research divisions.

In 2017, we carried out an in-depth and comprehensive DESY strategy process. The DESY competence teams developed many brilliant ideas, which will enter into the strategy for the coming decade. Most importantly, we were able to identify not only future priorities but also posteriorities. This will render our research centre very robust, enabling it to cope with the future challenges.

For particle and astroparticle physics, the DESY-2030 strategy has important implications. In general, we decided to further foster DESY's role as a national hub and as a

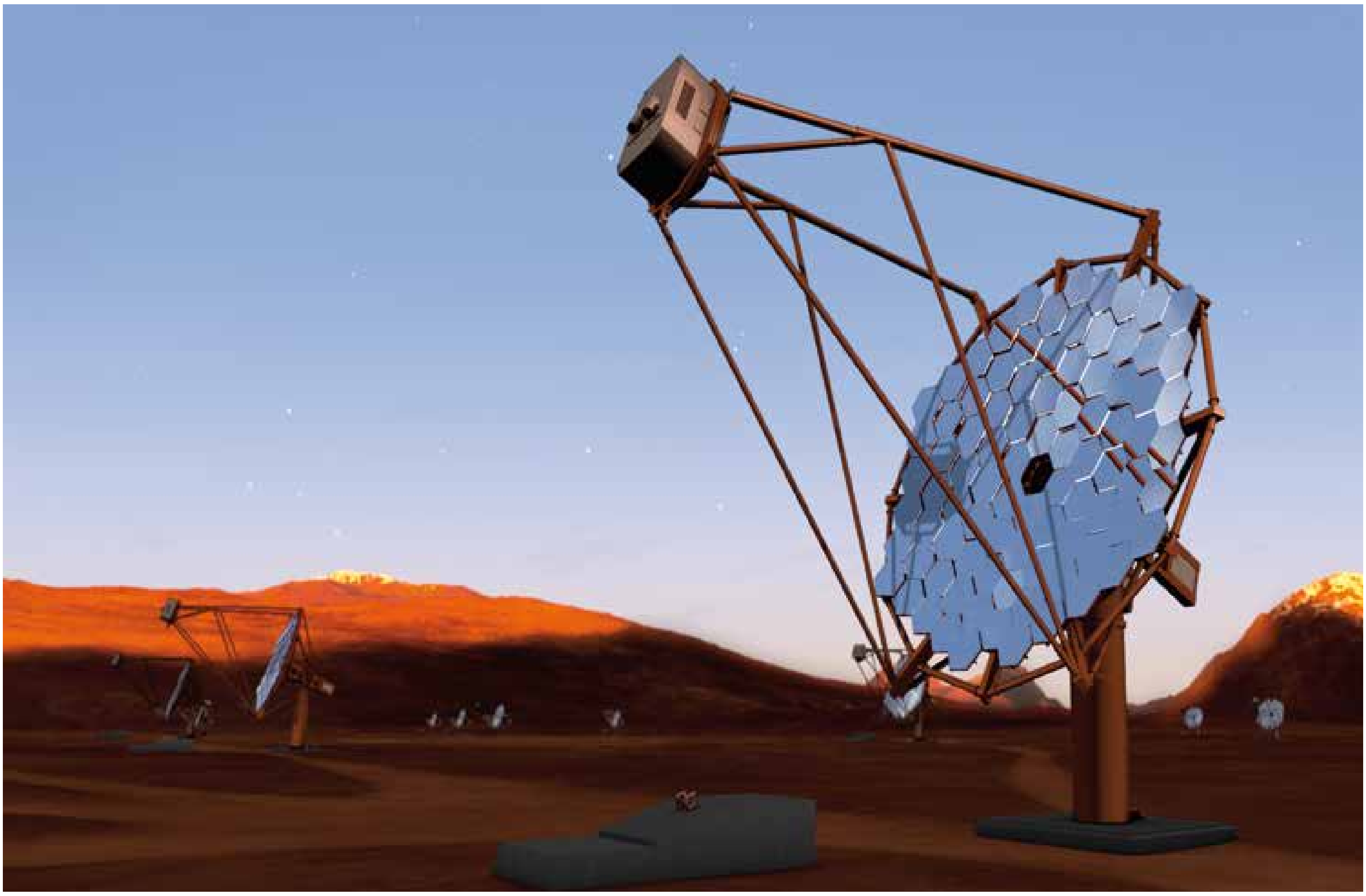

Figure 1

Artist's impression of the medium-sized telescopes that are being developed by DESY for the next-generation gamma-ray observatory CTA facilitator and driver of German contributions to international large-scale projects. In this spirit, key elements of the strategy are the successful delivery of our contributions to the upgrades of the ATLAS and CMS experiments at the Large Hardon Collider (LHC) at CERN near Geneva, Switzerland, and to the Belle II experiment at the SuperKEKB collider at KEK in Japan, as well as a massive engagement in the construction of the Cherenkov Telescope Array (CTA), the next-generation gamma-ray observatory (and the science exploitation of all these instruments).

As one of the globally largest players in particle and astroparticle physics, DESY also engages in the strategy developments for these fields. Consequently, we are also directing our efforts towards realising an upgrade of the IceCube neutrino observatory at the South Pole and towards defining the next global collider project beyond the LHC. DESY's voice is well heard in the German, European and international communities.

These international ambitions require a sound basis on site, and the DESY-2030 strategy consequently foresees a strong theory support for our experimental activities, a set of on-site experiments and a strengthening of our detector R&D activities. With the ALPS II experiment searching for hypothetical very weakly interacting ultralight particles, with ideas for successor experiments on site and with the Detector Assembly Facility (DAF) currently being used for the construction of the ATLAS and CMS tracker end-caps for the high-luminosity phase of the LHC, we are in a very good position to achieve our ambitions.

The DESY campuses in Hamburg and Zeuthen are developing very dynamically. In Hamburg, DESY is making a strategic handshake with the University of Hamburg, which is planning to relocate its physics and chemistry departments on the Bahrenfeld campus, in a later stage possibly also parts of the biology department. This move will foster novel cooperations and new opportunities for the training of students and young scientists. Together with the University, DESY is preparing *inter alia* a new Centre for Interdisciplinary Theoretical Physics, the Wolfgang Pauli Centre, which has the ambition of becoming an international meeting place for young theorists from all over the world. These developments have become possible thanks to special financial support by the German Parliament.

I would like to thank all the DESY staff members for their excellent work in the last years, and I am looking forward to the coming years, which will surely be more brilliant than ever.

Helmut Dosch
Chairman of the DESY Board of Directors

Particle and astroparticle physics at DESY.

Introduction

Dear Colleagues and Friends of DESY,

In 2017, DESY was vibrant with activities, in particle and astroparticle physics as well as in photon science and in accelerator development, and our campuses in Hamburg and Zeuthen saw many construction activities – a manifestation of our efforts to secure the research centre's future.

Two main processes kept us busy: the strategy process DESY-2030 and the preparation for the programme-oriented funding (POF) evaluation of the Helmholtz Association in February 2018. The POF evaluation will eventually lead to funding recommendations for the upcoming POF IV period, which will according to current planning start in 2020 and last for seven years. The DESY-2030 strategy process also has long-term consequences for our work. After intense discussions in dedicated competence teams and in the DESY strategy group, the DESY Board of Directors defined a clear roadmap for the next decade and beyond.

Figure 1

Installation of the BEAST II detector in the Belle II experiment at the SuperKEKB collider at KEK in Japan (November 2017)

In particle physics, the Large Hardon Collider (LHC) at CERN near Geneva, Switzerland, will remain our central activity for many years to come. DESY will focus on the upgrades of the ATLAS and CMS experiments and on their successful science exploitation. With strong groups in both experiments, and with the construction of the new tracker end-caps for ATLAS and CMS starting in mid-2018 in the Detector Assembly Facility (DAF) at DESY, we are very well prepared to achieve these goals.

A second cornerstone of DESY's particle physics strategy is the Belle II experiment at the SuperKEKB collider at KEK in Japan, which will start data taking in 2018 (Fig. 1). The PXD vertex detector contributed by German groups will be added in 2019. Data taking will last until around 2027, and hopes for exciting results are high.

A set of on-site experiments will complement DESY's particle physics portfolio: The ALPS II experiment, which aims to probe for hypothetical very weakly interacting ultralight particles (WISPs), will start data taking in 2020, and we are working hard on realising potential successor experiments, such as MADMAX or IAXO. In addition, we will further strengthen our efforts in detector and accelerator R&D.

Another key element in the DESY particle physics strategy is the theory group. We will strive to foster its broad spectrum of research topics and its position as a world-leading centre for theoretical physics.

Concerning the farther future, DESY will prepare for a leading participation in future global collider projects, and we will strive to strengthen our position as a hub for the German particle physics community, facilitating German contributions to international large-scale projects.

In astroparticle physics, one focus of DESY is on the preparation of the Cherenkov Telescope Array (CTA), the

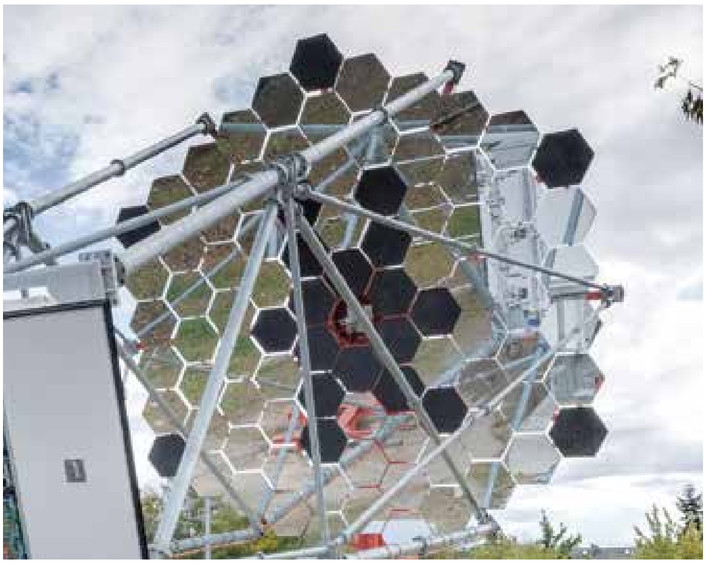

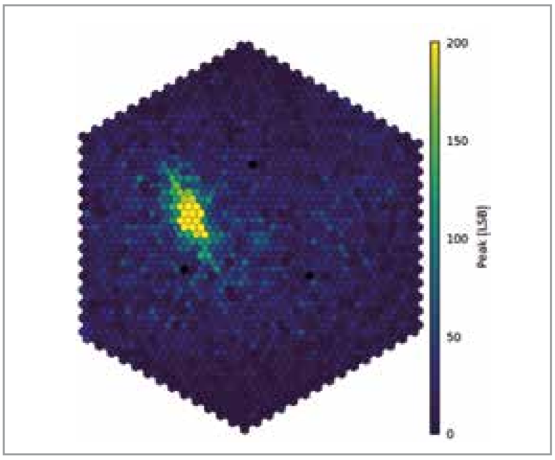

Figure 2

Left: Prototype of the mid-sized telescope for CTA in Berlin Adlershof.

Right: First image of an air shower in Cherenkov light.

next-generation gamma-ray observatory. We foresee a strong role of DESY in the construction and operation of the observatory, and CTA will enable us to drive prominent science topics. One 2017 highlight was the first observation of air showers with the mid-sized telescope prototype of CTA (Fig. 2). In neutrino astronomy, DESY will contribute to the exploitation of the IceCube experiment at the South Pole, and we will drive the upgrade programme towards IceCube-Gen2.

A particular emphasis is on the multimessenger approach to astronomy. DESY will extend its key role in real-time alert systems and in optical and gamma-ray follow-ups, and we will further develop the relevant synergies. The multimessenger approach already proved to be very fruitful: In 2017, for the first time, sources have been observed using several messengers at the same time.

Central to all our ambitions is the talent of our staff. In 2017, DESY has – again – been very successful in attracting a number of highly qualified scientists at different career levels. The Helmholtz Young Investigator Groups of Anna Franckowiak (neutrino astronomy, IceCube) and Elisa Pueschel (CTA) started working in 2017, and three new Young Investigator Groups were granted: The groups of Torben Ferber (Belle II), Abideh Jafari (CMS) and Priscilla Pani (ATLAS) will take up their work at DESY in early 2018. Furthermore, David Berge could be recruited to a leading scientist position in gamma-ray astronomy with the help of the Helmholtz recruitment initiative.

What will the future bring? With our efforts in the POF and DESY-2030 processes, we are clearly well prepared to tackle future challenges. At the same time, we are also putting our efforts into the ongoing German, European and international strategy considerations.

In particle physics, DESY has been actively contributing to the strategy process of the German Committee for Elementary Particle Physics (KET), which will conclude with a strategy workshop in May 2018. Here, a statement on the German views will be formulated as input to the currently beginning European strategy process – in which DESY will play a very active role.

More concretely, in 2018, DESY will face several decisive events: the start of data taking with Belle II, the end of LHC Run 2 and the start of the construction of the ATLAS and CMS tracker end-caps in the DAF. A decision on the realisation of the International Linear Collider (ILC) in Japan is also expected. The 250 GeV stage of the ILC was proposed in 2017, and it presents a scientifically sound case, as is documented not least in the positive statement of the International Committee for Future Accelerators (ICFA).

In astroparticle physics, DESY will begin the construction of the first preproduction telescopes for CTA and of the CTA Science Data Management Centre (SDMC). We will continue our multimessenger activities and expand the cross alerting of gamma-ray, neutrino and gravitational-wave events and X-ray and optical outbursts.

We have a successful year 2017 behind us, and we have ambitious plans for the future. I congratulate all of the DESY staff members on their successes, and I thank them very much for their continued effort for the research centre!

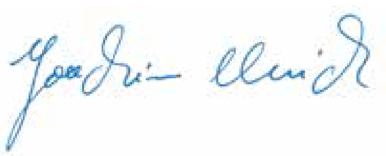

Joachim Mnich
Director in charge of Particle Physics
and Astroparticle Physics

News and events.

A busy year 2017

January

First electrons in European XFEL accelerator

In January, the European XFEL X-ray laser – the largest and most powerful X-ray free-electron laser in the world – reached an important milestone on the way to its operation phase: The accelerator team guided the first electrons from their source point in the facility's injector into the superconducting main linear accelerator, which is cooled to -271°C (2 K). After passing through the first four accelerator modules and a subsequent section in which the electron bunches are compressed, the particles were captured in an electron dump about 150 m away. As the largest shareholder of European XFEL, DESY is responsible for the construction and operation of the accelerator – the longest and most advanced superconducting linear accelerator ever built.

View into the European XFEL accelerator tunnel

FLASHForward accelerates first electron bunches

The plasma accelerator project FLASHForward at DESY's FLASH free-electron laser facility accelerated electron bunches in a plasma cell for the first time. The FLASHForward team used a high-power laser to ignite a plasma, in which electrons were accelerated to energies of around 100 MeV within a distance of just a few millimetres. The achievement allowed important preliminary studies for the planned beam-driven plasma experiment.

Plasma cell of the FLASHForward experiment

The FLASHForward project aims to test plasma wakefield acceleration. The electric fields produced in a plasma can be a thousand times stronger than those in conventional particle accelerators. Researchers all over the world are investigating whether this highly efficient method of particle acceleration can be used to develop extremely compact particle accelerators. The FLASHForward scientists aim to use the FLASH electron beam to generate a plasma in order to further accelerate other electron bunches from the FLASH accelerator or electron bunches that are formed in the plasma itself. FLASHForward is funded by grants from the Helmholtz Impulse and Networking Fund and supported by the Alexander von Humboldt Foundation.

Construction of the beamline (left) connecting the FLASHForward experiment to the FLASH accelerator

February

Youth science competition "Jugend forscht" 2017 at DESY

Participants of the regional "Jugend forscht" competition at DESY in Hamburg

For the fifth time, DESY hosted the regional "Jugend forscht" science competition in Hamburg-Bahrenfeld, one of four regional competitions in Hamburg. In mid-February, about 100 participants met at the DESY school lab, where, on the first day of the competition, they presented a total of around 50 projects to a group of honorary experts. Some of these projects were part of the "Schüler experimentieren" competition for pupils from fourth grade on. On the second day of the competition, many interested visitors used the opportunity to have a look at the projects explained by the young researchers. The science competition encourages achievements and talents in the fields of mathematics, computer science, the natural sciences and technology, with the aim to inspire lasting enthusiasm for these topics among young people.

Solving five big questions in particle physics in a SMASH

The extremely successful Standard Model of particle physics has an unfortunate limitation: The current version is only able to explain about 15 percent of the matter found in the universe. Although the model describes and categorises all the known fundamental particles and interactions, it does so only for the type of matter we are familiar with. However, astrophysical observations suggest that the mysterious dark matter is more than five times as common.

An international team of theoretical physicists came up with an extension to the Standard Model that could not only explain dark matter but also solve five major problems faced by particle physics at one stroke. Guillermo Ballesteros from the University of Paris-Saclay in France, Andreas Ringwald from the DESY theory group and their colleagues presented their Standard Model Axion Seesaw Higgs portal inflation (SMASH) model in the journal *Physical Review Letters*.

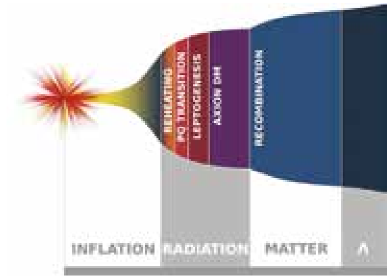

History of the universe according to the SMASH model, denoting the different phases of the epochs since the big bang

New eyes for the gamma-ray sky

The newly refurbished cameras of the High Energy Stereoscopic System (H.E.S.S.) gamma-ray telescopes in Namibia detected their first signals from a cosmic particle accelerator: The new cameras recorded Markarian 421 as their first target, a well-known blazar in the constellation Ursa Major. The active galactic nucleus, 400 million light years away, was detected during an active state and at high significance. After four years of development, testing, production and deployment, the achievement was the last big milestone of the H.E.S.S. I camera upgrade project, which was led by DESY. The success was also an important test for the next-generation gamma-ray observatory, the Cherenkov Telescope Array (CTA), which will use the same camera technology.

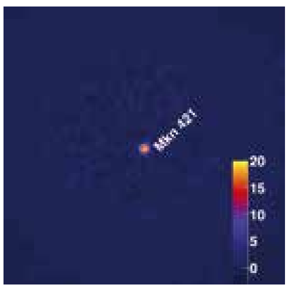

Cosmic gamma radiation from the active galactic nucleus Markarian 421, recorded by the new H.E.S.S. cameras

March

Progress on Belle II with tests of BEAST II at DESY

In early 2017, important components for the Belle II detector, due to start taking data at the SuperKEKB accelerator of the Japanese research centre KEK in 2018, were tested at the DESY II Test Beam Facility in Hamburg. Two new pixel detector modules delivered by the Max Planck Institute for Physics in Munich were installed and tested within a high-tech test detector called BEAST II, which will occupy the space of the extremely sensitive vertex detector until the Belle II team has gained a clear understanding of the particle background from the high-intensity particle collisions at SuperKEKB.

As the success of the Belle II project builds on an increase of the instantaneous luminosity by a factor of 40 during the first few years of operation, determining how the various background sources scale with beam intensity and luminosity is extremely important. Only once this is sufficiently well understood will the very sensitive vertex detector be installed in Belle II.

New modules installed in the test rig at the DESY Test Beam Facility

April

Best German particle physics PhD thesis produced at DESY

DESY scientist Simon Spannagel was awarded the 2017 Particle Physics Dissertation Prize of the German Physical Society (DPG), which he shared with Tim Dietrich of the University of Jena, who investigated merging neutron stars in his thesis on gravitational physics.

In his thesis, Spannagel focused on two distinct topics: He conducted ground-breaking studies on modern silicon pixel detectors for the CMS experiment at the Large Hadron Collider (LHC) at CERN near Geneva, Switzerland, and developed an alternative method for measuring the mass of the top quark. Spannagel worked in the DESY CMS group from 2013 to 2016, before moving on to a research fellowship at CERN. The DPG Particle Physics Dissertation Prize is worth 1500 euros.

Simon Spannagel

Astroparticle Physics Medal for Christian Spiering

DESY scientist Christian Spiering was awarded the prestigious O'Ceallaigh Medal for astroparticle physics by the Dublin Institute for Advanced Studies. Spiering was honoured "for his outstanding contributions to cosmic-ray physics and to the newly emerging field of neutrino astronomy in particular". The O'Ceallaigh Medal is awarded every second year. Spiering is the first German scientist to join the list of internationally renowned awardees.

Christian Spiering

Protesters, including from DESY, at the March for Science on the Hamburg City Hall square

March for Science

Those who criticise scientists for withdrawing into the ivory tower were probably not out and about on 22 April in Berlin, Hamburg and many other cities in Germany and all over the world. The international Earth Day was at the same time the day of the first global March for Science, on which people took to the streets for the freedom of science. The rally was initiated in the USA.

About 2000 people joined the March for Science in Hamburg, around 11 000 in Berlin. At both events, specially produced DESY-blue T-shirts bearing the slogan “Science Facts” stuck out from the crowd. In Germany, a total of 37 000 people demonstrated for the freedom of science and research. Worldwide, there were more than 600 marches with over 1.3 million participants.

The DESY staff and campus partners demonstrated for science with the explicit support of the DESY Directorate and the Helmholtz Association.

Science on Tap 3.0

For the third time, the outreach project “Wissen vom Fass” (Science on Tap) invited people thirsty for knowledge to meet at pubs and bars. On 27 April, Hamburg scientists left their computers and labs and went out to report on their research in vivid 30-minute talks, after which they answered questions from the audience. After its successful premiere in October 2015, the programme was already extended with a multitude of fascinating topics at the second event in November 2016. This time, “Wissen vom Fass” was on offer in about 50 pubs and bars.

May

First lasing of the European XFEL

On 2 May, the European XFEL achieved the last major milestone before its official opening: The 3.4 km long facility, most of which is located in underground tunnels, generated its first X-ray laser light. The X-ray light had a wavelength of 0.8 nm – about 500 times shorter than that of visible light. At first lasing, the laser had a repetition rate of one pulse per second, which will later increase to 27 000 per second.

The X-ray light of the European XFEL is extremely intense and a billion times brighter than that of conventional synchrotron light sources. The achievable laser light wavelength corresponds to the size of an atom, meaning that the X-rays can be used to make pictures and films of the nanocosmos at atomic resolution. The laser light was generated from an electron beam from the superconducting linear accelerator – the facility’s key component, which DESY had put into operation in the previous months.

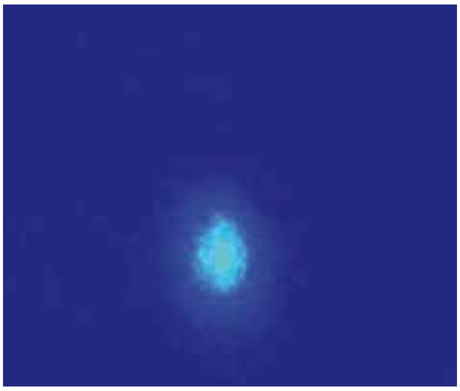

First laser light at the European XFEL, recorded by an X-ray detector at the end of the tunnel

DESY scientist Winfried Decking explaining operations in the DESY accelerator control room

June

Future Circular Collider Week in Berlin

The annual meetings of the worldwide Future Circular Collider study are major international events in which the progress in every domain relevant for the development of such a huge research infrastructure is reviewed. The FCC Week 2017 – held in Berlin from 29 May to 2 June – was jointly organised by CERN and DESY. It was the third in the series of FCC Weeks with more than 500 participants.

Conference poster announcing the Future Circular Collider Week 2017 in Berlin

The FCC Week comprised a scientific programme, an industrial partnership programme and exhibition as well as an innovation poster session. The dedicated poster session served as a platform to highlight advancements that are relevant for the study progress, have the potential for technological breakthroughs enabling a frontier particle accelerator infrastructure and may have significant societal and industrial impacts.

July

High Energy and Particle Physics Prize for Robert Klanner

For his contributions to the development and application of silicon microstrip detectors, DESY's former Director in charge of Particle and Astroparticle Physics Robert Klanner, together with Eric Heijne from CERN and the recently deceased Gerhard Lutz from the Max Planck Institute for Physics in Munich, was awarded the 2017 High Energy and Particle Physics Prize of the European Physical Society (EPS).

Robert Klanner

In the 1980s, the three physicists paved the way for the breakthrough of silicon microstrip detector technology, which has become an essential part of all current particle physics experiments. Klanner joined DESY in 1984, taking part as leading scientist in the detector and physics programme of the ZEUS experiment at the former HERA collider. In 1996, he became a professor at the University of Hamburg. He was research director at DESY from 1999 to 2005.

DESY welcomes 102 summer students from 28 countries

For seven weeks, 102 young scientists from 28 countries got a glimpse of the different areas of research carried out at DESY. The DESY summer student programme is one of the largest and most international summer schools in Germany.

DESY summer students in Hamburg …

In addition to learning the theoretical foundations of accelerator, particle, astroparticle and X-ray physics, the 85 students visiting the Hamburg site and the 17 students visiting the Zeuthen site were involved in the practical work in on-going research projects. The experience gave them a deep insight into day-to-day life as a scientist. It is above all the internationality and the practical experience that make DESY's annual summer student programme so popular among students.

Generally, the number of applications considerably exceeds the number of available places. The number of students interested in the 2017 DESY summer student programme was higher than ever before. The organisers listed about 670 applicants and had to make a difficult choice: Only about one in six students could be accepted for the programme.

… and Zeuthen

August

New carbon dioxide evaporative cooling for ATLAS

When particles collide with each other and the electronic components and sensors of particle detectors are working flat out, they generate a lot of heat, which poses a threat to the efficiency of those components and can, in the worst case, result in overheating. Particle detectors such as the huge ATLAS experiment at the LHC at CERN therefore have to be cooled all the time. A new carbon dioxide (CO_2) evaporative cooling scheme was successfully tested at DESY in summer 2017.

Under conditions of high pressure and low temperature, CO_2 is liquid rather than gaseous. Its particularly efficient cooling effect is caused by the liquid evaporating and in doing so absorbing heat from the detector. To conduct the test, the scientists used a prototype of one part of the end-cap under construction for use at the high-luminosity LHC, which they placed in a thermally isolated test chamber cooled by a

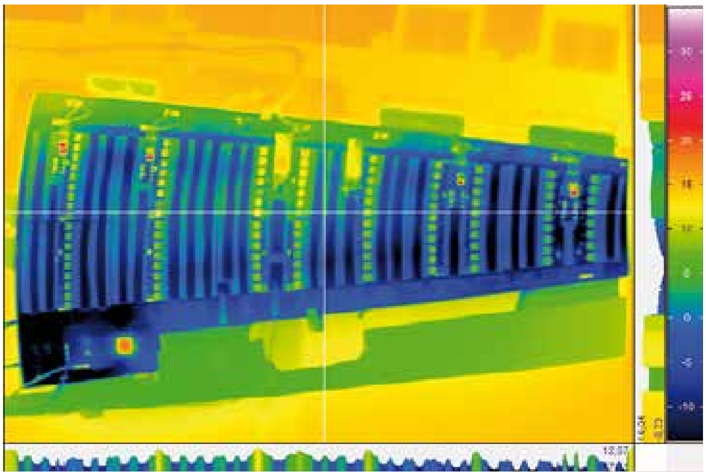

Using an infrared camera, the scientists can check the efficiency of their new cooling system.

cooling unit and then photographed using a thermographic camera. Among other things, the researchers had to take into account the angle from which they photographed the prototype, because silicon reflects any kind of heat and even the small amounts of heat produced by the camera would have disrupted the measurements. Ultimately, some 165 m^2 of silicon strip detectors are to be operated in ATLAS using the CO_2 evaporative cooling mechanism.

Cataloguing gamma-ray flares

Researchers at DESY have compiled an extensive catalogue of variable sources of cosmic gamma radiation, analysing almost 7.5 years of observational data from NASA's Fermi Gamma-Ray Space Telescope. Over that period, the Large Area Telescope (LAT) on board the satellite registered a total of 4547 bursts of gamma radiation, known as flares. Thanks to improved analytical methods, the flares could be assigned to 518 variable sources. The Fermi All-Sky Variability Analysis (FAVA) also lists 77 unknown sources, whose identity has not yet been determined. The scientists presented their catalogue in *The Astrophysical Journal.*

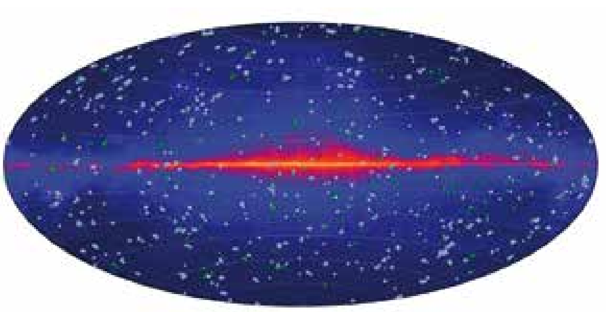

The gamma-ray sky as seen by NASA's Fermi Gamma-Ray Space Telescope. Each spot represents a localised gamma-ray flare.

September

David Berge new leading scientist at DESY

On 1 September, David Berge took up a position as a joint professor for particle and astroparticle physics at DESY in Zeuthen and at the Humboldt University (HU) in Berlin. Berge started his research carrier with a PhD in gamma-ray astronomy at the Max Planck Institute for Nuclear Physics in Heidelberg, before switching fields to work at CERN within the ATLAS collaboration for seven years during the LHC start-up phase. In 2013, he moved to Amsterdam as a faculty member of GRAPPA, a centre of excellence of the University of Amsterdam at the interface of particle and astroparticle physics.

His research at DESY and HU Berlin focuses on cosmic particle accelerators and on the search for dark matter. For the latter, he is concentrating on gamma-ray telescopes such as H.E.S.S. or the future CTA observatory as well as on the ATLAS experiment. With his strong background in LHC physics, Berge is ideally suited to pursue the synergies arising from a combination of methods and data from both particle and astroparticle physics.

David Berge

Integration through education

Qais Haidari, a refugee from Afghanistan who has been living in Hamburg since autumn 2015, started a training programme as a media and information service specialist at the DESY library on 1 September.

After graduating from high school in Kabul, Haidari successfully completed a two-year course of studies at the National Institute of Management and Administration (NIMA). However, he had to leave his country and his family after being threatened by the Taliban. After an adventurous escape across Turkey and the Mediterranean Sea, he finally reached Hamburg.

Eventually, with the help of the Hamburg coordination centre for continuing education and employment (KWB), which was established jointly by the Hamburg employer associations, social security office and employment agency, the 26-year-old applied for training as a media and information service specialist at DESY. Although the capacities of the library staff were almost exhausted, the common willingness at DESY to contribute to integration made his employment possible. The Helmholtz Association also provided support: It contributed half of the training costs in the first year as part of its refugee initiative.

Qais Haidari and Antje Daum of the DESY Hamburg library

Three new Helmholtz Young Investigator Groups at DESY

The Helmholtz Association awarded funding for three new Young Investigator Groups at DESY. With an annual grant of 300 000 euros each, three young scientists will set up and run their own research group at DESY for six years. The Helmholtz Association and DESY each pay half of the grant. All in all, the Helmholtz Association's 18 research centres are funding 16 new Young Investigator Groups.

Priscilla Pani and her group will focus on the search for dark matter by analysing the high-energy proton–proton collisions in the ATLAS detector at the LHC. The group will work together with the DESY ATLAS group and the Humboldt University in Berlin, in particular studying the scenario in which the interaction between dark matter and conventional matter is mediated by a new scalar particle that – like the Higgs boson – interacts mainly with heavy elementary particles. For this purpose, collisions in which pairs of top quarks are created and which are at the same time missing transverse energy are particularly interesting.

Abideh Jafari, who will be part of the CMS collaboration at the LHC, will take a closer look at a particular aspect of the electroweak force: She hopes to be the first to measure the interaction between the top quark and the *Z* boson directly and with high precision. Heavy elementary particles and their precise measurement play an important role in the search for new physical phenomena. Jafari will also work closely together with theorists at DESY and the Karlsruhe Institute of Technology (KIT).

Torben Ferber aims to use the Belle II detector at the SuperKEKB accelerator to search for dark matter and axion-like particles. His Young Investigator Group will work together with the DESY Belle II group and the University of Hamburg, in particular studying events that produce either a single or exactly three high-energy photons. To do this, as well as for his additional search for dark photons and axion-like particles, Ferber's group will promote the detector's electromagnetic calorimeter and push ahead with the reconstruction of its data, with a special focus on machine learning.

DESY school lab celebrates 20th anniversary

In 2017, the school lab on the DESY campus in Hamburg, named "physik.begreifen", celebrated its 20th anniversary. On the occasion, the school lab team organised a colourful festival, with about 100 guests attending the ceremony in the auditorium. "physik.begreifen" was the first school lab within the Helmholtz Association and as such truly trendsetting.

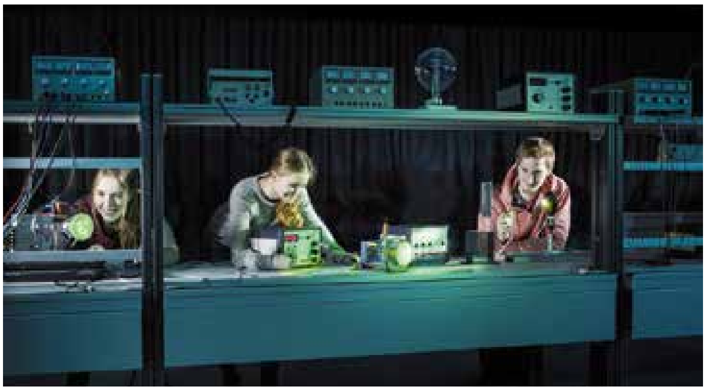

Pupils in the eLab of the DESY school lab in Hamburg

"It is our special concern and an important social mission as well to get young people enthusiastic about the natural sciences," said Hamburg School Senator Ties Rabe, whose ministry has been supporting the project from its inception. "The DESY physik.begreifen school lab is a wonderful example of cooperation between a top-class research institute and the Hamburg Ministry for School and Vocational Training."

A special honour was the visit of former DESY Director of Administration Helmut Krech, who initiated the project 20 years ago. Since then, more than 88 000 pupils have been taking advantage of the offer. Nowadays, the school lab welcomes up to ten school classes per week.

October

Art meets Science: Dark Matter

From 13 October to 9 November, the DESY campus turned into an art gallery, with 15 artists from all over Germany presenting their work on the theme of dark matter. The project goes back to an idea of CMS scientist Christian Schwanenberger and Hamburg artist Tanja Hehmann. The participating artists came from various fields: painting, graphics, photography and film, sculpture, installation, intervention as well as sound and multimedia.

In the planning phase, they got together with DESY scientists during a workshop to gather more information on the subject – why we know that there has to be dark matter, how we search for it and how its discovery might change our view of the world. The artists too spoke about their work and work processes. In the course of the workshop, it became clear that artists and scientists have much in common. Eagerness to experiment, problem-solving strategies, coping with failures and of course curiosity are common features of both professional groups.

The exhibition was open for guided tours. On 31 October, a dedicated event took place in the framework of the International Dark Matter Day. A few hundred enthusiasts took part, attending lectures in the DESY auditorium and visiting the exhibition on campus.

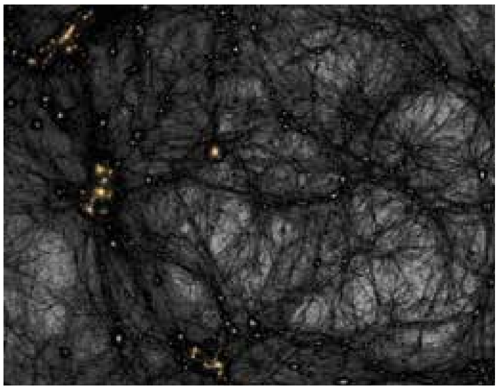

Visualisation of dark matter in the universe

Start of multimessenger astronomy

For the first time, the observatories LIGO in the USA and VIRGO in Italy registered gravitational waves from a merging pair of neutron stars. In an unprecedented worldwide observational campaign, in which DESY scientists participated alongside many other researchers, the source of the gravitational-wave event was found. The object was identified to be a so-called kilonova, a star that became very bright for a few days, which could be detected in visible light as well as in the infrared and X-ray wavelength ranges. DESY scientists were also involved in searches with the international gamma-ray observatory H.E.S.S. and the neutrino telescope IceCube:

H.E.S.S. in Namibia was the first ground-based telescope system to point to the direction of the gravitational waves, and IceCube at the South Pole had also been searching for evidence in almost real time.

The gamma-ray observatory H.E.S.S. in Namibia, in which DESY is involved, was the first ground-based telescope system to point to the direction of the gravitational waves.

MADMAX looking for axions

The nature of dark matter is probably one of the most pressing questions in modern physics. Although the existence of dark matter is difficult to refute, direct experimental detection in the laboratory is still missing. Particles called axions could solve the dark-matter mystery. On 18 October, scientists officially founded the MAgnetized Disc and Mirror Axion eXperiment (MADMAX) collaboration, which will use a novel experimental approach to detect such axions. MADMAX will be located in the hall of the H1 experiment at DESY's former HERA collider and complement the ALPS II experiment. ALPS II, which is currently under construction in the HERA accelerator tunnel, will look for axion-like particles. DESY is also involved in the International Axion Observatory (IAXO) proposal, designed to look for solar axions.

In addition to the group of the Max Planck Institute for Physics in Munich where the basic concept was developed, the MADMAX collaboration comprises research groups from the universities of Aachen, Hamburg and Tübingen in Germany, the University of Zaragoza in Spain, the French Institute of Research into the Fundamental Laws of the Universe (CEA-IRFU) in Saclay and DESY.

The members of the newly founded MADMAX collaboration at the experiment's future location at DESY in Hamburg

November

ZTF scans heavens for exploding stars

On 1 November, the Zwicky Transient Facility (ZTF) – a new US-based robotic camera facility – took its first image of the sky, showing a part of the constellation Orion in the northern sky featuring a turbulent star-forming region with the famous horsehead nebula. The ZTF will scan the sky every night to discover exploding stars, matter devouring black holes and other short-lived, violent phenomena in the cosmos. It can capture hundreds of thousands of stars and galaxies in a single shot and survey the night sky particularly fast. Led by the California Institute of Technology (Caltech), the ZTF collaboration includes various partners from around the world, among them DESY and the Humboldt University in Berlin, Germany.

The design and construction of the ZTF were technological challenges, especially as the camera had to fit into the comparatively small telescope tube. To make this possible, new solutions for technical requirements had to be developed. For instance, the camera's shutter, which is usually mounted right in front of it, was moved to the outside of the telescope and had to be built exceptionally big, with a diameter of 1.31 m. It was constructed and tested at DESY in cooperation with the company Bonn-Shutter in Germany.

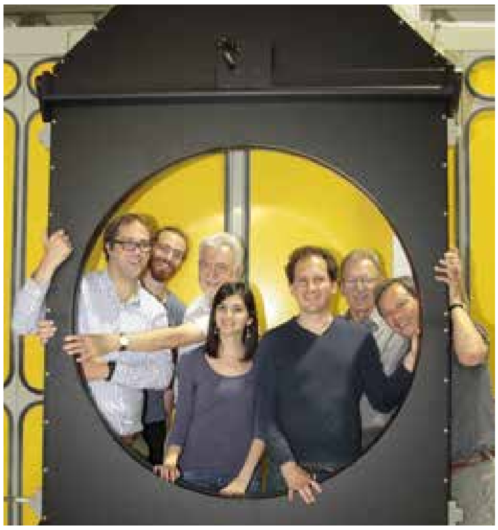

The ZTF camera features the largest shutter ever built for an astronomical instrument.

Record attendance at DESY DAY

The open day of DESY and its Hamburg campus partners on 4 November attracted more visitors than ever before, with 20 287 persons registered. More than 150 activities and attractions offered hands-on research for visitors to touch and grasp. In experimental halls, laboratories, accelerator tunnels, workshops, construction departments, the computer centre and the school lab, about 1000 helpers demonstrated what the research centre is all about. Also on display were the works of the "Art meets Science: Dark Matter" project, the first such project at DESY.

PhD Thesis Prizes 2017

As part of DESY's Science Day on 15 November, the Association of the Friends and Sponsors of DESY (VFFD) awarded its PhD Thesis Prizes 2017 in equal parts to Volodymyr Myronenko and Johann Haber, both of DESY and the University of Hamburg. The association presents the prize every year for one or two outstanding PhD theses from the two previous university terms. The prize was worth 2000 euros for each awardee.

Johann Haber's doctoral thesis deals with quantum optics as applied to hard X-rays and will help to further establish this new field of research at modern X-ray sources. In his doctoral thesis on physics at DESY's former HERA collider, Volodymyr Myronenko combines and analyses the inclusive neutral-current and charged-current cross sections for lepton–proton scattering measured in the H1 and ZEUS experiments.

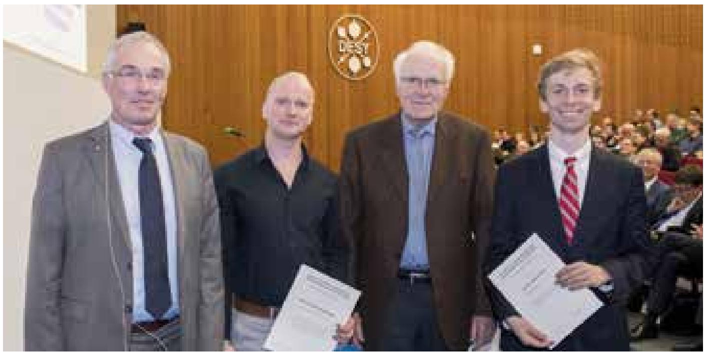

DESY Director Helmut Dosch, Volodymyr Myronenko, VFFD chairperson Friedrich-Wilhelm Büßer and Johann Haber (from left)

BEAST II detector installed in Belle II

Scientific and technical staff involved in the international Belle II collaboration at the Japanese research centre KEK installed a key component of the Belle II particle detector, which is currently under construction. The BEAST II test detector will spend several months measuring the radiation levels in the immediate vicinity of the interaction point, before being replaced by the new, highly sensitive vertex detector that is ultimately to be installed in its place.

Prior to the start of particle collisions, the central beam pipe for the particles needed to be installed inside the detector and connected to the focusing magnets of the SuperKEKB accelerator. Since there is very little room inside, the vacuum systems of the two components could not be connected by hand, as is usually done. Instead, a remote-controlled vacuum connection system was specially developed at DESY. The modernised electron–positron collider SuperKEKB will produce more particle collisions than ever before in the world, and the focusing magnets are key to achieving this world record.

Sixth International Cosmic Day

For the sixth International Cosmic Day, more than 1400 teenagers gathered in 20 countries around the world in late November to explore messenger particles from the universe. The students conducted their own experiments investigating cosmic rays, discussed the results with scientists and worked for one day like an international research collaboration. Scientific institutions worldwide opened their doors on the occasion to offer the high-school students – and about 30 teachers – an exciting insight into astroparticle physics. The event was initiated by DESY in cooperation with Netzwerk Teilchenwelt and the US particle physics centre Fermilab with its teachers' network QuarkNet.

Cosmic particle accelerator: the Crab Nebula in the constellation Taurus

December

Ahmed Ali elected APS Fellow

For his contributions to, among other things, precision tests of the Standard Model of particle physics, DESY scientist Ahmed Ali was elected Fellow of the American Physical Society (APS) – a special honour conferred on APS members in recognition of exceptional work. The society also emphasised Ali's role in the organisation and consultancy of international conferences and his constant efforts to advance the cooperation of physicists from numerous countries and cultures.

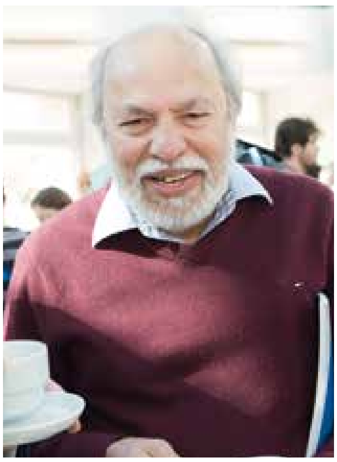

Ahmed Ali

Experimental particle physics.

Physics with protons has been at the heart of DESY's particle physics activities since the start-up of its electron–proton collider HERA in 1992. Today, the cornerstones of DESY's proton physics programme are its ATLAS and CMS groups, which are involved in a large variety of developments at the Large Hadron Collider (LHC) at CERN, from hardware design to data analysis. One activity paving the way to the discovery of new phenomena is the re-establishment of Standard Model measurements at the LHC. These include precise measurements of *Z*-boson cross sections by ATLAS (p. 23) as well as other Standard Model tests with electroweak gauge bosons or in the strong sector (p. 26). Another focus of the DESY LHC groups is the properties of the recently discovered Higgs boson. Enhanced accuracy has allowed the DESY ATLAS group to find first direct evidence of the coupling between the Higgs and the top quark (p. 24) and to study Higgs decays into tau leptons (p. 30) and bottom quarks (p. 28), which are formidable probes of extended Higgs sectors. Moreover, studies with discovery potential are continuously being performed, including searches for dark matter (p. 32) or supersymmetry (p. 29).

At the same time, the DESY LHC groups are preparing for the future LHC upgrades – in particular, the high-luminosity upgrade foreseen for the years after LHC Run 2 (p. 20). This includes the development of completely novel technologies, such as dedicated tomography of hardware with a large material budget (p. 22), but also the alignment of the newly installed tracker in the CMS experiment (p. 31).

Physics with lepton beams – and the R&D work for the necessary accelerators and detectors – constitutes the second pillar of DESY's particle physics activities. The focus here is on future linear colliders, particularly the International Linear Collider (ILC), and on the upgraded SuperKEKB accelerator with the Belle II experiment at the Japanese national particle physics laboratory KEK. The assembly of Belle II is in full swing (p. 34), and first physics data taking is planned to happen in 2019. Regarding a future electron–positron linear collider, the two main activities at DESY are detector development (p. 38 and p. 40) as well as projections of the discovery reach of a linear collider (p. 36). Last but not least, the ALPS II experiment at DESY approaches the design sensitivity of its optical cavities in preparation for its data run in 2020 (p. 42).

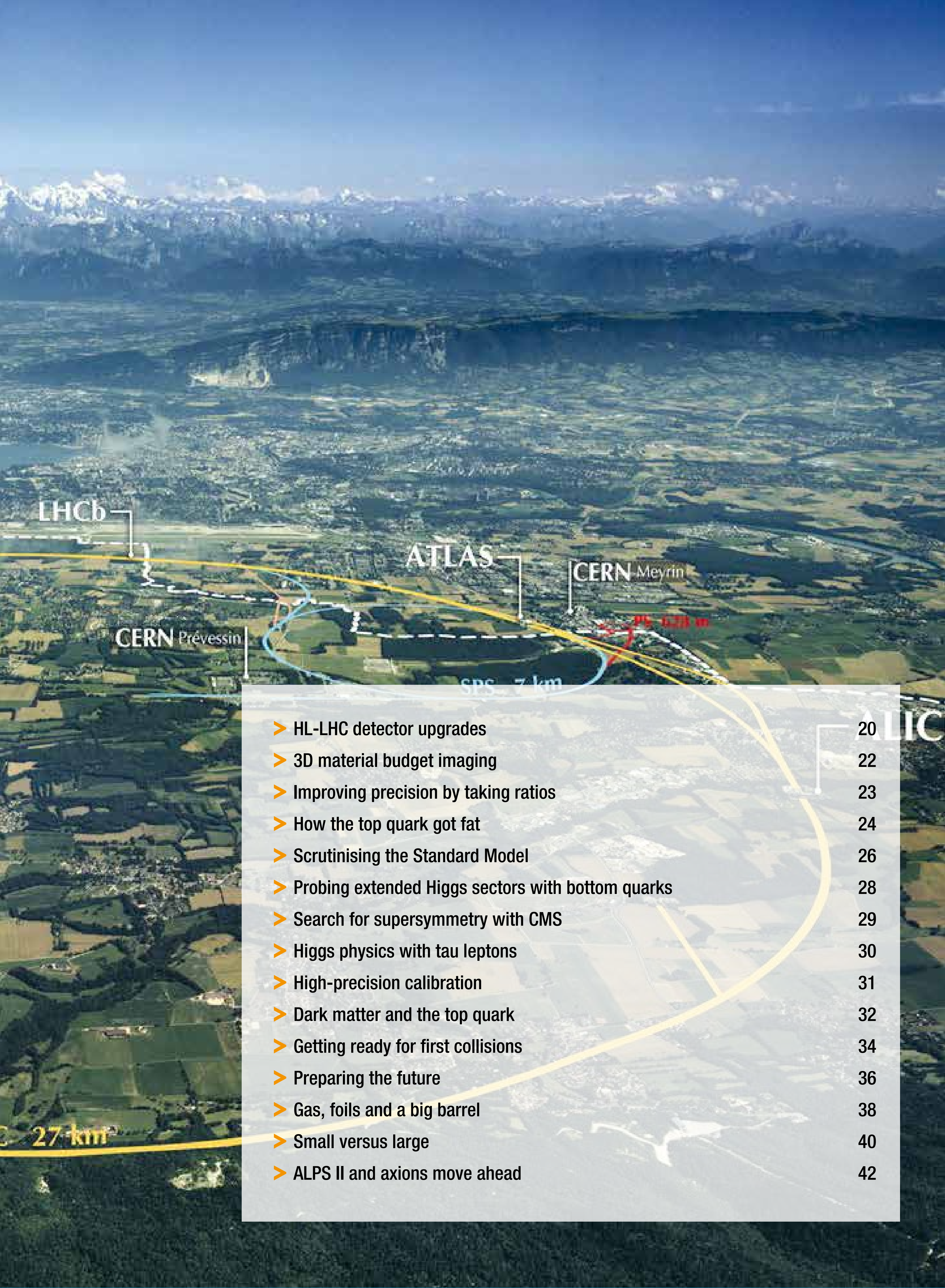
LHCb
ATLAS
CERN Meyrin
CERN Prévessin
SPS 7 km
PS 628 m
27 km

HL-LHC detector upgrades.

New tracking detectors for ATLAS and CMS

The ATLAS and CMS collaborations are preparing detector upgrades for the high-luminosity phase of the LHC (HL-LHC). Both experiments will replace their current tracking detectors with more radiation-hard and more precise silicon tracking detectors in a three-year shutdown starting in 2024. DESY, together with German institutes of the ATLAS and CMS collaborations, will deliver one end-cap detector for each experiment. This process will include module production, end-cap construction and integration at DESY. The technical design reports for the tracker upgrades of ATLAS and CMS were prepared with substantial contributions by DESY and submitted and approved in 2017. At DESY, relevant R&D for the production of the detector components has been performed, and the necessary infrastructure is currently being built and will be commissioned in 2018.

Infrastructure for the detector upgrades

DESY and its partners will deliver one end-cap detector each for the ATLAS inner tracker (ITk) and the CMS outer tracker (OT). The DESY LHC groups have committed to provide a substantial part of the silicon detector modules, the construction of mechanical parts for the end-caps as well as the full integration of the end-caps and the final system tests before the transportation to CERN.

For this purpose, a dedicated Detector Assembly Facility (DAF) is being prepared at DESY, which will be used for the production of silicon modules and comprise larger areas where these modules can be integrated onto the large end-cap structures of about 2.5 m radius and 2 m length. Two existing buildings at DESY were refurbished and the first of two cleanroom installations was built in 2017. As of early 2018, this ISO-6 cleanroom of ~250 m^2 is being commissioned. It will serve for the silicon sensor module R&D and production. A second cleanroom (ISO-7) of ~700 m^2 to be used for the integration of the full end-caps will be ready for commissioning by mid-2018.

Figure 1
ATLAS technical design report for the ITk strip detector

Both DESY LHC groups are actively preparing the production and performing the necessary R&D. They contributed significantly to the technical design reports for the tracker upgrades, which were submitted to the LHC Experiments Committee in 2017.

ATLAS detector upgrade activities at DESY

The DESY ATLAS detector upgrade activities focus on the design, prototyping and construction of one of the two end-caps for the ITk strip detector. An end-cap will consist of about 4000 silicon modules, distributed on six disks with 32 petals each. Petals are ultralow-mass wedge-shaped mechanical support structures in which cooling and data transmission are directly embedded. Each petal has nine modules on each side with six different sensor geometries to cover the wedge-shaped surface. As the largest institute in the ATLAS ITk collaboration, DESY will cover many aspects of the end-cap construction, including module construction, petal construction, end-cap assembly and full system tests.

A total of 2000 of the modules required for the end-cap will be constructed at both DESY sites, in Hamburg and Zeuthen. The remaining 2000 modules will be provided by the German partners from the universities of Berlin, Dortmund and

Freiburg. In 2017, the first end-cap-specific modules (R0) were constructed and tested in Freiburg and Zeuthen. Based on these and previous prototypes, DESY is now gearing up towards the full production of all six module types. The production is scheduled to last about three years.

A fast production of the modules is only possible thanks to the use of UV-curable glue, which was pioneered by DESY. The selection and detailed characterisation including radiation damage studies were performed by a DESY PhD student. The optimisation of the sensor back-side connection for the high voltage is also a DESY development. Using the DESY II Test Beam Facility, the performance of prototype modules was tested in detail, and the results were fed back into the design of the final readout system.

The DESY ATLAS group invented and prototyped a tool to insert the extremely valuable fully loaded petals into the end-cap structure with very high precision. Once the tool has been completed, a copy of the tool will be provided to the partner construction site of the second end-cap.

One major highlight of 2017 was the submission and approval of the ATLAS technical design report (TDR) for the ITk strip detector [1] (Fig. 1). It was drawn up with substantial contributions of DESY: Two-thirds of the editorial team, including the main editor, were from the DESY ATLAS group. The team was in charge of a high-quality write-up of all aspects of the overall project.

Preparing for CMS module production at DESY

The CMS end-cap will consist of five double disk structures, made up of four half-disks each. Two different types of silicon sensor modules will be used to equip the disks. On the outer radii, modules built out of two closely spaced silicon strip sensors of 10 x 10 cm^2 will be used (2S modules). The inner radii – up to 650 cm – will be equipped with so-called PS modules, sandwiches of a silicon strip and a silicon pixel sensor. In total, 1600 2S and 1400 PS modules are needed for one end-cap.

The DESY CMS group will produce 1000 PS modules for the future CMS tracker and mount these onto the mechanical structures of the end-cap, together with the 2S modules built by the German universities of Aachen and Karlsruhe. In preparation, a first 2S prototype module equipped with two CMS Binary Chip 2 (CBC2) application-specific integrated circuits (ASICs) was built and tested at DESY, reaching the required assembly precision.

The DESY CMS group has taken a leading role in the development of the data acquisition firmware of the front end. A test beam measurement was successfully performed with the 2S prototype module in the DESY test beam, using a pixel telescope as external reference and a fully integrated data acquisition system taking advantage of the developed firmware.

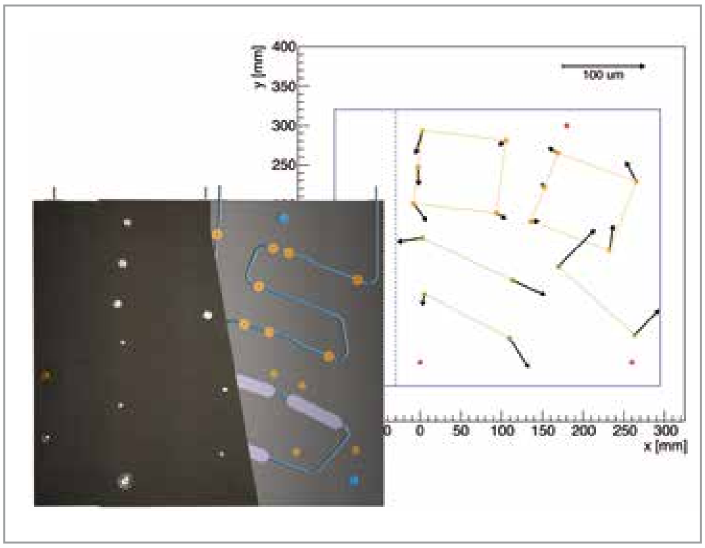

Figure 2

Second version of the small Dee prototype together with the corresponding metrology results

With the availability of the ASICs for the PS modules, DESY will continue with the PS module prototype production as the next step.

DESY will also be responsible for the mechanical parts of the end-cap and has started building prototypes of the half-disk substructures (Dee). A second version of the small Dee prototype was successfully built within the assembly precision specifications, and the assembly sequence was proven. Figure 2 shows the second version of the small Dee prototype together with the corresponding metrology results. The maximum deviation from the nominal position for all inserts is below 65 μm and well within the required precision of 100 μm.

As a next step, DESY is preparing a full-sized prototype of a Dee with 2.2 x 1.1 m^2 area, six embedded cooling sectors and close to 800 inserts. In addition, the group is developing the tooling to carry out the full integration chain.

A member of the DESY CMS group was co-author of the CMS tracker upgrade TDR, which was submitted in 2017, contributing finite element analysis (FEA) performance studies of all module types.

Contact:

Ingrid-Maria Gregor, ingrid.gregor@desy.de
Sergio Diez Cornell, sergio.diez.cornell@desy.de
Günter Eckerlin, guenter.eckerlin@desy.de
Andreas Mussgiller, andreas.mussgiller@desy.de

Reference:

[1] ATLAS-TDR-025, CERN-LHCC-2017-005.

3D material budget imaging.

Probing samples with a high-energy electron beam

The DESY CMS group has developed a new tomographic technique that, like X-ray-based computed tomography (CT), allows for the analysis of macroscopic samples of any given material type. It is based on the measurement of impact positions and deflection angles of electrons in the GeV range traversing the sample under test, enabling the reconstruction of the object's material budget distribution. Owing to the high penetration depth of high-energy electrons, this technique has the potential to overcome challenges of CT regarding samples of high-*Z* materials or with large material budgets.

Highly energetic charged particles undergo multiple Coulomb scattering when traversing any material, leading to an effective deflection of the particles. The shape of the distribution of these scattering angles depends on the amount and type of material traversed by the particle. Hence, a larger material budget, i.e. denser or thicker materials, results in a wider angular distribution.

In 2017, we used multi-GeV electrons delivered by the DESY Test Beam Facility to probe samples, precisely measuring the electrons' trajectories in front and behind the object and thereby the impact position and scattering angle at the sample. The distribution of the angular deflection is evaluated within a virtual plane through the sample, which is divided into image cells of 100 x 100 μm^2. For each image cell, only those particles are taken into account that traverse it. The widths of the angular distributions yield an estimate of the material budget for each image cell, forming a two-dimensional material budget image of the projected sample. In order to reconstruct the sample's three-dimensional material budget distribution, the measurement is repeated for different rotation angles of the sample, the corresponding data for all angles are combined, and an inverse radon transform is applied. Figure 1 (left) shows a single slice of the reconstructed material budget distribution for a coaxial adapter.

In order to investigate the limits of this technique, simulations were performed using samples made from aluminium and lead. The geometrically identical cubes with an edge length of 6 mm feature a rectangular cut-out at the bottom side and several holes of 0.1 mm to 1 mm in size. Figure 1 (right) shows the successful reconstruction of both cubes as two half-spaces. Note especially that a 6 mm lead cube constitutes about 38 attenuation lengths for a 100 keV photon beam, equivalent to a filtered 200 keV beam, rendering CT imaging of such samples impossible.

This track-based multiple scattering tomography was conducted at DESY for the first time, and the successful reconstruction of measured and simulated data for samples with large material budgets illustrates the potential of this technique, overcoming the limitations of conventional CT imaging.

Contact:

Hendrik Jansen, hendrik.jansen@desy.de

Paul Schütze, paul.schuetze@desy.de

Reference:

[1] H. Jansen and P. Schütze, Appl. Phys. Lett. 112 (14), 144101 (2018).

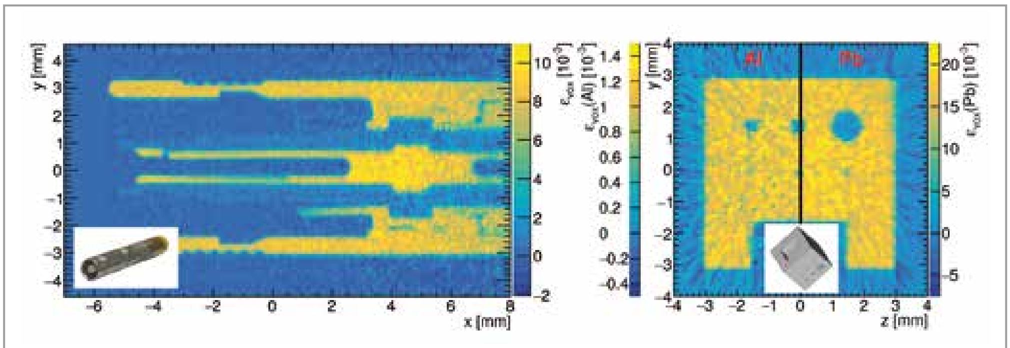

Figure 1

Left: Reconstructed slice of the measured three-dimensional material budget of a coaxial adapter. Right: Reconstructed slice of a structured aluminium resp. lead cube from simulated trajectories.

Improving precision by taking ratios.

Shedding light on the distribution of gluons and light sea quarks in the proton

The structure of the proton in different kinematic regimes can be tested using data sets collected with the ATLAS detector at the LHC during Run 1 and Run 2 at centre-of-mass energies of 7 TeV, 8 TeV and 13 TeV. The members of the DESY ATLAS group performed precise measurements of *Z*-boson cross sections using early data from proton–proton collisions at 13 TeV and calculated various ratios using new and previously published top-quark pair cross section measurements. Taking the ratios of the measurements is a powerful way to achieve the highest precision in measurements, thus allowing theoretical predictions to be tested and the understanding of proton structure to be improved.

Precision measurements of cross sections of different processes at different centre-of-mass energies provide a stringent test of Standard Model (SM) predictions. The top-quark pair and *Z*-boson cross section measurements at the LHC performed by the ATLAS and CMS collaborations are in good agreement with theoretical predictions. Ordinarily, experimental precision is limited by the accuracy with which the proton–proton collision luminosity can be determined, and theoretical predictions are subject to large uncertainties from parton distribution functions (PDFs).

A higher level of the precision can be achieved by measuring ratios between cross sections for various processes and energies. By taking ratios, important uncertainties can be cancelled out. This allows a study of the influence of the data on PDF constraints and, moreover, can be sensitive to physics beyond the SM.

At the LHC, the top quark is predominantly produced in pairs through gluon–gluon fusion, and its production is sensitive to the gluon distribution inside the proton. The production of *Z* bosons is dominated by quark–antiquark annihilation and therefore sensitive to the distribution of the light sea quarks in the proton. Consequently, the ratio has a significant sensitivity to the ratio of the gluon and quark PDFs.

The DESY ATLAS group performed the first measurement of inclusive *Z*-boson production in the dilepton channel at a centre-of-mass energy of 13 TeV, reaching a precision at the 0.5% level (excluding luminosity uncertainty). This process can be used to cross-normalise the top-quark pair measurement. In order to achieve the maximum cancellation of uncertainties, the event selection and the lepton selection were adopted from the one in the top-quark pair analysis at the same energy. The ratio of the top-quark pair production to the *Z*-boson production at the centre-of-mass energy of 13 TeV was

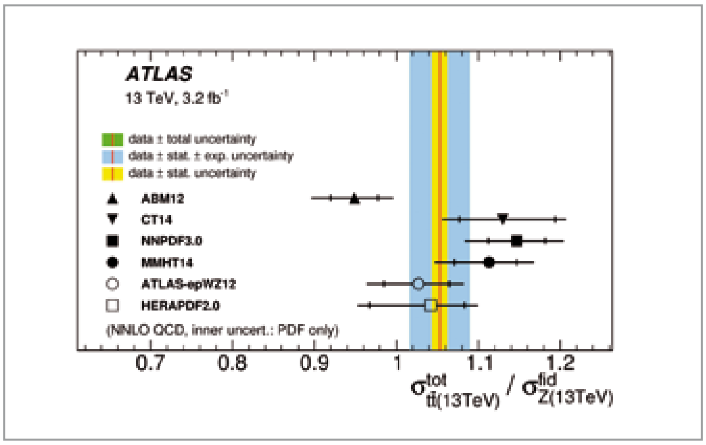

Figure 1

Top-quark pair to *Z*-boson ratio at a centre-of-mass energy of 13 TeV compared to predictions based on the different PDF sets. From [1].

compared to the different theoretical predictions performed at the highest available order in perturbative theory. The comparison demonstrated that the ATLAS data are more precise than the theoretical predictions, as shown in Fig. 1, and suggested constraints for the distribution of both the light sea quarks and the gluons using the ATLAS-epWZ12 PDF set [1]. Furthermore, an inclusion of these data in PDF fits can lead to a reduction in PDF uncertainties in the kinematic region that is sensitive to the top-quark production, thus improving the precision of the theoretical predictions.

Contact:

Alexandre Glazov, alexandre.glazov@desy.de
Artur Trofymov, arthur.trophimov@desy.de
Nataliia Zakharchuk, nataliia.zakharchuk@desy.de

Reference:

[1] ATLAS Collaboration, JHEP 02, 117 (2017).

How the top quark got fat.

Evidence for direct top–Higgs coupling observed

The DESY ATLAS group has observed evidence for the associated production of a Higgs boson with a top quark–antiquark pair for the first time. This process facilitates the direct measurement of the top–Higgs coupling, a crucial test of the Higgs mechanism, which aims at explaining the generation of particle masses. The data for this measurement was taken during LHC Run 2 in 2015 and 2016.

Introduction

Since the discovery of the Higgs boson at the LHC in 2012, the study of its properties has been a major research topic for particle physicists. In the Standard Model (SM), the presence of the Higgs field explains why some fundamental particles have mass: Particles couple to the Higgs field to acquire mass. The top quark is the heaviest particle in the SM. Therefore, its coupling to the Higgs boson is expected to be the strongest, and measuring the value of this coupling is hence of utmost importance for studying the Higgs mechanism.

While the top-quark coupling to the Higgs boson influences many Higgs-related measurements, such as the Higgs boson decay into a pair of photons, the top-associated Higgs boson production is the only way to measure this coupling directly. This is therefore a vital measurement to verify the SM and the nature of its associated Higgs field. A deviation of the expected coupling from the theoretical prediction could reveal the first signs of new phenomena beyond the SM.

The ATLAS experiment has observed evidence for this process for the first time, in a complex analysis using LHC data with a centre-of-mass energy of 13 TeV, in which the DESY ATLAS group played a leading role.

Finding the needle in the haystack

The DESY ATLAS group searched for events where the Higgs boson decays to two bottom (*b*) quarks ($t\bar{t}H$, $H \rightarrow b\bar{b}$), which is the most likely decay channel. Since the top quark almost always decays to a *W* boson and a *b* quark, the decay of $t\bar{t}H$ leads to complex final states with four *b*-quark jets (Fig. 1). These events are very rare and hidden under a huge amount of background. The dominant background process is

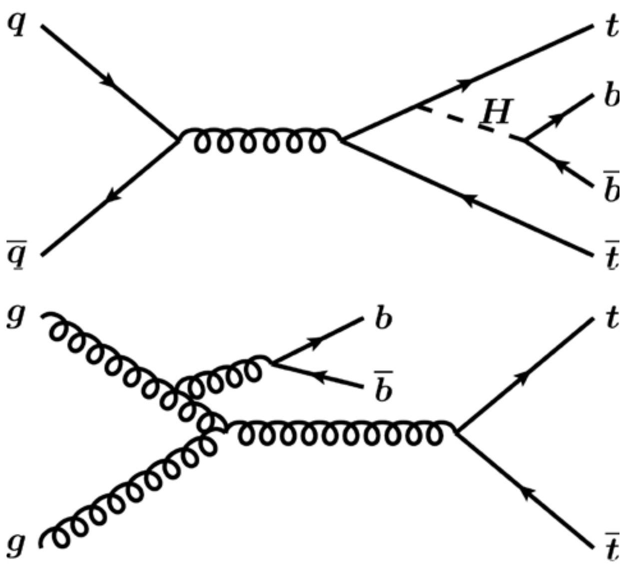

Figure 1

Example of Feynman graphs for $t\bar{t}H$ production with $H \rightarrow b\bar{b}$ decay (upper part) and $t\bar{t}b\bar{b}$ production (lower part). In both cases, four *b*-quark jets are present in the final state, two of which arise from the decay of top quarks.

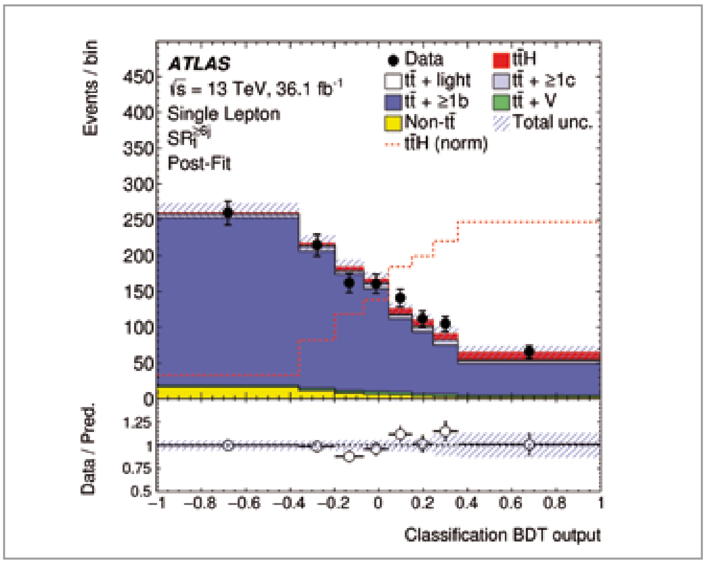

Figure 2

Distribution of the Classification BDT output in the most sensitive region with one electron or muon and at least six jets, of which four are identified as originating from the hadronisation of *b* quarks. The distribution is shown after the fit to the data. The $t\bar{t}H$ signal contribution is shown in red and the dominant $t\bar{t}b\bar{b}$ background in dark blue. From [1].

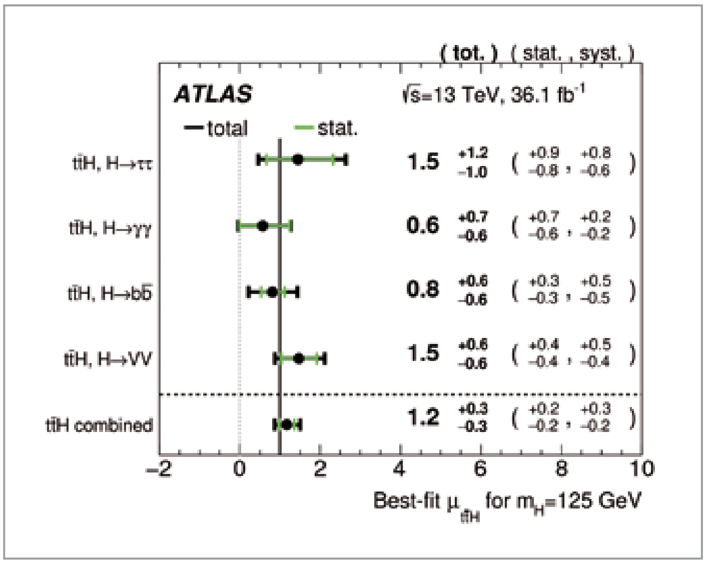

Figure 3

Fitted $t\bar{t}H$ signal strength μ as obtained from the four analysis channels. The total uncertainties are shown in black, together with the statistical uncertainties in green. The value obtained by the combination of the four channels is also shown. From [2].

the production of top-quark pairs, with a production rate 2000 times larger than the $t\bar{t}H$ signal. Especially, top-quark pair events with additional *b*-quark jets produced e.g. from a gluon instead of Higgs boson decay, as shown in Fig. 1, are almost indistinguishable.

The analysis was performed in the leptonic channels, where at least one of the *W* bosons, arising from the decay of the top quarks, decays into a charged lepton and a neutrino. This complex final state with large background requires the analysis to be split in regions of charged lepton multiplicity, jet multiplicity and number of *b*-quark jets. The regions have different sensitivity to signal and background processes. Even in the most sensitive region with exactly one charged lepton and at least six jets, of which four are *b*-quark jets, the signal-to-background ratio is only 5%.

In order to further disentangle signal from background events, machine learning techniques and advanced statistical tools were used in the analyses. These techniques can optimally exploit the full information of the final-state particles.

Figure 2 shows the result of the machine learning algorithm, called "Classification BDT output" in the most sensitive region, with one electron or muon and at least six jets, of which at least four are *b*-quark jets. The algorithm indicates $t\bar{t}H$ events (shown in red) with high values of BDT output. Even after optimisation, the signal yield is lower than the back-ground in all bins. A fit is performed on background and signal regions to extract the $t\bar{t}H$ signal from the difference it causes on the shape of the Classification BDT output distribution. This analysis is limited by the large systematic uncertainties on the modelling of the dominant $t\bar{t}b\bar{b}$ background.

Results

Figure 3 shows the result of the $t\bar{t}H$, $H \to b\bar{b}$ analysis combined with searches for $t\bar{t}H$ in other Higgs boson decay channels. The measurements use data collected in 2015 and 2016 that correspond to an integrated luminosity of about 36 fb^{-1}. The vertical line in the figure represents the SM prediction assuming a Higgs boson mass of 125 GeV. The signal strength μ indicates the measured $t\bar{t}H$ production rate in comparison to the value predicted by the SM.

The ratio of the measured $t\bar{t}H$ signal cross section to the SM expectation is found to be $\mu = 1.2 \pm 0.3$ in the ATLAS experiment, which disfavours the background-only hypothesis by 4.2 standard deviations, while the expected significance is 3.8 standard deviations.

Contact:

Judith Katzy, judith.katzy@desy.de
Timothée Theveneaux-Pelzer, timothee.theveneaux-pelzer@desy.de

References:

[1] ATLAS Collaboration, arXiv:1712.08895 [accepted by Phys. Rev. D].
[2] ATLAS Collaboration, arXiv:1712.08891 [accepted by Phys. Rev. D].

Scrutinising the Standard Model.

Towards a better understanding of particles and their interactions

The Standard Model (SM) of particle physics aims at describing the particles in the universe and their interactions up to high energies, including the energies obtained at the LHC at CERN. In 2017, the ATLAS and CMS groups at DESY have published further measurements testing this claim by scrutinising the SM to the edges of its predictive capabilities. The DESY ATLAS group measured the production of *W* bosons in association with jets and the *W*-boson pair production with no jet activity. The DESY CMS group provided new measurements of particle production at very small transverse momenta and of jet production at very large transverse momenta. These measurements are essential milestones for a better understanding of particles and their interactions within the SM.

ATLAS – Weak boson production at its best

The production of *W* bosons at the LHC is a powerful probe for looking into both the strong interactions and the electroweak interactions in the SM.

Production of *W* bosons in association with jets

The DESY ATLAS group published a measurement of *W*-boson production in association with jets, based on 20.2 fb^{-1} of data from proton–proton collisions at the centre-of-mass energy of $\sqrt{s} = 8$ TeV [1]. The emission of jets is described by the theory of strong interactions, quantum chromodynamics (QCD), and their presence can give the produced *W* boson significant transverse momentum (p_T). Differential cross sections, in particular at high p_T, provide a valuable test for QCD predictions in the perturbative regime.

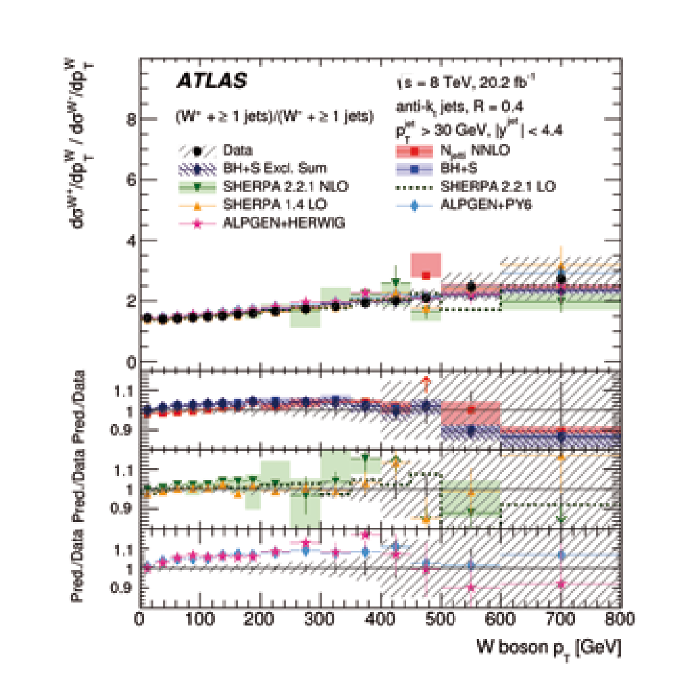

Figure 1

Ratio of the differential cross sections of W^+- and W^--boson production in association with at least one jet as a function of the *W*-boson p_T [1]

Depending on their charge, *W* bosons in association with at least one jet are produced from different partons in the proton: typically an up quark for W^+, a down quark for W^-, plus a gluon for both. In the cross section ratio of W^+ to W^-, the dominating theoretical and experimental uncertainties related to the jet production cancel, thus probing smaller effects in the predictions, such as the parton density functions (PDFs) in the proton. The cross section ratios of W^+ to W^- production were measured for the first time in association with jets in the publication by the DESY ATLAS group, including the ratio as a function of the *W*-boson p_T in the presence of at least one jet (Fig. 1).

Production of *W*-boson pairs

The measurement of the *W*-boson pair production (W^+W^-) is a challenging process that targets the fundamental structure of the electroweak interaction in the SM. One of the dominant

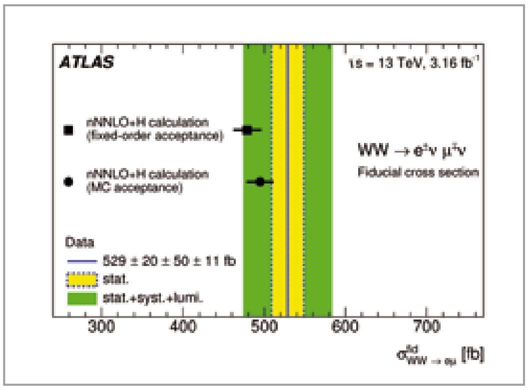

Figure 2

Measured W^+W^- production cross section in comparison with the two best available theoretical predictions [2] production modes of this process involves gauge boson self-interactions, which are not well constrained within the SM. Hence, a precision measurement of this process challenges our theoretical knowledge of the SM, whereas any observed deviation could hint at the existence of physics beyond the SM.

The DESY ATLAS group measured the cross section of W^+W^- production with no jet activity at a centre-of-mass energy of $\sqrt{s}$ = 13 TeV [2]. The measured cross section in a fiducial phase space close to the detector acceptance is in agreement with the two best available theoretical predictions (Fig. 2). With the current availability of a much larger data set, the DESY ATLAS group is now aiming for a more precise measurement with improved experimental uncertainties.

CMS – QCD at the extremes

Predictions obtained from the theory of QCD within the SM are in very good agreement with measurements in a region of phase space away from the extremes.

Measurements at very small transverse momenta

When the energy of the interacting partons becomes very small, the density of partons rises and the parton–parton cross section eventually diverges. The cross section of charged particles above a transverse momentum p_{Tmin} is a direct measurement of this behaviour [3].

The measurement (Fig. 3) at a centre-of-mass energy of 13 TeV [4], performed by the DESY CMS group, shows that the distribution falls at larger p_T, but approaches a constant value at small p_T. While the density of partons is very large in this region, they overlap and recombine, leading to the observed behaviour, which is confirmed by predictions of QCD calculations including those effects. The predictions describe the general behaviour, while significant differences are observed especially in the region of small p_T.

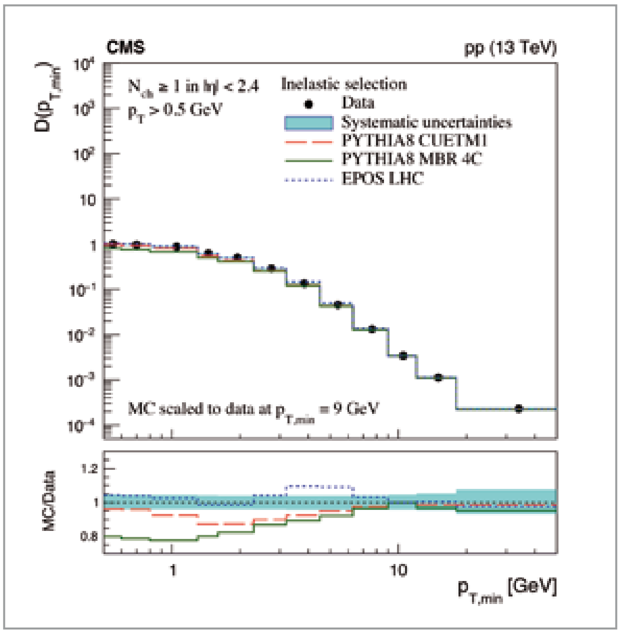

Figure 3

Normalised distribution of charged particles [4] with p_T larger than p_{Tmin}, compared to different theory predictions. The band shows the systematic uncertainty.

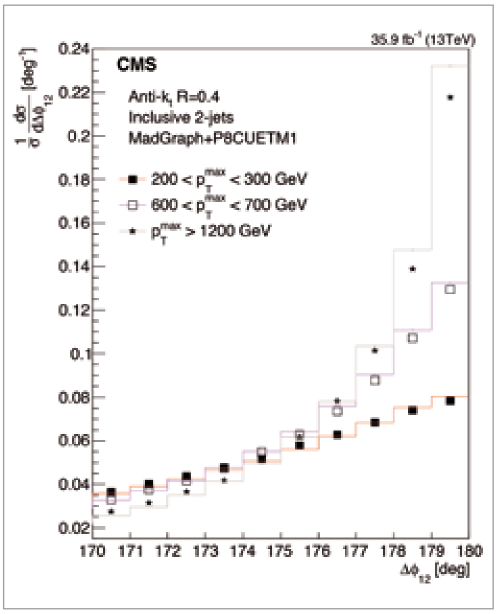

Figure 4

Normalised inclusive two-jet distributions as a function of the azimuthal difference of the two leading jets for three p_{Tmax} regions [5] compared to a theoretical calculation

Measurements at very large transverse momenta

Another region of phase space is reached when the p_T of jets becomes large and eventually reaches the kinematic limit. The DESY CMS group measured the correlation of two jets in the azimuthal plane [5]. Figure 4 shows the difference in azimuthal angle between the two jets with largest transverse momentum (p_{Tmax}) for different values of p_{Tmax} in the region where both jets are nearly back to back. For small and medium transverse momentum, one observes a significant decorrelation, while at largest p_{Tmax} (p_{Tmax} > 1.2 TeV), the two jets are mostly back to back. Higher-order parton radiation leads to a decorrelation of the two jets. When the transverse momentum of the two jets is very large, there is little phase space left for additional parton radiation.

The theoretical prediction describes the measurement reasonably well, except in the highest p_{Tmax} region, where significant differences are observed.

Although calculations agree reasonably well with most of the measurements obtained at the LHC, the extreme regions of small and very large transverse momenta of the particles and jets challenge the theory.

Contact:

Valerie Lang, valerie.lang@desy.de
Baishali Dutta, baishali.dutta@desy.de
Hannes Jung, hannes.jung@desy.de

References:

[1] ATLAS Collaboration, arXiv:1711.03296 [hep-ex].
[2] ATLAS Collaboration, Phys. Lett. B 773, 354 (2017).
[3] A. Grebenyuk et al., Phys. Rev. D86 117501 (2012).
[4] CMS Collaboration, CMS-PAS-FSQ-16-011.
[5] CMS Collaboration, CMS-PAS-SMP-17-009.

Probing extended Higgs sectors with bottom quarks.

Additional Higgs bosons may couple strongly to *b* quarks

At a centre-of-mass energy of 13 TeV, the LHC Run 2 offers unique sensitivity to additional bosons of an extended Higgs sector, especially in the decay to bottom quarks. The DESY CMS Higgs group used specialised triggers to hunt for close relatives of the well-established Higgs boson. The results show increased sensitivity, which is also extended towards higher masses.

Dominant decay mode

The search for additional Higgs bosons beyond the Standard Model (SM) is one of the most exciting topics at the LHC. The existence of a second Higgs doublet would directly lead to a rich Higgs sector. One example for a theory with two Higgs doublets is supersymmetry (SUSY). As we know, the SM Higgs boson decays most frequently into a pair of *b* quarks. In extended Higgs sectors, the coupling to *b* quarks may be further enhanced, which makes Higgs production with additional *b* quarks an attractive signature.

A challenging analysis

However, Higgs studies in purely hadronic final states are very challenging. A special trigger searching for *b*-quark jets already in the online selection is crucial to suppress the huge background rate from QCD multijet production. The analysis then searches for a resonance in the invariant mass of the two *b*-tagged jets with highest transverse momentum, accompanied by a third *b* candidate. The background is described by analytic functions with up to six shape parameters, and the fit is performed in three overlapping mass regions.

As shown in Fig. 1, the invariant-mass distribution is well described over a very wide range, and no signal is observed. The analysis provides unique limits on Higgs production in this topology. They are consequently interpreted within various models. In particular, Fig. 2 shows the exclusion in the flipped two-Higgs doublet model (2HDM), in which down-type quarks and leptons couple to different doublets. Shown is the result for a mass value of 500 GeV; the analysis gives unique bounds for this model.

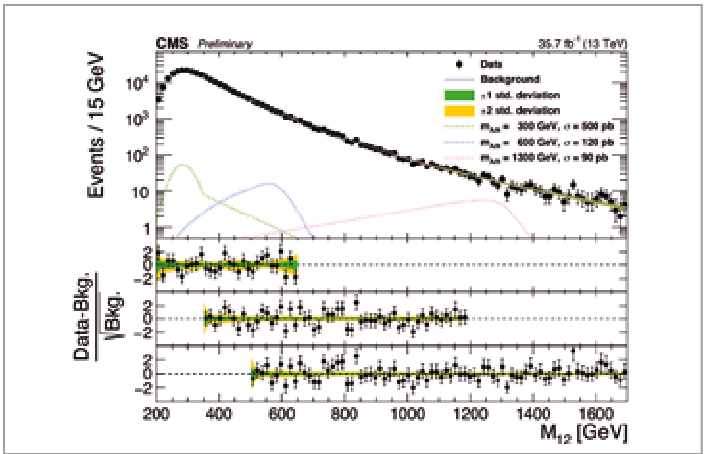

Figure 1

Invariant-mass distribution of the two leading, *b*-tagged jets together with background-only fits [1]. Expected signal shapes for three different Higgs masses are also shown.

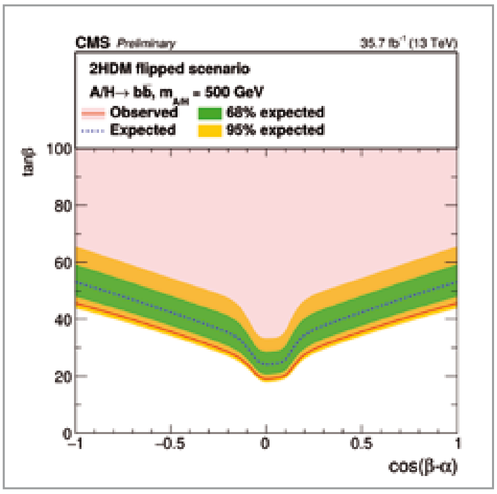

Figure 1

Excluded regions in the parameter plane of the flipped 2HDM model, for a Higgs mass of 500 GeV [1]

Contact:

Chayanit Asawatangtrakuldee, chayanit.asawatangtrakuldee@desy.de

Rainer Mankel, rainer.mankel@desy.de

Reference:

[1] CMS Collaboration, http://cds.cern.ch/record/2302331.

Search for supersymmetry with CMS.

Chasing superpartners of the tau lepton.

Supersymmetry is one of the most popular theories for physics beyond the Standard Model. Members of the DESY CMS group have performed a search for direct and indirect production of the supersymmetric partner of the tau lepton using data recorded by the CMS detector at the LHC in 2016.

Supersymmetry (SUSY) is a theory beyond the Standard Model (SM), which predicts for each SM particle a supersymmetric partner particle differing only in its spin (by ½). If the symmetry were perfect, the SUSY particles would have the same mass as their SM partner particle, and most of them would have already been discovered. Since no SUSY candidate has been observed yet, the symmetry must be broken, pointing to higher masses of the superpartners.

In the past, the DESY CMS group performed several searches for the superpartners that are produced in the strong interaction, e.g. the partners of the gluon [1] and the top quark [2].

The search for weakly produced particles, such as the partners of the leptons and the bosons, called neutralinos $(\widetilde{\chi}^0)$ and charginos $(\widetilde{\chi}^{\pm})$, is very challenging. Their production cross section is much lower than the one of strongly produced particles of similar mass. Therefore, more data have to be analysed to reach comparable sensitivity.

The DESY CMS group has performed a search for the superpartner of the tau lepton (τ), called stau ($\tilde{\tau}$), in direct pair production as well as in the decay of neutralinos and charginos, using data recorded by the CMS detector at the LHC in 2016 [3]. In the latter case, the second-lightest neutralino $(\widetilde{\chi}^0_2)$ decays to a stau and a tau lepton, while the chargino $(\widetilde{\chi}^{\pm}_1)$ decays to a stau and a neutrino. In all cases, the stau decays subsequently to a tau and the lightest SUSY particle, the LSP, which is assumed to be the lightest neutralino $(\widetilde{\chi}^0_1)$ in this analysis.

The search was performed in the channel where one tau finally decays to an electron or a muon and the other one decays to hadronic particles, or one tau decays to an electron and the other to a muon. As shown in Fig. 1, for the second-lightest neutralino and the chargino, masses below 560 GeV can be excluded if the LSP is nearly massless. For a stau mass of 90 GeV and a nearly massless LSP, no mass point could be excluded, and the group determined an upper limit of 0.66 pb.

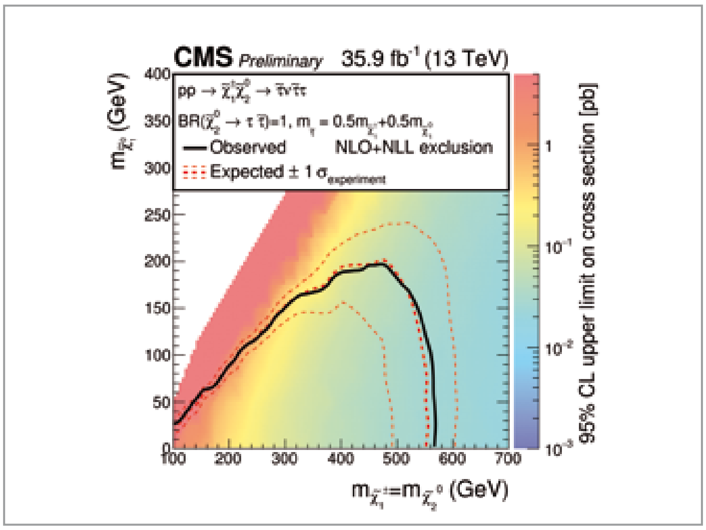

Figure 1

Expected and observed limits on the cross section for neutralino–chargino production with decay through the SUSY partner of the tau lepton, where the mass of the latter is taken in this search to be halfway between the two neutralinos. The area below the thick black curve represents the observed exclusion region, while the dashed red lines indicate the expected limits and their $\pm 1\sigma$ standard deviation ranges.

Contact:

Isabell-A. Melzer-Pellmann, isabell.melzer@desy.de

References:

[1] CMS Collaboration, CMS-PAS SUS-16-042.
[2] CMS Collaboration, JHEP 07, 027 (2016), Erratum: JHEP 09, 056 (2016).
[3] CMS Collaboration, CMS-PAS SUS-17-002.

Higgs physics with tau leptons.

Heaviest charged lepton helps to explore electroweak symmetry breaking

Elucidating the mechanism through which the Standard Model (SM) particles acquire mass is a cornerstone of the physics programme at the LHC. Final states with two oppositely charged tau leptons play an important role in the study of electroweak symmetry breaking. Using 36 fb^{-1} of the LHC Run 2 data collected at 13 TeV, the CMS collaboration analysed these final states with the aim to study the properties of the discovered Higgs boson and to search for additional Higgs bosons beyond the SM. The DESY CMS group was strongly involved in the analyses.

Measuring the fermionic couplings of the Higgs boson is the key step towards elucidating the mechanism of electroweak symmetry breaking. The DESY CMS group made significant contributions to one of the recently published measurements of this kind, namely the measurement of the Higgs boson coupling to τ leptons with LHC Run 2 data.

The study targeted three major production mechanisms of the Higgs boson: gluon–gluon fusion, both with the Higgs boson produced at low transverse momentum and with the Higgs boson produced in a highly boosted state, as well as vector boson fusion. Four decay modes of τ pairs were analysed: $\tau_e\tau_h$, $\tau_\mu\tau_h$, $\tau_h\tau_h$ and $\tau_e\tau_\mu$. Here, τ_e (τ_μ) stands for the leptonic decay of the τ into an electron (muon), and τ_h denotes the τ decay into hadrons. Combined with the LHC Run 1 data set, this measurement resulted in the first observation of the $H \to \tau\tau$ decay in a single experiment with a statistical significance of 5.9 σ.

Figure 1 illustrates the signal observed in the distribution of the mass of the two τ leptons. The combination of all analysed channels yields a measured value of the signal strength μ (defined as the probed $H \to \tau\tau$ rate relative to the value predicted in the SM) of $\mu = 1.09 \pm 0.27$ in agreement with the SM expectation ($\mu = 1$).

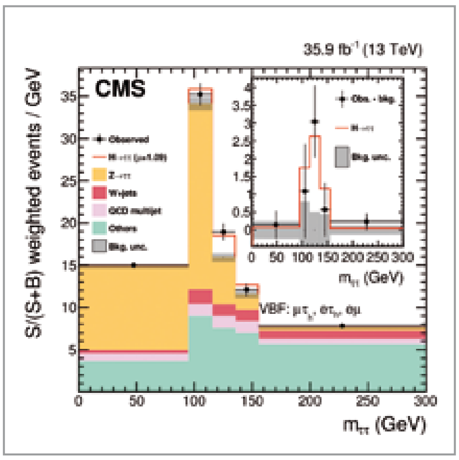

Figure 1

Observed and predicted distribution of the invariant mass of τ pairs in the CMS analysis of the $H \to \tau\tau$ decay channel

The study of final states with τ leptons is also crucial in searches for additional Higgs bosons appearing in theories beyond the SM. One example is the Minimal Supersymmetric Standard Model (MSSM), which features two Higgs doublets and predicts five physical states: two scalars (h, H), one pseudoscalar (A) and two charged bosons ($H^\pm$). The H/A boson decay rate into τ leptons in the MSSM is enhanced at high values of $\tan\beta$, the ratio of the vacuum expectation values of the two Higgs doublets. The DESY CMS group played an active role in the analysis, searching for additional heavy neutral Higgs bosons decaying into a pair of τ leptons in LHC Run 2 data.

The search exploited two production modes of supersymmetric Higgs bosons – gluon–gluon fusion and b-quark-associated production – and made use of the same τ pair decay modes as the aforementioned study of the discovered Higgs boson. The reach of the search was extended to masses of the heavy supersymmetric Higgs bosons beyond 1.5 TeV. The analysis revealed no signal, and stringent constraints on the MSSM parameters were derived. For the MSSM benchmark scenarios, in which the lightest scalar boson h is consistent with the measured properties of the discovered Higgs boson, the upper 95% confidence level limit on $\tan\beta$ ranges from 4 at m_A = 300 GeV to 60 at m_A = 1.7 TeV, where m_A is the mass of the Higgs boson A.

Contact:

Alexei Raspereza, alexei.raspereza@desy.de

References:

[1] CMS Collaboration, Phys. Lett. B 779, 283 (2018).

[2] CMS Collaboration, arXiv:1803.06553, submitted to JHEP.

High-precision calibration.

CMS tracker alignment and luminosity measurement

The DESY CMS group plays a leading role in the alignment of the track detectors and in the measurement of the luminosity. In 2017, a new pixel track detector with one additional layer was installed in the CMS experiment, leading to significant improvement of the track and vertex reconstruction. The DESY tracker alignment team led the preparation efforts and derived the first real-data alignment. The integrated luminosity is a crucial quantity for virtually all analyses. The DESY CMS group contributes to the online and offline precision calibration of the luminosity measurement.

Alignment of the upgraded pixel detector

In early 2017, a new upgraded pixel detector was installed in the CMS experiment, implying the need to newly determine all the positions, orientations and surface curvatures of the sensors. A precision of a few micrometres is required for optimal performance of the device. DESY led the preparation and implementation, including the upgrade of the CMS alignment software as well as simulation studies. In a multistep procedure, cosmic-ray and collision data were used to determine the displacements from the nominal positions. They were found to be as large as 3 mm in the end-cap and 2 mm in the barrel. Iteratively, the local precision was improved until it was better than 0.5 µm (Fig. 1), thus delivering high performance already shortly after the restart of the LHC after the winter shutdown.

Luminosity measurement

Luminosity is a measure of the particle collision rate and a crucial ingredient both for the operation of the LHC and the experiments and for the physics data analysis. The CMS group at DESY is involved in the operation and maintenance of the BCM1F detector, a device for real-time bunch-by-bunch measurement of the instantaneous LHC luminosity and beam backgrounds. DESY also makes key contributions to the precision calibration of the integrated luminosity using Van-der-Meer (VdM) scan data. In VdM scans, the event rate is measured as a function of the transverse separation of the two beams (Fig. 2). From the measured beam–beam profile and the beam currents, an absolute luminosity is determined. Permille-level corrections for residual correlations, non-linearities and time dependencies are determined in order to achieve a high-precision luminosity measurement [2]. DESY contributed several of these corrections.

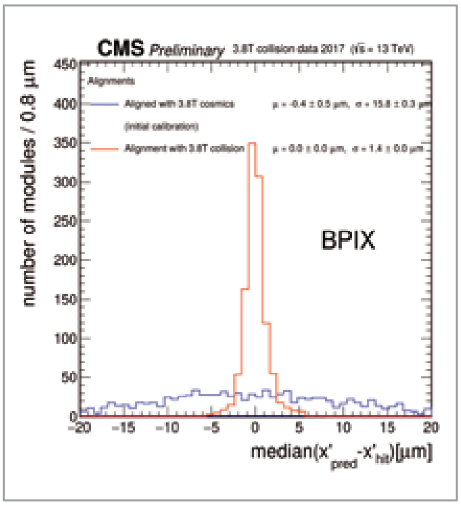

Figure 1

Distribution of median track hit residuals in the local *x*' direction of the pixel barrel (BPIX) modules. The tracks were fitted using the tracker geometry derived with cosmic-ray tracks (blue) and with the alignment derived with collision data (red). The latter distribution is well centred and very narrow, indicating an excellent local precision [1].

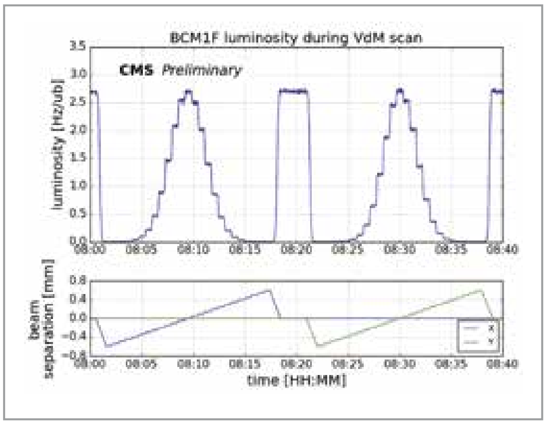

Figure 2

Luminosity measured by the BCM1F detector during a Van-der-Meer scan. The lower panel shows the transverse separation of the beams.

Contact:

Gregor Mittag, gregor.mittag@desy.de
Andreas Meyer, andreas.meyer@desy.de

References:

[1] CMS Collaboration, CMS-DP-2017-054 (2017).
[2] CMS Collaboration, CMS-PAS-LUM-17-004 (2018).

Dark matter and the top quark.

Exploring the unknown with the heaviest known elementary particle

Postulated more than 80 years ago by Swiss astronomer Fritz Zwicky, the phenomenon of dark matter is still one of the major unsolved puzzles in science today. While its existence is firmly established by a multitude of astrophysical and cosmological observations, such as measurements of the rotational velocity of galaxies and, more recently, the cosmic microwave background, its particle nature remains elusive. If dark matter is a so-called weakly interacting massive particle (WIMP), it could be produced at the LHC at CERN. The DESY ATLAS and CMS groups play a leading role in searches for dark matter at the LHC.

Dark-matter production at the LHC

Recently proposed simplified benchmark models for dark matter (DM) searches at the LHC [1] extend the particle content of the Standard Model (SM) by fermionic DM and a mediator particle connecting DM and SM particles. Some of these interesting models involve scalar (CP-even) and pseudoscalar (CP-odd) couplings to SM particles. Assuming Yukawa-like couplings for such (pseudo-)scalar mediators, the coupling strength scales with the mass of the SM fermion and is largest for the heaviest known elementary particle, the top quark.

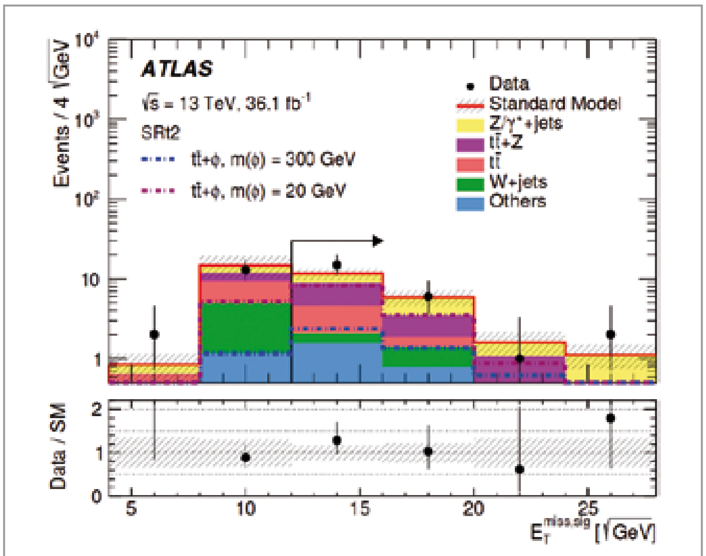

Figure 1

Comparison between the data and the SM background prediction as a function of the missing transverse momentum significance. The event selection requirement on the distribution shown is indicated by an arrow. For comparison, distributions of two signal scenarios that have been searched for are shown in addition.

WIMPs would not leave any signal in the detector. Their production would be detected as a large amount of missing transverse momentum recoiling against visible particles, such as a top quark–antiquark pair ($t\bar{t}$), due to momentum conservation (Fig. 1). Both the ATLAS group and the CMS group at DESY played a leading role in searches for a data excess in LHC proton–proton collisions with $t\bar{t}$ and large missing transverse momentum [2–5]. About 36 fb^{-1} of data recorded at a centre-of-mass energy of 13 TeV were analysed, exploring all $t\bar{t}$ decay channels.

The main background arises from the production of a top quark–antiquark pair, which dominates at low missing transverse momentum, and the production of a top quark–antiquark pair in association with a *Z* boson decaying into a pair of neutrinos. Such events represent a challenging and irreducible background. To suppress them and to maximise the sensitivity of the searches, distributions probing the spin correlation of the two top quarks have been studied. This is particularly interesting as it also allows searches to distinguish between CP-even and CP-odd mediator couplings to the top quark.

Figure 2 shows the upper limit on the $t\bar{t}$+DM cross section as a function of the mass of the scalar DM mediator, analysing final states with two leptons and high missing transverse momentum. In this scenario, masses up to about 100 GeV can be excluded. The sensitivity to pseudoscalar mediators is slightly lower because the cross section is smaller than for CP-even scalar mediators up to a mass of about 200 GeV.

The sensitivity of the search is currently still limited by data statistics and therefore offers very good prospects for future measurements with larger data sets.

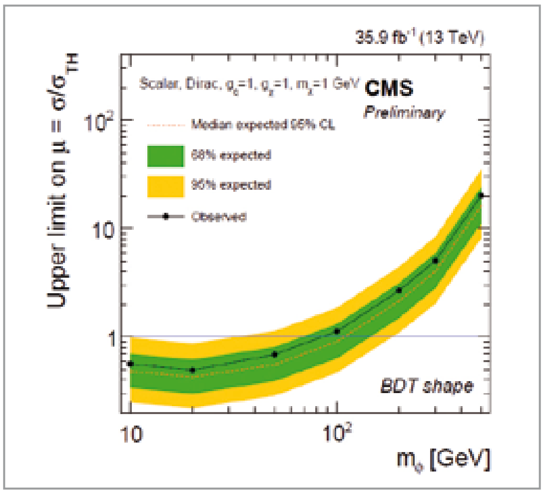

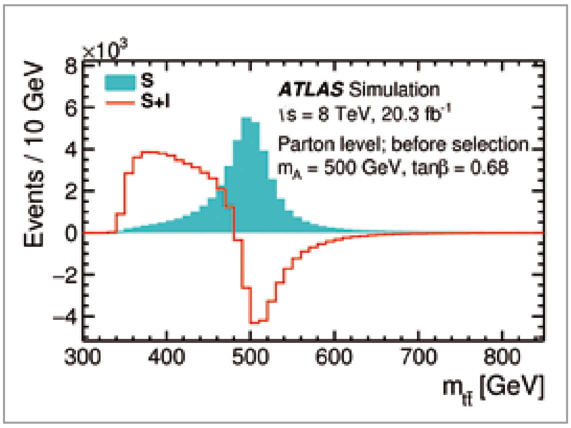

Figure 3

Signal shape for a heavy pseudoscalar Higgs boson *A* decaying to a top quark–antiquark pair with (red) and without (turquoise) interference effects considered

Figure 2

Recent searches for DM produced in association with a top quark–antiquark pair exclude CP-even scalar mediators up to about 100 GeV assuming an overall coupling scaling factor of 1.0 between the top quark and the DM mediator [4].

Probing complex signals of dark matter

A complementary approach in the search for evidence of DM at the LHC is to look for new particles predicted to participate in the interaction of DM and ordinary matter. Current simplified models typically predict a single DM particle and DM mediator each. However, more complex models are becoming increasingly popular due to their richer phenomenology, which allows them to be probed via a multitude of different signatures. In particular, they can motivate the exploration of new kinematic regimes and signatures.

One such model [6], developed partly by the DESY theory group, is currently studied as a new benchmark model in both ATLAS and CMS. It builds on the well-motivated assumption of the existence of a second Higgs field, leading to additional heavy scalar and pseudoscalar Higgs bosons. If these additional Higgs bosons are heavy enough, they would dominantly decay into a top quark–antiquark pair.

This signal process is particularly challenging to identify as it interferes strongly with SM background processes. Hence, these additional Higgs bosons would not appear as a localised peak in the invariant-mass spectrum of their decay products. Instead, they would result in a more complicated peak dip structure (Fig. 3) that depends significantly on the parameters of the model, such as the masses and the ratio of the vacuum expectation values of the two Higgs fields.

In 2017, the ATLAS collaboration published the first search for heavy Higgs bosons in this challenging decay mode [7]. The results are interpreted in the context of a minimal extension of the SM by a second Higgs field without making any assumptions about DM interactions. This search can also be used to constrain the extended two-Higgs doublet model with a pseudoscalar mediator [6].

Outlook

With the full data set of 140 fb^{-1} expected by the end of 2018, searches for DM produced in association with top quarks are expected to be among the most sensitive searches for DM interacting with ordinary matter via scalar or pseudoscalar mediators. The current searches will be improved and optimised in sensitivity. Furthermore, searches probing yet unexplored parameter regions of new models, such as models with two Higgs fields and an extra mediator particle, will be studied, looking for new and yet unexplored signal patterns. These two search approaches are complementary and will provide a unique opportunity to unravel the mystery of DM.

Contact:

Katharina Behr, katharina.behr@desy.de
Kelly Beernaert, kelly.beernaert@desy.de
Alexander Grohsjean, alexander.grohsjean@desy.de
Matthias Saimpert, matthias.saimpert@desy.de

References:

[1] D. Abercrombie et al., arXiv:1507.00966.
[2] ATLAS Collaboration, Eur. Phys. J. C 78, 18 (2018).
[3] ATLAS Collaboration, arXiv:1711.11520 (2018).
[4] CMS Collaboration, CMS PAS EXO-17-014 (2018).
[5] CMS Collaboration, CMS PAS EXO-16-049 (2018).
[6] Bauer et al., JHEP 1705, 138 (2017)
[7] ATLAS Collaboration, Phys. Rev. Lett. 119, 191803 (2017).

Getting ready for first collisions.

SuperKEKB and Belle II

DESY is strongly involved in the realisation of the second-generation B-factory SuperKEKB, an electron–positron collider at the KEK particle physics laboratory in Japan, and the corresponding Belle II experiment. In 2017, significant progress was made towards finalising the upgrade of the former KEKB accelerator and of the detector. The construction of the completely new damping ring for the positron beam was finished, the final focus magnets were commissioned, and their field was measured. The construction of the Belle II detector was completed with the exception of the vertex detector. The assembly of the pixel vertex detector and the strip detector is ongoing in Germany and at KEK, respectively. The assembly of the two devices on the final central beam pipe is foreseen for summer/autumn 2018. The start of physics data taking with the vertex detector installed is scheduled for the beginning of 2019.

Status of SuperKEKB and Belle II

An important step towards first data taking with colliding beams was reached on 11 April 2017, when the Belle II detector was rolled into beam position seven years after the end of beam operation of the predecessor experiment Belle (Fig. 1). With the exception of the new vertex detector (VXD), all Belle II subdetectors had been installed in the meantime. The VXD consists of two DEPFET pixel detector layers (PXD) surrounded by four layers of double-sided strip detector (SVD). The design and construction of the PXD are the main responsibility of the 12 German institutes involved in Belle II. The two superconducting final-focus magnets QCSL and QCSR – the central components of the upgraded SuperKEKB accelerator – were successfully installed in the interaction region in the months before the roll-in.

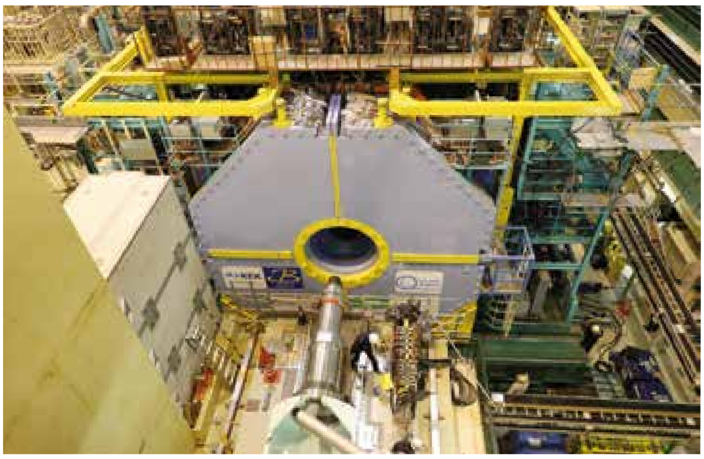

Figure 1

Belle II detector after rolling into beam position on 11 April 2017 together with the QCSR in its retracted position

Magnetic field measurements

In order to be able to reach the ultimate luminosity goal of 8×10^{35} $cm^{-2}s^{-1}$, the SuperKEKB machine physicists need to precisely control the field around the beam axis in the interaction region. Once all the different magnets inside the QCS cryostats are operated at their nominal currents, very large magnetic forces resulting from the interaction with the 1.5 T field of the Belle II solenoid will lead to small shifts in the position of the magnets, which will affect the magnetic field distribution on the beamline. In addition, small imperfections in the assembly procedure for the 55 individual magnets inside this highly complex system or saturation effects in their magnetic components may lead to distortions in the field configuration, which are impossible to predict. In order to understand the magnet properties in sufficient detail, the SuperKEKB magnet group performed an extensive measurement programme in summer 2017, including data taking with single stretched wires, harmonic coils and a Hall probe.

The DESY group used this period to complete its complementary magnetic field measurement campaign inside the Belle II tracking volume. An excellent knowledge of the magnetic field in this region is essential for high-precision tracking, which forms the basis for most physics analyses. While in summer 2016 a modified robot from CERN had been employed to measure the magnetic field of the Belle II solenoid just before the installation of the large central drift chamber (CDC), in 2017 the DESY group concentrated on the restricted volume to be occupied by the VXD and on the narrow gaps between the QCS cryostats and the inner envelope of the CDC. This additional data are needed to determine the influence of the significant stray field of the

QCS magnets inside the tracking volume and to tune the simulations done by the SuperKEKB magnet group. Mapping the field in the VXD volume required the design of a dedicated robotic system (Fig. 2) allowing remote and reliable operation in this area, which was completely inaccessible after the QCS magnets had been inserted.

The mechanical design and construction of the mapper were done by IFJ-PAN in Cracow, Poland, in close collaboration with DESY. More than 100 carefully calibrated 3D Hall probes provided by CERN on a loan basis were used to instrument the region. To exploit the full potential of the 3D information, a significant effort had to be made to precisely survey and align the mapper mechanics and the Hall probes before and after the installation of the device. The outer dimensions of the mapper were chosen so that it could be installed using the same tooling developed at MPP Munich in Germany for the complex installation procedure of the VXD proper.

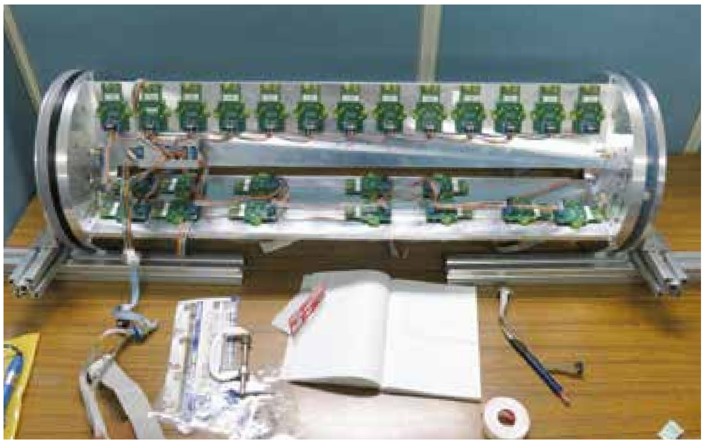

Figure 2

Magnetic field mapper for the VXD region. The device is driven by an ultrasonic piezo engine and equipped with more than 40 3D Hall probes to map the magnetic field in the VXD volume.

The successful installation of the mapper in April 2017 therefore also served as an important final rehearsal for this delicate operation. The data of the field measurement campaigns are still being analysed together with those obtained by the SuperKEKB magnet group. The combined information from all measurements will lead to a consistent and improved model of the magnetic field in the tracking volume and on the beamline, which will then be implemented into the reconstruction software of Belle II.

Getting ready for Phase 2 of SuperKEKB

The commissioning of the SuperKEKB accelerator complex proceeds in three phases. The commissioning of the main ring – still without the final focus system – was the main goal of Phase 1 in early 2016. Since then, the construction and instrumentation of the new damping ring for the positron beam has been finished. The start of the next commissioning phase is foreseen for spring 2018, when electron and positron beams will be brought to collision for the first time using the so-called nanobeam scheme. The goal of Phase 2 is to reach at least the design luminosity of the predecessor accelerator KEKB ($1x10^{34}$ $cm^{-2}s^{-1}$) at background conditions that are acceptable for the very sensitive VXD. After installation of the VXD in fall 2018, data taking (Phase 3) is scheduled to start at the beginning of 2019.

In order to be able to characterise the beam-related background as well as possible, the BEAST II system, consisting of a small sector of the final VXD plus several dedicated background monitoring devices, was constructed for Phase 2 operation. System integration and commissioning of the BEAST II components took place in February and March 2017 at the dedicated PERSY setup in the HERA hall West at DESY and at the DESY Test Beam Facility. After transportation of the individual components to Japan in fall 2017, the BEAST II setup was re-assembled on the fragile central beryllium beam pipe at KEK. Thanks to the experience gained with the magnetic field mapper, the installation of BEAST II into Belle II proceeded very smoothly in November (see News and Events section).

The interaction region is by far the most complicated area of the entire SuperKEKB accelerator, mainly because of severe space limitations. After installation of BEAST II and later the VXD together with the central beam pipe into Belle II, it will be impossible to connect the vacuum system of the accelerator with the central beam pipe using standard techniques. For this reason, DESY has proposed, designed and constructed the so-called remote vacuum connection (RVC). The RVC is based on a hydraulic system that allows remote closing of the vacuum seals, thereby fulfilling the high standards of ultrahigh-vacuum tightness set by the SuperKEKB vacuum group.

The full and reliable functioning of this complex system is absolutely crucial for the installation of the VXD and therefore mission-critical for the entire project. For this reason, the system was extensively tested and optimised over several years using a dedicated test stand at DESY (see cover picture of this annual report) before it was installed on the QCS cryostats in November 2017. A major common milestone was achieved for both the accelerator and the experiment when the RVC was successfully closed for the first time after the insertion of the QCS magnets in preparation for Phase 2 operation.

Belle II collaborative services and tools

In 2017, the Belle II membership management system became operational as an integral part of the collaborative services, which are hosted at DESY. The new system serves as the basis for e.g. author or mailing lists, votes, shift distribution or maintenance and operation costs.

Contact:
Carsten Niebuhr, carsten.niebuhr@desy.de

Preparing the future.

Physics case for the 250 GeV stage of the International Linear Collider

The International Linear Collider (ILC) is among the leading contenders as a future collider project for particle physics. Its polarised electron and positron beams could collide at centre-of-mass energies between 200 GeV and 1 TeV, annihilating to produce Higgs bosons, top quarks, *W* and *Z* bosons – and potentially also new exotic particles. The technical design report of the ILC, published in 2013, focused on 500 GeV as initial baseline energy. In 2017, with leading contributions from DESY, the global Linear Collider Collaboration (LCC) presented the design [1] and the physics case [2–3] for a first stage of the ILC operating at 250 GeV, the minimal energy needed for efficient production of the Higgs boson in electron–positron collisions.

Scrutinising the Higgs boson

The most famous target of the initial 250 GeV stage of the ILC is certainly the Higgs boson. Discovered in 2012 at the LHC at CERN, it is the youngest member of the particle family, but maybe the longest sought after. Since 2012, we have been learning a lot about the new kid on the block from the LHC, but still many questions remain: Is the Higgs boson really an elementary particle, the only one without spin, or rather a composite object? Why does it have such a special relation to the top quark, making the latter as heavy as a gold atom? Does the Higgs boson act as a portal to a whole dark sector, explaining the cosmologically observed dark matter?

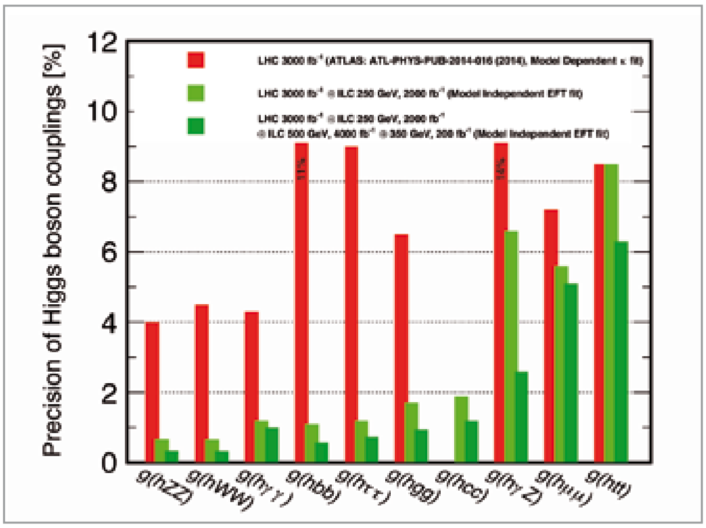

Figure 1

Precisions on Higgs boson couplings expected from the HL-LHC alone (red), in combination with the 250 GeV stage of the ILC (light green) and adding the 500 GeV stage of the ILC (dark green) [3]

It has been known for a long time that an electron–positron collider with sufficient energy and luminosity will be the ideal place to scrutinise the Higgs boson in great detail and in a model-independent way – a qualitative difference from measurements at hadron colliders. This characteristic was traditionally studied in the so-called κ-framework based on independent scaling factors for each Higgs coupling. Together with colleagues from SLAC, KEK and the University of Tokyo, the DESY ILC group now interpreted projections for Higgs measurements at the ILC in a more general and yet more powerful framework: effective field theory (EFT). Within the chosen EFT ansatz [2], the Higgs measurements can be combined with existing electroweak precision data from the former LEP and SLC colliders as well as with measurements of the interactions of the three electroweak gauge bosons expected from the ILC. It is the incorporation of these non-Higgs measurements that makes the 250 GeV stage of the ILC much more powerful than previously recognised.

Figure 1 shows the expected precision on the Higgs couplings to various other particles as obtained from this new EFT-based interpretation, for the 250 GeV stage of the ILC (light green) and including the 500 GeV stage (dark green) in combination with high-luminosity LHC (HL-LHC) measurements. At 250 GeV already, many couplings reach a precision of 1–2%, including the coupling to charm quarks, which is very hard to observe at the LHC. The 500 GeV data lead to further improvements, typically by a factor of 2. For comparison, the red bars show HL-LHC projections obtained from a model-dependent fit similar to the κ-framework.

In addition to the couplings displayed in Fig. 1, the ILC at 250 GeV would also provide an important constraint on the

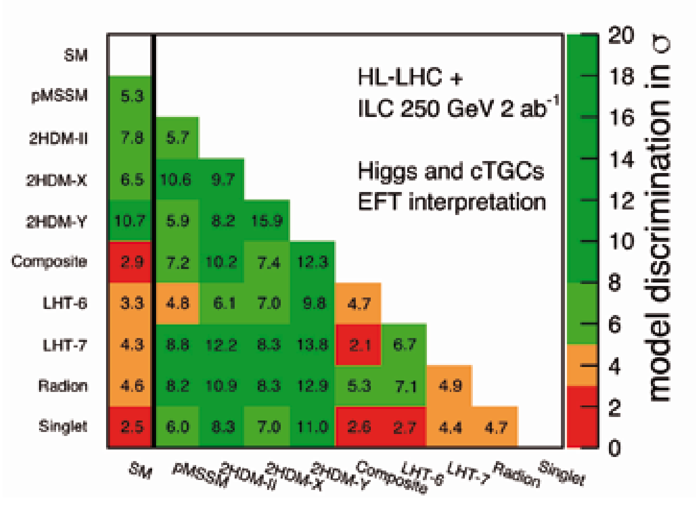

Significance for discriminating the Standard Model (SM) from various examples of extensions of the SM by the power of Higgs precision measurements as expected from the 250 GeV stage of the ILC [2]

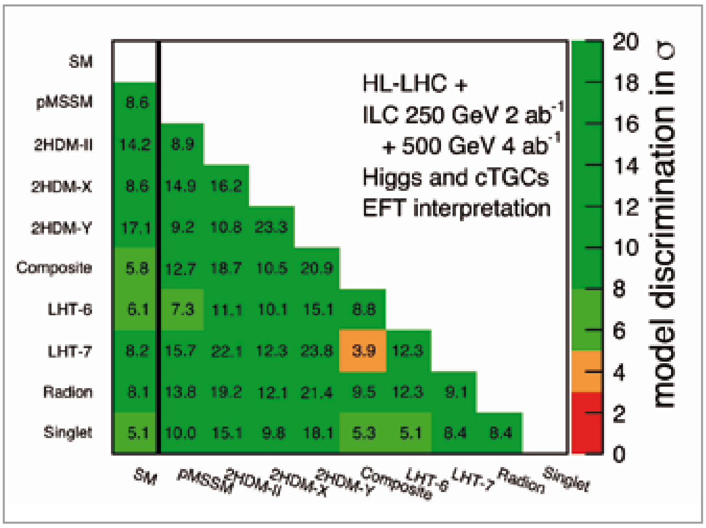

Figure 3

Same as Figure 2, but including the measurements expected from the 500 GeV stage of the ILC [2]

rate of "invisible" decays of the Higgs boson, for instance into dark-matter particles: If no such decays are observed at the ILC, their contribution must be less than 0.32% of all Higgs decays.

Probing beyond the Standard Model

Does it matter whether we know the properties of the Higgs boson to a precision of 1% or 5%? Yes, it does. As the LHC has so far not found other new particles beyond the Higgs boson, there are good reasons to assume that new particles are rather heavy. But the heavier the new particles are, the smaller their influence on the Higgs coupling will be. The 1–2% precision expected from the first stage of the ILC will enable us to probe significant new physics parameter space beyond the direct discovery reach of the LHC.

The DESY ILC group illustrated this potential by considering a variety of the most popular extensions of the Standard Model (SM) of particle physics. For each type of model, benchmark points were selected such that no new particle would be observed at the HL-LHC. In other words, they'd all look exactly like the SM in any HL-LHC measurement. If we compare the deviations of the Higgs couplings in these benchmarks from their SM values with the expected ILC precision, we can derive a significance (σ) for observing these deviations. For the 250 GeV stage of the ILC, the resulting significances for these benchmarks with respect to the SM and with respect to each other are displayed in Fig. 2. In particle physics, an effect with a significance larger than 3 (orange) is traditionally referred to as observation, while a significance larger than 5 (green) is required to claim a discovery.

Just a first step

While the initial 250 GeV stage of the ILC offers formidable physics prospects, it is only a first step towards the full programme including measurements at 500 GeV and even 1 TeV. The ability to extend the length of the accelerator and thereby increase the energy is an important feature of linear colliders.

Figure 3 shows how the significances in Fig. 2 will change when adding the 500 GeV Higgs coupling measurements. With the additional precision at 500 GeV, all example benchmarks will clearly be discoverable.

Most importantly, the extension of the ILC to 500 GeV (or beyond) will offer a whole new set of measurements, including the Higgs self-coupling, the top Yukawa coupling and of course a whole precision programme on the top quark, which has never been produced in electron–positron collisions before. The ILC at 250 GeV could be the first step on this journey.

Contact:

Jenny List, jenny.list@desy.de

References:

[1] Linear Collider Collaboration, arXiv:1711.00568.
[2] T. Barklow et al., Phys. Rev. D97, no.5, 053003 (2018).
[3] K. Fujii et al., arXiv:1710:07621.

Gas, foils and a big barrel.

A high-precision time projection chamber for future experiments

The international Linear Collider Time Projection Chamber (LCTPC) collaboration is developing a high-precision time projection chamber (TPC) for a future linear collider particle physics experiment. DESY is a key player in the development of a gas electron multiplier (GEM)-based readout system. In December 2016, a three-week-long test beam campaign with a large prototype TPC was performed at the DESY II Test Beam Facility. The analysis of the test beam data yielded promising results for the applicability of such a TPC in the final detector.

The physics programme at a future linear collider aims at high-precision measurements, which translates into the need for highly performant detectors, as e.g. the International Large Detector (ILD) concept. The tracking system has to provide a high resolution and excellent pattern recognition combined with a very low material budget. Implementing a TPC as the main tracker could fulfil these requirements. TPCs based on micropattern gaseous detectors can achieve a very good resolution and ensure excellent pattern recognition capabilities. In addition, a TPC allows for particle identification by measuring the specific energy loss *dE/dx*. Given that the sensitive volume consists of gas, TPCs can have a very low material budget.

The international LCTPC collaboration pursues R&D for such a TPC. DESY is a key player for the development of a readout using GEM foils, one candidate for the TPC readout. For these studies, a readout module with a design as foreseen for the final TPC is being developed.

In this step of the development, the main focus was on the construction techniques and the GEM foil flatness, which directly impacts the signal uniformity over the module area. To this end, special tooling was developed to ensure the flatness and the reproducibility of the GEM mounting. This resulted in a consistent improvement of the height deviations of the foil over the module area by almost a factor of 2.

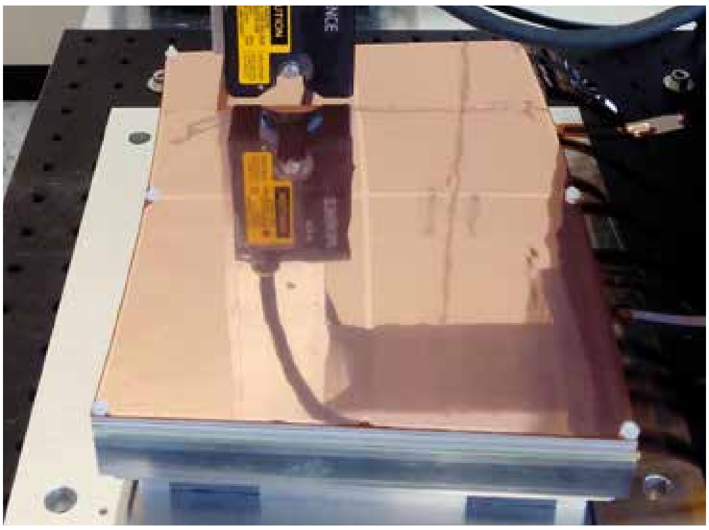

Figure 1

Fully assembled GEM readout module in the height profile measurement stand

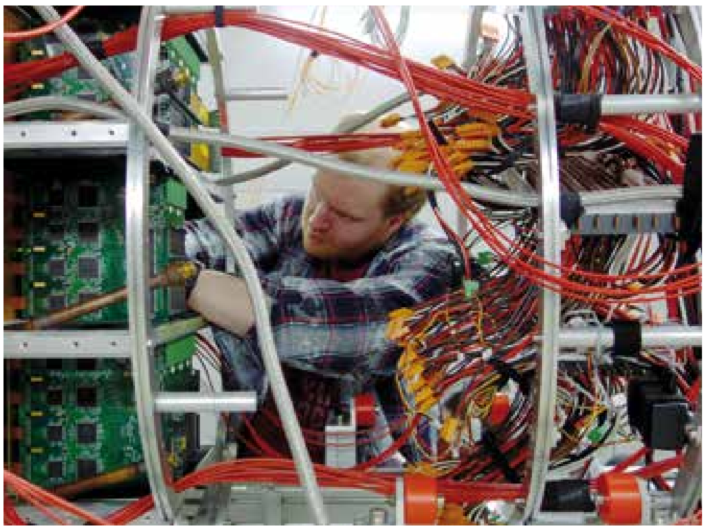

Figure 2

Mounting the TPC prototype readout electronics at DESY test beam area T24/1

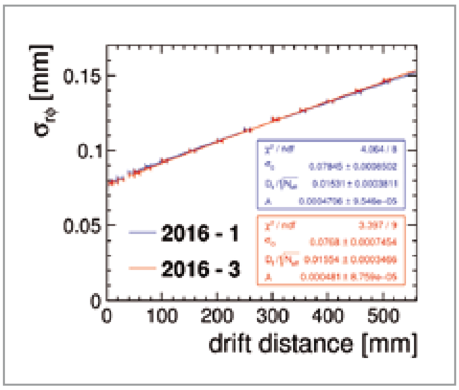

Figure 3

Point resolution of two measurement series with two weeks time in-between

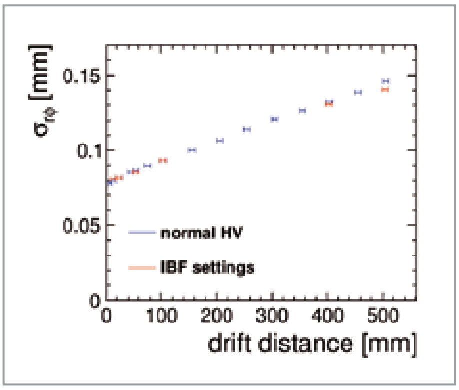

Figure 4

Comparison of point resolution of high-gain and minimal Ion back flow GEM settings

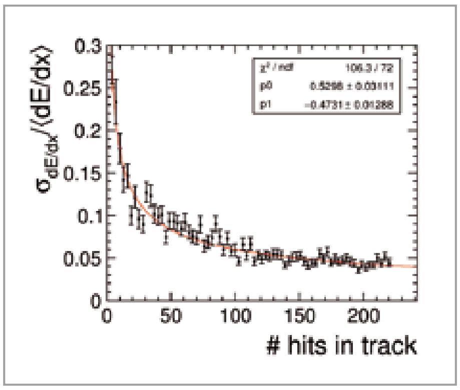

Figure 5

Extrapolation of the *dE/dx* resolution to a full-size TPC with 220 samples

Compared to the previous module generation, the RMS of the deviations shrank from 50–90 µm to 30–50 µm, which is well within the requirements. Figure 1 shows a fully assembled module in the height profile measurement stand.

Up to seven of these about 17 x 23 cm^2 large readout modules can be mounted into the end plate of a large TPC prototype with 75 cm diameter and 60 cm length. This prototype was developed for use at the DESY II Test Beam Facility. Here, together with the LCTPC collaboration and supported by the European EUDET and AIDA programmes, an extensive setup for gas detector tests was implemented, including a large-bore 1 T solenoid.

In December 2016, a three-week-long test beam campaign was performed using three of the GEM readout modules. Figure 2 shows the mounting of the readout electronics in the test beam area T24/1. In 400 measurement runs, 9.5 million events were recorded, including almost 6 million events measured with a half-a-radiation-length thick target in front of the prototype. The target was used to produce multitrack events from the single electron beam in order to study the pattern recognition and resolution of nearby particle tracks.

The spatial single-point resolution versus the drift length is shown in Fig. 3 for two measurements at the beginning and at the end of the test beam campaign, respectively. Both measurements agree very well, demonstrating the stability of the system. Scaling the results, obtained at 1 T, to the foreseen field of 3.5 T results (due to the lower electron diffusion in the gas) in a resolution below 100 µm, which is the requirement for the final TPC.

Figure 4 shows a resolution comparison between the GEM standard settings, which are optimised for high gain, and so-called minimal ion back flow (IBF) settings. The IBF settings are chosen such that only a minimal amount of the ions produced in the amplification stage flows back into the sensitive TPC volume [1]. This minimises distortions of the electric drift field caused by the positively charged ions. An important result for the final detector is that these settings don't deteriorate the spatial resolution.

As mentioned before, a TPC can be used to identify particles by measuring the specific energy loss. In a first test, this was done for the electron beam of the test beam facility. To extrapolate the results to the 220 samples, or hits, of the final TPC, shorter and longer tracks were composed out of the measured tracks of the prototype with 62 hits. The result is shown in Fig. 5, confirming that the envisaged *dE/dx* resolution of 5% can be reached in the final detector.

The analysis of the test beam campaign shows very promising results, confirming the applicability of a TPC for the main tracker in the ILD detector. Future development steps foresee the inclusion of an ion gate layer on the modules to suppress the back flow of ions into the sensitive volume to nearly zero.

Contact:

Ties Behnke, ties.behnke@desy.de
Ralf Diener, ralf.diener@desy.de

Reference:

[1] K. Zenker, DESY-Thesis-2014-044.

Small versus large.

Optimising a detector for the International Linear Collider

The International Linear Collider (ILC) is an electron–positron linear collider, which will in its first phase be operated at 250 GeV as a Higgs factory. It is planned to be built in Japan. The DESY FLC group plays an important role in the development of the International Large Detector (ILD) for the ILC. The design and optimisation of a modern particle physics detector would not be possible without sophisticated software tools and detailed simulation studies. DESY scientists are leading the design, development and application of the underlying software tools and have recently created two new detector models, one large and one small. Applying a novel technique, different calorimeter technologies are simulated in parallel. This allows the comparison of different choices for detector technologies and geometrical layouts with the same physics events.

Overview

The rich and unique physics programme planned for the ILC is imposing challenging requirements on the performance of a particle detector. The ILD detector is one of two detector concepts that have been developed to meet these challenges. It is optimised for "particle flow" (PFA) event reconstruction, which requires highly granular calorimeters and excellent track momentum resolution as well as the precise measurement of the track's impact parameter.

A yet unprecedented asymptotic transverse momentum resolution of 2×10^{-5} GeV^{-1} is required for the precise measurement of the Higgs mass in events where the produced Higgs boson is recoiling against a *Z* boson decaying into two muons. Excellent jet energy resolution is required for the many physics analyses that involve hadronic jets in the final state, such as Higgs branching ratio measurements. These also require very good heavy-flavour tagging capabilities provided through the impact parameter measurement. The ILD detector is a very mature detector concept, described in detail in the technical design report (TDR) [1]. The design also involves alternative technology proposals for some of the ILD subdetectors.

The TDR marks a milestone for the ILD detector but not the end of the road for R&D. An interesting question remains: Is it possible to find an alternative detector design that performs equally well but at lower cost? The main drivers of the cost are the large calorimeters inside the magnetic field and the surrounding coil. The ILD collaboration has started a new programme of detector optimisation that focuses on understanding the impact of reducing the detector size on the performance.

ILD simulation models in DD4hep

In order to study the effects of detector layout and subdetector technologies on the physics performance, very detailed models of the detector have to be defined in a suitable simulation model. The linear collider community has recently developed a new detector geometry toolkit called DD4hep [2], together with experts from CERN. DD4hep is a flexible, modular and generic software tool, which can be used for any particle physics detector and is also used by other future projects such as CLIC and FCC. DD4hep has been adopted

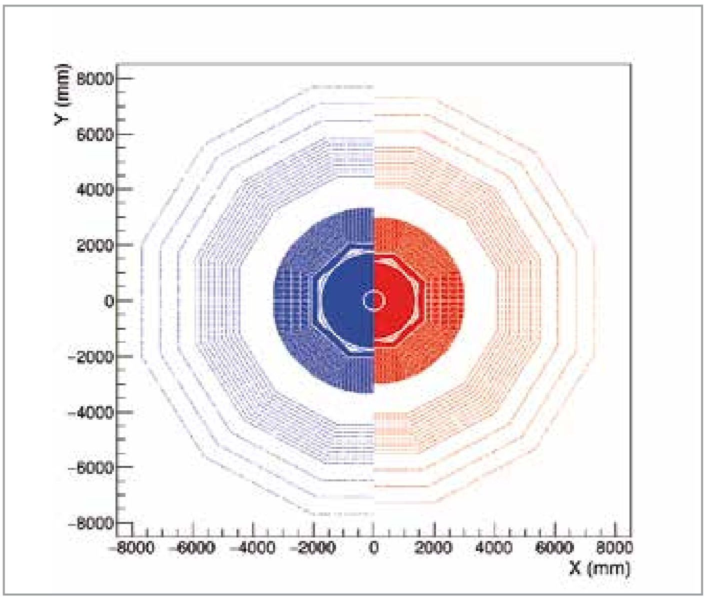

Figure 1

Simulated tracker and calorimeter hits in the large (blue) and in the small (red) ILD detector model, showing the dimensions of the geometrical layout of the two models

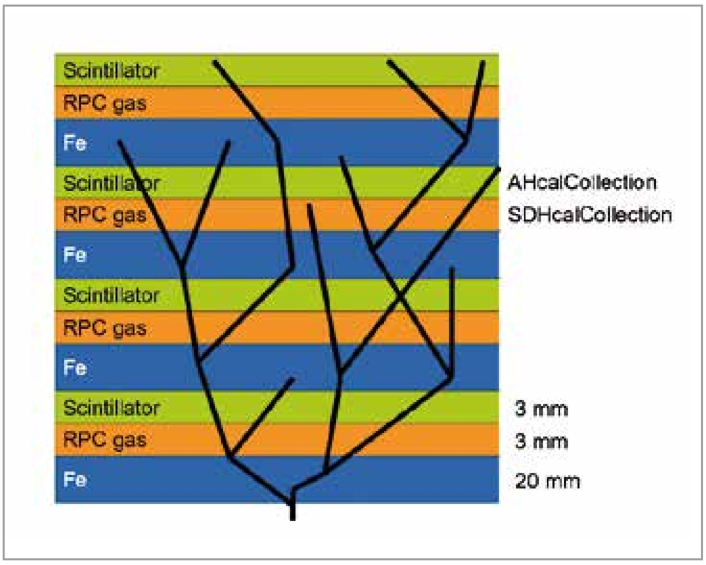

Figure 2

Schematic view of the multitechnology simulation model for the AHcal of the ILD. Two different technologies, the scintillator and the RPCs, are implemented in the stainless-steel absorber structure, allowing hits to be recorded for the same particle shower for both technologies.

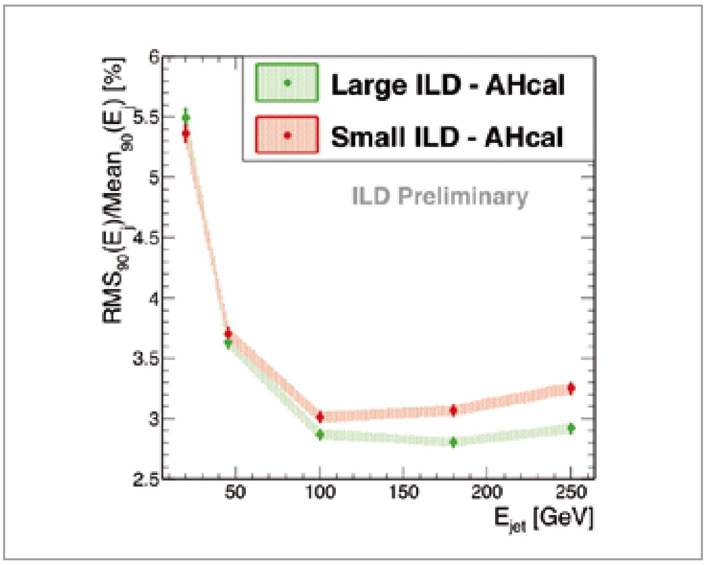

Figure 3

Jet energy resolution as a function of jet energy for the large and small ILD detector model using the AHcal technology option

by the HEP Software Foundation as one of its incubator projects, very much in line with the new paradigm in particle physics to increase the use and development of common software tools to address re-occurring common problems.

The ILD collaboration has created two different detector layouts in DD4hep, one with the original size and one with a reduced radius (Fig. 1). The collaboration will soon produce large Monte Carlo data sets in order to study the effect of the detector size on the performance with realistic physics analyses. As mentioned above, the ILD design also foresees several technology options for some of its subdetectors. In particular, there are two proposals for the main calorimeters: a silicon-based electromagnetic calorimeter (Si-Ecal) and an alternative using scintillator tiles (Sci-Ecal). Similarly, for the hadronic calorimeter, there is a scintillator-based analogue option (AHcal) and one that uses a semi-digital readout from resistive plate chambers (RPCs) (SDHcal).

Due to the required computing resources, it would be prohibitive to create large Monte Carlo data sets for all possible combinations of technology options and geometrical layouts. This issue is addressed by a novel technique that allows different technologies to be simulated at the same time – the multitechnology simulation. We achieve this by placing two different readout technologies and materials in between the absorber plates of the calorimeters, as is shown in Fig. 2 for the Hcal.

When a particle showers in the calorimeter, we record hit collections for both technologies at the same time. Detailed studies have shown that the resulting shower properties are equivalent to those achieved with stand-alone simulation models, where only one sensitive layer is used with additional electronics and services in the gap. With this novel technique, it will be possible to compare different technology options based on the exact same physics events.

First results and future studies

The complete software chain from the simulation over reconstruction to the analysis of detector performance benchmarks is currently being finalised and will very soon be frozen for the planned large-scale production.

A preliminary result for one important benchmark, the jet energy resolution, is shown in Fig. 3 for the large and small model. It shows that both detectors have a similar performance with some visible advantages of the larger model at higher energies.

Many more important comparisons are planned for the remainder of 2018 with the goal to better understand the cost vs. performance dependency and to ultimately decide on the size of the ILD detector.

Contact:

Frank Gaede, frank.gaede@desy.de

References:

[1] T. Behnke et al., arXiv:1306.6329.

[2] M. Frank, F. Gaede, C. Grefe, P. Mato, J. Phys. Conf. Ser. 513 022010 (2014).

ALPS II and axions move ahead.

DESY might become world-leading centre for axion searches

In 2017, the ongoing preparations for the ALPS II experiment at DESY by the Any Light Particle Search collaboration again met major milestones. In addition, two international collaborations working on other proposals to search for axions, IAXO and MADMAX, were formally founded at meetings at DESY. Both experiments could well be located at DESY in Hamburg.

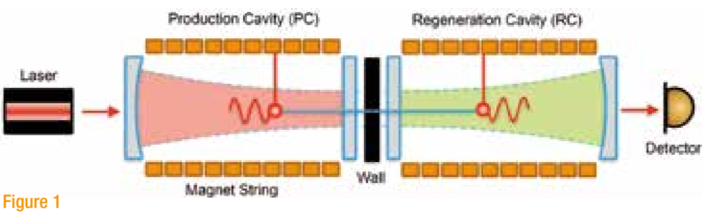

Figure 1

Schematic layout of the ALPS II experiment

The ALPS II experiment at DESY aims for generating and detecting axion-like particles and other so-called weakly interacting slim particles (WISPs) using the light-shining-through-a-wall (LSW) technique. Figure 1 shows a schematic sketch of the ALPS II setup: Light circulates inside a 100 m long optical resonator surrounded by ten modified dipole magnets from the former HERA proton accelerator. Through interaction of light with the magnetic field, axion-like particles might be produced, which could easily penetrate the light-tight wall shielding the second compartment of ALPS II. Here, axion-like particles might interact with the magnetic field to convert back to photons, giving the impression of light shining through the wall. The main experimental challenges refer to the proper modification of the HERA dipole magnets, the construction of two well-aligned and mode-matched optical resonators and the detection of extremely low photon fluxes.

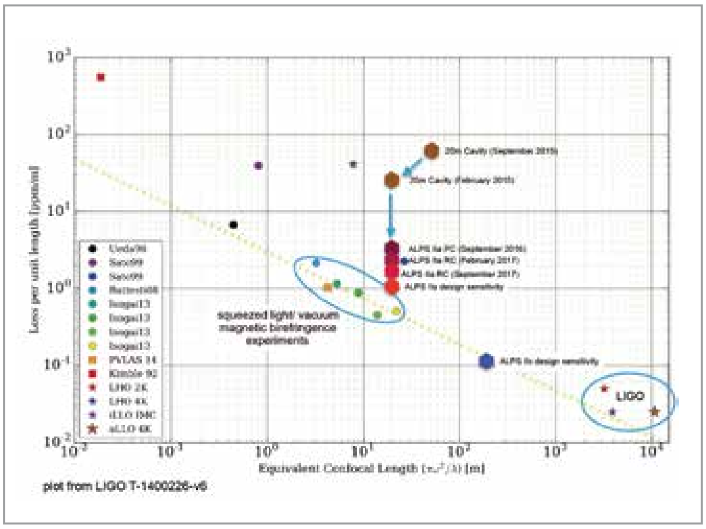

Figure 2

Comparison of the performance of optical resonators worldwide. The loss per unit length is displayed as a function of the equivalent confocal length. ALPS II has now nearly reached its specifications.

In 2017, the process of modifying the dipole magnets from the HERA accelerator so as to increase the horizontal aperture to the one required by ALPS II gained considerable speed. By the end of the year, seven magnets had been straightened successfully without any failure. The production rate approached the goal of one magnet per month.

The optics for ALPS II is being developed in a dedicated 20 m long laboratory in the HERA West hall at DESY. The major achievements are summarised in Fig. 2, which presents the worldwide performance of long-baseline optical resonators. The figure is adopted from the LIGO collaboration and displays the losses inside an optical resonator per length as a function of the length. In 2017, ALPS II nearly reached the empirical frontier indicated by the dotted line. With improved mirrors (see discussion in *DESY Particle Physics 2016*), it is expected to reach the goals labelled “ALPS IIa” (for the 20 m long system) and “ALPS IIc” (for the 200 m long installation in the HERA tunnel).

Another crucial milestone was reached by length-locking the regeneration cavity (RC, Fig. 1). To compensate for the ambient seismic noise, either the length of a cavity or the

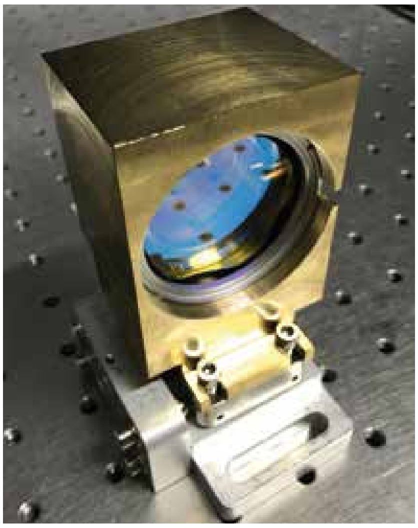

Figure 3

Custom-made piezo actuator moving the RC end mirror. The design shifts the first mechanical resonance to 6.3 kHz.

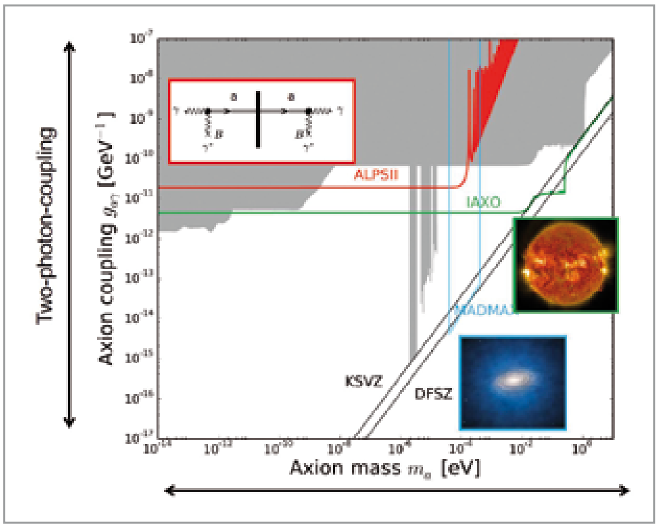

Figure 4

Parameter space for axion-like particles and reach of ALPS II (light-shining-through a wall), IAXO (looking for solar axion-like particles) and MADMAX (looking for axionic dark matter). "KSVZ" and "DSFZ" denote parameter lines for particular well-motivated axion models explaining the CP conservation of QCD. Note that ALPS II will probe for axion-like particles in a model-independent fashion, while IAXO relies on astrophysical assumptions and MADMAX on cosmological models.

wavelength of the circulating light have to be constantly adapted to meet the resonance condition. While for the production cavity this is realised by feeding back on the laser frequency, the RC has to rely on a length control. For this purpose, the ALPS collaboration constructed a piezo actuator moving the RC end mirror (Fig. 3), which was shown to fulfil all the requirements of ALPS IIc [1].

While ALPS II aims for starting the first data run in 2020, the worldwide interest in axions and axion-like particles is strongly rising, and more groups engage in plans for corresponding future international experiments. Due also to the visibility of ALPS II, two major international initiatives met at DESY to formally found collaborations. The first one took place in July 2017, when collaboration partners for the International Axion Observatory (IAXO) gathered in Hamburg. IAXO will search for axions and similar particles produced in the sun [2]. A first prototype could be ready in 2021, and DESY has offered to host the IAXO experiment. Moreover, in October 2017, the MAgnetized Disc and Mirror AXion (MADMAX) collaboration was founded in a meeting at DESY. MADMAX [3] aims for detecting axions as components of the dark matter all around us and would be located next to ALPS II in the HERA North hall.

ALPS II, IAXO and MADMAX would perfectly complement each other. All three will reach sensitivities significantly beyond present-day experiments and tackle the most promising parameter regions derived from theory and astrophysical considerations. Their sensitivities are compared in Fig. 4.

Over the last years, observational hints have been accumulating from astrophysics, pointing to the existence of excessive energy losses of stars in different stages of their evolution (red giants, helium-burning stars, white dwarfs) beyond the ones accounted for by neutrino emission. Intriguingly, these anomalies can be explained in a unified manner by the existence of a sub-keV-mass axion-like particle with a coupling to both electrons and photons. In 2017, a three-sigma hint for this hypothesis was established with DESY participation [4] (Fig. 5). The existence of such an axion-like particle can be probed both by ALPS II, if the mass is below 0.1 meV, and by IAXO, if it is below 10 meV.

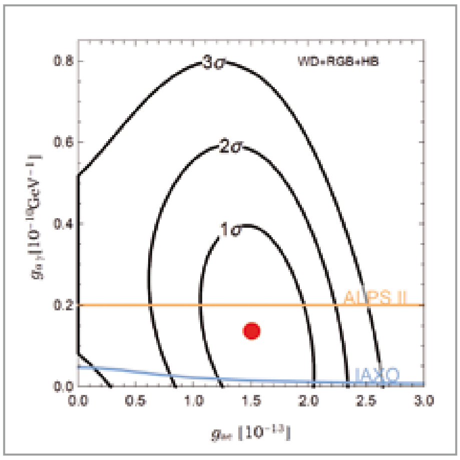

Figure 5

Combined analysis of the observational hints on excessive energy losses of white dwarfs (WD), red giant branch (RGB) and helium-burning (HB) stars in the parameter plane spanned by the photon and electron coupling of an axion-like particle [4]

Contact:

Axel Lindner, axel.lindner@desy.de
Andreas Ringwald, andreas.ringwald@desy.de

References:

[1] J. H. Põld, A. D. Spector, arXiv:1710.06634 [physics.ins-det].
[2] http://iaxo.web.cern.ch
[3] B. Majorovits et al., arXiv:1712.01062 [physics.ins-det].
[4] M. Giannotti, I.G. Irastorza, J. Redondo, A. Ringwald and K. Saikawa, JCAP 10, 010 (2017), [arXiv:1708.02111 [hep-ph]].

Astroparticle physics.

Astroparticle physics at DESY spans a broad range of topics, from theoretical studies to a plethora of experimental activities. Of these, the Cherenkov Telescope Array (CTA), the next-generation gamma-ray observatory, is currently the largest endeavour. The DESY CTA group is instrumental in numerous crucial aspects of the experiment, from software to telescope development (p. 47) and analysis of the physics case (p. 46).

DESY has extensive experience in gamma-ray astronomy. The research centre is an important contributor to the H.E.S.S. telescope system in Namibia, the first of the second generation of experiments in this field. In 2017, H.E.S.S. observed for the first time gamma rays from two massive stars orbiting each other (p. 48). Moreover, the analysis of data from the Fermi Gamma-Ray Space Telescope allowed enough information to be collected to compile a first gamma-ray novae catalogue (p. 51). Gamma-ray measurements continue to be one of the main probes of the universe, enabling studies of the intergalactic magnetic field (p. 50) and even of models of nuclear physics (p. 55). These experimental activities are supported by theoretical studies on shock acceleration of particles (p. 54).

The second major field of experimental activities in astroparticle physics is neutrino physics. DESY is strongly involved in the IceCube neutrino telescope at the South Pole, which continues to deliver high-quality data (p. 52).

Several new DESY research groups obtained third-party funding. Walter Winter was awarded a European Research Council (ERC) Consolidator Grant to study neutrinos and the origin of cosmic rays (p. 56). Two new Helmholtz Young Investigator Groups were granted for performing multimessenger observations of high-energy neutrinos (Anna Franckowiak, p. 57) and dark-matter searches with CTA (Elisa Pueschel, p. 58).

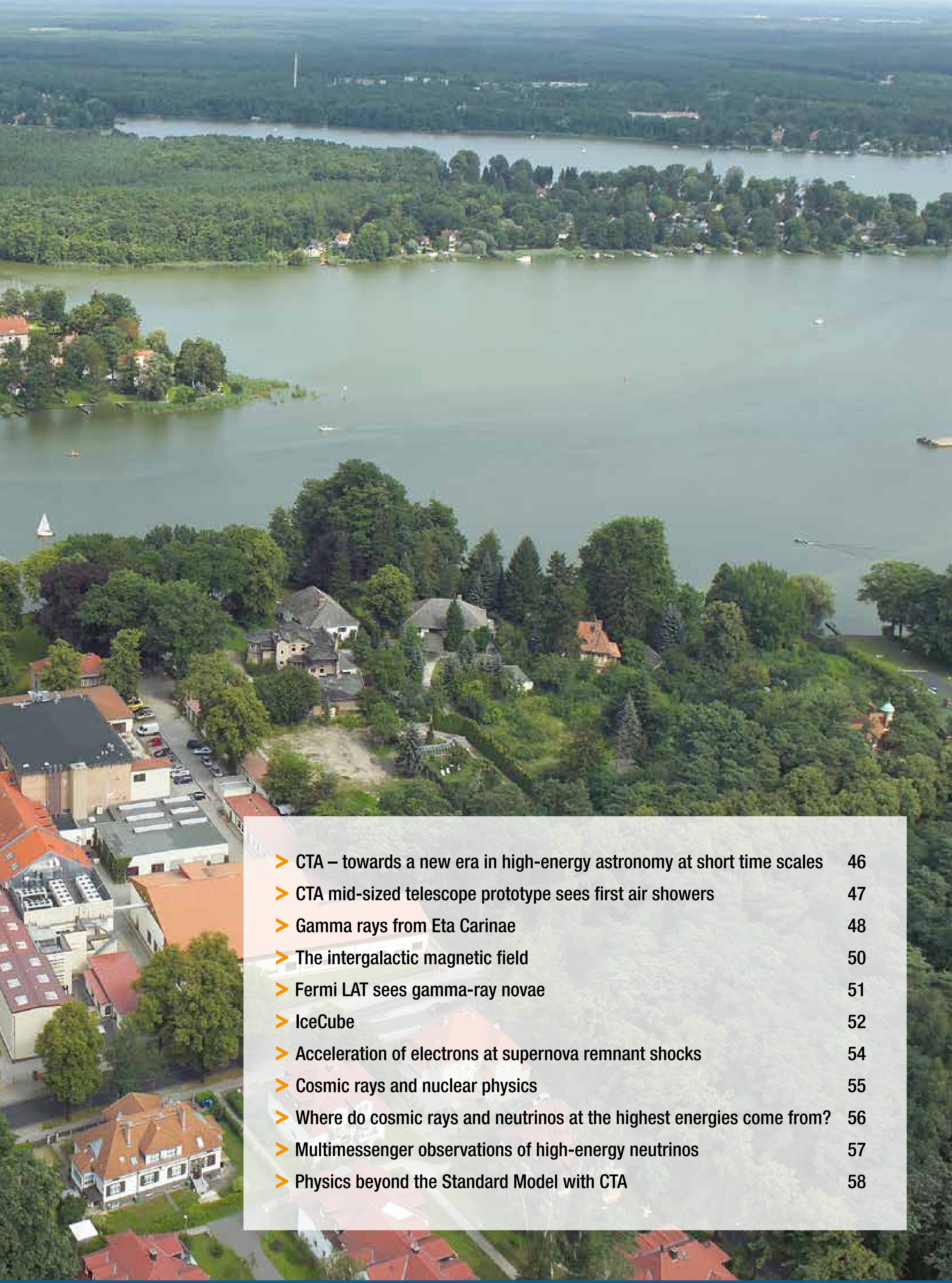

CTA – towards a new era in high-energy astronomy at short time scales.

How to catch short gamma-ray flares

The Cherenkov Telescope Array (CTA) is the next-generation gamma-ray observatory, built by a worldwide consortium with DESY among the key contributors. CTA will observe the highly active non-thermal universe at energies above 20 GeV with unprecedented clarity and sensitivity, especially for transient phenomena.

Variable phenomena on time scales from milliseconds to months are observed from many astrophysical objects, with telescopes covering the electromagnetic spectrum from radio waves to gamma rays, but also using neutrinos and gravitational waves. Sources explode or flare up, often in unpredictable ways, mostly in connection with catastrophic events, such as stellar collapses, and extreme environments, such as strong gravitational fields, fast spinning objects and huge magnetic fields. "High-speed" astrophysics is thus of great scientific interest.

Our view of the transient universe will change in the near future with the advent of the CTA gamma-ray observatory and the coordination of CTA observations with other instruments, such as the Large Area Telescope (LAT) on board the Fermi Gamma-Ray Space Telescope, the Zwicky Transient Facility (ZTF) wide-field optical telescope in California and the IceCube neutrino observatory at the South Pole. DESY is a key partner in all these observatories. The transient physics programme for CTA is a direct continuation of DESY's contributions to transient programmes in the H.E.S.S., MAGIC and VERITAS collaborations. Cooperation of CTA with big observatories in other wavelengths bands, such as ALMA and SKA, is also planned.

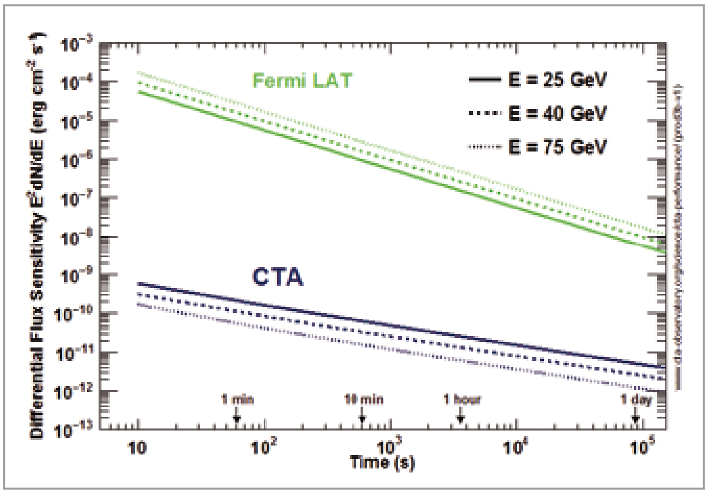

Figure 1

Differential flux sensitivity of CTA at selected energies as a function of observing time in comparison with the Fermi LAT instrument [1]

In extensive simulations, the CTA collaboration has now quantified the performance figures for CTA [1]. They show that CTA provides dramatic improvement in sensitivity compared to Fermi LAT for transient objects at different time scales (Fig. 1). CTA is so much better because of the much larger effective detector size for gamma rays (10^4–10^5 m^2), improved background rejection and imaging quality. The sensitivity of CTA at the lowest energies is provided by large-sized telescopes (23 m mirror diameter), which can rotate in less than 30 s to any point in the sky. The mid-sized telescopes (MSTs, developed at DESY) provide drastic improvement in imaging quality, effective detector area and field of view. They can be directed to any point of the sky in less than 90 s. Their seven-degree field of view allows efficient follow-up of transient alerts with large positional uncertainties. Transient alerts will be issued and received in near real time from any astronomical observatory through automatic alert pipelines in the CTA observation execution system software (designed mostly by DESY).

Contact:

Gernot Maier, gernot.maier@desy.de

Reference:

[1] https://www.cta-observatory.org/science/cta-performance

CTA mid-sized telescope prototype sees first air showers.

Successful test for CTA

The mid-sized telescope (MST) developed at DESY is the work horse of the Cherenkov Telescope Array (CTA). In total, 40 telescopes of this type will be built for the final setup. They will provide the best sensitivity between 100 GeV and 10 TeV, which is the core energy region of gamma-ray astronomy with Cherenkov telescopes.

In September 2017, an important milestone was reached on the way to constructing the CTA gamma-ray observatory. In order to form a fully functioning telescope, a complete FlashCam camera from MPIK in Heidelberg was placed on the MST prototype built by DESY in Berlin Adlershof. Function tests of the complete system were conducted, and already in the next night, the MST's powerful 12 m diameter eye was directed towards the sky, successfully recording its first Cherenkov light from air showers. By focusing the Cherenkov light from the relativistic shower particles onto the camera, a first shower image emerged (Fig. 1).

The test campaign proceeded, verifying the interfaces and integration procedure of the telescope and camera, the mirror alignment procedures and the routine and remote operation of the telescope and camera. Every component performed as expected, with the system integration proceeding smoother than anticipated. After six successful weeks, the camera was unmounted and returned to Heidelberg for further lab testing. The MST structure will be operated and tested for another year in Berlin. Integration and test of a French NectarCAM, the second camera proposed for the MSTs, are in preparation and planned for the second half of 2018.

Contact:
Markus Garczarczyk, markus.garczarczyk@desy.de

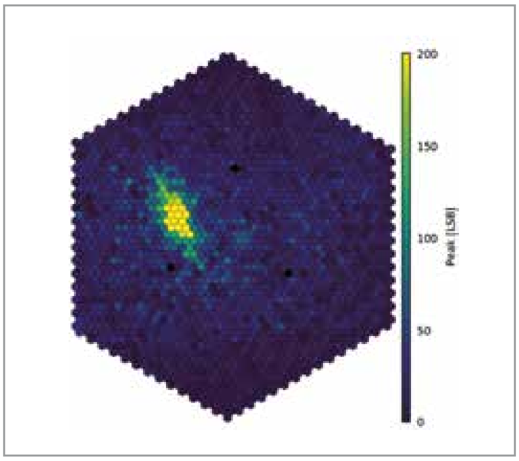

Figure 1

Left: Fully functional 12 m MST prototype in Berlin Adlershof. Right: Cherenkov light image of an air shower in the 2048 pixel FlashCam.

Gamma rays from Eta Carinae.

… and follow-up of a neutron star merger with H.E.S.S.

In a most challenging measurement with the telescopes of the High Energy Stereoscopic System (H.E.S.S.), a gamma-ray observatory in Namibia, very high-energy (VHE) gamma rays were detected for the first time from two massive stars orbiting each other. The system, called Eta Carinae, is a colliding-wind binary and emits gamma rays up to ~1 TeV. It is the first source of a new class and allows the study of particle acceleration in the extreme environment around massive stars.

Observing a late stage in the life of a massive star is of great importance to understand stellar evolution, in particular how massive stars enrich their surroundings with dense gas, which the supernova formed by the exploding star will eventually plough through, thereby accelerating particles. Eta Carinae is composed of a luminous blue variable star of ~100 solar masses and a companion of ~30 solar masses orbiting its more massive companion in a very eccentric orbit.

The stars drive fast (500–3000 km/s) and dense stellar winds. Where these winds hit each other, they form a colliding-wind region, in which charged particles can be accelerated. Although Eta Carinae was not predicted to be a gamma-ray emitter, the space-based Fermi Large Area Telescope (LAT) found it to be a strong gamma-ray source at GeV energies. The Fermi Gamma-Ray Space Telescope has observed Eta Carinae for years and established the gamma-ray emission to be variable and extending up to ~100 GeV.

With its much larger detector area for energies beyond 100 GeV, the H.E.S.S. gamma-ray observatory is perfectly suited to search for those gamma rays from Eta Carinae –

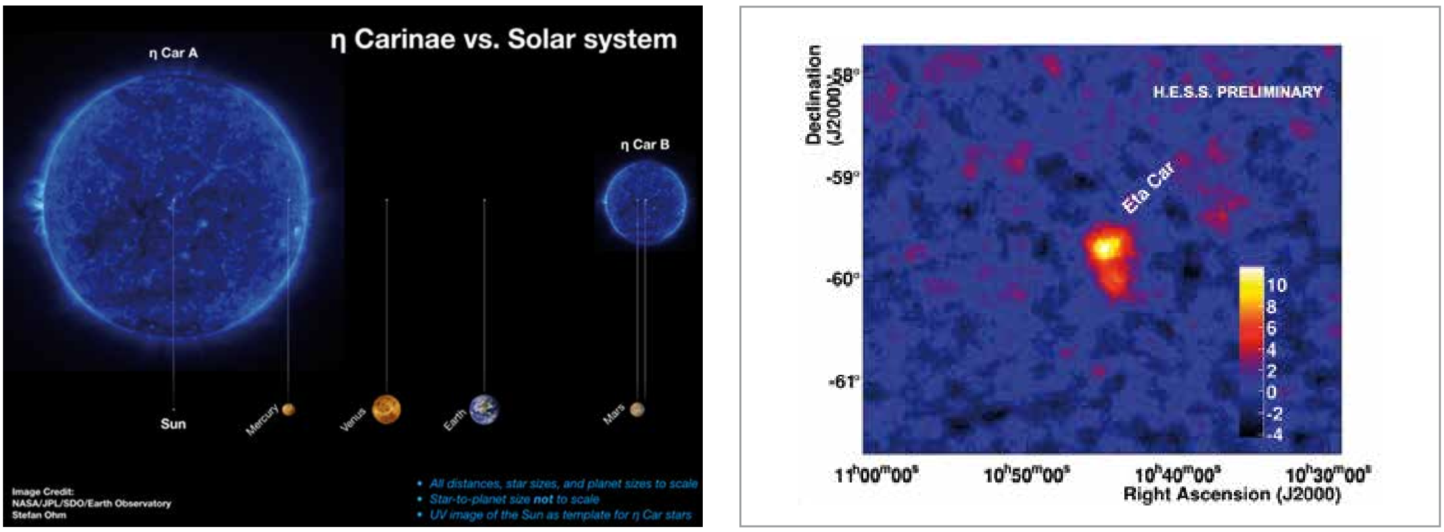

Figure 1

Left: Illustration of the size of Eta Carinae during periastron, compared to the solar system (bottom). Right: Preliminary H.E.S.S. gamma emission of Eta Carinae near periastron.

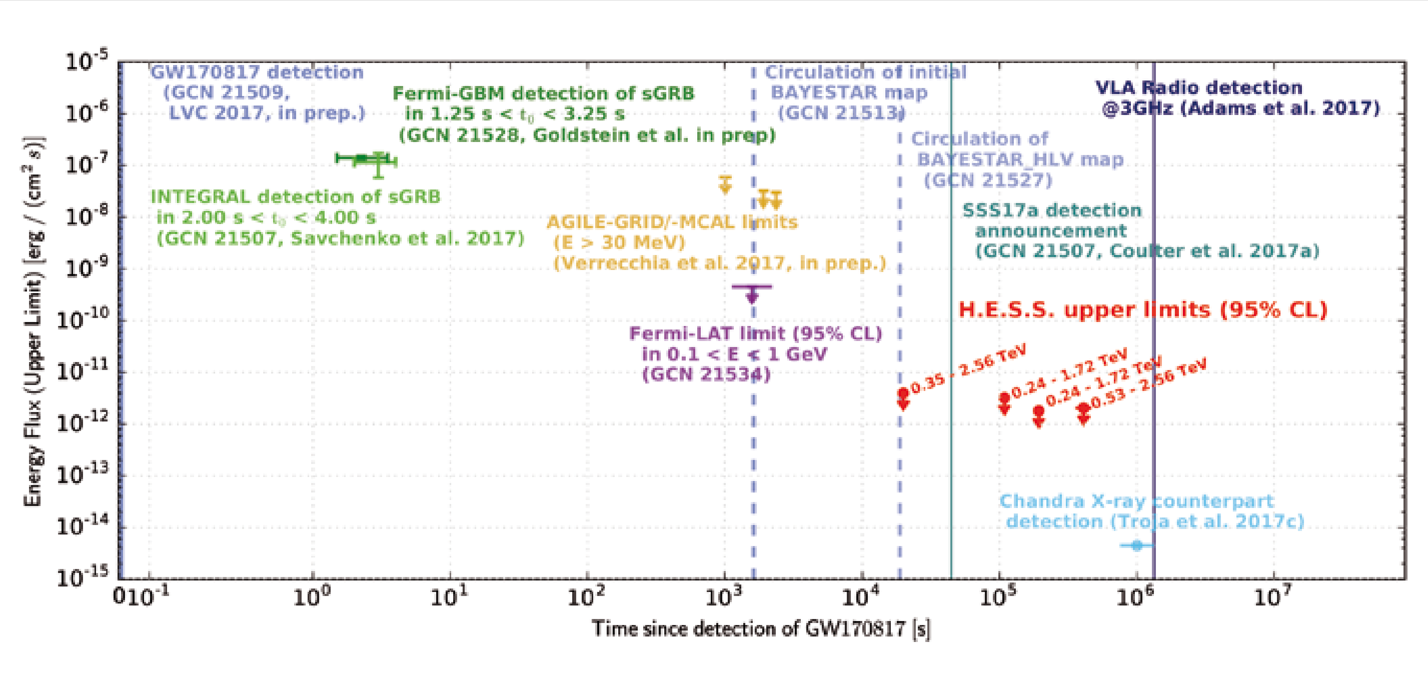

Figure 2

Observations of the gravitational-wave event GW170817 seen by LIGO and VIRGO and follow-up observations by different telescopes

there is just one problem. The optical and ultraviolet light of the Carina Nebula, which surrounds Eta Carinae, is so bright that Cherenkov telescopes randomly record this night sky background. Scientists from DESY and the University of Potsdam in Germany therefore modified the H.E.S.S. data taking, calibration and data analysis to deal with this background, eventually detecting Eta Carinae at very high energies (Fig. 1). The H.E.S.S. data set covered the time when the stars are closest to each other (periastron). The detection established colliding-wind binaries as a new class of VHE gamma-ray sources [1].

Scientists from DESY and the University of Potsdam implemented a new functionality that allows the H.E.S.S. telescopes to automatically receive, process and follow up on alerts from telescopes worldwide – including alerts about merger events detected by gravitational-wave observatories, which also emit electromagnetic radiation (first seen in 2017).

The non-thermal universe is not as quiet and steady as it appears to the human eye. Particle acceleration often occurs in the vicinity of fast-rotating neutron stars, or of black holes and collapsing massive stars that launch jets of plasma into their surroundings. The universe is thus highly variable. New instruments using X-ray, radio and optical wavelengths, but also neutrinos and gravitational waves give scientists increasing access to such transient phenomena, opening up completely new channels for the study of the most violent phenomena in the cosmos.

The DESY H.E.S.S. group implemented a prompt transient alert and follow-up system that efficiently deals with the fast reception, filtering and processing of alerts from survey instruments in space and on the ground from around the world, allowing for the fastest possible response of H.E.S.S. to short-lasting phenomena such as gamma-ray bursts [2].

When the LIGO/VIRGO collaboration issued the alert for their first-ever detected neutron star merger (GW170817), thanks to its location in Namibia and the vigilant shift crew, H.E.S.S. was the first ground-based instrument to follow up on the event (Fig. 2). Although H.E.S.S. did not detect gamma-ray emission [3] in this case, the scheduling and data taking worked perfectly. The event represented a perfect test for future alerts and recommended the H.E.S.S. real-time follow-up system also for the upcoming Cherenkov Telescope Array (CTA) gamma-ray observatory.

Contact:

Stefan Ohm, stefan.ohm@desy.de

References:

[1] H.E.S.S. Source of the Month, August 2017: Eta Carinae.
[2] The H.E.S.S. prompt alert and follow-up system, to be published.
[3] Abdallah, et al. (H.E.S.S. Collaboration), ApJ Letters 850, 2 (2017).

The intergalactic magnetic field.

Tracing activity in the early universe

Gamma-ray astronomy provides a means of probing the strength and structure of the intergalactic magnetic field (IGMF), an extremely weak magnetic field that exists in the voids between galaxies. This field is of particular interest for cosmology, as it may have been generated just after the big bang. Alternatively, it may have been produced much later in the evolution of the universe, e.g. during galaxy formation. Its measurement could thus provide important insight into the evolution of the universe.

As predictions for the strength and correlation length of the IGMF differ for the two cases, measurements determining these values will help decide between the models of how the IGMF is generated. Measuring the extremely weak field is an experimental challenge, but observations of distant gamma-ray emitters make it possible to probe a theoretically interesting range of IGMF strengths. As gamma rays travel from distant emitters to Earth, they interact with ambient photon fields *en route*: First, they scatter off photons of the extragalactic background light to produce electron–positron pairs, which then collide with lower-energy photons of the cosmic microwave background, upscattering them to higher energies. The energy of the initial photons is thus reprocessed to lower energies in a cascade process. The IGMF bends the charged electron and positron trajectories, giving the cascade emission a broader angular profile than the one of gamma rays that make it to Earth with no bending.

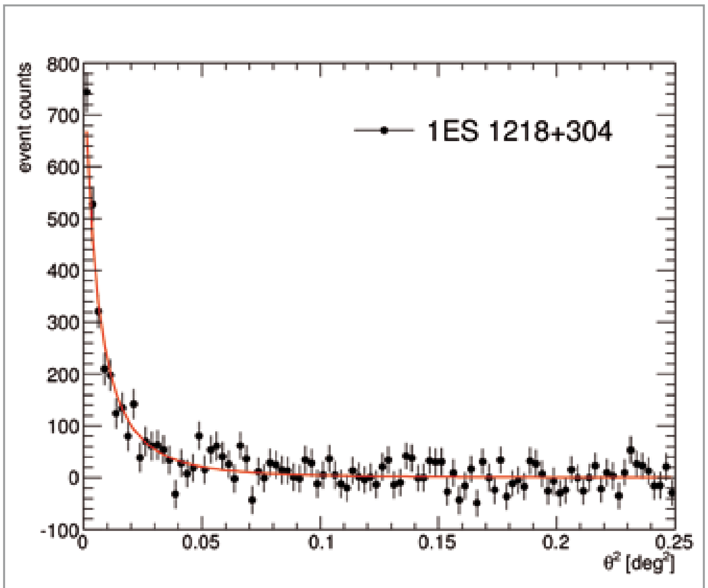

Figure 1

Angular profiles (measured and expected) of gamma rays from blazar 1ES 1218+304

Members of the DESY VERITAS group analysed observations of seven distant gamma-ray emitters above 160 GeV to search for “halos” showing broadening due to interaction with the IGMF. Source selection is key: Sources must be far enough from Earth for a cascade to develop. The angular profiles of the sources were compared with predictions from simulation (see Fig. 1 for the blazar 1ES 1218+304), assuming an angular extension only due to the instrument’s angular resolution and no broadening due to the IGMF (red line). In all cases, the angular profiles of the gamma-ray sources showed good agreement with simulated point sources. In the absence of broadening, it was possible to rule out a window of IGMF strengths of around 10^{-14} Gauss for a reasonable assumption of the correlation length (1 megaparsec). While current instruments are limited by their angular resolution and gamma-ray flux sensitivity, the upcoming Cherenkov Telescope Array (CTA) will be able to either detect or set more stringent constraints on the IGMF.

Contact:

Elisa Pueschel, elisa.pueschel@desy.de

Reference:

[1] Archambault et al, ApJ 835, 288 (2017).

Fermi LAT sees gamma-ray novae.

First novae catalogue

Novae are runaway thermonuclear explosions on the surface of a white dwarf in a binary system that accretes matter from its stellar companion (Fig. 1). This causes a sudden increase in brightness (i.e. the appearance of a bright "new" star), which slowly fades over several weeks or even months. The DESY Fermi group developed a unified analysis method to find gamma-ray novae in data of the Large Area Telescope (LAT) on board the Fermi Gamma-Ray Space Telescope.

In 2010, for the first time, gamma-ray emission (>100 MeV) was discovered from the Nova V407 Cygni in data of the Fermi LAT [1]. This particular nova exploded in a binary system of a white dwarf accompanied by a red-giant star. In that case, high-energy particles can be accelerated in a blast wave driven by the high-density circumstellar wind of the red giant. Surprisingly, Fermi LAT discovered more gamma-ray novae in the following years, also mostly classical novae with a main-sequence star companion instead of a red giant [2].

For better understanding, the DESY Fermi group analysed a larger sample of novae using the latest Fermi LAT data set (Pass 8) and compiled a catalogue of 75 optically detected galactic novae recorded during the Fermi mission (Fig. 2). Based on the six previously detected gamma-ray novae, we developed a unified analysis method, which was then applied to all novae in the sample [3]. The new analysis correctly identified the six previously detected novae and found indications for two new novae candidates. Thus, not all novae are gamma-ray emitters. The gamma-emitting ones require special features, yet to be identified.

Contact:
Anna Franckowiak, anna.franckowiak@desy.de

References:
[1] A. A. Abdo et al. (Fermi-LAT Coll.), Science 329, 817, 2010.
[2] M. Ackermann et al. (Fermi-LAT Coll.), Science 345, 554–558, 2014.
[3] A. Franckowiak, P. Jean, M. Wood, C. C. Cheung, S. Buson, A&A 609, A120, 2018.

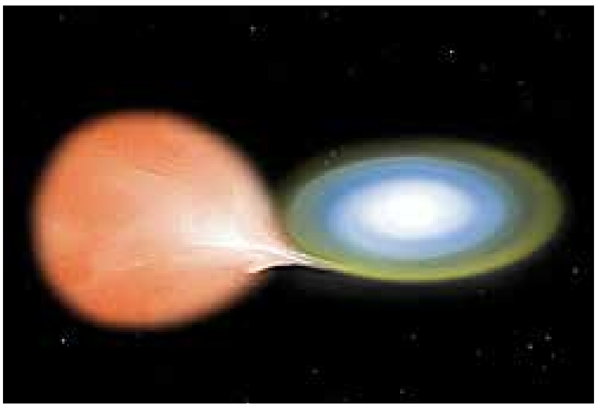

Figure 1

Artist's conception of a binary star system, consisting of a white dwarf accreting hydrogen from a larger companion.

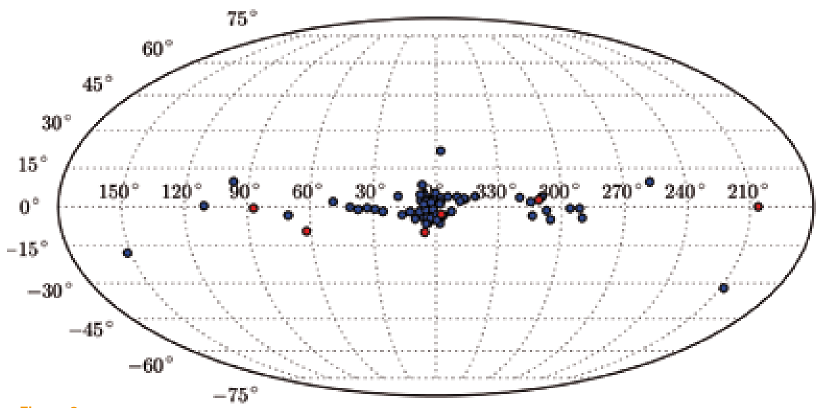

Figure 2

Spatial distribution in galactic coordinates of 75 novae (red and blue) optically detected from the start of the Fermi mission in August 2008 to the end of 2015. Previously seen gamma-ray novae are marked in red [3].

IceCube.

Searching for neutrino sources and tau neutrinos

DESY plays a leading role in the operation and data analysis of the world's largest particle detector, the IceCube neutrino observatory at the South Pole. In the last years, the DESY IceCube group worked on studies of supernovae as sources of the diffuse neutrino flux, the setup of a real-time follow-up programme linking observatories around the world and the search for tau neutrinos.

Searching for supernova neutrino sources

After IceCube discovered a diffuse flux of high-energy cosmic neutrinos in 2013 [1], the origin of those neutrinos is still unknown. Prime candidates are powerful stellar explosions. In the most extreme case of stellar death, the stellar core collapses to a black hole, which rapidly accretes material forming a relativistic jet. Those jets are detected thanks to extremely bright, short flashes of gamma rays outshining the entire universe for a few seconds.

Gamma-ray bursts (GRBs) were among the prime candidates for sources of high-energy neutrinos, but are largely ruled out now because too few neutrino events show a coincident gamma-ray emission [2]. However, GRBs might be just a small part among a much larger population of "failed" GRBs, so called "choked-jet supernovae", which could potentially produce the measured neutrino signal. A certain class of GRBs is associated with Type Ic supernova explosions, which could be the only signature of failed GRBs. In addition to choked-jet supernovae, supernovae that explode in a dense circumstellar medium are promising neutrino source candidates [3]. In that case, the supernova ejecta collide with the dense medium and can thereby produce high-energy particles (Fig. 1).

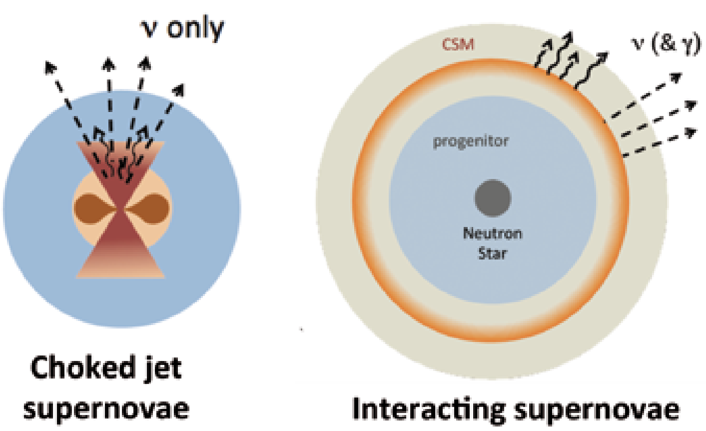

Figure 1

Illustration of supernovae with a choked jet (left) and supernovae that explode in a dense circumstellar medium with which the supernova ejecta can interact (right)

The DESY IceCube group compiled a catalogue of ≈1000 supernovae, detected in the optical range since the start of IceCube operation, and searched for spatial and temporal coincidences with high-energy neutrinos. No significant excess of neutrinos from the supernova directions was found, limiting the contribution of supernovae to the measured diffuse neutrino flux to less than 50% [4].

Real-time follow-up programme

To increase the sensitivity to transient or variable neutrino sources, the IceCube collaboration set up a real-time neutrino search that alerts other observatories, which can then search for an electromagnetic counterpart to the neutrino signal. Interesting neutrino events are identified within seconds after their detection in the IceCube neutrino detector, and their direction is passed on to follow-up instruments around the

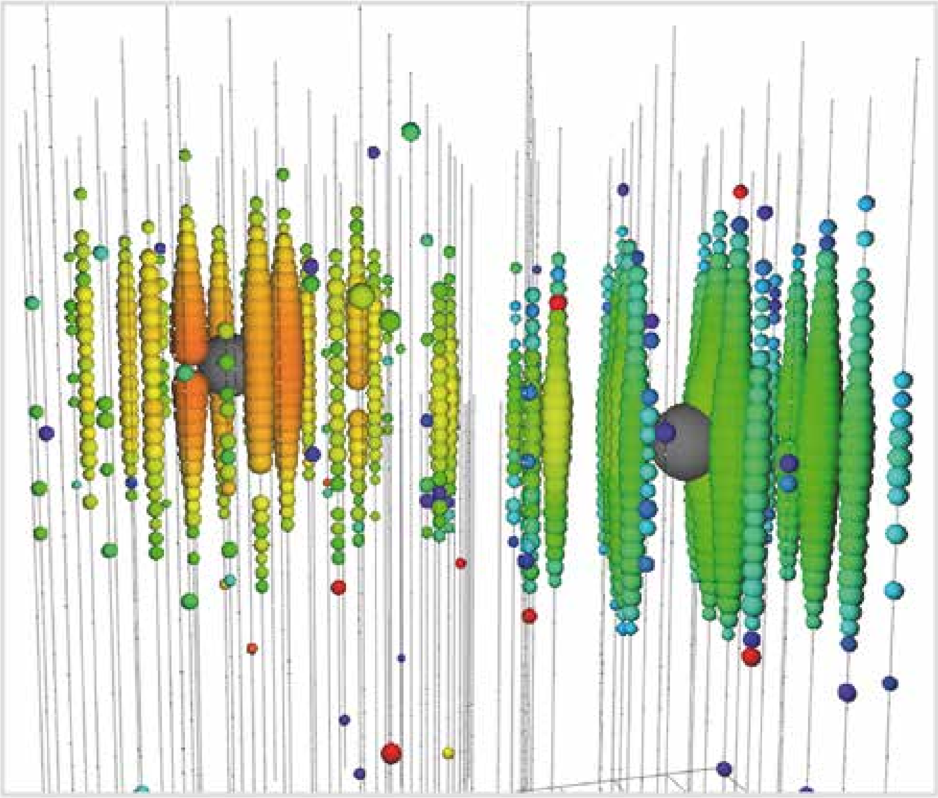

Figure 2

Simulated multi-PeV tau–neutrino interaction in IceCube. The two grey spheres indicate the generation and decay points of the tau lepton produced in the neutrino interaction.

world on the ground and in space [5]. Such interesting events are either single very high-energy neutrinos or neutrino multiplets, i.e. two or more neutrinos that arrive within a short time interval and could originate from the same direction.

On 17 February 2016, IceCube detected the most significant multiplet since the start of the follow-up programme: three neutrinos consistent with the same point of origin appeared within 100 seconds. Following the alert, eight other observatories searched for associated electromagnetic radiation, from visible light up to gamma rays [6]. Such a neutrino triplet is expected to occur by chance only once in 13.7 years. This suggests that a nearby or extremely energetic source (e.g. a core collapse supernova, a gamma-ray burst or a flare of an active galactic nucleus) produced these three neutrinos.

Several ground-based optical observatories (ASAS-SN, LCO and MASTER) had been searching for emission at the time of the IceCube triplet alert and before. The Swift X-ray satellite observed the position of the neutrino triplet within a minute after its detection. Gamma-ray observatories (Fermi LAT, VERITAS and HAWC) looked for electromagnetic emission. All these observations failed to detect any electromagnetic radiation. The optical observations ruled out a nearby supernova, the X-ray telescopes excluded brighter-than-average GRBs and the gamma-ray observatories precluded active galactic nuclei. This work thus demonstrated the potential of follow-up programmes and multiwavelength and multimessenger astronomy.

Tau neutrinos

About 1/3 of astrophysical neutrinos are expected to be tau neutrinos. At energies above 100 TeV, they can produce a unique signature in IceCube. The Cherenkov light from the hadron shower generated with the tau lepton in the neutrino interaction can be separated from the particle shower through its decay (Fig. 2). A new analysis by a DESY PhD student [7] improved the identification potential for these events by about a factor of two. The student analysed six years of IceCube high-energy neutrino events. About two tau neutrinos were expected, but none was found. While this is still compatible with fluctuations, the analysis has greatly increased the potential to identify the first cosmic tau neutrinos in the near future.

Contact:

Anna Franckowiak, anna.franckowiak@desy.de
Markus Ackermann, markus.ackermann@desy.de

References:

[1] M.G. Aartsen (IceCube Collaboration), Science 342, 1242856 (2013).
[2] M.G. Aartsen (IceCube Collaboration), ApJ 843, 2 (2017).
[3] K. Murase, T. A. Thompson, B. Lacki, J. Beacom, PRD 84, 043003 (2011).
[4] A. Stasik, DESY, PhD thesis, 2017, http://dx.doi.org/10.18452/18729.
[5] M.G. Aartsen (IceCube Collaboration), Astropart. Phys. 92, 30 (2017).
[6] M.G. Aartsen (IceCube Collaboration), A&A 607, A115 (2017).
[7] M. Usner for the IceCube Collaboration, Proceedings of Science 974 (ICRC 2017).

Acceleration of electrons at supernova remnant shocks.

Towards more realistic numerical models

Computer simulations are a powerful instrument for studying plasma and shock physics. High-resolution simulations are used to explore the physics of shocks for parameters that permit extrapolation to the conditions in young supernova remnants. Numerical experiments of the astroparticle theory group at DESY in Zeuthen sample a representative portion of the shock surface and demonstrate in detail the shock physics and the variety of electron acceleration processes.

It is generally assumed that galactic cosmic rays are produced by diffusive shock acceleration in shocks of supernova remnants. This mechanism requires a pre-acceleration that is the most difficult and still unresolved issue of the theory. Our DESY group simulates shocks with parameters such as those that occur in shocks in young supernova remnants. The shock transition consists of undisturbed plasma (upstream), a “foot”, “ramp” and “overshoot” region and the downstream region (Fig. 1a). Two instabilities occur in the shock transition: electrostatic Buneman instability in the foot region (Fig. 1c) and Weibel-type filamentation instability in the ramp region (Fig. 1b).

The Buneman instability results from the interaction of the shock-reflected ions with incoming cold electrons and leads to an oscillating electric field. If that field is strong enough to efficiently trap electrons, these electrons can be accelerated up to relativistic energy, producing a high-energy tail in the electron spectra in the downstream region. This acceleration mechanism is known as shock surfing acceleration, and we found that its efficiency strongly depends on the magnetic-field configuration and the temperature of the upstream region [1].

The second (Weibel-type) instability is excited because of interactions of reflected ions with incoming ions. The deformation of magnetic field lines by the Weibel instability can lead to magnetic reconnection, meaning a change of magnetic-field topology and the conversion of magnetic energy into kinetic energy of particles. Tracing individual particles in our simulations permits the identification of four individual acceleration processes that are spawned by magnetic reconnection [2]. These results are an important step towards ever more realistic models of particle acceleration in astrophysical plasmas.

Contact:
Martin Pohl, martin.pohl@desy.de

References:

[1] A. Bohdan et al., ApJ 847, 71 (2017).
[2] A. Bohdan et al., Proceedings of Science (ICRC2017), 587.

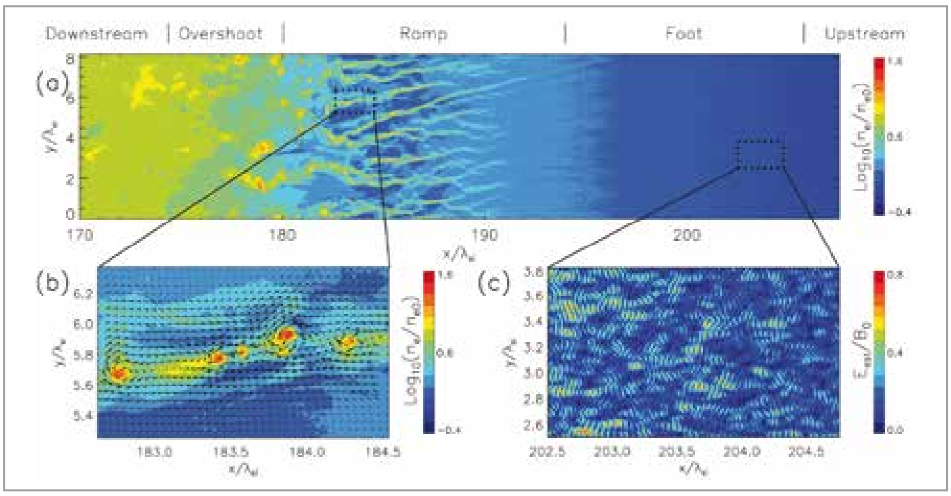

Figure 1

Structure of high-Mach-number perpendicular shocks:
(a) electron density in the shock region,
(b) electron density with overlapping magnetic field in a region of magnetic reconnection,
(c) electrostatic field strength in the Buneman instability region.

Cosmic rays and nuclear physics.

When interdisciplinarity matters

Ultrahigh-energy particles bombard the Earth from outer space. Despite huge efforts, their sources are still unknown. Measurements indicate that particles with more than 100 EeV (=10^{20} eV) could be heavier than protons. In this case, the deflection of nuclei in intergalactic magnetic fields would preclude pointing back at – and thus identifying – their sources. The astroparticle theory group at DESY in Zeuthen strives to model the interactions of accelerated nuclei in their sources and during their travel through extragalactic space.

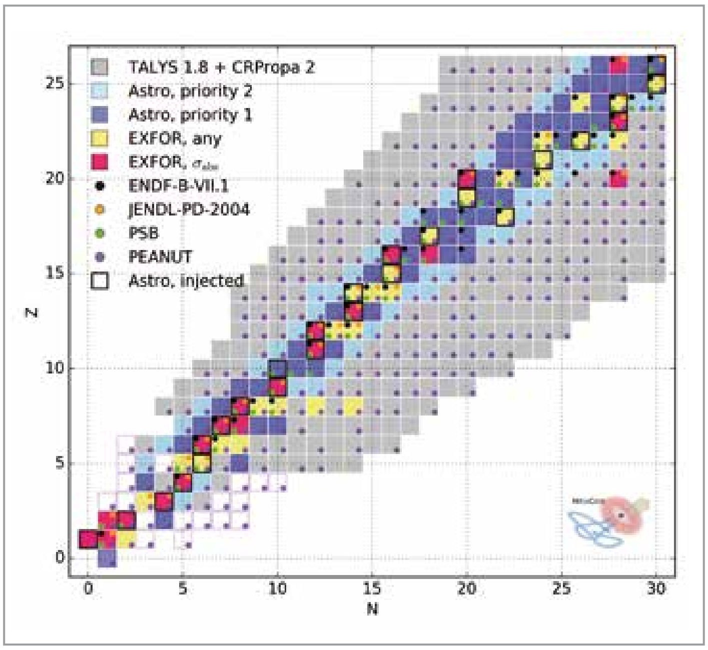

Figure 1

Nuclide chart (as a function of Z and N) showing the isotopes with relevance for cosmic-ray astrophysics (dark blue, light blue, grey, black rectangles) and the experimental knowledge (measured: red, yellow; modelled: dots)

Ambient radiation fields affect the initial energy and composition of cosmic rays, as photo-meson production and nuclear disintegration can occur. In this process, a whole cascade of nuclides is produced. For all relevant nuclides, information on interaction cross sections, lifetimes and particle production is then needed. We have collected information on all relevant nuclides and nuclear processes and assessed their influence on astrophysical observables of cosmic rays and neutrinos. For many nuclides, no measurements exist and model predictions are partly very uncertain.

Our group also studied the impact of nuclear models on the nuclear cascade within a gamma-ray burst radiation field [1]. It could be demonstrated that the impact of nuclear model uncertainties is potentially larger in environments with non-thermal radiation fields than in the cosmic microwave background. Figure 1 shows the experimental status. Isotopes with the highest priority for astroparticle physics are the dark and light blue ones (priority 1 and 2, respectively). The grey isotopes are also relevant, as they are used in popular propagation and nuclear reaction programs. Isotopes that are injected in our propagation simulations are framed by black rectangles (i.e. the most abundant stable isotope for each Z).

However, measurements of the relevant nuclear properties exist only for the red and yellow isotopes. Isotopes for which at least model predictions exist are shown with dots.

Ultimately, close cooperation with the nuclear physics community is needed to provide systematic measurements and improved predictability for unmeasured isotopes. This is urgently required for progress in the search for the sources of cosmic rays at the highest energies.

Contact:

Denise Boncioli, denise.boncioli@desy.de

Reference:

[1] D. Boncioli, A. Fedynitch, W. Winter, Scientific Reports 7, 4882 (2017).

Where do cosmic rays and neutrinos at the highest energies come from?.

Studying the universe with multiple messengers challenges theory

Charged cosmic rays at the highest energies come from outside the Milky Way. It is difficult to reveal their origin because they travel in random paths, deflected by magnetic fields. The recent observation of extragalactic neutrinos, which travel undeflected between their source and Earth, has opened a new window onto the origin of cosmic rays. Funded by the European Research Council (ERC), the "Neutrinos and the origin of cosmic rays" (NEUCOS) group at DESY develops a picture of astrophysical sources assuming a common origin of cosmic rays and neutrinos at the highest energies.

Astrophysical objects are often observed through different messengers, such as high-energy gamma rays, cosmic rays, neutrinos or even gravitational waves, all coming from very violent environments. These environments likely produce (some of) the messengers at the same time. Theory is challenged to consistently describe the observed fluxes of various messengers in the sources.

Neutrinos and cosmic rays are intimately connected because neutrinos are produced in interactions of energetic protons or, less efficiently, nuclei in or near the source. The NEUCOS project aims to understand this connection, in view of the fact that cosmic rays have recently been proven to be a mix of nuclei (and not just protons). Major efforts are undertaken to model sources with a heavier cosmic-ray composition, find ways to test neutrino properties by their propagation and optimise future in-ice and deep-sea experiments for particle physics (e.g. measurement of the neutrino mass hierarchy) and astroparticle physics (e.g. search for astrophysical neutrino sources).

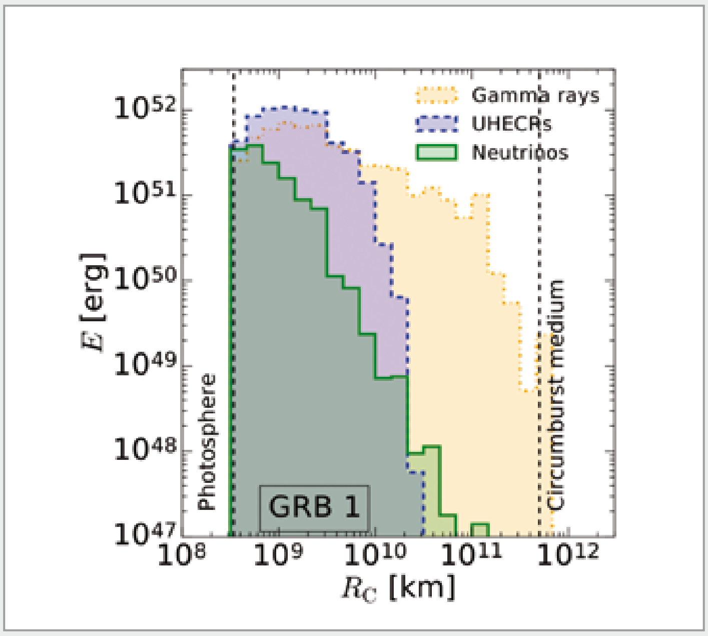

Figure 1

Gamma ray, ultrahigh-energy cosmic ray (UHECR) and neutrino production in a gamma-ray burst as a function of the radius R_c from a central engine for a specific model. Different messengers come from different regions around the same object. Relating them requires a detailed description of the source as a whole.

The ERC group is multidisciplinary, with particle physicists working on interactions in the sources and astrophysicists modelling specific source classes, such as gamma-ray bursts and active galactic nuclei. Together, we aim to develop multimessenger descriptions of the observations for plausible scenarios of the origin of ultrahigh-energy cosmic rays and neutrinos.

ERC Consolidator Grant

"NEUCOS: Neutrinos and the origin of cosmic rays"

Contact:

Walter Winter, walter.winter@desy.de

References:

[1] M. Bustamante et al., ApJ 837, no. 1, 33 (2017).
[2] https://astro.desy.de/theory/neucos/index_eng.html

Multimessenger observations of high-energy neutrinos.

Neutrino alerts followed up by two new optical survey instruments

The most promising neutrino source candidates are of transient or variable nature, such as supernovae, tidal disruption events and flaring active galactic nuclei (AGN). To catch the rapidly fading counterparts, neutrinos need to be reconstructed in real time to allow immediate follow-up observations of the patch of sky where the neutrino came from. New follow-up instruments in combination with sophisticated real-time data analysis pipelines will improve the sensitivity to transient neutrino sources. The Helmholtz Young Investor Group (YIG) "Identifying the Sources of High-Energy Neutrinos with Multimessenger Observations" at DESY is strongly involved in these endeavours.

To get access to several years of archival data overlapping with operations of the IceCube neutrino observatory and to quickly follow up on neutrino alerts, the members of the YIG joined the optical All-Sky Automated Survey for Supernovae (ASAS-SN). ASAS-SN currently consists of four units around the globe, each with four robotic 14 cm telescopes. ASAS-SN has been monitoring the visible sky to magnitude 17 in the V-band on a two to three day cadence. It has followed up ten IceCube neutrino alerts. One was observed 37 seconds after the alert was received, including scheduling the observation and slewing the telescope. Furthermore, ASAS-SN long-term all-sky monitoring provides useful information to study AGN variability [1]. The YIG works with ASAS-SN data to exploit the temporal overlap with archival IceCube data and to develop new cross-correlation algorithms for the next generation of optical survey instruments.

The Zwicky Transient Facility (ZTF) is a novel optical survey instrument on Mount Palomar in California, USA. With a field of view of 47 square degrees, it is able to scan the entire Northern sky every night to a magnitude of 20.5 (much deeper than ASAS-SN). ZTF saw first light in November 2017 (Fig. 1), and first science results were produced during engineering runs [2]. ZTF will find a vast amount of optical transients and thus provide a valuable catalogue of potential neutrino sources. The challenge is to classify the large number of recorded transients. Robust source classification requires a spectroscopic follow-up with another instrument. As a member of ZTF, the DESY astroparticle physics group has access to spectroscopic resources located on the same mountain and to additional spectroscopic resources awarded to the DESY group and the Humboldt University, Berlin. A real-time stream of IceCube neutrinos will play a crucial role in preselecting interesting optical transients for spectroscopic follow-ups. The YIG currently develops and implements new algorithms to cross-correlate neutrinos in location and time with optical transients.

The unprecedented list of sources that ZTF will provide will boost our sensitivity for probing supernovae and tidal disruption events as sources of high-energy neutrinos.

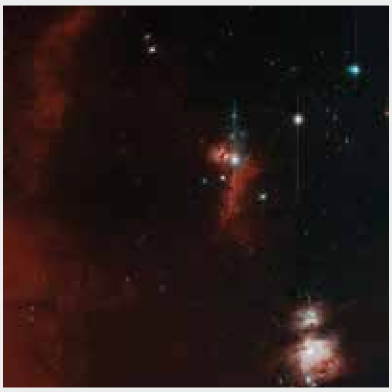

Figure 1

"First-light" image of ZTF on 1 November 2017. The full-resolution image has more than 24 000 x 24 000 pixels. Each ZTF image covers a sky area equal to 247 full moons. The Orion nebula is at the lower right.

Helmholtz Young Investigator Group

"Identifying the Sources of High-Energy Neutrinos with Multimessenger Observations"

HELMHOLTZ ASSOCIATION

Contact:

Anna Franckowiak, anna.franckowiak@desy.de

References:

[1] A. Franckowiak et al., The Astronomer's Telegram, 10794 (2017).
[2] S.R. Kulkarni on behalf of the ZTF collaboration, The Astronomer's Telegram, 11266 (2018).

Physics beyond the Standard Model with CTA.

Search for dark-matter particles in astrophysics data

The nature of physics beyond the Standard Model (BSM) of particle physics is as much a driving question for astrophysicists as it is for particle physicists. In particular, astrophysical measurements show that more than 80 percent of the matter in the universe is not accounted for by visible matter, pointing to a new particle or a set of particles that make up this so-called dark matter. A Helmholtz Young Investigator Group (YIG) at DESY was formed to study the nature of BSM physics using the upcoming Cherenkov Telescope Array (CTA) gamma-ray observatory.

The signature of dark-matter particles decaying to a final state with photons could be seen as spectral features such as bumps or spectral cut-offs in the normally smooth spectra of astrophysical objects, occurring at energies that depend on the mass of the dark-matter particle. However, current gamma-ray telescopes have a limited energy resolution. The YIG seeks to exploit the much better energy resolution and gamma-ray flux sensitivity of CTA to search for signatures of BSM particles.

In preparation for CTA data analysis, the YIG uses VERITAS data as test. In particular, the group investigated a large set of blazars observed by VERITAS. These cosmic particle accelerators, with energetic jets of particles pointing towards Earth, produce high-energy photons whose spectra could show hints of BSM particles in case they couple to photons. No evidence for tell-tale bumps has been found, and while spectral cutoffs are observed in some of the spectra, they occur at different energies, indicating an astrophysical origin.

The YIG also performs simulation studies on how the energy and angular resolution of CTA can be improved through suitable event selections either for precision studies or for analyses where event statistics is more important. As shown in Fig. 1, the energy resolution can be improved significantly by retaining only the best-reconstructed events (type 0).

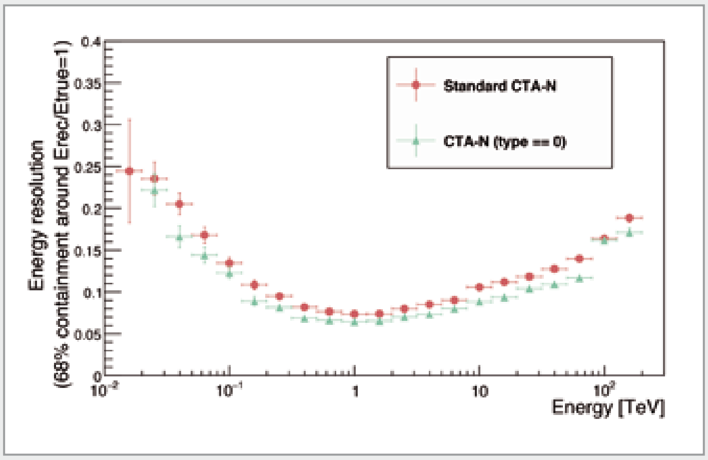

Figure 1

CTA energy resolution for the standard setup (red) and retaining only the best-reconstructed events (type 0, green)

Helmholtz Young Investigator Group

"Opening a New Window on Physics Beyond the Standard Model Using the Cherenkov Telescope Array"

Contact:
Elisa Pueschel, elisa.pueschel@desy.de

Theoretical particle physics.

The DESY theory group covers a broad range of topics – from particle phenomenology and lattice gauge theory to cosmology and string theory. This scientific breadth is a unique asset of the group and of DESY, as it provides a setting for many fruitful interactions.

In particle phenomenology, results from the Large Hadron Colllider (LHC) at CERN are at the centre of current activities. These include general techniques for precision calculations (p. 66) and their application to Higgs physics (p. 64).

Particle phenomenology activities at DESY are strongly connect to efforts in both lattice gauge theory and cosmology. Lattice gauge theory, pursued by the DESY NIC group, is steadily approaching the goal of producing results for the limits of vanishing lattice spacing, infinite volume and physical quark masses. In 2017, their efforts led to an improved understanding of the spin structure of the proton (p. 68).

Moreover, theoretical efforts in cosmology enabled much progress in our understanding of how dark matter and inflation could be embedded into a framework with supersymmetry at high energy scales (p. 62).

The last core activity of the group, string theory, has recently provided deeper insights into the bootstrap method for studying gauge theories (p. 70). The ultimate goal of these studies is to improve our understanding of the theories relevant for particle phenomenology.

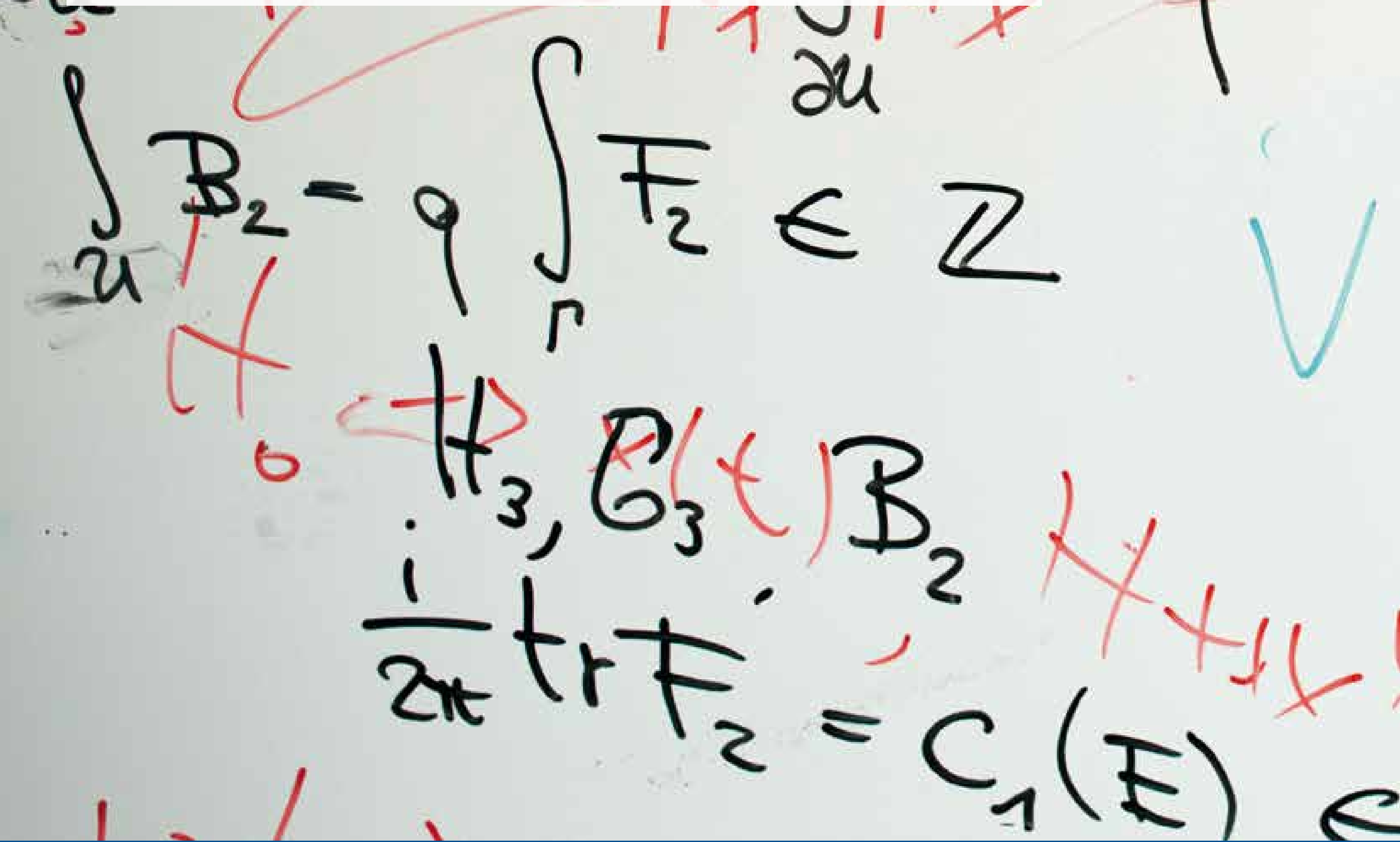

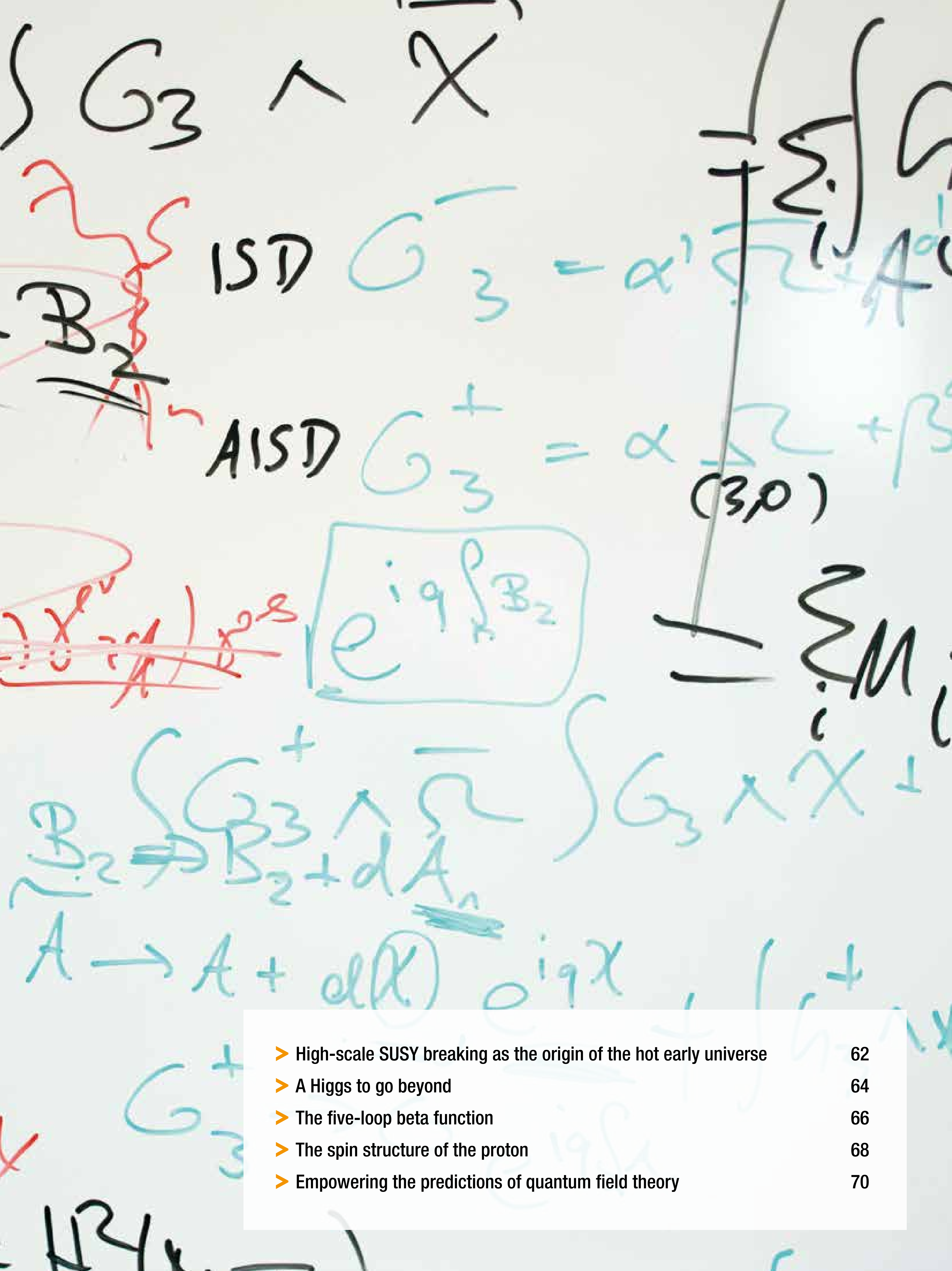
ISD
AISD
(3,0)

High-scale SUSY breaking as the origin of the hot early universe.

A unified particle physics model for the early universe

The early universe can be seen as a laboratory for testing theories of high-energy physics far beyond the reach of colliders. Observations such as the cosmic microwave background, the existence of dark matter and the baryon asymmetry of the universe provide clues on the properties of these theories. A convincing particle physics model aiming at extending the Standard Model of particle physics to energies close to the Planck scale should be capable of explaining all these observations within a single framework. In this article, we provide an example of such a framework, which intimately links supersymmetry breaking, inflation and leptogenesis. The only dimensionful parameter is generated by a strongly interacting hidden-sector gauge group, analogously to the QCD scale.

The Standard Model (SM) of particle physics is stunningly successful in describing physics up to the energy scales of the most powerful colliders we can currently build (e.g. 14 TeV centre-of-mass energy at the LHC). However, the energies reached in the early universe may have been much higher than this, possibly close to the Planck scale of 10^{18} GeV. And somewhere in this vast range of energies, new physics beyond the SM must arise: Firstly, the homogeneity of the cosmic microwave background (CMB) and the extremely large-scale correlations of its tiny fluctuations require some mechanism to bring a huge part of the early universe into causal contact. Secondly, the observed matter–antimatter asymmetry in our universe requires some mechanism to create a tiny imbalance between the baryon and antibaryon content of the hot primordial plasma. Thirdly, the observation of the gravitational effects of dark matter, for example in galaxy rotation curves, requires some new very weakly interacting particle. The SM cannot accomplish any of these tasks.

Over the past decades, many theories and paradigms have been developed to address the questions above. Cosmic inflation, a phase of exponential expansion in the early universe, driven by vacuum energy with negative pressure, successfully explains our CMB observations. The matter–antimatter asymmetry can be generated dynamically if the so-called Sakherov conditions are fulfilled: violation of baryon number as well as of C and CP symmetry in an out-of-equilibrium environment. An example is (thermal) leptogenesis, where these conditions are met in the production and decay of right-handed neutrinos in a minimal extension of the SM. Finally, out of several well-motivated theories that predict viable dark-matter candidates, we would like to emphasise the role of supersymmetry (SUSY). Doubling the particle content of the SM, it not only provides candidates for dark matter and for the inflaton (the particle driving inflation), but its gauged version, supergravity, also offers a way to link the SM with general relativity. Not a theory of quantum gravity itself, it can be viewed as a low-energy limit of e.g. string theory. If supersymmetry is realised at a relatively low energy scale, it can provide a solution to the hierarchy problem, explaining the smallness of the Higgs mass compared to the Planck scale. Given the absence of supersymmetric signals at the LHC, we will however abandon this last idea in this article and instead focus on supersymmetry broken at a very high energy scale.

These cosmological problems and their proposed solutions have so far mainly been discussed independently. However, any viable theory extending the SM to high energy scales will have to address all these issues simultaneously. In particular, a solution proposed to address only one of the problems may actually change one of the other problems for the worse. A well-known example is the interplay between inflation and supersymmetry breaking: The dynamics in one sector typically back-reacts on the other sector, potentially destroying the fine calibration needed to produce the required results. In Ref. [1], we therefore studied in detail an explicit model that addresses all of these issues simultaneously. With only few free parameters, all possible correlations and back-reactions are fully calculable, and we show that they are actually crucial in obtaining the observed values for e.g. the CMB observables.

The proposed setup consists of a strongly interacting SU(2) gauge group in a hidden sector with a residual U(1) flavour symmetry, which we (weakly) gauge and identify as $U(1)_{B-L}$, the symmetry associated with the difference of baryon and

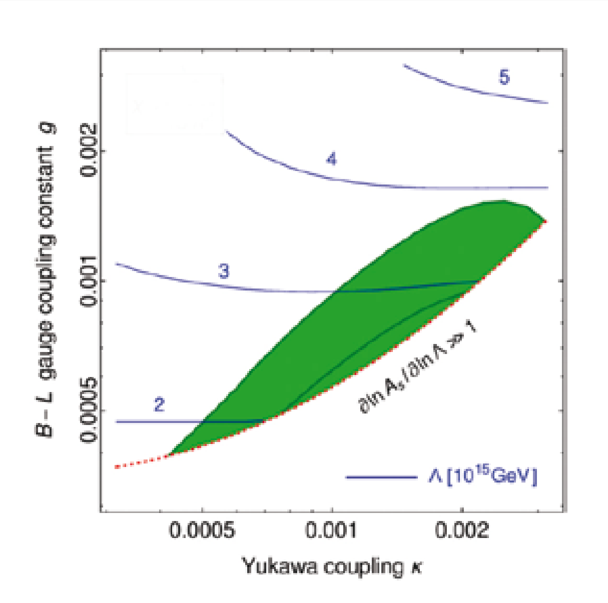

Figure 1

Viable parameter space (marked in green) fulfilling all theoretical and observational constraints. The region below the dashed red line is excluded since it requires significant fine-tuning in the inflation sector.

lepton number. Below the dynamical scale Λ, determined by the Landau pole of the SU(2) gauge symmetry, the degrees of freedom of this hidden sector confine into composite particles, analogously to the mesons of QCD. This phase transition spontaneously breaks supersymmetry (this is known as the IYIT model of SUSY breaking [2]) and B-L, thereby generating an effective Fayet Iliopoulos (FI) term for the $U(1)_{B-L}$. This FI term provides the vacuum energy for cosmic inflation, a scenario dubbed D-term inflation [3]. At the end of inflation, the $U(1)_{B-L}$ plays a key role, providing the necessary couplings to the SM to populate the primordial thermal bath with SM particles. In particular, gauging $U(1)_{B-L}$ entails three right-handed neutrinos, which are abundantly produced at the end of inflation, leading to leptogenesis through a mixture of thermal and non-thermal processes. This entire setup is embedded in supergravity.

After ensuring the theoretical self-consistency of the model, we are left with only three free parameters for the inflation and supersymmetry breaking sector: the dynamical scale Λ, which sets the overall energy scale, the gauge coupling g of the $U(1)_{B-L}$ and a Yukawa coupling κ in the inflation sector, which contributes to the inflaton potential through loop corrections. In addition, there are the mass and mixing parameters of the (right-handed) neutrino sector. Out of these parameters, the dynamical scale κ is essentially fixed by the measured amplitude of the scalar CMB fluctuations, $\Lambda \sim 10^{15}$ GeV, a value interestingly close to the energy scale of grand unified theories. The viable parameter space for the coupling constants g and κ is shown in Fig. 1. Non-trivially, there is a region in parameter space (marked in green in Fig. 1) where all observational constraints (mainly CMB observations) are met. This fixes the remaining free parameters g and κ up to about a factor of order 1.

The dark-matter candidate in this model is a neutralino (a supersymmetric partner of a gauge boson), which at the cost of fine-tuning can be ensured to have the correct relic abundance. The production of a thermal bath and of the observed matter–antimatter asymmetry proceeds very similarly to the scenario discussed in Ref. [4]. That study was in fact part of my PhD projects at DESY six years ago, at the time already triggering some of the questions that we have been able to address now. The coupled set of Boltzmann equations of Ref. [4] tracks the number densities of all particle species throughout the phase transition at the end of inflation. In particular, the entire vacuum energy of the inflation sector gets transmitted to the SM thermal bath through an intermediate decay into right-handed neutrinos, thereby providing a very efficient leptogenesis mechanism.

In summary, we find that the three major cosmological puzzles mentioned in the introduction can be resolved within a single theoretical framework. Due to the high energy scales involved, direct tests of this model are unfortunately very difficult. Depending on the details of the phase transition at the end of inflation, further clues might be found in the future in the cosmic gravitational wave background.

Contact:

Valerie Domcke, valerie.domcke@desy.de

References:

[1] Domcke and Schmitz, Phys. Rev. D 95, no. 7, 075020 (2017) and arXiv:1712.08121.
[2] K. I. Izawa and T. Yanagida, Prog. Theor. Phys. 95, 829 (1996); K. A. Intriligator and S. D. Thomas, Nucl. Phys. B 473, 121 (1996).
[3] P. Binetruy and G. R. Dvali, Phys. Lett. B 388, 241 (1996); E. Halyo, Phys. Lett. B 387, 43 (1996).
[4] Buchmüller, Domcke, Schmitz, Nucl. Phys. B 862, 587–632 (2012).

A Higgs to go beyond.

Using the Higgs boson in the quests for an extension of the Standard Model

While providing an astonishingly accurate description of many observations, the Standard Model (SM) of particle physics also fails to account for others. The Higgs boson, discovered in 2012 at the LHC, now serves as a privileged exploration tool for physics beyond the SM. Two approaches to this quest can be envisioned: testing specific theories such as the minimal supersymmetric extension of the SM, or employing a general parameterisation of the theory space directly surrounding the SM. The DESY theory group has been engaged in both directions, studying the constraints deriving from existing measurements and the reach of possible future experiments.

The quests for an extension of the SM

Particle physics currently finds itself in a challenging position. On the one hand, in spite of successfully describing most measurements made so far, the SM is known to be incomplete. It does for instance not account for the observation of dark matter (DM) or for the vast predominance of matter over antimatter in the universe. On the other hand, measurements have so far not allowed us to unambiguously single out a specific theory that could supersede it. Testing scenarios and identifying allowed directions of extension are therefore important tasks for both theorists and experimentalists. The newly discovered Higgs boson, whose properties now need to be determined precisely, could be especially sensitive to physics beyond the Standard Model (BSM) and constitute a prime exploration tool.

The LHC at CERN, which smashes protons against each other at the largest energies ever accessed in controlled conditions, plays a major role in this quest for BSM physics. Its experiments aim for the direct production of new particles and for a precise characterisation of known ones, including the Higgs boson. At lower energies, other experiments for instance look for DM particles (e.g. LUX) or are able to reach astounding precision on quantities such as the anomalous magnetic moment of the muon. These measurements are confronted with the predictions of the SM and its extensions. BSM modelling is possible through specific theories or systematic parameterisations. We will discuss one approach of each type followed in the DESY theory group.

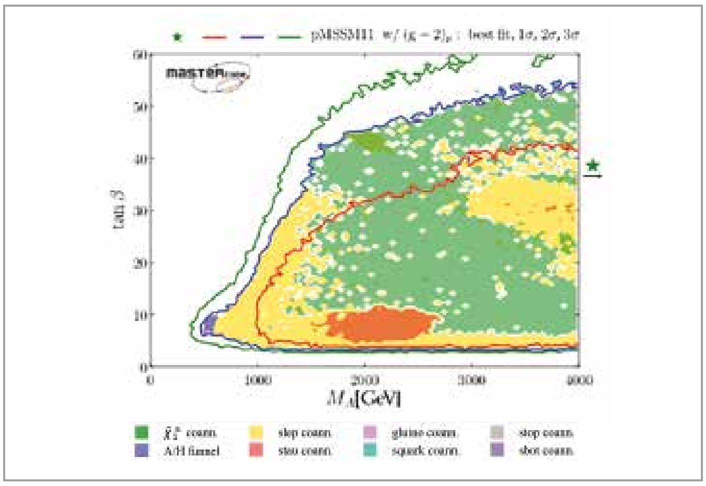

Figure 1

Likelihood profiles of the pMSSM11 in the two-dimensional plane of the pseudoscalar mass (M_A) and tanβ. The shadings indicate the active DM mechanism, which allows the constraint coming from the observed DM relic density to be satisfied.

Testing supersymmetric models

Given a specific extension of the SM, one can determine in which region of parameter space it complies with existing measurements. Constraints on the existence of new particles should also be satisfied. Supersymmetry is a well-motivated hypothesis upon which specific extensions of the SM can be constructed. Members of the MasterCode collaboration at DESY have focused their efforts [1] on understanding how a phenomenological version of the Minimal Supersymmetric Standard Model (MSSM) with eleven parameters, the so-called pMSSM11, fares against current experimental measurements and bounds. While this study goes well beyond the Higgs sector, striving to fully encompass the richness and complexity of supersymmetric phenomenology (also beyond the LHC), it is still significantly impacted by the measured Higgs properties and by the limits on the existence of heavier Higgs bosons.

To understand how the experimental Higgs physics programme and the MSSM interrelate, we need to recall a few general features of the latter. First of all, in the MSSM, for each SM particle there is a superpartner with spin differing by half a unit. Moreover, for theoretical reasons, two Higgs doublets are required in the MSSM instead of just one in the SM. As a consequence, there are five physical Higgs particles: three neutral ones (the CP-even *h* and *H*, as well as the CP-odd *A*) and two charged ones.

One of the most important constraints relevant for the Higgs particle *h*, which we identify with the one observed at the LHC, arises from its precisely measured mass. In contrast with the SM, where it is a free parameter, the MSSM makes a prediction for this quantity. The inclusion of sophisticated loop corrections depending on many parameters is required for the model to match the observed Higgs mass value. Bounded from above by m_Z , the tree-level prediction of the MSSM is indeed plainly contradicted experimentally. In our study, we found that this constraint can be satisfied. The observed SM-like Higgs production rates can also be reproduced, even with relatively light superpartners.

Of course, the LHC experiments are also looking for the other Higgs particles. In Fig. 1, we show the likelihood profiles in the (M_A, tanβ) plane. For larger values of tanβ – the ratio of the vacuum expectation values of the two MSSM Higgs doublets – important bounds derive from searches for heavy Higgs bosons decaying to tau leptons ($y^{A/H}_{\tau} \propto$ tanβ). At lower values of tanβ, other constraints become relevant but, for tanβ of order 10, masses as low as 500 GeV are still allowed for the CP-odd *A*.

Employing systematic parameterisations

Besides testing specific models, it is also possible to systematically parameterise the theory space in direct vicinity of the SM. Assuming that no new particle is light enough to be produced with the energies experimentally available, a so-called effective field theory (EFT) can be constructed using SM particles and established symmetries as building blocks. Such an EFT naturally embeds the SM and consistently extends it with new interactions of unknown strengths and higher dimensions. Consistency at the quantum level and the power of its systematic theory space coverage are in general only preserved when all interactions up to a given dimension are considered simultaneously. A global approach including various measurements is then required to constrain all possible directions of SM extension.

The interactions of the Higgs boson in particular can be modified. Its self-interactions are key to understanding the mechanism through which the Higgs provides masses to SM particles. These self-interactions could help us understand why the weak interaction – responsible for radioactivity – is so strong compared to gravity, or shed light on the absence of significant amounts of antimatter around us in the universe. A modification of the interaction between three Higgs bosons, denoted $\delta\kappa_\lambda$, will be probed to a limited extent in the next high-luminosity phase of the LHC (HL-LHC). The DESY theory group contributed to a global EFT analysis in which the HL-LHC sensitivity gained at leading order (LO), in Higgs pair

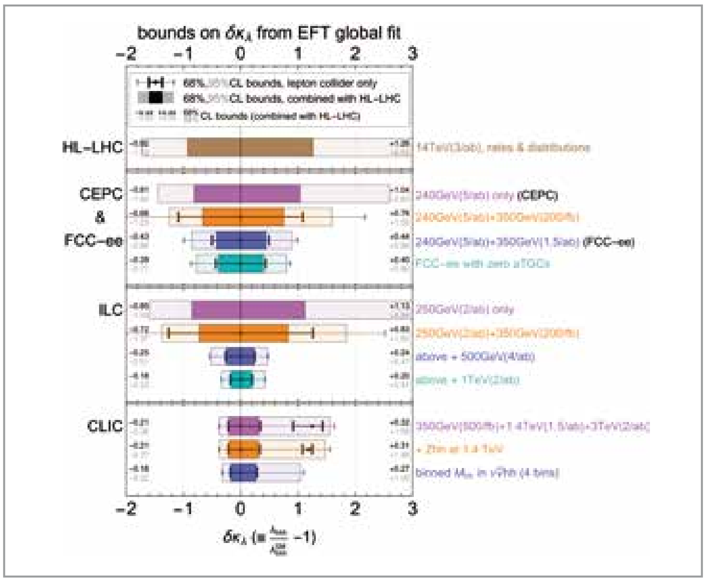

Figure 2

Global EFT constraints on a modification of the interaction between three Higgs bosons $\delta\kappa_\lambda$ obtainable at various circular (CEPC and FCC-ee) and linear (ILC and CLIC) electron–positron colliders, in comparison with the one that the high-luminosity phase of the LHC (HL-LHC) would yield. See Ref. [3] for details.

production, and the one gained at next-to-leading order (NLO), in single Higgs production, were both included [2]. New colliders are needed for more precise determinations. Proton collisions at energies an order of magnitude above LHC ones would yield the best sensitivity but require at least 25 years of technology development and construction.

With global EFT studies, the DESY theory group was also instrumental in demonstrating that new electron–positron colliders, which could be realised on shorter time scales, would also bring valuable information on $\delta\kappa_\lambda$ [3], in addition to measuring Higgs interactions with SM particles precisely [4]. Several scenarios were considered. Figure 2 shows that circular colliders such as the CEPC or FCC-ee, having only a NLO sensitivity to $\delta\kappa_\lambda$ in single Higgs production, could significantly improve HL-LHC constraints. Runs at two different energies would be fully complementary. Linear colliders such as the ILC or CLIC could yield higher precisions by reaching energies sufficient for producing pairs of Higgs bosons and therefore gaining LO sensitivity to $\delta\kappa_\lambda$. In these studies, we stressed the complementarity between Higgsstrahlung and *WW* fusion Higgs pair production modes as well as the additional sensitivity brought by a differential measurement of the invariant mass of the Higgs pair.

Contact:

Emanuele Bagnaschi, emanuele.bagnaschi@desy.de
Gauthier Durieux, gauthier.durieux@desy.de

References:

[1] E. Bagnaschi et al, Eur. Phys. J. C78 (2018).
[2] S. Di Vita, C. Grojean, G. Panico, M. Riembau, T. Vantalon, JHEP 09, 069 (2017).
[3] S. Di Vita, G. Durieux, C. Grojean, J. Gu, Z. Liu, G. Panico, M. Riembau, T. Vantalon, JHEP 02, 178 (2018).
[4] G. Durieux, C. Grojean, J. Gu, K. Wang, JHEP 09, 014 (2017).

The five-loop beta function.

Pushing perturbative QCD to the limit

In 2017, within an international collaboration, a member of the DESY theory group in Zeuthen calculated the beta function in perturbative quantum chromodynamics (QCD) up to five-loop order for a general gauge group.

Anomalous dimensions are fundamental objects of gauge theories. In QCD, the beta function and the anomalous dimension of the quark masses play a particularly important role. The beta function describes the evolution of the strong coupling constant under change of the renormalisation scale. For large scales, this leads to asymptotic freedom and for small scales to confinement. The anomalous mass dimension determines the dependence of the mass on the scale choice.

The beta function was first determined in seminal works by David Gross, Frank Wilczek and David Politzer at one-loop order in 1973, establishing QCD as the theory of strong interactions. During the following decades, it was calculated up to five-loop order in perturbative QCD.

The beta function and the anomalous mass dimension of QCD can be obtained using a number of different approaches, e.g. by calculating different combinations of renormalisation constants. Since the beta function and the anomalous mass dimension are both gauge-independent, they can be obtained by employing a particular choice of gauge, e.g. the background field gauge, during the calculation. Although this choice of gauge simplifies the approach, not choosing a particular gauge during the analysis serves as a welcome check for the final result.

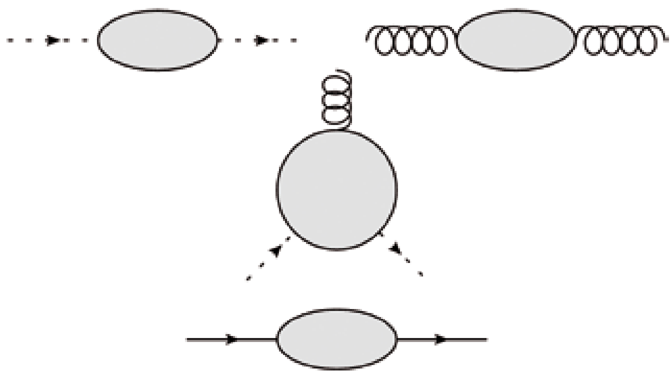

Figure 1

Sample diagrams required to calculate the beta function and the anomalous mass dimension. Dotted, curly and straight lines indicate ghosts, gluons and quarks, respectively.

In our calculation, we chose to evaluate the ghost and gluon self-energies and the ghost–ghost–gluon vertex. Together with the quark self-energy, these are sufficient to obtain all renormalisation constants of QCD thanks to Ward identities. Samples of the relevant Feynman diagrams are shown in Fig. 1. In total, we had to calculate about 80 000 Feynman diagrams each for the ghost and quark self-energies, 500 000 for the gluon self-energy and 1 500 000 for the ghost–ghost–gluon vertex. Although the ghost–ghost–gluon vertex contains the most diagrams, the calculation of the gluon self-energy is the most demanding part. The analysis greatly benefitted from the available high-performance computing infrastructure of the theory group at DESY in Zeuthen.

To perform the calculation, we first had to separate ultraviolet from infrared singularities. To achieve this, we introduced a mass on all internal lines. This mass serves as an infrared regulator and removes all infrared divergences but does not change the ultraviolet ones. There is a small price to pay, though: The procedure leads to an artificial mass for the gluon and requires the use of a gluon mass counterterm. After introducing the mass regulator, we can set all external momenta to zero and are left with vacuum diagrams. The prototypes of these vacuum diagrams are shown in Fig. 2.

The calculation is then performed using standard techniques. We use integration-by-parts identities to relate the millions of Feynman integrals appearing in the course of the calculation and express them as linear combinations of basis integrals. These basis integrals then need to be calculated from first principles. A very attractive approach to their evaluation is the method of factorial series, which leads to very precise numerical results. For the Feynman integrals at hand, we obtained numerical results with up to a few hundred digits of

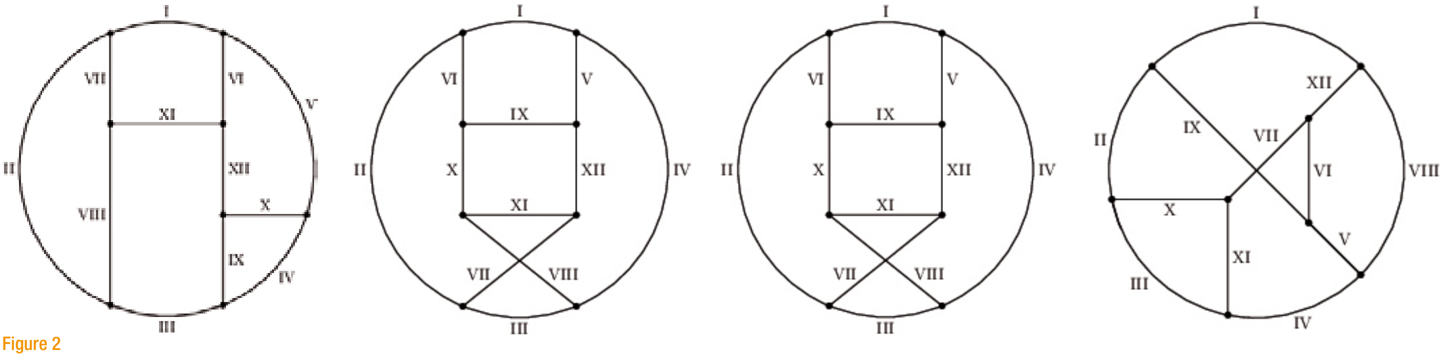

Figure 2

Families of five-loop vacuum integrals required to calculate the beta function

precision. The precision for the individual integrals is sufficiently high to be able to fit the final result to a small number of zeta values.

Finally, we would like to present our results. Recalling the definition of the beta function
$\partial_{\ln(\mu^2)} a = -a(\epsilon - \beta)$ with $a = \dfrac{C_A g^2(\mu)}{16\pi^2}$,

where C_A denotes the eigenvalue of the quadratic Casimir operator in the adjoint representation and g the strong coupling constant, and writing it as a power series in the strong coupling constant
$-\beta = b_0 a + b_1 a^2 + b_2 a^3 + b_3 a^4 + b_4 a^5$,
we obtain at one-loop order the well-known result
$3b_0 = -4n_f + 11,$

where $n_f = \dfrac{N_f T_F}{C_A}$,

with N_f denoting the number of active quark flavours.

At higher orders in the perturbative series, the expressions become more complicated and too lengthy to display here for a general gauge group. We therefore specialise on QCD, i.e. $SU(N_c)$ with the number of colours $N_c = 3$. The result for the five-loop coefficient of the beta function then reads

$$
\begin{aligned}
b_4 \;=\; & \left(\frac{1205}{708588} - \frac{152\zeta_3}{19683}\right) N_f^4 \\
& + \left(-\frac{48722\zeta_3}{59049} + \frac{1618\zeta_4}{6561} \right. \\
& \left. + \frac{460\zeta_5}{2187} - \frac{630559}{1417176}\right) N_f^3 \\
& + \left(\frac{698531\zeta_3}{19683} - \frac{10526\zeta_4}{2187} \right. \\
& \left. - \frac{381760\zeta_5}{19683} + \frac{25960913}{472392}\right) N_f^2 \\
& + \left(-\frac{4811164\zeta_3}{19683} + \frac{33935\zeta_4}{1458} \right. \\
& \left. + \frac{1358995\zeta_5}{6561} - \frac{336460813}{472392}\right) N_f \\
& + \frac{207295\zeta_3}{162} - \frac{363\zeta_4}{2} \\
& - \frac{10670\zeta_5}{9} + \frac{8157455}{3888}
\end{aligned}
$$

Next to the beta function, the quark mass anomalous dimension γ_m is of big importance. It is also gauge-independent and defined in a similar way to the beta function
$\partial_{\ln(\mu^2)} \ln m_q(\mu) = \gamma_m(a) = c_f\, a\,(3 + \gamma_{m1} a + \cdots)$,
where $c_f = C_F/C_A$, with C_F the eigenvalue of the quadratic Casimir operator in the fundamental representation.

For the five-loop contribution, we obtain, again for QCD,

$$
\begin{aligned}
\gamma_{m4} \;=\; & \left(-\frac{320\zeta_3}{59049} + \frac{64\zeta_4}{6561} - \frac{260}{59049}\right) N_f^4 \\
& + \left(\frac{12848\zeta_3}{19683} + \frac{448\zeta_4}{2187} - \frac{5120\zeta_5}{6561} + \frac{91865}{354294}\right) N_f^3 \\
& + \left(\frac{46400\zeta_3^2}{6561} + \frac{2010824\zeta_3}{59049} - \frac{166300\zeta_4}{6561} \right. \\
& \quad \left. - \frac{264040\zeta_5}{19683} + \frac{92000\zeta_6}{6561} + \frac{1320742}{177147}\right) N_f^2 \\
& + \left(-\frac{75680\zeta_3^2}{2187} - \frac{12538016\zeta_3}{19683} \right. \\
& \quad + \frac{2038742\zeta_4}{6561} + \frac{49876180\zeta_5}{59049} \\
& \quad \left. - \frac{638000\zeta_6}{2187} - \frac{1820000\zeta_7}{6561} - \frac{150736283}{354294}\right) N_f \\
& + \frac{96800\zeta_3^2}{243} + \frac{46402466\zeta_3}{59049} - \frac{698126\zeta_4}{2187} \\
& \quad - \frac{231757160\zeta_5}{59049} + \frac{242000\zeta_6}{243} + \frac{412720\zeta_7}{243} \\
& \quad + \frac{99512327}{39366}
\end{aligned}
$$

All the results we obtained are in full agreement with results from groups at KIT and NIKHEF.

Contact:

Peter Marquard, peter.marquard@desy.de

References:

[1] T. Luthe, A. Maier, P. Marquard, Y. Schroeder, JHEP 1710, 166 (2017).
[2] T. Luthe, A. Maier, P. Marquard, Y. Schroeder, JHEP 1703, 020 (2017).
[3] T. Luthe, A. Maier, P. Marquard, Y. Schroeder, JHEP 1701, 081 (2017).

The spin structure of the proton.

Towards solving the proton spin puzzle using lattice QCD

The John von Neumann Institute for Computing (NIC) group at DESY in Zeuthen, in collaboration with the Cyprus Institute, has carried out lattice QCD simulations to compute the individual contributions of quarks and gluons to the proton spin. The result confirms the experimental data collected during the past 30 years, which indicates that only a small fraction of the proton spin is carried by the intrinsic spin of the quarks.

The origin of the proton spin puzzle

Protons and neutrons, also called nucleons, are the building blocks of atomic nuclei. Together with the much lighter electrons, they make up basically all of the stable matter surrounding us on Earth. The intrinsic angular momentum of the nucleons (and electrons) as quantum mechanical particles is exactly 1/2 in units of ħ and gives rise to the magnetic properties of many materials. For more than half a century, understanding the internal structure of the nucleons has posed an enormous experimental and theoretical challenge.

The symmetries and regular patterns in the properties of the nucleons and the zoo of further hadrons observed in high-energy physics experiments have led to the picture that nucleons are bound states of three constituents, called quarks. Their binding force must be strong at large distances in order to explain “confinement”, i.e. the fact that quarks cannot be directly observed in experiments but remain confined inside hadrons.

However, somewhat surprisingly, deep-inelastic scattering experiments with a polarised proton target, carried out by the European Muon Collaboration (EMC) at CERN in the late 1980s (and subsequently, e.g. at SLAC and DESY), found that only a small fraction of the proton spin can be attributed to the spin of the individual quarks within the proton. This astonishing result was often called the “proton spin puzzle” because it is in contrast to the theoretical expectation from constituent-quark models.

In these models, the nucleon is considered to be a bound state of just three massive quarks. The mass of such constituent quarks is large (about a third of the nucleon mass) because it effectively accounts for part of the binding energy from strong interactions. In this picture, even when relativistic effects are taken into account, the quark models predict that

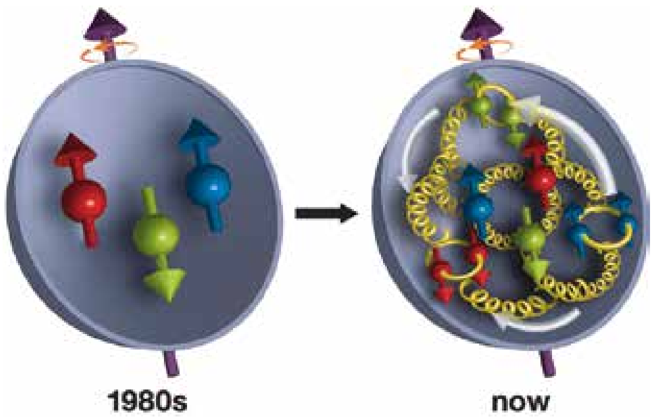

Figure 1

Illustration of how the understanding of the proton structure evolved from a bound state of three constituent quarks (left) to a complex object formed by valence quarks, sea quark–antiquark pairs and gluons (right).

a large fraction of the nucleon spin is carried by the quarks, and they thus cannot explain the experimental results.

The proton in QCD

The situation became different, but not less challenging (Fig. 1), in the framework of quantum chromodynamics (QCD) – the relativistic quantum field theory that describes the strongly interacting sector of the Standard Model of particle physics. The strong interactions are mediated by massless gauge fields, called gluons. The quark fields of QCD have a relatively small mass of only a few percent of the proton mass. These QCD quarks are related in a very complicated dynamical way to the physical nucleon states – and to the constituent quarks of the naive quark models.

In the fully dynamical framework of QCD, gluons and the orbital angular momentum of the quarks can also contribute to the total nucleon spin. This can be described by the following sum rule

$$\sum_{q=u,d,s,\ldots}(S^q + L^q) + J^g = \frac{1}{2} \qquad (1)$$

where S^q is the contribution from the intrinsic quark spin, L^q is the quark orbital angular momentum and J^g is the gluon total angular momentum.The quark contributions also include effects of sea quarks (i.e. virtual quark–antiquark pairs) and are summed over all quark flavours $q = u, d, s, c$ ... (not only the valence quarks u and d of the nucleon). Some care is also needed to properly define L^q and J^g such that all three contributions in the decomposition above are gauge-invariant. Moreover, due to non-trivial renormalisation effects, each term on the left-hand side of Eq. (1) may become dependent on the momentum transfer Q^2 in the scattering process, while the right-hand side is of course independent of Q^2.

The quantitative test of the sum rule Eq. (1) using experimental data or theory predictions poses a huge challenge: Disentangling the quark and gluon contributions requires deep-inelastic scattering experiments in which different particles, in particular leptons (as in the EMC experiment) and protons (as in recent experiments at RHIC), are used to probe the polarised protons within a fixed target or a second beam. Then, the measured structure functions need to be integrated (and usually extrapolated) over suitable kinematical regions to extract the individual contributions in Eq. (1).

The computation of these quantities is extremely difficult also on the theory side, because the formation of the proton as a complicated bound state of the quarks and gluons in QCD involves highly non-linear effects. These cannot be computed perturbatively, i.e. by an expansion in the coupling strength of QCD, because this coupling becomes large at the energy scales relevant for the hadronic bound states. Only numerical simulations within lattice QCD, where the theory is formulated on a discrete and finite space–time lattice, allow for a non-perturbative treatment of QCD in the low-energy regime.

The proton spin from lattice QCD

In collaboration with the Cyprus Institute, the DESY NIC group has carried out extensive lattice QCD simulations with four dynamical quarks with degenerate and approximately physical mass values for u and d quarks, and non-perturbatively improved twisted-mass action to reduce discretisation effects. In lattice QCD, the individual contributions to the proton spin according to Eq. (1) can be obtained from matrix elements of suitable renormalised local operators O_i between proton states. To extract these matrix elements, one computes ratios of correlation functions between two interpolating fields that create and annihilate proton states at large Euclidian time separation and with or without insertion of O_i. Different methods have been used to compute these ratios to verify that the time separations are sufficiently large to suppress contributions from excited nucleon states.

Correlation functions where the operator couples only to gluon fields or to quarks that are not directly connected to the proton fields, so-called disconnected diagrams, have an inherently bad signal-to-noise ratio. This difficulty has been overcome by using novel algorithms and exploiting special properties of twisted-mass fermions.

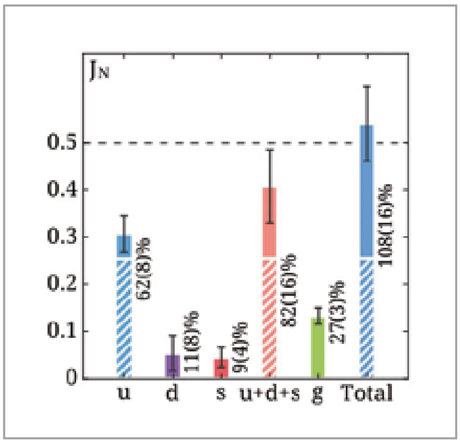

Figure 2

Relative contributions to the proton spin in the $\overline{MS}$ scheme at 2 GeV. Striped segments show (connected) contributions from valence quarks and solid segments show (disconnected) contributions from sea quarks or gluons.

Results

The results for the individual contributions to the proton spin, $S^q + L^q$ and J^q according to Eq. (1), computed at $Q^2 = 0$, are summarised in Fig. 2. Since these values have been obtained from simulations at a single lattice spacing of about 0.09 fm, no continuum extrapolation has been performed yet. Within the statistical and systematic uncertainties, the sum of all contributions nicely adds up to ½ as expected from Eq. (1).

Adding up only the intrinsic spin contributions (S^q) from all the quarks, we find that only about 20% of the total proton spins arise from the spin of the quarks, in accordance with the experimental data. The remaining proton spin is due to the gluons and the angular momentum of the quarks (which are both absent e.g. in simple quark model predictions). This result is in line with phenomenological analyses and an important step towards resolving the proton spin puzzle, which originates from the simplified picture of a proton made up effectively only of constituent quarks without orbital angular momentum and without explicitly including gluons.

In addition, the contributions of gluons and (valence and sea) quarks to the linear momentum of the proton have been computed and found to consistently add up to the overall linear momentum of the proton.

Contact:

Karl Jansen, karl.jansen@desy.de
Stefan Schäfer, stefan.schaefer@desy.de
Hubert Simma, hubert.simma@desy.de
Rainer Sommer, rainer.sommer@desy.de

References:

[1] A. Adare et al., (PHENIX Collaboration), Phys. Rev. D 90, no. 1, 012007 (2014).
[2] C. Adolph et al. (COMPASS Collaboration), Phys. Rev. Lett. B 753, 18 (2016).
[3] C. Alexandrou et al., Phys. Rev. Lett. 119, 142002 (2017).
[4] A. Abdel-Rehim et al., Phys. Rev. D 89, no. 3, 034501 (2014).

Empowering the predictions of quantum field theory.

From beautiful mathematics to particle collisions

Scattering amplitudes form a bridge connecting theoretical particle physics with the real world of collider experiments. Although their computation by means of Feynman diagrams quickly becomes prohibitive and is only valid when the particles are interacting weakly, international collaborations led by members of the DESY theory group are making significant progress addressing these shortcomings: On the one hand, new efficient methods lead to the determination of amplitudes at weak interaction strength by exploiting their analytic structure, also revealing intriguing connections to contemporary mathematics. On the other hand, the analysis of kinematic regions where the phenomenon of integrability miraculously emerges, paves the way for describing scattering at any interaction strength.

Simple models for hard problems

Based on the gauge theories underlying the Standard Model, scattering amplitudes provide predictions for specific outcomes to be detected by an observer, after quantum particles that were initially far apart approach each other and interact. Scattering amplitudes are therefore essential for comparison of the theory with the results of collider experiments, in order to identify phenomena beyond our current description of nature.

When the interaction strength, or coupling, is weak, the standard method for computing amplitudes is perturbation theory. Here, more accurate values of the amplitudes are approached by iteratively including corrections that are controlled by increasing powers of a small parameter, and which may be systematically obtained with the help of Feynman diagrams. In practice, however, the complexity increases rapidly at each order of correction. Perhaps more importantly, for quantum chromodynamics (QCD), the theory of the strong force, this framework becomes inapplicable at low energies, where the theory is strongly coupled.

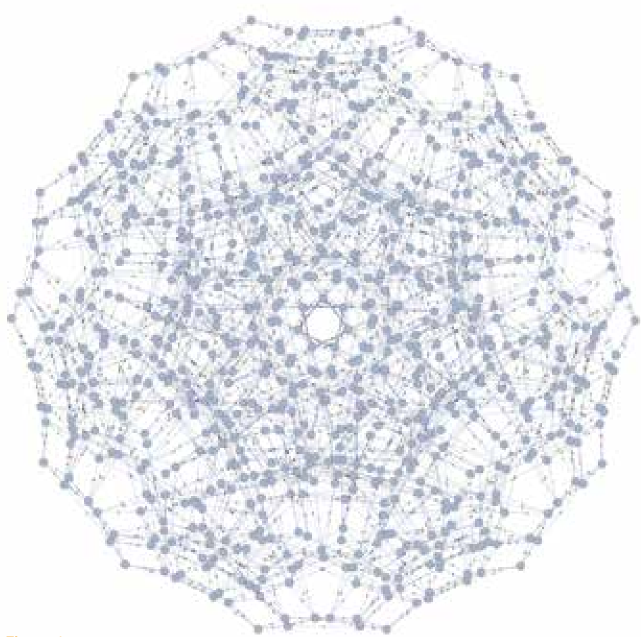

Figure 1

E6 cluster algebra, relevant for seven-gluon scattering. It contains clusters, denoted by nodes, with lines connecting them corresponding to a relation between them, known as mutation.

In order to address these pressing issues, a fruitful strategy is to first focus on idealised models, which allow for progress by disentangling some sources of complexity, while maintaining the essential features of reality. The example of the harmonic oscillator, and the central role it has played in understanding more intricate dynamical systems, may serve as an illustration of this approach.

For gauge theories, the analogue of the harmonic oscillator is known as maximally supersymmetric Yang–Mills theory. It is a cousin of QCD, additionally possessing supersymmetry, i.e. a symmetry between bosonic particles, such as the gluons that carry the strong force, and fermionic particles, which typically describe the matter we are made of. In the last decades, it has served as an excellent theoretical laboratory for developing computational methods, before applying them to QCD.

Record-breaking perturbative results

One of the avenues for overcoming the inefficiencies of conventional perturbation theory, which the study of maximally supersymmetric Yang–Mills theory has opened, is the “amplitude bootstrap” programme. The key idea is to fully exploit the expected analytic behaviour of the amplitude, as a function of the external momenta, in order to uniquely identify it. The amplitude bootstrap was initiated by Lance Dixon, James Drummond and Johannes Henn in 2011 for the six-gluon amplitude, as symmetry alone suffices to fix lower-point amplitudes.

In a series of papers, we were able to upgrade this procedure to the next frontier, the seven-gluon amplitude, thanks to exciting implications of contemporary mathematics [1] and fundamental physics principles [2] for its analytic structure. First, it turns out that the singularities of the amplitude are dictated by a mathematical object known as cluster algebra, shown in Fig. 1. And second, the double discontinuities of the amplitude are restricted by a set of relations, formulated by Othmar Steinmann, that follow from simple considerations such as the conservation of probability.

In this manner, we computed the third- and fourth-order perturbative correction to the most complicated part of the amplitude, and we surprisingly found that our framework in a sense becomes more powerful as we increase the number of external gluons from six to seven! Does this simplicity persist at higher points? Apart from the phenomenological importance of high-multiplicity results for new physics searches, there is evidence that all amplitudes of our model may be solvable even non-perturbatively, as we describe next.

Towards high-energy scattering at any coupling

Another remarkable feature of the gauge theory we are focusing on is integrability: This is the property of a physical system to have as many conserved quantities as degrees of freedom, which guarantees exact solvability. For scattering amplitudes, integrability only appears in special kinematic regions, but fortunately, one of these regions is quite relevant: As depicted in Fig. 2, it amounts to the frequently occurring collision of two high-energy gluons, which only mildly changes their trajectories, but also produces additional gluons.

Integrability has allowed Benjamin Basso, Simon Caron-Huot and Amit Sever to obtain the 2 → 4 amplitude in this region, non-perturbatively in integral form. It would be of course very exciting if the same could be achieved for any number of produced gluons. However, previous attempts stumbled on a serious difficulty: Starting with the 2 → 5 amplitude, the general form of its corresponding integral contained divergences that made no sense.

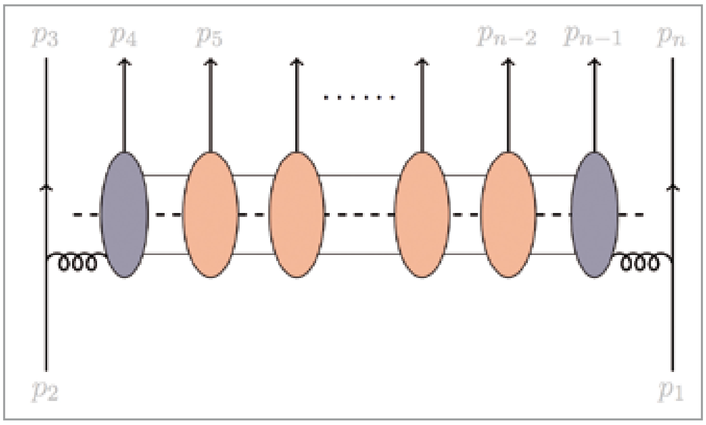

Figure 2

2 → n-2 high-energy or multi-Regge kinematics. Time evolves from bottom to top.

After a long effort, which among other things included thoroughly understanding the relevant space of functions in these kinematics [3], these divergences were recently cured [4]. This significant achievement paves the way for a description of all high-energy amplitudes at any coupling, and work on uncovering the form of the non-perturbative integrand is under way.

In conclusion, the DESY theory group is strongly involved in international collaborations that may for the first time provide an exact solution of an interacting four-dimensional gauge theory and also lead to significant applications for more realistic theories making contact with experiment. This aim will be further facilitated by our participation in the recently approved Innovative Training Network of the European Commission “Scattering Amplitudes: From Geometry to Experiment”.

Contact:

Georgios Papathanasiou, georgios.papathanasiou@desy.de

References:

[1] J.M. Drummond, G. Papathanasiou and M. Spradlin, JHEP 1503, 072 (2015).

[2] L.J. Dixon, J. Drummond, T. Harrington, A.J. McLeod, G. Papathanasiou and M. Spradlin, JHEP 1702, 137 (2017).

[3] V. Del Duca, S. Druc, J. Drummond, C. Duhr, F. Dulat, R. Marzucca, G. Papathanasiou and B. Verbeek, JHEP 1608, 152 (2016).

[4] V. Del Duca, S. Druc, J. Drummond, C. Duhr, F. Dulat, R. Marzucca, G. Papathanasiou and B. Verbeek, arXiv:1801.10605.

Infrastructure and services.

The experimental and theoretical research activities at DESY would not be possible without the contributions and support from numerous groups and people. One important service offered by DESY is its Test Beam Facility at the DESY II synchrotron. Scientists from all over the world are using the facility to subject newly developed detector components, e.g. for the International Linear Collider (ILC) or the LHC upgrades, to tests with electron or positron beams (p. 74). Other examples include the work of the DESY electronics groups, which design and manufacture important components for particle physics detectors (p. 76), or the development of laser plasma accelerators (p. 78).

Computing too is a crucial ingredient of research at DESY. The DESY IT group is constantly striving to improve its services for all users and needs – from the Grid and the National Analysis Facility (NAF) to high-performance computing platforms (p. 82). Big data in particular has gained in importance, leading to a European initiative spearheaded by DESY (p. 80).

As the DESY research campus is rapidly growing, comprising an increasing number of users, facilities and partner laboratories across multiple scientific disciplines, the Digital Campus helps to cope with the rising number of service requests (p. 84). Meanwhile, the DESY library group is promoting the open-access movement and working towards increasing the user-friendliness of the publishing process at DESY (p. 86).

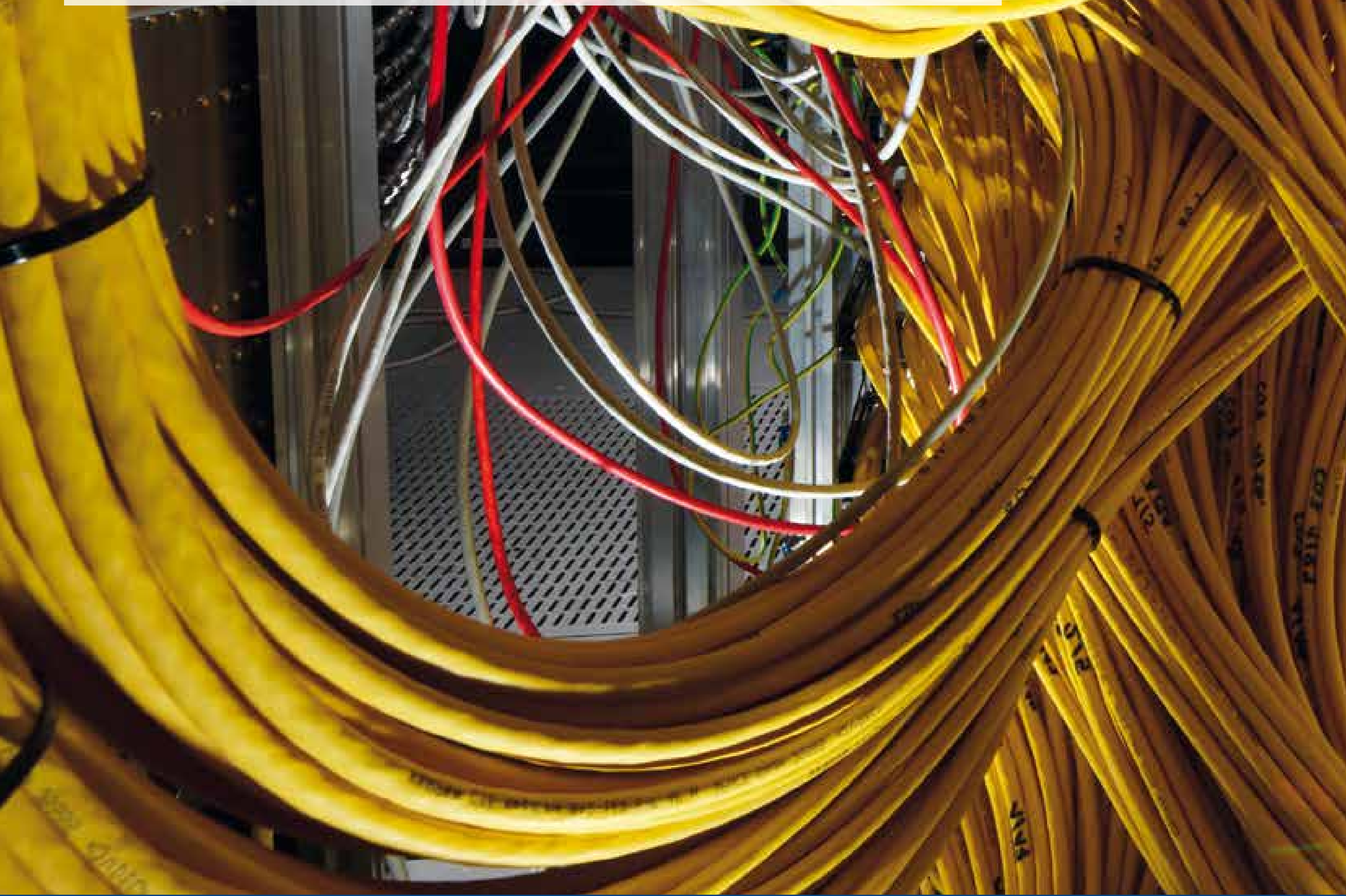

Oops, we did it again.

Another successful year for the DESY II Test Beam Facility

DESY operates the DESY II test beam facility for R&D projects of the global detector community. After the Christmas shutdown 2016, the facility started running again in February 2017 and, excluding a short summer shutdown, delivered reliable beam to users until Christmas 2017. User groups ranging from the upcoming LHC upgrades to small groups pursuing generic R&D made extensive use of the facility, appreciating the world-class infrastructures at DESY, such as the EUDET-style pixel beam telescopes or the large-bore magnets. To understand the future needs of the community, a test beam user workshop was held for the first time in fall 2017.

The DESY II Test Beam Facility

The DESY II Test Beam Facility makes use of the DESY II synchrotron, which predominantly serves as an injector for the PETRA III synchrotron radiation source, to parasitically generate beams of electrons and positrons in the energy range of 1–6 GeV. These are provided to users at three beamlines, which the users can control individually. The ease of use and the excellent infrastructure available make the DESY II test beam a very popular facility within the global user community. The test beam support team constantly adds improvements to the beamlines and strives to keep it a world-class facility for detector R&D.

The EU-funded AIDA-2020 project continues to support activities at the DESY II Test Beam Facility in many ways. Under its Transnational Access programme, it helps users from outside Germany to come to DESY and perform their tests at the facility. In addition, AIDA-2020 also supports existing infrastructure, such as the beam telescopes, and the installation of new infrastructure. In 2017, this included the construction and installation of a common monitoring system that logs general condition values, such as temperature, humidity, air pressure and others, using industry-grade back-ends. This information can then be integrated into the users' data streams.

Figure 1

Belle II test beam using the PCMAG 1 T solenoid

Furthermore, AIDA-2020 supported the design and test of the EUDAQ2 framework, which allows different detectors to run using a common data acquisition (DAQ) framework. The CALICE and ATLAS collaborations thoroughly and successfully tested this approach.

Highlights from 2017

In 2017, the DESY II Test Beam Facility was operated for 38 weeks in total. Over all the beamlines, this resulted in 114 user weeks, 67% of which were used. In total, 283 users from 17 countries came to the facility, with 62% from Germany, 17% from other EU countries and 11% from outside the EU. 49% of the users came for the first time to the DESY test beam, and 52% were students, underlining the importance of the facility as a training site for the next generation of detector experts.

Among the user communities, the LHC groups dominated with 58% of requests. As usual, however, groups from many different fields, ranging from Belle II or ILC detector R&D to experiments at FAIR, made use of the facility. The beam telescopes were again in high demand, with 75% of the groups requesting their use.

In February 2017, the Belle II group performed its final beam test at DESY (Fig. 1). A complete slice of the silicon tracking system for Belle II (pixel detector PXD and silicon strip tracker

SVD) was installed inside the PCMAG 1 T solenoid and read out by the final DAQ system, including the track-based data readout of the PXD detector. The collaboration will now move ahead to install the final system into the Belle II detector in Japan in 2018.

Use of the test beam facility is not restricted to high-energy physics. CBM is a proposed experiment for the upcoming FAIR facility at GSI in Darmstadt, Germany. One of the main subdetectors is the transition radiation detector, which will be used for particle identification. A first large-scale prototype was successfully tested at DESY, providing valuable input for the upcoming CBM technical design report.

Finally, educational use of the beamlines is by now part of the programme. Summer students conducted experiments at the test beam, as did the participants of the course "Particle Physics for Teachers", run by the DESY further education group.

DESY test beam user workshop

On 5 and 6 October 2017, DESY hosted the DESY test beam user workshop "Future Opportunities for Test Beams at DESY". Fifty participants from different user communities, ranging from LHC (ALICE, ATLAS, CMS, LHCb) to FAIR (CBM, PANDA), DUNE, Belle II, future linear colliders (ILC, CLIC) and generic detector R&D, presented their experience with the DESY II Test Beam Facility, their concrete plans for the upcoming years and a first estimate of their needs for beam time in the long-term future beyond 2025. A special focus was on additional improvements to the facility beyond its current capabilities. The findings of the workshop are summarised in [1]. A key point made by the users is that they are very happy with the current facility, especially with its reliability, the available infrastructure and the support. In terms of upgrades, the key requirement is higher rates, especially at the higher energies.

One possibility to meet this requirement would be to use the current R-Weg line, which was the former transfer line from DESY II to the DORIS storage ring, as a fourth beamline. Here, the primary bunches would be used, providing 6.3 GeV electrons with intensities of up to 10^{10} electrons per bunch. In practice, the beam would have to be reduced in intensity and broadened in order to offer usable rates for detector tests. Given the time scales for the high-luminosity LHC (HL-LHC) detector upgrades, realising this upgrade in the next years would be highly desirable.

The workshop outcome regarding the mid-term future of the facility is that the need for test beams – while difficult to exactly specify a decade in advance – will not diminish after the completion of the HL-LHC upgrades. Firstly, experience

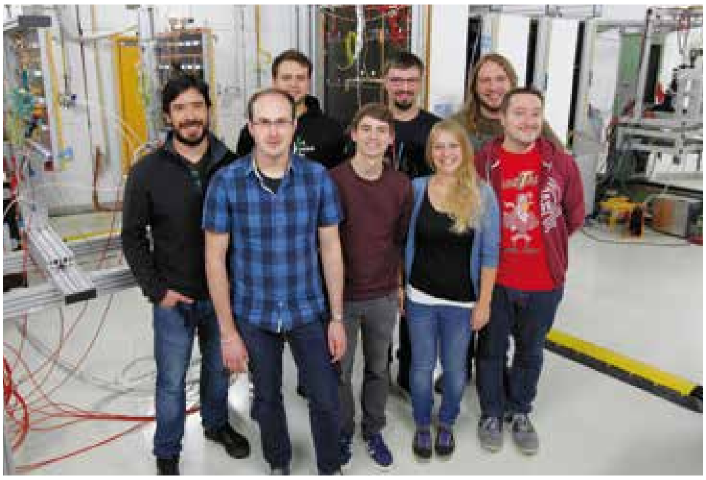

Figure 2

CBM transition radiation detector tested at DESY

shows that the need for test beams continues after the installation of upgraded detector systems to improve the understanding of the systems. Secondly, detector development activities for future facilities will continue to require high-quality test beams for many years to come.

Outlook for 2018 and beyond

The Christmas shutdown 2017 will again be a busy time for the facility. The complete Ethernet infrastructure will be upgraded, including a new core switch and the replacement of the complete cabling. From this point on, the whole test beam will feature gigabit connections and be ready for 10 gigabit operation. At the same time, the old beamline controls will be replaced to provide a better user experience.

The year 2018 will be equally busy. Beam time will start on 12 February and run till Christmas with a four-week-long summer shutdown. As of December 2017, 55% of the slots are booked and requests for beam time keep coming in. With 47.5% of requests, the LHC users are again the dominant user community. With the shutdown of the test beams at CERN in 2019 and 2020, DESY will operate the only multi-GeV test beam in Europe, and demand is expected to be even higher during that period.

Contact:

testbeam-coor@desy.de
Ralf Diener, ralf.diener@desy.de
Norbert Meyners, norbert.meyners@desy.de
Marcel Stanitzki, marcel.stanitzki@desy.de

References:

http://testbeam.desy.de
[1] J.-H. Arling et al., DESY-18-019.

Ultrafast and superlight.

Designing and manufacturing the ATLAS EoS board

DESY is strongly involved in the upgrade of the ATLAS experiment for the high-luminosity upgrade of the LHC (HL-LHC). An essential part of the ATLAS upgrade is the construction of a new inner tracking system. The inner tracker (ITk) consists of two major subsystems: the silicon strip tracker and the pixel detector. One of the key components for which DESY is responsible is the End-of-Substructure (EoS) card, which is the interface card between the building blocks of the silicon strip tracker upgrade, the so-called staves and petals, and the off-detector components. The challenge is to provide high-speed communication with minimum power consumption and a very reliable design with a lifetime of 15 years, use as little space as possible and make the device very radiation-hard. The EoS card is being developed and produced in close collaboration between the DESY ATLAS group and the DESY electronics groups (FE and ZE).

The ATLAS inner tracker upgrade

While the LHC is currently running very successfully and the ATLAS experiment is taking data with high efficiency, preparations have already started long ago for a high-luminosity upgrade of the LHC. The HL-LHC is supposed to deliver a factor 10 more luminosity than the current LHC. The HL-LHC programme will start in 2026 after a two-year shutdown, during which the accelerator will be upgraded. The current ATLAS tracking system will have reached the end of its life at this point, and in order to exploit the physics potential of the HL-LHC, it needs to be upgraded as well. The ATLAS collaboration decided to completely replace its current tracker with a new inner tracker. The ITk will be an all-silicon-based solution consisting of a silicon pixel detector and a silicon-strip-based tracker. The challenge regarding the ITk in general is to design a robust radiation-hard detector and to increase the granularity of the system while at the same time significantly reducing the material budget and the power consumption.

The strip tracker consists of one barrel with four double-sided layers and two end-caps with six doubled-sided disks each. The barrel is made up of so-called staves, which host the individual silicon strip modules on both sides on a common mechanical structure and provide all the services (power, data lines, cooling) to the detector modules. For the end-cap, the approach is quite similar, but in this case, the wedge-shaped building blocks are called petals (Fig. 1). The EoS cards, which act as the central interface between the stave or petal and the off-detector electronics, are located at the end of each stave or petal.

The technical design report for the ITk Strip Tracker [1] was approved in 2017. DESY is responsible for the construction of one of the strip tracker end-caps and has several other responsibilities, including the design, production and testing of all EoS cards.

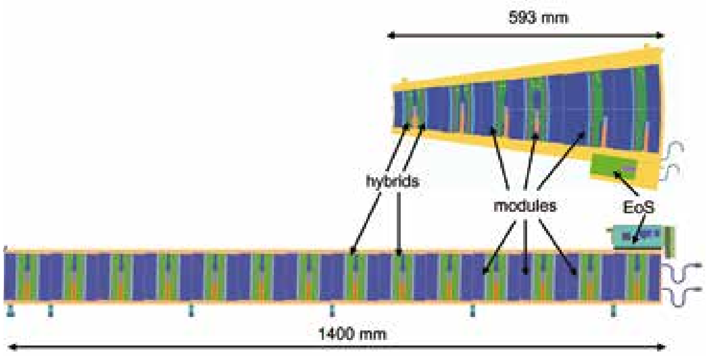

Figure 1

Drawing of a barrel stave (bottom) and an end-cap petal (top) for the ATLAS ITk strip tracker [1]

The EoS card

The EoS card is a key component of the strip tracker upgrade. It provides both low voltage (LV) and high voltage (HV) to the individual detector modules. The data communication uses a high-speed optical link with 10 GBit/s, which hands the commands to the modules and receives the data from the modules. The EoS card is the only location at which the entire stave or petal is electrically and optically connected to the outside world, which makes the reliability of the component a core issue. Besides the requirements on material budget and reliability, the space requirements are also quite stringent, e.g. the total height of the populated board may not exceed 5 mm.

For the HL-LHC, dedicated radiation-hard application-specific integrated circuits (ASICs) are being developed centrally at CERN and will be provided to all the LHC experiments. For high-speed communication between the detectors and the data acquisition, the low-power Gigabit Transceiver (lpGBT) ASIC is being developed, which can multiplex up to 40 data streams from the detector modules on a 10 GBit/s uplink. It distributes commands from the downlink to up to 14 modules on a stave or petal. The Versatile Link+ (VL+) converts the electrical signal from the lpGBT into an optical signal and vice versa. The optical link is essential to transfer data at 10 GBits/s over large distances.

To reduce the total amount of material required for services such as cabling, the input voltage to the staves and petals is set to 11 V. A dedicated DC-DC converter stage is used on each EoS card to generate the voltages suitable for the lpGBT and the VL+. DC-DC converters are designed to convert between different DC voltage levels with very high efficiency. While DC-DC converters are extensively used in industry, developing a DC-DC system that is radiation-hard and works in a strong magnetic field is a problem unique to the LHC experiments. It involves designing radiation-hard ASICs to control the DC-DC conversion and shielding the coils of the DC-DC system. To simplify the development, CERN has also taken on the task of providing the radiation-hard ASICs for the DC-DC converters to all the LHC experiments.

Designing the EoS card for 10 GBit/s and high-density interconnects such as ball grid arrays (BGA) and at the same time for robustness and minimal material consumption is a challenge. Reliability recommendations include e.g. using wider traces and thicker printed circuit boards (PCBs), which is of course not beneficial for reducing the amount of material. High-density BGA packages save space but require smaller structures, which may be less reliable. The DESY groups have put significant effort into establishing a solution that meets all the requirements with a focus on the highest reliability feasible.

To reduce the amount of material even further and simplify integration, only one power connector will be used to power both EoS cards of the stave or petal. This requires daisy-chaining both EoS cards in a master–slave configuration. As the interface between the petals and staves, the EoS card also has to meet many integration requirements, including tight space requirements.

As the DC-DC converters are operated in a magnetic field of 2 T, shield boxes for the coils are required, which makes these boxes the highest components on the EoS, exceeding the 5 mm envelope by 1 mm. Hence, the DC-DC package will be put on a separate thin PCB placed in a cut-out on the EoS PCB and then connected using wire bonds. This setup saves 1.5 mm and thus meets the stringent height requirements. Placing the DC-DC packages for both EoS on one side alleviates additional worries during integration by increasing the distance between two staves or petals.

Prototyping the current generation

The EoS card will use all the common ASICs provided by CERN in its final design, but currently none of these ASICs are available yet. For the prototyping, the first-generation GBTx/VL, which was designed for the LHC Phase I upgrades in 2018,

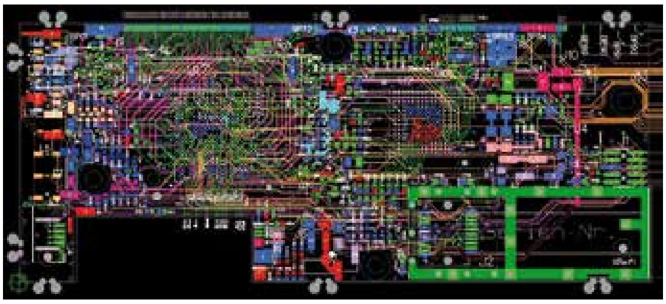

Figure 2

Layout of the EoS prototype

had to be used. A first set of prototypes was designed and produced at DESY (Fig. 2). The tests illustrated the validity of design and its robustness and were also a good test run for the ZE group to prepare for the final production, which will be done at DESY.

Heading for production

With the ATLAS upgrade components moving closer and closer to production, the EoS team at DESY (Fig. 3) is also getting ready for the major challenge. A total of 2000 EoS boards in six different variants need to be designed, produced and thoroughly tested till the end of 2020. Once inserted into ATLAS, they will become inaccessible for the next 15 years, so quality control and quality assurance are essential. The EoS team at DESY is currently designing the test stand infrastructure, which will allow the team to exercise all the cards, qualify them and then provide a detailed test report for each unit. All this will be highly automated to reduce the amount of time needed for testing during production – yet another challenge the team is currently addressing.

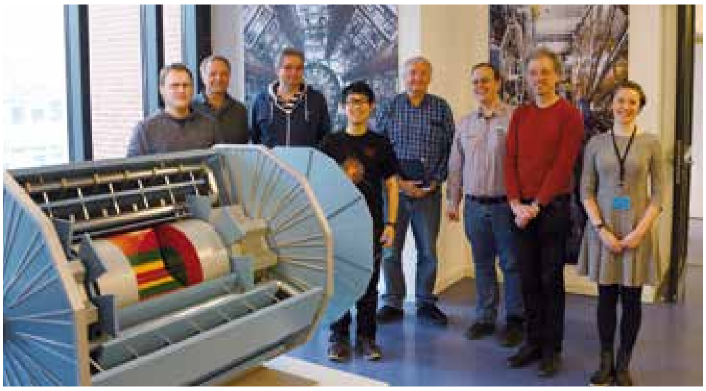

Figure 3

The team behind the project, combining skills and expertise from the DESY ATLAS and electronics groups (FE and ZE)

Contact:

Peter Göttlicher, peter.goettlicher@desy.de
Marcel Stanitzki, marcel.stanitzki@desy.de
Otto Zeides, otto-christian.zeides@desy.de

Reference:

[1] ATLAS Collaboration, CERN-LHCC-2017-005, https://cds.cern.ch/record/2257755.

Electron beams from lasers.

Electrons can “surf” in the wake of a laser to 100 MeV energies in distances of millimetres

The use of lasers to generate relativistic electron beams was proposed in 1979, and the field has since evolved to demonstrate multi-GeV electron beams. At the heart of these very compact accelerators is an interaction between a laser and plasma, where the intense laser pulse drives a charge separation wave trailing behind it. The use of plasma media allows for accelerating fields of the order of hundreds of gigavolts per metre, thus reducing the overall dimensions of the accelerator manifold. At DESY, such an accelerator is generating electron beams used for many applications, from advanced electron beam diagnostics to future uses in creating medically relevant X-ray sources.

Surfing the plasma wave

The seminal work of Toshiki Tajima and John Dawson outlining the principle of the laser wakefield accelerator (LWFA) was published in 1979 [1], describing how an intense laser pulse generates an electron wave as it travels through a plasma. This happens due to the ponderomotive force of the laser pulse – a force that acts on all charged particles and pushes them away from regions of high laser intensity. The electrons swiftly move away from the body of the laser pulse while the heavy and sluggish ions stay put. This creates a charge separation, where the excess positive charge density near the laser axis acts so as to pull the electrons back towards their initial positions. The electrons overshoot their initial location, and an electron oscillation is set up – similarly to a wake formed behind a speeding boat in water (Fig. 1, Panels a and b).

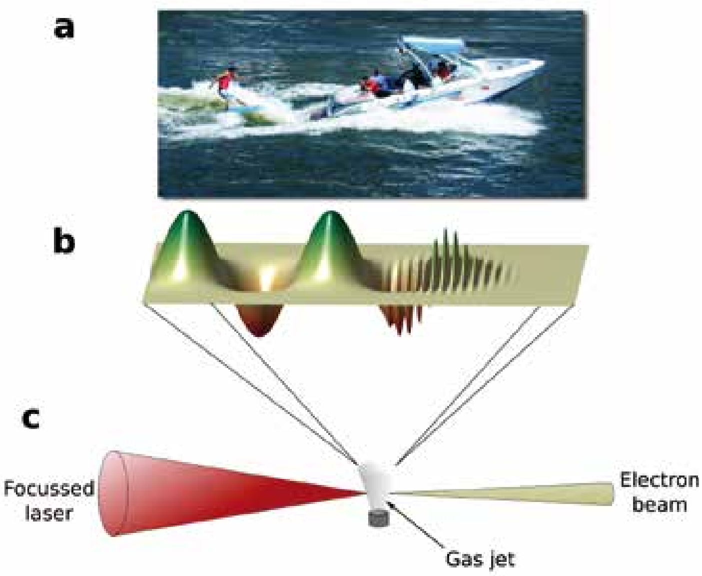

Figure 1

Example schematic of laser plasma accelerators (Panel c). The laser drives a wave in a plasma (Panel b), similarly to a boat in water (Panel a).

This Langmuir wave has a wavelength of $\lambda_p = 2\pi\, c/\omega_p$, where $\omega_p = (q_e^2 n_e/\varepsilon_0\, m_e)^{1/2}$ is the electron plasma frequency, with n_e being the electron plasma density. For electron densities of 10^{19} cm^{-3}, the wake wavelength is of the order of tens of micrometres. To resonantly excite such a plasma wave, laser pulses with a spatial extent and temporal duration of this order are required, restricting the focal spot size to tens of micrometres and the pulse length to tens of femtoseconds.

The amplitude of the plasma wave is proportional to the laser intensity, and thus very high laser intensities are required to create large accelerating fields. Extremely high laser strengths can actually lead to complete evacuation of electrons from the plasma wave, resulting in an ion “bubble” behind the laser pulse. The accelerating electric field strength in such a bubble can be estimated using Gauss’ law, and for $n_e = 10^{19}$ cm^{-3} and $\lambda_p = 10$ µm, yields $E \approx 300$ GeV/m. These field strengths are more than three orders of magnitude higher than the maximum gradients of state-of-the-art radio-frequency cavities, allowing 100 MeV energies to be reached in millimetres.

Electrons that are injected into the cavity gain energy by effectively “surfing” (as depicted in Fig. 1) on the steep accelerating gradient in the bubble, gaining energy in this cavity as the laser traverses the plasma at relativistic speed. As the electrons will rapidly gain enough energy to move relativistically with a velocity very close to c, they will overrun

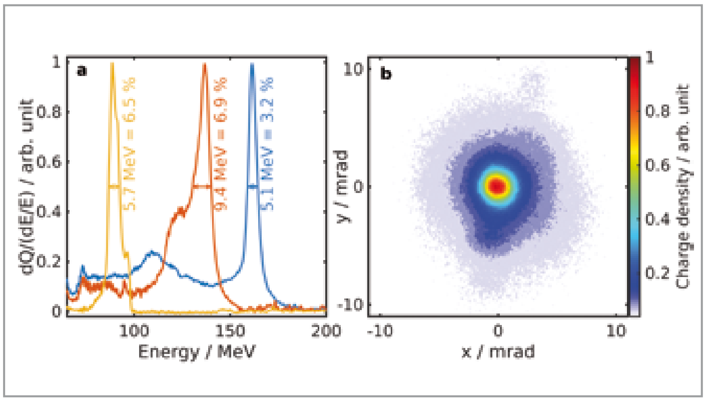

Figure 2

Example energy spectra (a) and beam profile (b) of electron beams generated with the compact laser wakefield accelerator

the plasma wake moving at the group velocity of the laser pulse. This is an inherent limitation for the maximum energy gain, and for a laser with angular frequency ω_0, it is given by $\Delta W = 2\ \omega_0^2 / \omega_p^2 m_e c^2$ [1].

If driven to high enough amplitudes, the plasma wave can break and some electrons can become trapped in the cavity. In addition to relying on such wave breaking, electrons can be injected into the plasma wave in a few different ways, and the method of choice will affect the properties of the electron beam. For the self-injection method, where some electrons will be driven to dephase from the collective wave motion, the correct experimental parameters can lead to the generation of very high-quality beams. These electron bunches typically have charges of the order of tens of picocoulombs, a divergence of the order of a few milliradians and relative energy spreads of a few percent at ~100 MeV energy level. Some typical experimentally measured spectra and a beam profile are shown in Fig. 2.

Using the beams

Such a compact source can be very versatile, and the generated electron beams can be used for many different applications. One such application is testing, commissioning and calibrating of advanced beam diagnostics later to be used on the FLASHForward plasma accelerator at DESY's FLASH free-electron laser facility [2]. The availability of the beams and flexibility of the setup allows us to cross-calibrate and compare non-invasive charge diagnostics, such as the DaMon dark-current monitor [3] and integrating current transformers, with standard methods, such as profile screens. Additionally, transition radiation studies will be performed to gain understanding about the temporal structure of the femtosecond-duration electron beams, allowing for the development of more such diagnostics.

Work to characterise active plasma lenses [4] – compact plasma-based beam optics providing very strong and linear radially symmetric focusing forces – will be performed using this electron source. Such experiments allow the fine properties of the lens to be determined. Once characterised, the compactness of these plasma lenses will enable us to perform focusing scan measurements to determine the electron beam emittance.

The electrons injected into the plasma cavity also undergo betatron oscillations in the strong linear transverse focusing fields and emit radiation known as betatron X-rays. This radiation can be used to understand the properties of the electron beam dynamics within the plasma itself, allowing for non-invasive and "free" diagnosis of the beam emittance. This can prove another valuable diagnostic for the FLASH-Forward experiment, which is currently being commissioned, with first plasma experiments planned for mid-2018.

The short temporal duration of the electron beams – of the order of the plasma wavelength on the femtosecond scale – makes them ideal for probing transient phenomena. One approach for such probing is scattering another laser pulse off the accelerated electron beam. In a process called inverse Thomson scattering, the photon energy is upconverted to $\omega_t = 4\gamma_e^2\omega_0$ with γ_e being the electron gamma factor. Using an 80 MeV electron beam, photon energies of 100 keV are produced. This kind of X-ray energies would allow fluorescent imaging of biological materials, an exciting new avenue in diagnosing tumorous tissue and tracking the evolution of antibodies and drugs throughout the body.

More to come

The field of laser wakefield accelerators is quickly growing, and the research performed at DESY is providing excellent input for the overall developments. Using genetic algorithms to optimise the setup for any required electron beam property will soon allow for even better control over the relativistic electron beams, proving invaluable insight into the underlying plasma physics and generating even more useful beams for advanced prototyping and testing applications.

Contact:

Kristjan Poder, kristjan.poder@desy.de

References:

[1] T. Tajima and J. Dawson, Phys. Rev. Lett. 43, 267 (1979).
[2] http://forward.desy.de
[3] D. Lipka et al., DESY Technical Note, 2008-01.
[4] J. van Tilborg et al., Phys. Rev. Lett. 115, 184802 (2015).

The European Open Science Cloud.

DESY's contribution to a shared European computing infrastructure for science

Almost ten years ago, the European Commission launched the idea of a European Open Science Cloud (EOSC), a programme to support European scientists in taking the lead in all areas of data-driven sciences. Initiated and monitored by a High Level Expert Group, a series of large European-wide projects was launched to evaluate possible governance models, infrastructures and underlying technologies, with the aim to finally implement the first prototype by 2020. In 2017, the European Commission published the first official EOSC Declaration, signed already by over 80 stakeholders. From the very beginning, DESY has been a partner in a well-selected set of projects within the EOSC, accepted as a world-class expert in all areas of data management and data analytics.

The idea of a European Open Science Cloud

In 2005, the European Commission initiated the idea of a European Open Science Cloud (EOSC, Fig. 1) [1] "to give Europe a global lead in scientific data infrastructures and to ensure that European scientists reap the full benefits of data-driven science", targeting its first implementation for 2020. Besides putting in place a High Level Expert Group composed of members from a wider range of sciences in Europe and advisors from all over the world, charged with defining the EOSC objectives, a continuous stream of calls for proposals was released in preparation within the EU Horizon 2020 framework.

The corresponding projects should aim to establish a sustainable governance model, to unify the already implemented European-wide scientific e-infrastructures and to provide the necessary software and technology stacks in the areas of high-throughput computing (HTC) and high-performance computing (HPC). In doing so, they should use emerging cloud methodologies wherever possible and enable the integration of national initiatives on one hand and connect to worldwide private and public cloud providers on the other.

Moreover, in addition to the political and technological prerequisites, the High Level Expert Group suggested a set of data management policies that the European Commission should encourage or enforce for future data-driven scientific projects. One important requirement is that all projects expecting financial support from the European Commission should present a Data Management Plan precisely describing the flow and governance of precious data during and after the project's lifetime. Especially important is the implementation of the principles of findability, accessibility, interoperability and reusability (FAIR), regarded as the primary building blocks for a successful and responsible use and reuse of scientific data.

DESY and the EOSC

As the DESY computing facility is mandated to support large international projects with outstanding data management challenges, such as the Worldwide LHC Computing Grid (WLCG), the European XFEL, CTA and others, becoming an active part in the EOSC is inevitable for the research centre in order to ensure DESY-related sciences the best starting point for their future success.

The EOSCpilot project

An essential prerequisite for building an EOSC infrastructure is the establishment of a sustainable governance model, allowing the EOSC members not only to share compute, storage and network resources but also to buy into external private cloud offerings. This requires a clear understanding of ownership and industry-level payment procedures. All this is pioneered within the EOSCpilot project (Fig. 2), which was launched at the beginning of 2017 and will conclude at the end of 2018.

Besides the governance model, the project aims at presenting a catalogue of services that either are available

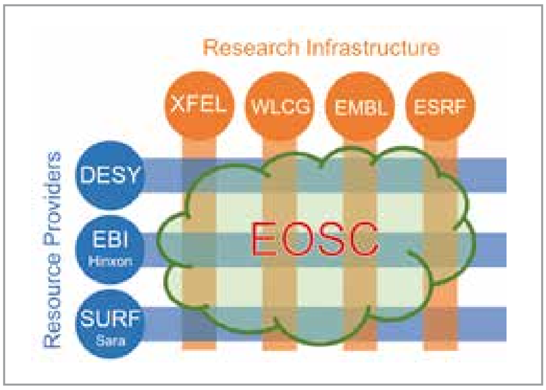

Figure 1
Design of the European Open Science Cloud

today or have been identified as likely to become important in the future. As those services have either to be federated or at least to interoperate, a work package has been established on the European-wide interoperability of services, in which DESY is primarily involved. As a side effect, the DESY computing facility is building its own cloud service infrastructure, prepared to interact with other services within the European science ecosystem. To synchronise this important development and infrastructure work with realistic requirements by the various scientific groups, DESY took over so-called "shepherdships" for some of the communities involved in the EOSCpilot project. This work is embedded in the context of Pilot Science Demonstrators, a work package responsible for synchronising the scientific requirements with the work of the development and infrastructure working groups.

dCache, INDIGO and eXtreme DataCloud

In addition to supporting DESY's particular interest in helping to shape the governance and policies of the European open science ecosystem, the DESY IT group has been continuously participating in a series of technology projects, in particular in the area of big data. The product DESY has to offer here is dCache, a technology for storing and delivering huge amounts of data on a variety of storage media. dCache.org is a collaboration between DESY, Fermilab and the Nordic Data Grid Facility, with the University of Applied Sciences in Berlin as an associated partner, aiming to attract students to the challenges of scientific data management. The dCache technology is used at more than 60 data-intensive sites around the world and serves a variety of sciences.

Within INDIGO-DataCloud, a consortium of 26 European partners from 11 countries, dCache got funding to adjust the technology's security subsystem to the requirements of a common European federated authentication system. Furthermore, storage providers from KIT, INFN, the Poznań Supercomputing and Networking Centre (PSNC) and DESY agreed on a common schema of data qualities in storage by initiating a working group in the framework of the Research Data Alliance. Subsequently, those definitions were integrated into a standard industry protocol, supervised by the Storage Networking Industry Association (SNIA). As a result, five locations in Europe interconnected their storage resources within a prototype field experiment and made them available through common protocols encompassing standard mechanisms to select the quality of the required storage space, including tape and low-latency storage devices.

In November 2017, the data management part of INDIGO-DataCloud was continued in the Horizon 2020 eXtreme-DataCloud project (XDC).

dCache, XDC and the European Data Lake

With the results of the INDIGO-DataCloud project, the vision of XDC is to build a European Data Lake supporting data-intensive scientific communities as well as the long tail of science with the already existing European computing infrastructures. Thanks to the data lake concept, existing and in particular new distributed European e-infrastructures will have to spend significantly less efforts on designing and implementing their data management architectures.

Figure 2
The European Open Science Cloud pilot project

Figure 3
The two data-driven Horizon 2020 projects DESY is involved in.

Data management core services, with well-defined interfaces, will be available across Europe and only need to be customised according to the needs of the particular community and their financial capacity. Those core services will include but not be limited to the secure storage of data and the automatic and secure transfer of massive amounts of data between data centres, following customised data lifecycle workflows. The workflows include the predefined transition of data between different storage qualities and between different authentication policies, essentially implementing the data management plans of the data owners.

Thanks to the long experience of the data centres and communities involved in this project, valuable blueprints for such a highly distributed data orchestration can be provided. Similarly, with a robust data lake in terms of data storage, security, safety and transfer, as well as a basic data orchestration machinery, large parts of the core data management operations of the individual experiments can be replaced by the experiment's agnostic lake functionality. As such, the core data management operations benefit from the advantages of common interfaces and the expertise of the data centre operations teams.

Moreover, as the data lake concept significantly simplifies the implementation of the FAIR principles, it is an enabling technology for combining high-quality data from different communities exploring new areas in science.

Contact:

Patrick Fuhrmann, patrick.fuhrmann@desy.de

Reference:

[1] "Realizing the European Open Science Cloud", doi:10.2777/940154.

An interdisciplinary scientific computing centre.

Providing services for all DESY branches of science

DESY carries out research in many different branches and at different locations, both at the two DESY sites and at remote sites, such as CERN, various astroparticle experiments or remote light sources. It is the mission of the DESY computing groups in Hamburg and Zeuthen to best serve all DESY communities, and increasingly also external groups and guests. As a general concept, the DESY computing groups aim for large, multipurpose infrastructures to efficiently serve different communities, while creating specialised infrastructures when necessary. This article briefly presents all infrastructures of the interdisciplinary Scientific Computing Centre at DESY.

Grid and NAF at DESY in Hamburg

The DESY Grid infrastructure provides a large portfolio of Grid services.

The actual workhorses are a large common batch system based on HTCondor, with about 20 000 cores, and high-capacity dCache storage elements. These resources serve different projects as multipurpose infrastructures:

- Worldwide LHC Computing Grid (WLCG) Tier-2 for the ATLAS, CMS and LHCb experiments
- Grid for the HEP collaborations Belle II and ILC
- Additional share of resources within the National Analysis Facility (NAF) for researchers of German institutes participating in the Helmholtz Alliance “Physics at the Terascale” – mainly ATLAS, CMS, ILC, and Belle II
- Analysis effort of the former HERA experiments (“HERA legacy”)
- Numerous small communities

In addition, the NAF has been in operation at DESY since 2007. It complements the DESY and German Grid resources. The facility was set up in the framework of the Helmholtz Alliance “Physics at the Terascale” and was initially intended for researchers of German institutes working for ATLAS, CMS, LHCb, Belle II and ILC. In the meantime, however, HERA legacy analysis efforts are also being supported, as well as German Belle activities. As the NAF supports direct interactive access, it allows for fast-response workflows necessary for development, debugging, testing and small-scale private production – important complements to the Grid infrastructure, which provides computing resources for a continuous massive production albeit has higher latencies.

Although there is a natural difference between job profiles running on the NAF and those running on the Grid, there are convenient commonalities arising from the intrinsic massive “embarrassing parallelism” in most high-energy physics data analysis and simulation jobs.

The dCache storage elements provide long-term storage for experimental and user data with several petabytes in curation for each group. Deployment and management of the storage elements have been automated and can be easily scaled thanks to the distributed setup, thus allowing for high parallelised input and output. NAF and Grid users have identical access to these central data stores. Additionally, NAF users have access to a fast scratch space for more direct and interactive work.

In addition to compute and storage resources, DESY also offers underlying services such as file catalogues and membership services. Since 2016, DESY has been operating the Belle II collaborative services. As the last missing piece, a collaboration membership management system was developed and put into production in 2017.

Infrastructures at DESY in Zeuthen

HPC

High-performance parallel computing (HPC) has a long history in Zeuthen, starting with special-purpose architectures for lattice quantum chromodynamics (LQCD) simulations developed by INFN and DESY up to a server cluster installation containing about 1800 CPU cores. Though LQCD projects (under the umbrella of the John von Neumann Institute for Computing, NIC) are still dominating the cluster utilisation, theoretical astroparticle physics applications are catching up. The computing components of the cluster are connected via a low-latency Fourteen Data Rate (FDR) InfiniBand network. To ensure fast data transfer, all nodes are connected to a distributed parallel Lustre storage system.

Figure 1

New cold aisle containment inside the RZ1 data centre at DESY in Zeuthen

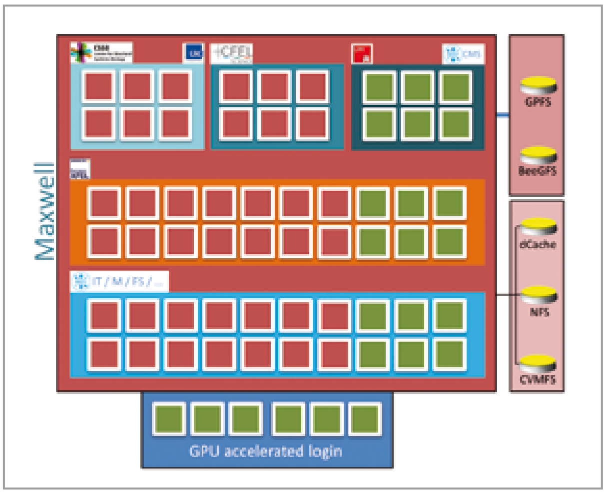

Figure 2

Layout of the Maxwell HPC cluster

Grid and compute farms

The Zeuthen computer centre operates the European Tier-1 centre for the IceCube neutrino experiment, supports the Cherenkov Telescope Array (CTA) and runs the WLCG ATLAS Tier-2 (4000 cores) and a local compute farm (3000 cores). In addition to CPU resources, about 100 general-purpose graphics processing units (GPGPUs) are used mainly by IceCube. The Grid and compute farms are connected to a large dCache storage system (5 PB) as well as to a Lustre-based parallel file system (2 PB). Figure 1 shows a view into a computing room in Zeuthen.

Project support

Members of the Zeuthen computer centre are responsible for the design and definition of the on-site information and communications technology infrastructure at the two CTA sites and are strongly integrated into the IceCube computing strategy. In the context of the photoinjector test facility PITZ, they contribute system administrative activities (data acquisition and storage) and a significant part of embedded software development.

Maxwell HPC cluster at DESY in Hamburg

Launched in 2011, the Maxwell HPC cluster has quickly grown into a massive HPC platform. The Maxwell cluster is a truly collaborative and cross-disciplinary compute infrastructure open also for different tenants.

The Maxwell cluster (Fig. 2) serves a wide range of different applications, ranging from data analysis (PETRA III, European XFEL, etc.) over deep learning (high-energy physics) to massive parallel computational tasks (simulations for laser wakefield accelerators and PETRA IV design studies, molecular dynamics and photon–matter interactions, etc.).

In 2017 and at the beginning of 2018, the computational resources of the Maxwell cluster were increased by almost a factor of 4, largely driven by the start-up of the European XFEL. The HPC platform meanwhile comprises close to 500 compute nodes, serving roughly 24 000 compute threads, and 180 TB of memory. AI-based frameworks in particular benefit from GPGPU acceleration. Currently, 60 nodes are equipped with a total of 90 GPGPUs.

Data storage is offered for PETRA III, FLASH, the European XFEL and others using the GPFS cluster file system (currently 4.5 PB) and BeeGFS (currently 400 TB) via the fast InfiniBand network. As of early 2018, the dCache instance of the European XFEL is also being integrated into the cluster.

Convenient access to the HPC platform is provided by five GPGPU-accelerated graphical login nodes – the Maxwell display – to graphical applications (ANSYS, Avizo, COMSOL Multiphysics, MATLAB, ParaView, etc.). The Maxwell display also enables collaborative workflows using a desktop-sharing technology.

Contact:

Andreas Gellrich, andreas.gellrich@desy.de
Thomas Hartmann, thomas.hartmann@desy.de
Yves Kemp, yves.kemp@desy.de
Frank Schlünzen, frank.schluenzen@desy.de
Peter Wegner, peter.wegner@desy.de

References:

[1] www.dcache.org; grid.desy.de; naf.desy.de
[2] dv-zeuthen.desy.de/services/grid; hpc.desy.de
[3] confluence.desy.de/display/IS/Maxwell

Towards a Digital Campus.

DESY's Computer-Aided Facility Management (CAFM) platform

The DESY campus is a rapidly growing multidisciplinary research campus, which attracts increasing numbers of users, guests and partner institutes. A Digital Campus helps to cope with the rising number of service requests.

Motivation and challenges

Top-level research needs the best environments. The DESY campus is hosting world-class research facilities, making it a busy environment with large numbers of on-site users. Many additional infrastructures, such as specialist workshops, computing infrastructure, meeting and conference rooms, guest houses and recreation areas, make the campus a welcoming and efficient place for excellent research.

Being well prepared is one of the important ingredients to effective on-site activities, and in many cases preparation starts in places away from the facilities, often even outside the campus: Maintenance work is planned in offices and meetings before being carried out at the facilities; components of experimental setups are prepared at partner laboratories, before being shipped to DESY; visits to the campus – finding on-site contacts, locating meeting rooms, booking accommodation in the guest house – are organised while still at home, before entering the premises.

The aim of the Digital Campus is to enable users to access campus services and facilities even when they are not at their location. The Digital Campus addresses both guests who are still off-site and preparing a stay on the campus as well as campus staff in their offices who are planning activities at a facility elsewhere on the campus. The tasks of the Digital Campus include providing orientation to users, increasing the accessibility and effectiveness of services, supporting operation and maintenance work at research infrastructures and strengthening cooperation.

The DESY CAFM

The primary concept of the Digital Campus is to provide visual, location-based access to services and information. Figure 1 shows a digital campus map, where services and special facilities are marked as points of interest. These POIs provide access to web services and further information.

Figure 1

Digital Campus mobile map with points of interest (POI) representing services

Figure 2

Functional components of computer-aided facility management at DESY

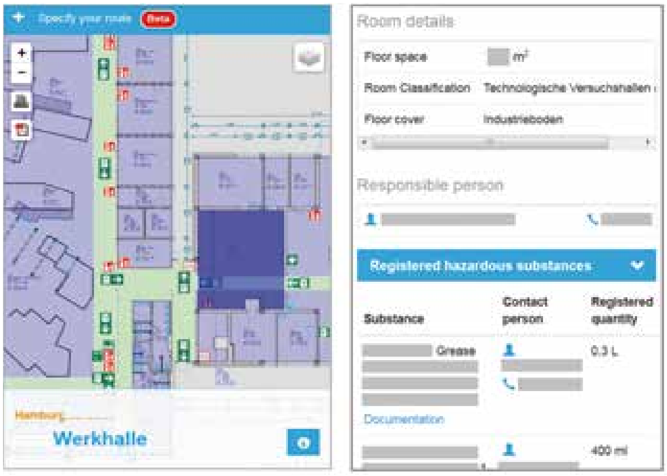

Figure 3

Room book visual and textual representation

Figure 4

Site map with navigator and POI selector

Campus map and navigation are the most prominent and visible components of the Digital Campus, but they reflect only a very small fraction of the available data pool. Behind the scenes, the Digital Campus holds data and plans for building management, campus and terrain documentation, technical safety, information and communications technology (ICT) infrastructure and many other technical disciplines.

The Digital Campus is based on the DESY Computer Aided Facility Management (CAFM) system, which is illustrated in Fig. 2: A collection of expert tools for providing and maintaining the many different campus services are integrated in such a way that they operate on a single source of standardised data and processes.

Offering expert tools enables service providers to easily extend their portion of the information pool and keep it up to date, which in turn will benefit other users in their work. Based on integrated and well-maintained data, workflows can be optimised, time-consuming searches and duplicate work can be avoided, and collaboration can be strengthened.

Objective: one digital lab

A central element of the Digital Campus is the digital room book. Figure 3 shows an example that records the characteristics of rooms and their current occupancy in conjunction with the floor plan. Additional records list safety technology, locks and keys, ICT connectors, hazardous substances and many other technical installations.

The openly visible part of the room book helps DESY staff members and visitors to find contacts and locations. Service providers use specialised tools for tasks such as cleaning management, key management, inspections of technical installations, safety inspections, outfitting, maintaining and repairing equipment and many more.

Figure 4 shows a part of the digital site plan, the second important central pillar of the Digital Campus. The plan notes the location of buildings and roads, numerous service points (POIs) and many routes of supply lines. For visitors and DESY staff members, the site plan provides orientation and navigation to e.g. contact persons, service facilities, conference rooms and guest houses. Service providers use the site plan in the planning and execution of construction projects.

With kilometre-long accelerator systems, located in tunnels underneath the campus, passing through several buildings, connected with numerous utilities and operated from central control rooms, the room book and the site plan of course form one tightly integrated entity.

@home, @work, @anywhere

An essential element of the Digital Campus is user interfaces that are tailored to the needs and capabilities of the users. Only intuitive user experience can ensure the Digital Campus is extensively used.

A large group of users are people coming to DESY who access the Digital Campus while on their way. They are offered a high-performance user interface for mobile devices, which primarily includes the site plan, navigation, contacts and POI-based information. For users who need information at their office desk, a more comprehensive web interface is available, which offers advanced information searches and evaluations. Service providers have dedicated applications available for e.g. editing building, site and installation plans and updating the various databases.

Contact:
Jens Kreutzkamp, jens.kreutzkamp@desy.de
Lars Hagge, lars.hagge@desy.de

Synergies in library systems.

From platform(s) to hub

At the end of 2000, DESY was one of the first customers of the company ExLibris in Germany to implement the library system ALEPH. A self-checkout system that allows automatic borrowing and return was introduced at the DESY central library in Hamburg over 15 years ago. The introduction of a modern radio-frequency identification (RFID)-based identification system in 2015 for all media was a first step towards the migration of the DESY library from the commercial library system towards open-source software.

Since 2006, publications created with DESY participation have been made visible and accessible through the DESY publication database. The first version of this system was based on proprietary software developed at Forschungszentrum Jülich. In 2013, the JOIN^2 collaboration, which includes DESY and Forschungszentrum Jülich as well as other Helmholtz centres and RWTH Aachen University, was founded, and the DESY library group migrated the publication database to the JOIN^2 software, which is based on the INVENIO system developed at CERN.

Migration preparations

Since INVENIO can also be used as a library system, it was a good idea to integrate the publication database and catalogue in order to be able to provide a uniform user interface. GSI in Darmstadt was another JOIN^2 project partner that wanted to use INVENIO as a library system. And the CERN library too was successfully migrated from the library system ALEPH to the current CERN Document Server (CDS) as a library system several years ago.

Therefore, the DESY library group was confident that the migration could successfully be carried out at DESY. Although the task was quite elaborate, it was successfully completed in summer 2017. In retrospect, it should be noted that, in addition to the actual data migration and the planned redevelopments of the self-booking interface, further adjustments were needed, which significantly increased the complexity of the project.

Data consolidation and clean-up

The members of the library groups at both DESY sites tirelessly consolidated and adjusted data throughout the migration phase. Data adjustment was urgently needed especially for the user data, since ALEPH had its own user administration, whereas the new system accesses the data of the DESY registry. Since summer 2017, all DESY media across all locations, including the DESY publications, can be searched worldwide in a common system based on JOIN^2.

Figure 1

RFID self-check-out station at the DESY central library in Hamburg

Figure 2

Terminal providing access to the DESY library homepage and databases

Open access and open article processing charges

DESY centrally supports various open-access options for authors either through international initiatives (e.g. arXiv, SCOAP[3]) or locally (DESY publication database). For individual publications, article processing charges are paid centrally for open-access journals. Open-access publications in hybrid journals are discouraged. To demonstrate how reporting on fee-based open-access publishing can be made more transparent and reproducible across institutions, DESY contributes to the database of the Open APC initiative, a project that provides cost data on 48 605 open-access journal articles, amounting to over 93 million euros and contributed by 153 institutions.

open access

Synergies

The well-known high-energy physics database INSPIRE, the data of which is supplemented and curated by the DESY library group, is also based on INVENIO. However, the speed of development of INSPIRE is so high that JOIN² cannot compete here, resulting in fewer synergies than hoped for. However, in the workflow of DESY publishing products, such as dissertations (DESY thesis series), DESY proceedings and "DESY red reports", which are also included in INSPIRE, the group was able to exploit synergies and to simplify and accelerate processes through the open interfaces of the new system.

Users can log into the new library system with the usual DESY access data, view their media account, renew media and place pre-orders. A comfortable search in the catalogue with focus on the different locations is possible. Even the display of relevant media that are not in stock (so-called "book proposals") is available. The user can order these online as reservations, and the library will make them available as soon as possible.

iNSPIRE

Outlook

In the future, articles delivered by interlibrary loan will also be made available to the users through the library system in the private group areas. Along with easy access, this method has the advantage that, in addition to the article, the associated bibliographic information is also provided, and the article is immediately available to other group members. These data can thus be used e.g. for citations in the users' own publications. With BibTeX, EndNote and RIS, the DESY library offers export formats that are compatible with current literature management programs. The DESY publication database is thus becoming more and more a central hub for the various library services that DESY is offering to all users across its campuses. For all questions about the use of the new system and the supply of literature, the DESY library team in Hamburg and Zeuthen is always at your disposal.

LIBRARIES PDF >>

Contact:

l.desk@desy.de and library.zeuthen@desy.de

References:

http://library.desy.de

http://library-zeuthen.desy.de


NUCLEAR
SCIENCE
VOL. 12
1962
OF
NUCLEAR
SCIENCE
VOL. 13
1963

References

Committees.

DESY Foundation Council

Representatives of the Federal Republic of Germany

A. Hohlt
(Federal Foreign Office)

MinR'in **O. Keppler**
(Federal Ministry of Education and Research)

MinR Dr. **V. Dietz** (Chair)
(Federal Ministry of Education and Research)

Representatives of the Free and Hanseatic City of Hamburg

LRD Dr. **R. Greve**
(Ministry of Education and Research)

N. Abend
(Ministry of Education and Research)

Representatives of the Federal State of Brandenburg

H. Roth
(Ministry of Finance)

C. Feller
(Ministry of Science, Research and Culture)

Representatives from science and industry

Prof. Dr. **U. Beisiegel**
(President, Georg-August-Universität Göttingen)

Dr. **M. Kraas**
(Olympus Surgical Technologies)

Dr. **G. Mecke**
(AIRBUS)

Dr. **C. Quitmann**
(Lund University)

Guests

Chair of the DESY Scientific Council
Prof. Dr. **P. Drell** (SLAC, USA)

Chair of the DESY Scientific Committee
Dr. **M. Kasemann**

President of the Hermann von Helmholtz Association
Prof. Dr. **O. Wiestler**

DESY Equal Opportunity Officer
A.-C. Jauch

Chair of DESY Works Council
K. Lando

DESY Board of Directors

Dr. **R. Brinkmann**
(Accelerator Division)

Prof. Dr. **H. Dosch**
(Chairman of the DESY Board of Directors)

Prof. Dr. **J. Mnich**
(Particle Physics and Astroparticle Physics Division)

C. Scherf (until 31 October 2015)
C. Harringa (acting since 1 November 2015)
(Administrative Division)

Prof. Dr. **E. Weckert**
(Photon Science Division)

Prof. Dr. **C. Stegmann**
(Representative of the Directorate in Zeuthen)

DESY Scientific Council

Dr. **R. Abela**
PSI (CH)

Prof. Dr. **O. Botner**
Uppsala University (SE)

Prof. Dr. **J. Daillant**
Soleil Synchrotron (FR)

Prof. Dr. **P. Drell** (Chair)
SLAC (USA)

Prof. Dr. **G. Hoffstaetter**
Cornell University (USA)

Prof. Dr. **K. Hämäläinen**
University of Helsinki (FIN)

Prof. Dr. **Y.-K. Kim**
University of Chicago (USA)

Prof. Dr. **T. Lohse**
Humboldt University Berlin (DE)

Prof. Dr. **L. Merminga**
TRIUMF (CA)

Dr. **B. Murphy**
Christian-Albrechts-University Kiel (DE)

Prof. Dr. **S. Ritz**
University of California (USA)

Prof. Dr. **L. Rivkin**
PSI (CH)

Dr. **E. Shaposhnikova**
CERN (CH)

Prof. Dr. **J. Womersley**
STFC (UK)

Prof. Dr. **N. Wermes**
University of Bonn (DE)

Prof. Dr. **L. Young**
ANL (USA)

and the chairs of

DESY MAC: Dr. **O. Bruening**
CERN (CH)

DESY PRC: Dr. **P. Burrows**
University of Oxford (UK)

DESY PSC: Dr. **Ch. David**
PSI (CH)

DESY Scientific Committee: Dr. **M. Kasemann**
DESY

European XFEL: Prof. Dr. **R. Feidenhans'l**
European XFEL (DE)

DESY Scientific Committee

M. Aldaya Martin (DESY)
R. Aßmann (DESY)
F. Beckmann (HZG)
T. Behnke (DESY)
M. Bieler (DESY)
I. Bloch (DESY)
K. Borras (DESY)
W. Buchmüller (DESY)
A. Burkhardt (DESY)
K. Büßer (DESY)
F. Calegari (DESY)
H. Chapman (DESY)
M. Diehl (DESY)
R. Doehrmann (DESY)
J. Dreyling-Eschweiler (DESY)
W. Drube (DESY)
S. Fiedler (EMBL)
T. Finnern (DESY)
B. Foster (DESY)
A. Frey (KET)
E. Gallo (DESY)
H. Graafsma (DESY)
I.-M. Gregor (DESY)
Ch. Grojean (DESY)
G. Grübel (DESY)
V. Gülzow (DESY)
B. Heinemann (DESY)
M. Hempel (DESY)
K. Honkavaara (DESY)
K. Jansen (DESY)
R. Kammering (DESY)
M. Kasemann (DESY, Chair)
C. Kluth (DESY)
M. Kowalski (DESY)
G. Kube (DESY)
F. X. Kärtner (DESY)
M. Martins (U Hamburg)
N. Meyners (DESY)
K. Mönig (DESY)
S. Molodtsov (European XFEL)
B. Murphy (KfS)
A. Mußgiller (DESY)
T. Naumann (DESY)
C. Niebuhr (DESY)
D. Nölle (DESY)
K. Peters (DESY)
E. Plönjes-Palm (DESY)
M. Pohl (DESY)
D. Reuther (DESY)
R. Röhlsberger (DESY)
R. Santra (DESY)
M. Schmitz (DESY)
V. Schomerus (DESY)
S. Schreiber (DESY)
Ch. Schroer (DESY)
H. Schulte-Schrepping (DESY)
A. Schulz (DESY)
Ch. Schwanenberger (DESY)
U. Schwanke (HU Berlin)
A. Schwarz (DESY)
T. Schörner-Sadenius (DESY)
G. Servant (DESY)
S. Spannagel (DESY)
A. Stierle (DESY)
K. Tackmann (DESY)
S. Techert (DESY)
M. Tischer (DESY)
R. Treusch (DESY)
Y. Umhey (DESY)
J. Viefhaus (DESY)
M. Vogt (DESY)
N. Walker (DESY)
G. Weiglein (DESY)
H. Weise (DESY)
H.-Ch. Wille (DESY)
K. Wittenburg (DESY)
W. Wurth (DESY)
H. Yan (DESY)

Machine Advisory Committee (MAC)

Prof. Dr. **R. Bartolini** (U Oxford, UK)
Dr. **O. Brüning** (CERN, CH, Chair, from May 2017)
Dr. **A. Faus-Golfe** (IFIC Valencia, SP)
Dr. **M. Ferrario** (INFN, IT)
Dr. **Z. Huang** (SLAC, USA)
Prof. Dr. **A. Jankowiak** (HZB, DE, Chair, until April 2017)
Dr. **P. Raimondi** (ESRF, FR)
Prof. Dr. **A. Wolski** (U Liverpool, UK)
Dr. **Ch. Steier** (LBNL, USA)

Physics Research Committee (PRC)

Prof. Dr. **P. Burrows** (U Oxford, UK, Chair)
Prof. Dr. **A. Boehnlein** (JLab, USA)
Prof. Dr. **L. Covi (**U Göttingen, DE)
Prof. Dr. **L. Feld** (RWTH Aachen, DE)
Prof. Dr. **J. Fuster Verdú** (IFIC Valencia, SP)
Prof. Dr. **L. Köpke** (U Mainz, DE)
Prof. Dr. **R. Ong** (UCLA, USA)
Prof. Dr. **L. Rosenberg** (U Washington, USA)
Prof. Dr. **R. Wallny** (ETH Zürich, CH)

Ex-officio members:
Prof. Dr. **H. Dosch** (DESY)
Prof. Dr. **J. Mnich** (DESY)
Prof. Dr. **E. Weckert** (DESY)
Dr. **R. Brinkmann** (DESY)
Prof. Dr. **C. Stegmann** (DESY)

German Committee for Particle Physics (KET)

Prof. Dr. **S. Bethke** (MPP München)
Prof. Dr. **K. Borras** (DESY)
Prof. Dr. **V. Büscher** (U Mainz)
Prof. Dr. **K. Desch** (U Bonn)
Dr. **M. Elsing** (CERN)
Prof. Dr. **A. Frey** (U Göttingen)
Prof. Dr. **T. Hebbeker** (RWTH Aachen)
Prof. Dr. **W. Hollik** (MPP München)
Prof. Dr. **M. Kobel** (TU Dresden)
Prof. Dr. **J. Mnich** (DESY)
Prof. Dr. **P. Schlepe**r (U Hamburg)
Prof. Dr. **M. Schumacher** (U Freiburg)
Prof. Dr. **G. Weiglein** (DESY)
Prof. Dr. **C. Zeitnitz** (U Wuppertal, Chair)
Prof. Dr. **D. Zeppenfeld** (KIT)

German Committee for Astroparticle Physics (KAT)

Prof. Dr. **J. Blümer** (KIT)
Prof. Dr. **K. Danzmann** (U Hannover)
Dr. **A. Haungs** (KIT)
Prof. Dr. **M. Lindner** (MPP München)
Prof. Dr. **L. Oberauer** (TU München)
Prof. Dr. **M. Pohl** (DESY)
Prof. Dr. **E. Resconi** (TU München)
Prof. Dr. **C. Stegmann** (DESY)
Prof. Dr. **S. Wagner** (U Heidelberg)
Prof. Dr. **C. Weinheimer** (U Münster)
Prof. Dr. **K. Zuber** (TU Dresden)

Memberships.

Accelerator Test Facility (ATF), Program Advisory Committee
Ralph Aßmann

ACOT - Advisory Committee of TRIUMF (Canada)
Kerstin Borras

AIDA-2020
Felix Sefkow (Coordinator)

Akademie der Wissenschaften Hamburg
Wilfried Buchmüller

ArXiv Member Advisory Board
Martin Köhler

ATLAS Collaboration Board
Klaus Mönig

ATLAS Tracker Upgrade Management Board
Ingrid Gregor

AWAKE Experiment CERN Collaboration Board
Ralph Aßmann

BELLE II Institutional Board
Carsten Niebuhr

BELLE II Scrutiny Group
Bernd Löhr

BMBF "Physik der kleinsten Teilchen", Gutachterausschuss
Joachim Mnich

CALICE Steering Board
Felix Sefkow (Chair)

CERN Science Policy Committee
Reinhard Brinkmann, Beate Heinemann

CMS Collaboration Board
Kerstin Borras, Matthias Kasemann (Chair)

CMS Tracker Institution Board
Günter Eckerlin

Computing Resources Review Board (CERN)
Volker Gülzow

Deutsches Forschungsnetz DFN, Betriebsausschuss
Volker Gülzow

Deutsches Forschungsnetz DFN, Verwaltungsrat
Joachim Mnich

DPG National Prize Committee
Georg Weiglein

DPG Wissenschaftlicher Beirat des Physikzentrums
Georg Weiglein

ERC Panel
Georg Weiglein

EuCARD2 European Coordination for Accelerator R&D
Ralph Aßmann, Nicoleta-Ionela Baboi, Jens Osterhoff

EuPRAXIA
Ralph Aßmann, Reinhard Brinkmann,
Jens Osterhoff (Chair of WP9)

European Committee for Future Accelerators (ECFA)
Kerstin Borras (Plenary member),
Joachim Mnich (Ex-officio member)

European Network for Novel Accelerators (EuroNNAc), Steering Group
Jens Osterhoff

European Particle Physics Communication Network
Thomas Zoufal

European Physical Society Accelerator Group (EPS AG)
Ralph Aßmann

Excellence Cluster Universe, Scientific Advisory Committee
Wilfried Buchmüller

Future Circular Collider (FCC), Collaboration Board
Ralph Aßmann

Galileo Galilei Institute (INFN), Scientific Committee
Christophe Grojean

GATIS Marie Curie Project, Supervisory Board
Volker Schomerus (Chair)

Gauß-Allianz
Volker Gülzow

German Executive LHC Outreach Group (GELOG)
Matthias Kasemann, Thomas Naumann, Christian Mrotzek,
Barbara Warmbein, Thomas Zoufal

GridKa Technical Advisory Board
Martin Gasthuber, Brigit Lewendel

Hamilton Mathematics Institute, Trinity College Dublin, Advisory Board
Volker Schomerus

Helmholtz Arbeitskreis Bibliotheks- und Informationsmanagement
Martin Köhler

Helmholtz Arbeitskreis Open Science
Florian Schwennsen

Helmholtz Data Federation Executive Board
Volker Gülzow, Brigit Lewendel

Helmholtz IT-Koordinierungsausschuss (KoDa)
Volker Gülzow

Helmholtz Lenkungsausschuss Materie
Ties Behnke, Helmut Dosch, Joachim Mnich,
Christian Stegmann

Helmholtz Programme Matter and Technologies
Ties Behnke (Programme spokesperson)

Helmholtz Think Tank
Kerstin Borras, Hans Weise

Humboldt Awards, Selection Committee
Wilfried Buchmüller

ICFA Beam Dynamics Panel
Rainer Wanzenberg

IEEE CANPS Technical Committee
Günter Eckerlin

IEEE Radiation Instrumentation Steering Committee
Ingrid-Maria Gregor

IEEE Real-Time Systems, Scientific Committee
Günter Eckerlin

ILC European Action Plan Working Group
Nicholas Walker

ILC Physics and Experiment Board and Executive Board
Ties Behnke, Karsten Büßer

ILD Institute Assembly
Felix Sefkow

INSPIRE Directorate
Kirsten Sachs

INSPIRE High-Energy Physics Literature Database, International Advisory Board
Jürgen Reuter

Institut d'Etudes Scientifiques de Cargese (IESC), Scientific Committee
Géraldine Servant

Interactions Collaboration Board
Christian Mrotzek

International Committee for Future Accelerators (ICFA)
Joachim Mnich (Chair)

John Adams Institute, Advisory Board
Reinhard Brinkmann

John von Neumann Institute for Computing (NIC), Directorate
Joachim Mnich

Joint Institute for Nuclear Research (JINR), Programme Advisory Committee for Particle Physics
Joachim Mnich

Joint Institute of Nuclear Research (JINR), Scientific Council
Joachim Mnich

KIT Center for Elementary Particle and Astroparticle Physics (KCETA), Advisory Board
Joachim Mnich

Komitee für Astroteilchenphysik (KAT)
Martin Pohl, Christian Stegmann

Komitee für Beschleunigerphysik (KfB)
Jens Osterhoff

Komitee für Elementarteilchenphysik (KET)
Kerstin Borras, Joachim Mnich, Georg Weiglein

LCC Physics and Detector Executive Board
Ties Behnke, Karsten Büßer

LHC Resources Review Board
Manfred Fleischer

LHC Resources Scrutiny Group
Frank Gaede, Carsten Niebuhr

Linear Collider Board (LCB)
Joachim Mnich

Max Planck Institute for Gravitational Physics, Potsdam, Advisory Committee
Wilfried Buchmüller

Max Planck Institute for Physics, Munich, Scientific Advisory Board
Joachim Mnich (Chair)

Munich Institute for Astro- and Particle Physics (MIAPP), Scientific Committee
Géraldine Servant

NIKHEF Scientific Advisory Committee (SAC)
Joachim Mnich

Oxford e-Science Research Centre Management Committee, University of Oxford
Brian Foster (Chair)

Particle Data Group
Brian Foster, Klaus Mönig, Andreas Ringwald, Georg Weiglein

Paul Scherrer Institut, Particle Physics Review
Joachim Mnich

PIER Executive Board (Research field Particle & Astroparticle Physics)
Georg Weiglein

SCOAP3 Repository Steering Working Group, Executive Committee
Florian Schwennsen

SFB 676 Vorstand
Elisabetta Gallo, Christian Schwanenberger

STFC, Accelerator Strategy Board (ASB)
Reinhard Brinkmann

SuperKEKB Machine Advisory Committee
Ralph Aßmann

TTC Executive Committee
Hans Weise

TTC Technical Board
Detlef Reschke

US LHC Accelerator Research Program Advisory Committee
Kay Wittenburg

Publications.

ALPS

Published

G. Ballesteros et al.
Standard Model—axion—seesaw—Higgs portal inflation. Five problems of particle physics and cosmology solved in one stroke.
Journal of cosmology and astroparticle physics, 1708(08):001, and PUBDB-2017-08981, DESY-16-184; arXiv:1610.01639.
doi: 10.1088/1475-7516/2017/08/001.

G. Ballesteros et al.
Unifying Inflation with the Axion, Dark Matter, Baryogenesis, and the Seesaw Mechanism.
Physical review letters, 118(7):071802, and PUBDB-2017-00981, DESY 16-049.
doi: 10.1103/PhysRevLett.118.071802.

M. Giannotti et al.
Stellar recipes for axion hunters.
Journal of cosmology and astroparticle physics, 1710(10):010, and PUBDB-2017-11543, DESY-17-116; arXiv:1708.02111.
doi: 10.1088/1475-7516/2017/10/010.

ATLAS

Published

M. Aaboud et al.
Electron efficiency measurements with the ATLAS detector using 2012 LHC proton–proton collision data.
The European physical journal / C, 77(3):195, and PUBDB-2017-08780.
doi: 10.1140/epjc/s10052-017-4756-2.

M. Alhroob et al.
Custom real-time ultrasonic instrumentation for simultaneous mixture and flow analysis of binary gases in the CERN ATLAS experiment.
Nuclear instruments & methods in physics research / A, 845:273, and PUBDB-2018-00522.
doi: 10.1016/j.nima.2016.04.104.

M. Alhroob et al.
Custom ultrasonic instrumentation for flow measurement and real-time binary gas analysis in the CERN ATLAS experiment.
Journal of Instrumentation, 12(01):C01091, and PUBDB-2018-00523.
doi: 10.1088/1748-0221/12/01/C01091.

ATLAS Collaboration.
A measurement of the calorimeter response to single hadrons and determination of the jet energy scale uncertainty using LHC Run-1 pp-collision data with the ATLAS detector.
The European physical journal / C, 77(1):26, and PUBDB-2017-00944, CERN-EP-2016-149; arXiv:1607.08842.
doi: 10.1140/epjc/s10052-016-4580-0.

ATLAS Collaboration.
Analysis of the Wtb vertex from the measurement of triple-differential angular decay rates of single top quarks produced in the t-channel at $\sqrt{s}$ = 8 TeV with the ATLAS detector.
Journal of high energy physics, 1712(12):017, and PUBDB-2018-00344, CERN-EP-2017-089; arXiv:1707.05393.
doi: 10.1007/JHEP12(2017)017.

ATLAS Collaboration.
Correction to: Identification and rejection of pile-up jets at high pseudorapidity with the ATLAS detector.
The European physical journal / C, 77:712, and PUBDB-2018-00343, CERN-EP-2017-055; arXiv:1705.02211.
doi: 10.1140/epjc/s10052-017-5245-3.

ATLAS Collaboration.
Determination of the strong coupling constant α_s from transverse energy-energy correlations in multijet events at $\sqrt{s} = 8$ TeV using the ATLAS detector.
The European physical journal / C, 77(12):872, and PUBDB-2017-13878, CERN-EP-2017-093; arXiv:1707.02562.
doi: 10.1140/epjc/s10052-017-5442-0.

ATLAS Collaboration.
Electromagnetic processes in ultra-peripheral Pb+Pb collisions with ATLAS.
Nuclear physics / A, 967:281, and PUBDB-2018-00550.
doi: 10.1016/j.nuclphysa.2017.04.043.

ATLAS Collaboration.
Erratum to: Measurement of the charge asymmetry in top-quark pair production in the lepton-plus-jets final state in pp collision data at $\sqrt{s} = 8\,\mathrm{T}eV$ with the ATLAS detector.
The European physical journal / C, 77(2):564, and PUBDB-2018-00313, CERN-PH-EP-2015-217; arXiv:1509.02358.
doi: 10.1140/epjc/s10052-017-5089-x.

ATLAS Collaboration.
Evidence for light-by-light scattering in heavy-ion collisions with the ATLAS detector at the LHC.
Nature physics, 13(9):852, and PUBDB-2018-00351, CERN-EP-2016-316; arXiv:1702.01625.
doi: 10.1038/nphys4208.

ATLAS Collaboration.
Evidence for the $H \to b\bar{b}$ decay with the ATLAS detector.
Journal of high energy physics, 1712(12):024, and PUBDB-2018-00367, CERN-EP-2017-175; arXiv:1708.03299.
doi: 10.1007/JHEP12(2017)024.

ATLAS Collaboration.
Fiducial, total and differential cross-section measurements of t-channel single top-quark production in pp collisions at 8 TeV using data collected by the ATLAS detector.
The European physical journal / C, 77(8):531, and PUBDB-2018-00360, CERN-EP-2016-223; arXiv:1702.02859.
doi: 10.1140/epjc/s10052-017-5061-9.

ATLAS Collaboration.
High-E_{T} isolated-photon plus jets production in pp collisions at $\sqrt{s}$ = 8 TeV with the ATLAS detector.
Nuclear physics / B, 918:257, and PUBDB-2017-01513, CERN-EP-2016-252; arXiv:1611.06586.
doi: 10.1016/j.nuclphysb.2017.03.006.

ATLAS Collaboration.
Jet energy scale measurements and their systematic uncertainties in proton-proton collisions at $\sqrt{s} = 13$ TeV with the ATLAS detector.
Physical review / D, 96(7):072002, and PUBDB-2018-00345, CERN-EP-2017-038; arXiv:1703.09665.
doi: 10.1103/PhysRevD.96.072002.

ATLAS Collaboration.
Measurement of b-hadron pair production with the ATLAS detector in proton-proton collisions at $\sqrt{s} = 8$ TeV.
Journal of high energy physics, 1711(11):62, and PUBDB-2018-00507, CERN-EP-2017-057; arXiv:1705.03374.
doi: 10.1007/JHEP11(2017)062.

ATLAS Collaboration.
Measurement of charged-particle distributions sensitive to the underlying event in $\sqrt{s} = 13$ TeV proton-proton collisions with the ATLAS detector at the LHC.
Journal of high energy physics, 1703(03):157, and PUBDB-2018-00339, CERN-EP-2016-28; arXiv:1701.05390.
doi: 10.1007/JHEP03(2017)157.

ATLAS Collaboration.
Measurement of detector-corrected observables sensitive to the anomalous production of events with jets and large missing transverse momentum in pp collisions at $\sqrt{s}$ = 13 TeV using the ATLAS detectorlabora.
The European physical journal / C, 77(11):765, and PUBDB-2017-13285, CERN-EP-2017-116; arXiv:1707.03263.
doi: 10.1140/epjc/s10052-017-5315-6.

ATLAS Collaboration.
Measurement of forward-backward multiplicity correlations in lead-lead, proton-lead, and proton-proton collisions with the ATLAS detector.
Physical review / C, 95(6):064914, and PUBDB-2018-00335, CERN-EP-2016-124; CERN-PH-EP-2016-124; arXiv:1606.08170.
doi: 10.1103/PhysRevC.95.064914.

ATLAS Collaboration.
Measurement of inclusive and differential cross sections in the $H \to ZZ^* \to 4\ell$ decay channel in pp collisions at $\sqrt{s} = 13$ TeV with the ATLAS detector.
Journal of high energy physics, 1710(10):132, and PUBDB-2018-00510, CERN-EP-2017-139; arXiv:1708.02810.
doi: 10.1007/JHEP10(2017)132.

ATLAS Collaboration.
Measurement of jet activity produced in top-quark events with an electron, a muon and two b-tagged jets in the final state in pp collisions at $\sqrt{s} = 13$ TeV with the ATLAS detector.
The European physical journal / C, 77(4):220, and PUBDB-2018-00357, CERN-EP-2016-218; arXiv:1610.09978.
doi: 10.1140/epjc/s10052-017-4766-0.

ATLAS Collaboration.
Measurement of jet fragmentation in Pb+Pb and pp collisions at $\sqrt{s_{\mathrm{NN}}} = 2.76$ TeV with the ATLAS detector at the LHC.
The European physical journal / C, 77(6):379, and PUBDB-2018-00350, CERN-EP-2017-005; arXiv:1702.00674.
doi: 10.1140/epjc/s10052-017-4915-5.

ATLAS Collaboration.
Measurement of jet p_{T} correlations in Pb+Pb and pp collisions at $\sqrt{s_{\mathrm{NN}}}$ = 2.76 TeV with the ATLAS detector.
Physics letters / B, 774:379, and PUBDB-2018-00338, CERN-EP-2017-054; arXiv:1706.09363.
doi: 10.1016/j.physletb.2017.09.078.

ATLAS Collaboration.
Measurement of lepton differential distributions and the top quark mass in $t\bar{t}$ production in pp collisions at $\sqrt{s} = 8$ TeV with the ATLAS detector.
The European physical journal / C, 77(11):804, and PUBDB-2018-00511, CERN-EP-2017-200; arXiv:1709.09407.
doi: 10.1140/epjc/s10052-017-5349-9.

ATLAS Collaboration.
Measurement of multi-particle azimuthal correlations in pp, p+Pb and low-multiplicity Pb+Pb collisions with the ATLAS detector.
The European physical journal / C, 77(6):428, and PUBDB-2018-00346, CERN-EP-2017-048; arXiv:1705.04176.
doi: 10.1140/epjc/s10052-017-4988-1.

ATLAS Collaboration.
Measurement of the cross section for inclusive isolated-photon production in pp collisions at $\sqrt{s} = 13$ TeV using the ATLAS detector.
Physics letters / B, 770:473, and PUBDB-2018-00340, CERN-EP-2016-291; arXiv:1701.06882.
doi: 10.1016/j.physletb.2017.04.072.

ATLAS Collaboration.
Measurement of the cross-section for electroweak production of dijets in association with a Z boson in pp collisions at $\sqrt{s}$ = 13 TeV with the ATLAS detector.
Physics letters / B, 775:206, and PUBDB-2018-00364, CERN-EP-2017-115; arXiv:1709.10264.
doi: 10.1016/j.physletb.2017.10.040.

ATLAS Collaboration.
Measurement of the Drell-Yan triple-differential cross section in pp collisions at $\sqrt{s} = 8$ TeV.
Journal of high energy physics, 1712(12):059, and PUBDB-2018-00365, CERN-EP-2017-152; arXiv:1710.05167.
doi: 10.1007/JHEP12(2017)059.

ATLAS Collaboration.
Measurement of the inclusive cross-sections of single top-quark and top-antiquark t-channel production in pp collisions at $\sqrt{s}$ = 13 TeV with the ATLAS detector.
Journal of high energy physics, 1704(04):086, and PUBDB-2018-00328, CERN-EP-2016-197; arXiv:1609.03920.
doi: 10.1007/JHEP04(2017)086.

ATLAS Collaboration.
Measurement of the inclusive jet cross-sections in proton-proton collisions at $\sqrt{s} = 8$ TeV with the ATLAS detector.
Journal of high energy physics, 1709(9):20, and PUBDB-2018-00353, CERN-EP-2017-043; arXiv:1706.03192.
doi: 10.1007/JHEP09(2017)020.

ATLAS Collaboration.
Measurement of the prompt J/ψ pair production cross-section in pp collisions at $\sqrt{s} = 8$ TeV with the ATLAS detector.
The European physical journal / C, 77(2):76, and PUBDB-2017-00970, CERN-EP-2016-211; arXiv:1612.02950.
doi: 10.1140/epjc/s10052-017-4644-9.

ATLAS Collaboration.
Measurement of the $t\bar{t}$ production cross section in the τ + jets final state in pp collisions at $\sqrt{s} = 8$ TeV using the ATLAS detector.
Physical review / D, 95(7):072003, and PUBDB-2018-00362, CERN-EP-2016-288; arXiv:1702.08839.
doi: 10.1103/PhysRevD.95.072003.

ATLAS Collaboration.
Measurement of the $\mathrm{t\bar{t}Z}$ and $\mathrm{t\bar{t}W}$ production cross sections in multilepton final states using 3.2 fb^{-1} of pp collisions at $\sqrt{\mathrm{s}} =$ 13 TeV with the ATLAS detector.
The European physical journal / C, 77(1):40, and PUBDB-2017-00945, CERN-EP-2016-185; arXiv:1609.01599.
doi: 10.1140/epjc/s10052-016-4574-y.

ATLAS Collaboration.
Measurement of the W boson polarisation in $t\bar{t}$ events from pp collisions at $\sqrt{s}$ = 8 TeV in the lepton + jets channel with ATLAS.
The European physical journal / C, 77(4):264, and PUBDB-2018-00356, CERN-EP-2016-219; CERN-PH-2016-219; arXiv:1612.02577.
doi: 10.1140/epjc/s10052-017-4819-4.

ATLAS Collaboration.
Measurement of the W^+W^- production cross section in pp collisions at a centre-of-mass energy of $\sqrt{s}$ = 13 TeV with the ATLAS experiment.
Physics letters / B, 773:354, and PUBDB-2018-00501, CERN-EP-2016-267; arXiv:1702.04519.
doi: 10.1016/j.physletb.2017.08.047.

ATLAS Collaboration.
Measurement of the ZZ production cross section in proton-proton collisions at $\sqrt{s} = 8$ TeV using the $ZZ \to \ell^-\ell^+\ell'^-\ell'^+$ and $ZZ \to \ell^-\ell^+\nu\bar{\nu}$ channels with the ATLAS detector.
Journal of high energy physics, 1701(01):099, and PUBDB-2018-00332, CERN-EP-2016-194; arXiv:1610.07585.
doi: 10.1007/JHEP01(2017)099.

ATLAS Collaboration.
Measurement of $W^\pm W^\pm$ vector-boson scattering and limits on anomalous quartic gauge couplings with the ATLAS detector.
Physical review / D, 96(1):012007, and PUBDB-2018-00336, CERN-EP-2016-167; arXiv:1611.02428.
doi: 10.1103/PhysRevD.96.012007.

ATLAS Collaboration.
Measurements of $\psi(2S)$ and $X(3872) \to J/\psi\pi^+\pi^-$ production in pp collisions at $\sqrt{s} = 8$ TeV with the ATLAS detector.
Journal of high energy physics, 1701(01):117, and PUBDB-2017-00947, CERN-EP-2016-193; arXiv:1610.09303.
doi: 10.1007/JHEP01(2017)117.

ATLAS Collaboration.
Measurements of charge and CP asymmetries in b-hadron decays using top-quark events collected by the ATLAS detector in pp collisions at $\sqrt{s} = 8$ TeV.
Journal of high energy physics, 1702(02):071, and PUBDB-2017-01289, CERN-EP-2016-221; arXiv:1610.07869.
doi: 10.1007/JHEP02(2017)071.

ATLAS Collaboration.
Measurements of electroweak Wjj production and constraints on anomalous gauge couplings with the ATLAS detector.
The European physical journal / C, 77(7):474, and PUBDB-2018-00504, CERN-EP-2017-008; arXiv:1703.04362.
doi: 10.1140/epjc/s10052-017-5007-2.

M. Aaboud et al.
Measurements of integrated and differential cross sections for isolated photon pair production in pp collisions at $\sqrt{s} = 8$ TeV with the ATLAS detector.
11. Rencontres de Moriond QCD and High Energy Interactions, La Thuile (Italy), 25 Mar 2017 - 1 Apr 2017.
APS, Woodbury, NY.
doi: 10.1103/PhysRevD.95.112005.

ATLAS Collaboration.
Measurements of long-range azimuthal anisotropies and associated Fourier coefficients for pp collisions at $\sqrt{s} = 5.02$ and 13 TeV and p+Pb collisions at $\sqrt{s_{\mathrm{NN}}} = 5.02$ TeV with the ATLAS detector.
Physical review / C, 96(2):024908, and PUBDB-2018-00358, CERN-EP-2016-200; arXiv:1609.06213.
doi: 10.1103/PhysRevC.96.024908.

ATLAS Collaboration.
Measurements of the production cross section of a Z boson in association with jets in pp collisions at $\sqrt{s} = 13$ TeV with the ATLAS detector.
The European physical journal / C, 77(6):361, and PUBDB-2018-00330, CERN-EP-2016-297; arXiv:1702.05725.
doi: 10.1140/epjc/s10052-017-4900-z.

ATLAS Collaboration.
Measurements of top quark spin observables in $t\bar{t}$ events using dilepton final states in $\sqrt{s}$ = 8 TeV pp collisions with the ATLAS detector.
Journal of high energy physics, 1703(03):113, and PUBDB-2017-11953.
doi: 10.1007/JHEP03(2017)113.

ATLAS Collaboration.
Measurements of top-quark pair differential cross-sections in the $e\mu$ channel in pp collisions at $\sqrt{s} = 13$ TeV using the ATLAS detector.
The European physical journal / C, 77(5):292, and PUBDB-2018-00333, CERN-EP-2016-220; CERN-PH-2016-220; arXiv:1612.05220.
doi: 10.1140/epjc/s10052-017-4821-x.

ATLAS Collaboration.
Measurements of top-quark pair differential cross-sections in the lepton+jets channel in pp collisions at $\sqrt{s} = 13$ TeV using the ATLAS detector.

Journal of high energy physics, 1711(11):191, and PUBDB-2018-00342, CERN-EP-2017-058; arXiv:1708.00727.
doi: 10.1007/JHEP11(2017)191.

ATLAS Collaboration.
Measurements of top-quark pair to Z-boson cross-section ratios at $\sqrt{s} = 13, 8, 7$ TeV with the ATLAS detector.
Journal of high energy physics, 1702(02):117, and PUBDB-2017-01290, CERN-EP-2016-271; arXiv:1612.03636.
doi: 10.1007/JHEP02(2017)117.

ATLAS Collaboration.
Performance of algorithms that reconstruct missing transverse momentum in $\sqrt{s} = 8$ TeV proton-proton collisions in the ATLAS detector.
The European physical journal / C, 77(4):241, and PUBDB-2018-00427, CERN-EP-2016-134; arXiv:1609.09324.
doi: 10.1140/epjc/s10052-017-4780-2.

ATLAS Collaboration.
Performance of the ATLAS Transition Radiation Tracker in Run 1 of the LHC: tracker properties.
Journal of Instrumentation, 12(05):P05002, and PUBDB-2018-00419, CERN-EP-2016-311; arXiv:1702.06473.
doi: 10.1088/1748-0221/12/05/P05002.

ATLAS Collaboration.
Performance of the ATLAS trigger system in 2015.
The European physical journal / C, 77(5):317, and PUBDB-2018-00500, CERN-EP-2016-241; arXiv:1611.09661.
doi: 10.1140/epjc/s10052-017-4852-3.

ATLAS Collaboration.
Precision measurement and interpretation of inclusive W^+, W^- and Z/γ^* production cross sections with the ATLAS detector.
The European physical journal / C, 77(6):367, and PUBDB-2018-00363, CERN-EP-2016-272; arXiv:1612.03016.
doi: 10.1140/epjc/s10052-017-4911-9.

ATLAS Collaboration.
Probing the W tb vertex structure in t-channel single-top-quark production and decay in pp collisions at $\sqrt{s} = 8$ TeV with the ATLAS detector.
Journal of high energy physics, 1704(04):124, and PUBDB-2018-00509, CERN-EP-2017-011; arXiv:1702.08309.
doi: 10.1007/JHEP04(2017)124.

ATLAS Collaboration.
Reconstruction of primary vertices at the ATLAS experiment in Run 1 proton–proton collisions at the LHC.
The European physical journal / C, 77(5):332, and PUBDB-2018-00423, CERN-EP-2016-150; arXiv:1611.10235.
doi: 10.1140/epjc/s10052-017-4887-5.

ATLAS Collaboration.
Search for anomalous electroweak production of WW/WZ in association with a high-mass dijet system in pp collisions at $\sqrt{s} = 8$ TeV with the ATLAS detector.
Physical review / D, D95(3):032001, and PUBDB-2017-00971, CERN-EP-2016-171; arXiv:1609.05122.
doi: 10.1103/PhysRevD.95.032001.

ATLAS Collaboration.
Search for dark matter at $\sqrt{s} = 13$ TeV in final states containing an energetic photon and large missing transverse momentum with the ATLAS detector.
The European physical journal / C, 77(6):393, and PUBDB-2018-00349, CERN-EP-2017-044; arXiv:1704.03848.
doi: 10.1140/epjc/s10052-017-4965-8.

ATLAS Collaboration.
Search for dark matter in association with a Higgs boson decaying to two photons at $\sqrt{s}$ = 13 TeV with the ATLAS detector.
Physical review / D, 96(11):112004, and PUBDB-2018-00373, CERN-EP-2017-079; arXiv:1706.03948.
doi: 10.1103/PhysRevD.96.112004.

ATLAS Collaboration.
Search for Dark Matter Produced in Association with a Higgs Boson Decaying to $\mathrm{b\bar{b}}$ using 36 fb^{-1} of pp Collisions at $\sqrt{\mathrm{s}}$ = 13 TeV with the ATLAS Detector.
Physical review letters, 119(18):181804, and PUBDB-2017-13299, CERN-EP-2017-117; arXiv:1707.01302.
doi: 10.1103/PhysRevLett.119.181804.

ATLAS Collaboration.
Search for direct top squark pair production in events with a Higgs or Z boson, and missing transverse momentum in $\sqrt{s} = 13$ TeV pp collisions with the ATLAS detector.
Journal of high energy physics, 1708(8):6, and PUBDB-2018-00517, CERN-EP-2017-106; arXiv:1706.03986.
doi: 10.1007/JHEP08(2017)006.

ATLAS Collaboration.
Search for Heavy Higgs Bosons A/H Decaying to a Top Quark Pair in pp Collisions at $\sqrt{s} = 8$ TeV with the ATLAS Detector.
Physical review letters, 119(19):191803, and PUBDB-2017-11903, arXiv:1707.06025.
doi: 10.1103/PhysRevLett.119.191803.

ATLAS Collaboration.
Search for heavy resonances decaying into a W or Z boson and a Higgs boson in final states with leptons and b-jets in 36 fb^{-1} of $\sqrt{\mathrm{s}} = 13$ TeV pp collisions with the ATLAS detector.
Journal of high energy physics, 1:52, and PUBDB-2017-13775, arXiv:1712.06518; CERN-EP-2017-250.
doi: 10.3204/PUBDB-2017-13775.

ATLAS Collaboration.
Search for heavy resonances decaying to a W or Z boson and a Higgs boson in the $q\bar{q}^{(\prime)}b\bar{b}$ final state in pp collisions at $\sqrt{s} = 13$ TeV with the ATLAS detector.
Physics letters / B, 774:494, and PUBDB-2018-00514, CERN-EP-2017-111; arXiv:1707.06958.
doi: 10.1016/j.physletb.2017.09.066.

ATLAS Collaboration.
Search for lepton-flavour-violating decays of the Higgs and Z bosons with the ATLAS detector.
The European physical journal / C, 77(2):70, and PUBDB-2017-00969, CERN-EP-2016-055; arXiv:1604.07730.
doi: 10.1140/epjc/s10052-017-4624-0.

ATLAS Collaboration.
Search for new high-mass phenomena in the dilepton final state using 36 fb^{-1} of proton-proton collision data at $\sqrt{s} = 13$ TeV with the ATLAS detector.
Journal of high energy physics, 1710(10):182, and PUBDB-2018-00417, CERN-EP-2017-119; arXiv:1707.02424.
doi: 10.1007/JHEP10(2017)182.

ATLAS Collaboration.
Search for new phenomena in a lepton plus high jet multiplicity final state with the ATLAS experiment using $\sqrt{s} = 13$ TeV proton-proton collision data.
Journal of high energy physics, 1709(09):088, and PUBDB-2018-00420, CERN-EP-2017-053; arXiv:1704.08493.
doi: 10.1007/JHEP09(2017)088.

ATLAS Collaboration.
Search for new phenomena in dijet events using 37 fb^{-1} of pp collision data collected at $\sqrt{s}$ =13 TeV with the ATLAS detector.
Physical review / D, 96(5):052004, and PUBDB-2018-00508, CERN-EP-2017-042; arXiv:1703.09127.
doi: 10.1103/PhysRevD.96.052004.

ATLAS Collaboration.
Search for new phenomena in events containing a same-flavour opposite-sign dilepton pair, jets, and large missing transverse momentum in $\sqrt{s} = 13$ pp collisions with the ATLAS detector.
The European physical journal / C, 77(3):144, and PUBDB-2017-01512, CERN-EP-2016-260; CERN-PH-2016-260; arXiv:1611.05791.
doi: 10.1140/epjc/s10052-017-4700-5.

ATLAS Collaboration.
Search for new phenomena in high-mass diphoton final states using 37 fb^{-1} of proton–proton collisions collected at $\sqrt{s} = 13$ TeV with the ATLAS detector.
Physics letters / B, 775:105, and PUBDB-2018-00372, CERN-EP-2017-132; arXiv:1707.04147.
doi: 10.1016/j.physletb.2017.10.039.

ATLAS Collaboration.
Search for new phenomena with large jet multiplicities and missing transverse momentum using large-radius jets and flavour-tagging at ATLAS in 13 TeV pp collisions.
Journal of high energy physics, 1712(12):034, and PUBDB-2018-00371, CERN-EP-2017-138; arXiv:1708.02794.
doi: 10.1007/JHEP12(2017)034.

ATLAS Collaboration.
Search for pair production of heavy vector-like quarks decaying to high-$\mathrm{p_T}$ W bosons and b quarks in the lepton-plus-jets final state in pp collisions at $\sqrt{s} = 13$ TeV with the ATLAS detector.
Journal of high energy physics, 1710(10):141, and PUBDB-2018-00366, CERN-EP-2017-094; arXiv:1707.03347.
doi: 10.1007/JHEP10(2017)141.

ATLAS Collaboration.
Search for pair production of vector-like top quarks in events with one lepton, jets, and missing transverse momentum in $\sqrt{s} = 13$ TeV pp collisions with the ATLAS detector.
Journal of high energy physics, 1708(8):52, and PUBDB-2018-00416, CERN-EP-2017-075; arXiv:1705.10751.
doi: 10.1007/JHEP08(2017)052.

ATLAS Collaboration.
Search for supersymmetry in events with b-tagged jets and missing transverse momentum in pp collisions at $\sqrt{s} = 13$ TeV with the ATLAS detector.
Journal of high energy physics, 1711(11):195, and PUBDB-2018-00368, CERN-EP-2017-154; arXiv:1708.09266.
doi: 10.1007/JHEP11(2017)195.

ATLAS Collaboration.
Search for supersymmetry in final states with two same-sign or three leptons and jets using 36 fb^{-1} of $\sqrt{s} = 13$ TeV pp collision data with the ATLAS detector.
Journal of high energy physics, 1709(09):084, and PUBDB-2018-00370, CERN-EP-2017-108; arXiv:1706.03731.
doi: 10.1007/JHEP09(2017)084.

ATLAS Collaboration.
Search for the dimuon decay of the Higgs boson in pp collisions at $\sqrt{s} = 13$ TeV with the ATLAS detector.
Physical review letters, 119(5):051802, and PUBDB-2018-00516, CERN-EP-2017-078; arXiv:1705.04582.
doi: 10.1103/PhysRevLett.119.051802.

ATLAS Collaboration.
Search for top quark decays $t \to qH$, with $H \to \gamma\gamma$, in $\sqrt{s} = 13$ TeV pp collisions using the ATLAS detector.
Journal of high energy physics, 1710(10):129, and PUBDB-2018-00369, CERN-EP-2017-118; arXiv:1707.01404.
doi: 10.1007/JHEP10(2017)129.

ATLAS Collaboration.
Search for triboson $W^{\pm}W^{\pm}W^{\mp}$ production in pp collisions at $\sqrt{s} = 8$ TeV with the ATLAS detector.
The European physical journal / C, 77(3):141, and PUBDB-2018-00327, CERN-EP-2016-172; arXiv:1610.05088.
doi: 10.1140/epjc/s10052-017-4692-1.

ATLAS Collaboration.
Searches for Exotic Physics in ATLAS using Substructure Techniques.
Journal of physics / Conference Series, 878:012007, and PUBDB-2017-13366.
doi: 10.1088/1742-6596/878/1/012007.

ATLAS Collaboration.
Searches for the $Z\gamma$ decay mode of the Higgs boson and for new high-mass resonances in pp collisions at $\sqrt{s} = 13$ TeV with the ATLAS detector.
Journal of high energy physics, 1710(10):112, and PUBDB-2018-00375, CERN-EP-2017-095; arXiv:1708.00212.
doi: 10.1007/JHEP10(2017)112.

ATLAS Collaboration.
Studies of $Z\gamma$ production in association with a high-mass dijet system in pp collisions at $\sqrt{s} = 8$ TeV with the ATLAS detector.
Journal of high energy physics, 1707(07):107, and PUBDB-2018-00347, CERN-EP-2017-046; arXiv:1705.01966.
doi: 10.1007/JHEP07(2017)107.

ATLAS Collaboration.
Study of ordered hadron chains with the ATLAS detector.
Physical review / D, 96(9):092008, and PUBDB-2018-00513, CERN-EP-2017-092; arXiv:1709.07384.
doi: 10.1103/PhysRevD.96.092008.

ATLAS Collaboration.
Study of the material of the ATLAS inner detector for Run 2 of the LHC.
Journal of Instrumentation, 12(12):P12009, and PUBDB-2018-00354, CERN-EP-2017-081; arXiv:1707.02826.
doi: 10.1088/1748-0221/12/12/P12009.

ATLAS Collaboration.
Study of $WW\gamma$ and $WZ\gamma$ production in pp collisions at $\sqrt{s}=8$ TeV and search for anomalous quartic gauge couplings with the ATLAS experiment.
The European physical journal / C, 77(9):646, and PUBDB-2018-00414, CERN-EP-2017-096; arXiv:1707.05597.
doi: 10.1140/epjc/s10052-017-5180-3.

ATLAS Collaboration.
Topological cell clustering in the ATLAS calorimeters and its performance in LHC Run 1.
The European physical journal / C, 77(7):490, and PUBDB-2018-00312, CERN-PH-EP-2015-304; arXiv:1603.02934.
doi: 10.1140/epjc/s10052-017-5004-5.

ATLAS Collaboration.
Top-quark mass measurement in the all-hadronic $t\bar{t}$ decay channel at $\sqrt{s}=8$ TeV with the ATLAS detector.
Journal of high energy physics, 1709(09):118, and PUBDB-2018-00421, CERN-EP-2016-264; arXiv:1702.07546.
doi: 10.1007/JHEP09(2017)118.

V. Bertone et al.
Impact of the heavy-quark matching scales in PDF fits.
The European physical journal / C, 77(12):837, and PUBDB-2018-00530, DESY-17-101; arXiv:1707.05343.
doi: 10.1140/epjc/s10052-017-5407-3.

C. Englert, J. Ferrando and K. Nordström.
Constraining new resonant physics with top spin polarisation information.
The European physical journal / C, 77(6):407, and PUBDB-2017-14032.
doi: 10.1140/epjc/s10052-017-4964-9.

N. Flaschl et al.
Thermal and hydrodynamic studies for micro-channel cooling for largearea silicon sensors in high energy physics experiments.
Nuclear instruments & methods in physics research / A, 863:26, and PUBDB-2017-05447.
doi: 10.1016/j.nima.2017.05.003.

Gregor, Ingrid-Maria and ATLAS Collaboration.
Identification and rejection of pile-up jets at high pseudorapidity with the ATLAS detector.
The European physical journal / C, 77(9):580, and PUBDB-2017-10473, CERN-EP-2017-055; arXiv:1705.02211.
doi: 10.1140/epjc/s10052-017-5081-5.

Gregor, Ingrid-Maria and ATLAS Collaboration.
Measurement of the k_{t} splitting scales in $Z\to\ell\ell$ events in pp collisions at $\sqrt{s}=8$ TeV with the ATLAS detector.
Journal of high energy physics, 1708(08):026, and PUBDB-2017-10498, CERN-EP-2017-033; arXiv:1704.01530.
doi: 10.1007/JHEP08(2017)026.

Gregor, Ingrid-Maria and ATLAS Collaboration.
Measurement of $WW/WZ\to\ell\nu qq'$ production with the hadronically decaying boson reconstructed asone or two jets in pp collisions at $\sqrt{s}$ = 8 TeV with ATLAS, and constraints on anomalous gauge couplings.
The European physical journal / C, 77(8):563, and PUBDB-2017-10494, CERN-EP-2017-060; arXiv:1706.01702.
doi: 10.1140/epjc/s10052-017-5084-2.

T. Harenberg et al.
Online production validation in a HEP environment.
The European physical journal / C, 77(3):188, and PUBDB-2018-00497, arXiv:1611.10112.
doi: 10.1140/epjc/s10052-017-4755-3.

K. Kanisauskas et al.
Radiation hardness studies of AMS HV-CMOS 350 nm prototype chip HVStripV1.
Journal of Instrumentation, 12(02):P02010, and PUBDB-2018-00559.
doi: 10.1088/1748-0221/12/02/P02010.

S. Kuehn et al.
Prototyping of hybrids and modules for the forward silicon strip tracking detector for the ATLAS Phase-II upgrade.
Journal of Instrumentation, 12(05):P05015, and PUBDB-2017-10562.
doi: 10.1088/1748-0221/12/05/P05015.

A. Luszczak and H. Kowalski.
Dipole model analysis of highest precision HERA data, including very low Q^2.
Physical review / D, D95(1):014030, and PUBDB-2017-00952, DESY-16-231; DESY-REPORT-16-231; arXiv:1611.10100.
doi: 10.1103/PhysRevD.95.014030.

A.-L. Poley.
Investigations into the impact of bond pads and p-stop implants on the detection efficiency of silicon micros-trip sensors.
Journal of Instrumentation, 12(07):P07006, and PUBDB-2017-08777, DESY-16-218; arXiv:1611.06114.
doi: 10.1088/1748-0221/12/07/P07006.

E. G. Villani et al.
HVMUX, a high voltage multiplexing for the ATLAS Tracker upgrade.
Journal of Instrumentation, 12(01):C01076, and PUBDB-2018-00493.
doi: 10.1088/1748-0221/12/01/C01076.

xFitter Developers' team Collaboration.
The photon PDF from high-mass Drell–Yan data at the LHC.
The European physical journal / C, 77(6):400, and PUBDB-2017-06655, arXiv:1701.08553; DESY-17-015.
doi: 10.1140/epjc/s10052-017-4931-5.

Ph.D. Thesis

M. Bessner.
Measurement of differential di-photon plus jet cross sections using the ATLAS detector.
Universität Hamburg, Hamburg, 2017.

R. Naranjo Garcia.
Measurements of top-quark properties at 8 TeV using the ATLAS detector at the LHC.
Bergische Universität Wuppertal, 2017.

R. Peschke.
Characterisation of the ATLAS ITK Strips Front-End Chip and Development of EUDAQ 2.0 for the EUDET-Style Pixel Telescopes.
Universität Hamburg, Hamburg, 2017.

A. Trofymov.
Measurements of $W^{\pm}$ and top-quark pair to Z-boson cross-section ratios at $\sqrt{s}$ = 13, 8, 7 TeV with the ATLAS detector.
Universität Hamburg, Hamburg, 2018.

E. Yildirim.
Collected Charge and Lorentz Angle Measurement on Non-irradiated and Irradiated ATLAS Silicon Micro-Strip Sensors for the HL-LHC.
Universität Hamburg, Hamburg, 2017.

Astroparticle physics

Published

M. G. Aartsen et al.
First search for dark matter annihilations in the Earth with the IceCube detector.
The European physical journal / C, 77(2):82, and PUBDB-2018-00005, arXiv:1609.01492.
doi: 10.1140/epjc/s10052-016-4582-y.

M. G. Aartsen et al.
Measurement of the Multi-TeV Neutrino Interaction Cross-Section with IceCube Using Earth Absorption.
Nature, 551:596, and PUBDB-2017-12817, arXiv:1711.08119.
doi: 10.1038/nature24459.

M. G. Aartsen et al.
Multiwavelength follow-up of a rare IceCube neutrino multiplet.
Astronomy and astrophysics, 607:A115, and PUBDB-2017-12822, arXiv:1702.06131.
doi: 10.1051/0004-6361/201730620.

M. G. Aartsen et al.
Search for neutrinos from dark matter self-annihilations in the center of the Milky Way with 3 years of IceCube/DeepCore.
The European physical journal / C, 77(9):627, and PUBDB-2017-11474, arXiv:1705.08103.
doi: 10.1140/epjc/s10052-017-5213-y.

B. P. Abbott et al.
Multi-messenger Observations of a Binary Neutron Star Merger.
The astrophysical journal / 2, 848(2):L12, and PUBDB-2017-12237, LIGO-P1700294, VIR-0802A-17, arXiv:1710.05833.
doi: 10.3847/2041-8213/aa91c9.

S. Abdollahi et al.
The second catalog of flaring gamma-ray sources from the Fermi All-sky Variability Analysis.
The astrophysical journal, 846(1):34, and PUBDB-2017-10908, arXiv:1612.03165.
doi: 10.3847/1538-4357/aa8092.

A. U. Abeysekara et al.
Discovery of Very-high-energy Emission from RGB J2243+203 and Derivation of Its Redshift Upper Limit.
The astrophysical journal / Supplement series, 233(1):7, and PUBDB-2017-12233, arXiv:1709.05403.
doi: 10.3847/1538-4365/aa8d76.

M. Ackermann et al.
Fermi-LAT Observations of High-energy Behind-the-limb Solar Flares.
The astrophysical journal, 835(2):219, and PUBDB-2017-01058.
doi: 10.3847/1538-4357/835/2/219.

M. Ackermann et al.
Gamma-Ray Blazars within the First 2 Billion Years.
The astrophysical journal, 837(1):L5, and PUBDB-2017-01366.
doi: 10.3847/2041-8213/aa5fff.

M. Ackermann et al.
Observations of M31 and M33 with the *Fermi* Large Area Telescope: A Galactic Center Excess in Andromeda?
The astrophysical journal, 836(2):208, and PUBDB-2017-01367.
doi: 10.3847/1538-4357/aa5c3d.

M. Ackermann et al.
Search for Extended Sources in the Galactic Plane Using Six Years of Fermi -Large Area Telescope Pass 8 Data above 10 GeV.
The astrophysical journal, 843(2):139, and PUBDB-2017-08796, arXiv:1702.00476.
doi: 10.3847/1538-4357/aa775a.

F. A. Aharonian, M. V. Barkov and D. Khangulyan.
Scenarios for Ultrafast Gamma-Ray Variability in AGN.
The astrophysical journal, 841(1):61, and PUBDB-2017-05457.
doi: 10.3847/1538-4357/aa7049.

M. L. Ahnen et al.
Constraining Lorentz Invariance Violation Using the Crab Pulsar Emission Observed up to TeV Energies by MAGIC.
The astrophysical journal / Supplement series, 232(1):9, and PUBDB-2017-11470, arXiv:1709.00346.
doi: 10.3847/1538-4365/aa8404.

M. L. Ahnen et al.
Observations of Sagittarius A* during the pericenter passage of the G2 object with MAGIC.
Astronomy and astrophysics, 601:A33, and PUBDB-2018-00432, arXiv:1611.07095.
doi: 10.1051/0004-6361/201629355.

M. L. Ahnen et al.
Performance of the MAGIC telescopes under moonlight.
Astroparticle physics, 94:29, and PUBDB-2017-10006, arXiv:1704.00906.
doi: 10.1016/j.astropartphys.2017.08.001.

M. Ajello et al.
3FHL: The Third Catalog of Hard Fermi -LAT Sources.
The astrophysical journal / Supplement series, 232(2):18, and PUBDB-2017-11473, arXiv:1702.00664.
doi: 10.3847/1538-4365/aa8221.

A. Albert et al.
Search for high-energy neutrinos from gravitational wave event GW151226 and candidate LVT151012 with ANTARES and IceCube.
Physical review / D, 96(2):022005, and PUBDB-2017-08787, arXiv:1703.06298.
doi: 10.1103/PhysRevD.96.022005.

C. Allen et al.
Very-High-Energy γ-Ray Observations of the Blazar 1ES 2344+514 with VERITAS.
Monthly notices of the Royal Astronomical Society, 471(2):2117, and PUBDB-2017-11453, arXiv:1708.02829.
doi: 10.1093/mnras/stx1756.

R. Aloisio et al.
SimProp v2r4: Monte Carlo simulation code for UHECR propagation.
Journal of cosmology and astroparticle physics, 1711(11):009, and PUBDB-2018-00466, arXiv:1705.03729.
doi: 10.1088/1475-7516/2017/11/009.

ANTARES Collaboration and IceCube Collaboration and Pierre Auger Collaboration and LIGO Scientific Collaboration and Virgo Collaboration.
Search for High-energy Neutrinos from Binary Neutron Star Merger GW170817 with ANTARES, IceCube, and the Pierre Auger Observatory.
The astrophysical journal / 2, 850(2):L35, and PUBDB-2017-13802.
doi: 10.3847/2041-8213/aa9aed.

S. Archambault et al.
Gamma-Ray Observations of Tycho's Supernova Remnant with VERITAS and *Fermi*.
The astrophysical journal, 836(1):23, and PUBDB-2017-01040.
doi: 10.3847/1538-4357/836/1/23.

S. Archambault et al.
Gamma-ray observations under bright moonlight with VERITAS.
Astroparticle physics, 91:34, and PUBDB-2017-01615.
doi: 10.1016/j.astropartphys.2017.03.001.

S. Archambault et al.
Search for Magnetically Broadened Cascade Emission from Blazars with VERITAS.
The astrophysical journal, 835(2):288, and PUBDB-2017-01041.
doi: 10.3847/1538-4357/835/2/288.

L. Arrabito et al.
The Cherenkov Telescope Array production system for Monte Carlo simulations and analysis.
22nd International Conference on Computing in High Energy and Nuclear Physics, San Francisco (USA), 10 Oct 2016 - 14 Oct 2016.
IOP Publ., Bristol.
doi: 10.1088/1742-6596/898/5/052013.

D. Biehl et al.
Astrophysical Neutrino Production Diagnostics with the Glashow Resonance.
Journal of cosmology and astroparticle physics, 1701(01):033, and PUBDB-2017-01282, arXiv:1611.07983.
doi: 10.1088/1475-7516/2017/01/033.

D. Boncioli, A. Fedynitch and W. Winter.
Nuclear Physics Meets the Sources of the Ultra-High Energy Cosmic Rays.
Scientific reports, 7(1):4882, and PUBDB-2017-08954, arXiv:1607.07989.
doi: 10.1038/s41598-017-05120-7.

N. Budnev et al.
TAIGA experiment: present status and perspectives.
Journal of Instrumentation, 12(08):C08018, and PUBDB-2018-00473.
doi: 10.1088/1748-0221/12/08/C08018.

N. Budnev et al.
The TAIGA experiment: From cosmic-ray to gamma-ray astronomy in the Tunka valley.
Nuclear instruments & methods in physics research / A, 845:330, and PUBDB-2018-00469.
doi: 10.1016/j.nima.2016.06.041.

M. Cerruti et al.
Luminous and high-frequency peaked blazars: the origin of the γ-ray emission from PKS 1424+240.
Astronomy and astrophysics, 606(A68):10, and PUBDB-2017-09410, arXiv:1707.00804.
doi: 10.1051/0004-6361/201730799.

Cherenkov Telescope Array Consortium.
Prospects for Cherenkov Telescope Array Observations of the Young Supernova Remnant RX J1713.7-3946.
The astrophysical journal, 840(2):74, and PUBDB-2017-04984, arXiv:1704.04136.
doi: 10.3847/1538-4357/aa6d67.

A. De Angelis et al.
The e-ASTROGAM mission.
Experimental astronomy, 44(1):25, and PUBDB-2017-11455, arXiv:1611.02232.
doi: 10.1007/s10686-017-9533-6.

Fermi-LAT Collaboration.
Cosmic-ray electron-positron spectrum from 7 GeV to 2 TeV with the Fermi Large Area Telescope.
Physical review / D, 95(8):082007, and PUBDB-2017-13651, arXiv:1704.07195.
doi: 10.1103/PhysRevD.95.082007.

Fermi-LAT Collaboration.
MAGIC detection of very high energy γ-ray emission from the low-luminosity blazar 1ES 1741+196.
Monthly notices of the Royal Astronomical Society, 468(2):1534, and PUBDB-2017-07766.
doi: 10.1093/mnras/stx472.

Fermi-LAT Collaboration.
Search for Cosmic-Ray Electron and Positron Anisotropies with Seven Years of Fermi Large Area Telescope Data.
Physical review letters, 118(9):091103, and PUBDB-2017-01364.
doi: 10.1103/PhysRevLett.118.091103.

Fermi-LAT Collaboration.
The Fermi Galactic Center GeV Excess and Implications for Dark Matter.
The astrophysical journal, 840(1):43, and PUBDB-2017-03387, arXiv:1704.03910.
doi: 10.3847/1538-4357/aa6cab.

Fermi-LAT Collaboration and H.E.S.S. Collaboration.
Gamma-ray blazar spectra with H.E.S.S. II mono analysis: The case of PKS 2155-304 and PG 1553+113.
Astronomy and astrophysics, 600:A89, and PUBDB-2017-00449, arXiv:1612.01843.
doi: 10.1051/0004-6361/201629427.

F. Fraschetti and M. Pohl.
Particle acceleration model for the broad-band baseline spectrum of the Crab nebula.
Monthly notices of the Royal Astronomical Society, 471(4):4856, and PUBDB-2017-11472, arXiv:1702.00816.
doi: 10.1093/mnras/stx1833.

S. Gao, M. Pohl and W. Winter.
On the direct correlation between gamma-rays and PeV neutrinos from blazars.
The astrophysical journal, 843(2):109, and PUBDB-2017-08770, arXiv:1610.05306.
doi: 10.3847/1538-4357/aa7754.

G. Giavitto et al.
The upgrade of the H.E.S.S. cameras.
Nuclear instruments & methods in physics research / A, 876:35, and PUBDB-2018-00555.
doi: 10.1016/j.nima.2016.12.057.

A. Goldstein et al.
Fermi Observations of the LIGO Event GW170104.
The astrophysical journal / 2, 846(1):L5, and PUBDB-2017-11471.
doi: 10.3847/2041-8213/aa8319.

O. Gress et al.
The wide-aperture gamma-ray telescope TAIGA-HiSCORE in the Tunka Valley: Design, composition and commissioning.
Nuclear instruments & methods in physics research / A, 845:367, and PUBDB-2018-00304.
doi: 10.1016/j.nima.2016.08.031.

T. Hassan et al.
Monte Carlo performance studies for the site selection of the Cherenkov Telescope Array.
Astroparticle physics, 93:76, and PUBDB-2017-07767.
doi: 10.1016/j.astropartphys.2017.05.001.

H.E.S.S. Collaboration.
A polarized fast radio burst at low Galactic latitude.
Monthly notices of the Royal Astronomical Society, 469(4):4465, and PUBDB-2018-00585, arXiv:1705.02911.
doi: 10.1093/mnras/stx1098.

H.E.S.S. Collaboration.
Extended VHE γ-Ray Emission Towards SGR1806-20, LBV1806-20, and Stellar Cluster Cl*1806-20.
Astronomy and astrophysics, X:10, and PUBDB-2017-11577, arXiv:1606.05404.
doi: 10.1051/0004-6361/201628695.

H.E.S.S. Collaboration.
Measurement of the EBL Spectral Energy Distribution Using the VHE γ-ray Spectra of H.E.S.S. Blazars.
Astronomy and astrophysics, 606:A59, and PUBDB-2017-11578, arXiv:1707.06090.
doi: 10.1051/0004-6361/201731200.

H.E.S.S. Collaboration.
TeV Gamma-Ray Observations of the Binary Neutron Star Merger GW170817 with H.E.S.S.
The astrophysical journal / 2, 850(2):L22, and PUBDB-2017-12826, arXiv:1710.05862.
doi: 10.3847/2041-8213/aa97d2.

X. Huang et al.
The Extinction Properties of and Distance to the Highly Reddened Type IA Supernova 2012cu.
The astrophysical journal, 836(2):157, and PUBDB-2018-00499.
doi: 10.3847/1538-4357/836/2/157.

IceCube Collaboration.
Astrophysical neutrinos and cosmic rays observed by IceCube.
Advances in space research, x:S0273117717303757, and PUBDB-2018-00003.
doi: 10.1016/j.asr.2017.05.030.

IceCube Collaboration.
Constraints on Galactic Neutrino Emission with Seven Years of IceCube Data.
The astrophysical journal, 849(1):67, and PUBDB-2017-12245, arXiv:1707.03416.
doi: 10.3847/1538-4357/aa8dfb.

IceCube Collaboration.
Extending the Search for Muon Neutrinos Coincident with Gamma-Ray Bursts in IceCube Data.
The astrophysical journal, 843(2):112, and PUBDB-2017-07768.
doi: 10.3847/1538-4357/aa7569.

IceCube Collaboration.
Measurement of the ν_μ energy spectrum with IceCube-79.
The European physical journal / C, 77(10):692, and PUBDB-2017-11704, arXiv:1705.07780.
doi: 10.1140/epjc/s10052-017-5261-3.

IceCube Collaboration.
PINGU: A Vision for Neutrino and Particle Physics at the South Pole.
Journal of physics / G, 44(5):054006, and PUBDB-2017-09958, arXiv:1607.02671.
doi: 10.1088/1361-6471/44/5/054006.

IceCube Collaboration.
Search for annihilating dark matter in the Sun with 3 years of IceCube data.
The European physical journal / C, 77(3):146, and PUBDB-2017-01471.
doi: 10.1140/epjc/s10052-017-4689-9.

IceCube Collaboration.
Search for Astrophysical Sources of Neutrinos Using Cascade Events in IceCube.
The astrophysical journal, 846(2):136, and PUBDB-2017-11452, arXiv:1705.02383.
doi: 10.3847/1538-4357/aa8508.

IceCube Collaboration.
Search for sterile neutrino mixing using three years of IceCube DeepCore data.
Physical review / D, 95(11):112002, and PUBDB-2017-06711.
doi: 10.1103/PhysRevD.95.112002.

IceCube Collaboration.
The contribution of Fermi-2LAC blazars to the diffuse TeV-PeV neutrino flux.
The astrophysical journal, 835(1):45, and PUBDB-2017-00648, arXiv:1611.03874.
doi: 10.3847/1538-4357/835/1/45.

IceCube Collaboration.
The IceCube Neutrino Observatory: instrumentation and online systems.
Journal of Instrumentation, 12(03):P03012, and PUBDB-2017-01470, arXiv:1612.05093.
doi: 10.1088/1748-0221/12/03/P03012.

IceCube Collaboration.
The IceCube realtime alert system.
Astroparticle physics, 92:30, and PUBDB-2017-04973, arXiv:1612.06028.
doi: 10.1016/j.astropartphys.2017.05.002.

IceCube Collaboration and IceCube Collaboration.
All-sky Search for Time-integrated Neutrino Emission from Astrophysical Sources with 7 yr of IceCube Data.
The astrophysical journal, 835(2):151, and PUBDB-2018-00004, arXiv:1609.04981.
doi: 10.3847/1538-4357/835/2/151.

S. Klepser.
The optimal on-source region size for detections with counting-type telescopes.
Astroparticle physics, 89:10, and PUBDB-2017-01945.
doi: 10.1016/j.astropartphys.2017.01.005.

O. Kobzar et al.
Spatio-temporal evolution of the non-resonant instability in shock precursors of young supernova remnants.
Monthly notices of the Royal Astronomical Society, 469(4):4985, and PUBDB-2017-13687.
doi: 10.1093/mnras/stx1201.

M. Krause, E. Pueschel and G. Maier.
Improved γ/hadron separation for the detection of faint γ-ray sources using boosted decision trees.
Astroparticle physics, 89:1, and PUBDB-2017-01279.
doi: 10.1016/j.astropartphys.2017.01.004.

J. C. Lau et al.
Interstellar gas towards the TeV γ-ray sources HESS J1640−465 and HESS J1641−463.
Monthly notices of the Royal Astronomical Society, 464(3):3757, and PUBDB-2017-02480.
doi: 10.1093/mnras/stw2692.

S. Lombardo et al.
SCALA: In situ calibration for integral field spectrographs.
Astronomy and astrophysics, 607:A113, and PUBDB-2018-00309.
doi: 10.1051/0004-6361/201731076.

V. López-Barquero et al.
TeV Cosmic-Ray Anisotropy from the Magnetic Field at the Heliospheric Boundary.
The astrophysical journal, 842(1):54, and PUBDB-2017-10020.
doi: 10.3847/1538-4357/aa74d1.

G. Lucchetta et al.
Scientific Performance of a Nano-satellite MeV Telescope.
The astronomical journal, 153(5):237, and PUBDB-2017-13641.
doi: 10.3847/1538-3881/aa6a1b.

C. Lunardini and W. Winter.
High energy neutrinos from the tidal disruption of stars.
Physical review / D, 95(12):123001, and PUBDB-2017-08952, arXiv:1612.03160.
doi: 10.1103/PhysRevD.95.123001.

MAGIC Collaboration.
A cut-off in the TeV gamma-ray spectrum of the SNR Cassiopeia A.
Monthly notices of the Royal Astronomical Society, 472(3):2956, and PUBDB-2018-00436, arXiv:1707.01583.
doi: 10.1093/mnras/stx2079.

MAGIC Collaboration.
First Multi-wavelength Campaign on the Gamma-ray-loud Active Galaxy IC 310.
Astronomy and astrophysics, 603:A25, and PUBDB-2018-00463, arXiv:1703.07651.
doi: 10.1051/0004-6361/201630347.

MAGIC Collaboration.
MAGIC observations of the microquasar V404 Cygni during the 2015 outburst.
Monthly notices of the Royal Astronomical Society, 471(2):1688, and PUBDB-2018-00465, arXiv:1707.00887.
doi: 10.1093/mnras/stx1690.

MAGIC Collaboration.
Multiwavelength observations of a VHE gamma-ray flare from PKS 1510−089 in 2015.
Astronomy and astrophysics, 603:A29, and PUBDB-2018-00435, arXiv:1610.09416.
doi: 10.1051/0004-6361/201629960.

MAGIC Collaboration.
Observation of the Black Widow B1957+20 millisecond pulsar binary system with the MAGIC telescopes.
Monthly notices of the Royal Astronomical Society, 470(4):4608, and PUBDB-2017-10005, arXiv:1706.01378.
doi: 10.1093/mnras/stx1405.

MAGIC Collaboration.
Search for very high-energy gamma-ray emission from the microquasar CygnusX-1 with the MAGIC telescopes.
Monthly notices of the Royal Astronomical Society, 472(3):3474, and PUBDB-2018-00864, arXiv:1708.03689.
doi: 10.1093/mnras/stx2087.

MAGIC Collaboration.
Very-high-energy gamma-ray observations of the Type Ia Supernova SN 2014J with the MAGIC telescopes.
Astronomy and astrophysics, 602:A98, and PUBDB-2018-00433, arXiv:1702.07677.
doi: 10.1051/0004-6361/201629574.

MAGIC Collaboration and VERITAS Collaboration.
Multiband variability studies and novel broadband SED modeling of Mrk 501 in 2009.
Astronomy and astrophysics, 603:A31, and PUBDB-2017-09408, arXiv:1612.09472.
doi: 10.1051/0004-6361/201629540.

I. de Medeiros Varzielas, R. W. Rasmussen and J. Talbert.
Bottom-up discrete symmetries for Cabibbo mixing.
International journal of modern physics / A, 32(06n07):1750047, and PUBDB-2017-01466.
doi: 10.1142/S0217751X17500476.

R. D. Monkhoev et al.
The Tunka-Grande experiment.
Journal of Instrumentation, 12(06):C06019, and PUBDB-2018-00515.
doi: 10.1088/1748-0221/12/06/C06019.

K.-I. Nishikawa et al.
Microscopic Processes in Global Relativistic Jets Containing Helical Magnetic Fields: Dependence on Jet Radius.
Galaxies, 5(4):58, and PUBDB-2017-12238, arXiv:1708.07740.
doi: 10.3390/galaxies5040058.

S. Ohm and C. Hoischen.
On the expected γ-ray emission from nearby flaring stars.
Monthly notices of the Royal Astronomical Society, 474(1):1335, and PUBDB-2018-00067, arXiv:1710.09385.
doi: 10.1093/mnras/stx2806.

M. Perucho, V. Bosch-Ramon and M. Barkov.
Impact of red giant/AGB winds on active galactic nucleus jet propagation.
Astronomy and astrophysics, 606:A40, and PUBDB-2018-00443.
doi: 10.1051/0004-6361/201630117.

Pierre Auger Collaboration.
Combined fit of spectrum and composition data as measured by the Pierre Auger Observatory.
Journal of cosmology and astroparticle physics, 2017(04):038, and PUBDB-2017-08950, arXiv:1612.07155; FERMILAB-PUB-16-618.
doi: 10.1088/1475-7516/2017/04/038.

Pierre Auger Collaboration.
Muon counting using silicon photomultipliers in the AMIGA detector of the Pierre Auger observatory.
Journal of Instrumentation, 12(03):P03002, and PUBDB-2017-01365, FERMILAB-PUB-16-656-AD-CD-TD.
doi: 10.1088/1748-0221/12/03/P03002.

M. Pohl et al.
Electron Pre-Acceleration at Nonrelativistic High-Mach-Number Perpendicular Shocks.
The astrophysical journal, 847(1):71, and PUBDB-2017-11075.
doi: 10.3847/1538-4357/aa872a.

O. Porth et al.
Modelling Jets, Tori and Flares in Pulsar Wind Nebulae.
Space science reviews, 207(1-4):137, and PUBDB-2017-07734.
doi: 10.1007/s11214-017-0344-x.

J. L. Racusin et al.
Searching the Gamma-Ray Sky for Counterparts to Gravitational Wave Sources: Fermi Gamma-Ray Burst Monitor R and Large Area Telescope Observations of LVT151012 and GW151226.
The astrophysical journal, 835(1):82, and PUBDB-2018-00589.
doi: 10.3847/1538-4357/835/1/82.

I. Rafighi et al.
Plasma effects on relativistic pair beams from TeV blazars. PIC simulations and analytical predictions.
Astronomy and astrophysics, 607:A112, and PUBDB-2017-11454.
doi: 10.1051/0004-6361/201731127.

R. W. Rasmussen et al.
Astrophysical neutrinos flavored with beyond the Standard Model physics.
Physical review / D, 96(8):083018, and PUBDB-2017-13831, DESY-17-107; arXiv:1707.07684.
doi: 10.1103/PhysRevD.96.083018.

S. J. Smartt et al.
A kilonova as the electromagnetic counterpart to a gravitational-wave source.
Nature, 551:75, and PUBDB-2017-12239, arXiv:1710.05841.
doi: 10.1038/nature24303.

I. Sushch and B. van Soelen.
Gamma–Gamma Absorption in the γ-ray Binary System PSR B1259-63/LS 2883.
The astrophysical journal, 837(2):175, and PUBDB-2018-00464.
doi: 10.3847/1538-4357/aa62ff.

I. Sushch et al.
Radio Observations of the Region Around the Pulsar Wind Nebula HESSJ1303−631 with ATCA.
Astronomy and astrophysics, 605:A115, and PUBDB-2017-11467, arXiv:1706.05891.
doi: 10.1051/0004-6361/201527871.

VERITAS Collaboration.
Dark matter constraints from a joint analysis of dwarf Spheroidal galaxy observations with VERITAS.
Physical review / D, 95(8):082001, and PUBDB-2017-02490, arXiv:1703.04937.
doi: 10.1103/PhysRevD.95.082001.

VERITAS Collaboration and Fermi-LAT Collaboration.
A Luminous and Isolated Gamma-Ray Flare from the Blazar B2 1215+30.
The astrophysical journal, 836(2):205, and PUBDB-2017-01281.
doi: 10.3847/1538-4357/836/2/205.

VERITAS Collaboration and MAGIC Collaboration.
A search for Spectral Hysteresis and Energy-Dependent Time Lags from X-Ray and TeV Gamma-Ray Observations of Mrk 421.
The astrophysical journal, 834(1):2, and PUBDB-2017-13701.
doi: 10.3847/1538-4357/834/1/2.

D. C. Warren et al.
Nonlinear Particle Acceleration and Thermal Particles in GRB Afterglows.
The astrophysical journal, 835(2):248, and PUBDB-2018-00544.
doi: 10.3847/1538-4357/aa56c3.

M. Zacharias, X. Chen and S. J. Wagner.
Attenuation of TeV γ-rays by the starlight photon field of the host galaxy.
Monthly notices of the Royal Astronomical Society, 465(3):3767, and PUBDB-2018-00545.
doi: 10.1093/mnras/stw3032.

Master Thesis

H. Breede.
Entwicklung eines kompakten Ionisationsprofilmonitors(3D-IPM) zur Online-Bestimmung von Profil und Positioneines Röntgenlaserstrahls.
Beuth Hochschule für Technik Berlin, 2017.

F. Dietrich.
Simulationsgestützte Gestaltung konstruktiver Varianten des strahlungsgekühlten Targets für die Positronenquelle des International Linear Collider (ILC).
Technische Hochschule Wildau, 2017.

Ph.D. Thesis

S. D. Altmann.
Search for TeV neutrinos from point-like sources in the southern sky using four years of IceCube data.
Humboldt Universität, 2017.

H. Fleischhack.
Measurement of the iron spectrum in cosmic rays with the VERITAS experiment.
Humboldt-Universität zu Berlin, 2017.

H. Fleischhack.
Measurement ofthe Iron Spectrum in Cosmic Rayswith the VERITAS Experiment.
Humboldt-Universität zu Berlin, 2017.

M. Giomi.
A catalog of variable high-energy gamma-ray sources and prospects for polarization measurement with the Fermi Large Area Telescope.
Humboldt-Universität zu Berlin, 2017.

M. Huetten.
Prospects for Galactic dark matter searches with the Cherenkov Telescope Array (CTA).
Humboldt-Universität zu Berlin, 2017.

M. Krause.
High-sensitivity analysis of the Cygnus region observed with VERITAS.
Humboldt-Universität zu Berlin, 2017.

A. K. Mallot.
The energy spectrum of cosmic electrons measured with the MAGIC telescopes.
Humboldt Universität, 2017.

Belle II

Published

Belle Collaboration.
Erratum to: Search for B decays to final states with the η_c meson.

Journal of high energy physics, 1702(02):088, and PUBDB-2018-00355, BELLE-PREPRINT-2015-1; KEK-PREPRINT-2014-42.
doi: 10.1007/JHEP02(2017)088.

Belle Collaboration.
Evidence for Isospin Violation and Measurement of CP Asymmetries in $B \to K^*(892)\gamma$.
Physical review letters, 119(19):191802, and PUBDB-2017-12046, BELLE-PREPRINT-2017-08; KEK-PREPRINT-2017-4; arXiv:1707.00394.
doi: 10.1103/PhysRevLett.119.191802.

Belle Collaboration.
First measurement of T-odd moments in $D^0 \to K_S^0\pi^+\pi^-\pi^0$ decays.
Physical review / D, 95(9):091101, and PUBDB-2017-05887, BELLE-PREPRINT-2017-01; KEK-PREPRINT-2016-62; arXiv:1703.05721.
doi: 10.1103/PhysRevD.95.091101.

Belle Collaboration.
Invariant-mass and fractional-energy dependence of inclusive production of di-hadrons in e^+e^- annihilation at $\sqrt{s} = 10.58$ GeV.
Physical review / D, 96(3):032005, and PUBDB-2017-10924, BELLE-DRAFT-2017-13-; KEK-DRAFT-2017-09; arXiv:1706.08348; BELLE-DRAFT-2017-13-KEK-DRAFT-2017-09.
doi: 10.1103/PhysRevD.96.032005.

Belle Collaboration.
Lepton-Flavor-Dependent Angular Analysis of $B \to K^*\ell^+\ell^-$.
Physical review letters, 118(11):111801, and PUBDB-2017-02387.
doi: 10.1103/PhysRevLett.118.111801.

Belle Collaboration.
Measurement of branching fraction and direct CP asymmetry in charmless $B^+ \to K^+K^-\pi^+$ decays at Belle.
Physical review / D, 96(3):031101, and PUBDB-2017-10774, KEK-PREPRINT-2017-5; BELLE-PREPRINT-2017-09; arXiv:1705.02640.
doi: 10.1103/PhysRevD.96.031101.

Belle Collaboration.
Measurement of the branching fraction and CP asymmetry in $B^0 \to \pi^0\pi^0$ decays, and an improved constraint on ϕ_2.
Physical review / D, 96(3):032007, and PUBDB-2017-10772, BELLE-PREPRINT-2017-11; KEK-PREPRINT-2017-7; arXiv:1705.02083.
doi: 10.1103/PhysRevD.96.032007.

Belle Collaboration.
Measurement of the decays $B \to \eta\ell\nu_\ell$ and $B \to \eta'\ell\nu_\ell$ in fully reconstructed events at Belle.
Physical review / D, D96(9):091102, and PUBDB-2017-13979, arXiv:1703.10216.
doi: 10.1103/PhysRevD.96.091102.

Belle Collaboration.
Measurement of the τ lepton polarization and $R(D^*)$ in the decay $\bar{B} \to D^*\tau^-\bar{\nu}_\tau$.
Physical review letters, 118(21):211801, and PUBDB-2017-05882, KEK-PREPRINT-2016-53; BELLE-PREPRINT-2016-14; arXiv:1612.00529.
doi: 10.1103/PhysRevLett.118.211801.

Belle Collaboration.
Observation of an alternative $\chi_{c0}(2P)$ candidate in $e^+e^- \to J/\psi D\bar{D}$.
Physical review / D, 95(11):112003, and PUBDB-2017-05893, BELLE-PREPRINT-2017-07; KEK-PREPRINT-2017-3; arXiv:1704.01872.
doi: 10.1103/PhysRevD.95.112003.

Belle Collaboration.
Observation of $D^0 \to \rho^0\gamma$ and Search for CP Violation in Radiative Charm Decays.
Physical review letters, 118(5):051801, and PUBDB-2017-00973, BELLE-CONF-1601; BELLE-PREPRINT-2016-11; arXiv:1603.03257.
doi: 10.1103/PhysRevLett.118.051801.

Belle Collaboration.
Search for $B \to h\nu\bar{\nu}$ decays with semileptonic tagging at Belle.
Physical review / D, 96(9):091101, and PUBDB-2017-13973, arXiv:1702.03224.
doi: 10.1103/PhysRevD.96.091101.

Belle Collaboration.
Search for $\Lambda_c^+ \to \phi p\pi^0$ and branching fraction measurement of $\Lambda_c^+ \to K^-\pi^+p\pi^0$.
Physical review / D, 96(5):051102, and PUBDB-2017-12039, BELLE-PREPRINT-2017-12; KEK-PREPRINT-2017-08; UCHEP-2017-06; arXiv:1707.00089.
doi: 10.1103/PhysRevD.96.051102.

Belle Collaboration.
Search for CP Violation and Measurement of the Branching Fraction in the Decay $D^0 \to K_S^0K_S^0$.
Physical review letters, 119(17):171801, and PUBDB-2017-12038, Belle-Preprint-2017-03; KEK-Preprint-2016-64; arXiv:1705.05966.
doi: 10.1103/PhysRevLett.119.171801.

Belle Collaboration.
Search for D^0 decays to invisible final states at Belle.
Physical review / D, 95(1):011102(R), and PUBDB-2017-00974, BELLE-PREPRINT-2013-13; KEK-PREPRINT-2013-51; BELLE-PREPRINT-2016-13; KEK-PREPRINT-2016-51; arXiv:1611.09455.
doi: 10.1103/PhysRevD.95.011102.

Belle Collaboration.
Search for light tetraquark states in $\Upsilon(1S)$ and $\Upsilon(2S)$ decays.
Physical review / D, D96(11):112002, and PUBDB-2017-13989, BELLE-PREPRINT-2017-21; KEK-PREPRINT-2017-30; arXiv:1711.01690.
doi: 10.1103/PhysRevD.96.112002.

Belle Collaboration.
Search for the 0^{--} Glueball in $\Upsilon(1S)$ and $\Upsilon(2S)$ decays.
Physical review / D, 95(1):012001, and PUBDB-2017-00117, BELLE-PREPRINT-2016-12; KEK-PREPRINT-2016-50; arXiv:1611.07131.
doi: 10.1103/PhysRevD.95.012001.

Belle Collaboration.
Study of η and dipion transitions in $\Upsilon(4S)$ decays to lower bottomonia.
Physical review / D, 96(5):052005, and PUBDB-2017-12047, BELLE-PREPRINT-2017-16; KEK-PREPRINT-2017-17; arXiv:1707.04973.
doi: 10.1103/PhysRevD.96.052005.

M. J. Dolan et al.
Revised constraints and Belle II sensitivity for visible and invisible axion-like particles.
Journal of high energy physics, 1712(12):094, and PUBDB-2018-00299, DESY-17-127; arXiv:1709.00009.
doi: 10.1007/JHEP12(2017)094.

CMS

Published

I. Abt et al.
Investigation into the limits of perturbation theory at low Q^2 using HERA deep inelastic scattering data.
Physical review / D, 96(1):014001, and PUBDB-2017-10569, DESY-17-051; arXiv:1704.03187.
doi: 10.1103/PhysRevD.96.014001.

A. Albert et al.
Towards the next generation of simplified Dark Matter models.
Physics of the Dark Universe, 16:49, and PUBDB-2017-12522, arXiv:1607.06680.
doi: 10.1016/j.dark.2017.02.002.

S. P. Baranov and A. Lipatov.
Prompt charmonia production and polarization at LHC in the NRQCD with k_T-factorization. Part III: J/ψ meson.
Physical review / D, D96(3):034019, and PUBDB-2017-11046, arXiv:1611.10141; DESY-17-039.
doi: 10.1103/PhysRevD.96.034019.

S. P. Baranov et al.
Associated production of Z bosons and b-jets at the LHC in the combined k_T + collinear QCD factorization approach.
The European physical journal / C, 77(11):772, and PUBDB-2017-12705, DESY-17-126; arXiv:1708.07079.
doi: 10.1140/epjc/s10052-017-5369-5.

S. P. Baranov et al.
Testing the parton evolution with the use of two-body final states.
The European physical journal / C, 77(1):2, and PUBDB-2017-00314, DESY-16-180; arXiv:1609.03546.
doi: 10.1140/epjc/s10052-016-4562-2.

CMS Collaboration.
Alignment of the CMS Tracker: Latest Results from LHC Run-II.
Journal of physics / Conference Series, 898:042014, and PUBDB-2017-12756.
doi: 10.3204/PUBDB-2017-12756.

CMS Collaboration.
Characterisation of irradiated thin silicon sensors for the CMS phase II pixel upgrade.
The European physical journal / C, 77(8):567, and PUBDB-2017-10157.
doi: 10.1140/epjc/s10052-017-5115-z.

CMS Collaboration.
Charged-particle nuclear modification factors in PbPb and pPb collisions at $\sqrt{s_{NN}} = 5.02$ TeV.
Journal of high energy physics, 1704(04):039, and PUBDB-2017-02289, CMS-HIN-15-015; CERN-EP-2016-242; arXiv:1611.01664.
doi: 10.1007/JHEP04(2017)039.

CMS Collaboration.
Coherent J/ψ photoproduction in ultra-peripheral PbPb collisions at $\sqrt{s_{NN}}$ = 2.76 TeV with the CMS experiment.
Physics letters / B, 772:489, and PUBDB-2017-11800, CMS-HIN-12-009; CERN-EP-2016-098; arXiv:1605.06966; FERMILAB-PUB-16-194-CMS.
doi: 10.1016/j.physletb.2017.07.001.

CMS Collaboration.
Constraints on anomalous Higgs boson couplings using production and decay information in the four-lepton final state.
Physics letters / B, 775:1, and PUBDB-2017-11806, CMS-HIG-17-011; CERN-EP-2017-143; arXiv:1707.00541.
doi: 10.1016/j.physletb.2017.10.021.

CMS Collaboration.
Cross section measurement of t-channel single top quark production in pp collisions at $\sqrt{s} = 13$ TeV.
Physics letters / B, 772:752, and PUBDB-2017-10113, CMS-TOP-16-003; CERN-EP-2016-233; arXiv:1610.00678.
doi: 10.1016/j.physletb.2017.07.047.

CMS Collaboration.
Erratum to: Search for dark matter and unparticles in events with a Z boson and missing transverse momentum in proton-proton collisions at $\sqrt{s} = 13$ TeV.
Journal of high energy physics, 1709(09):106, and PUBDB-2018-00599, CMS-EXO-16-010; CERN-EP-2016-309; arXiv:1701.02042.
doi: 10.1007/JHEP09(2017)106.

CMS Collaboration.
Erratum to: Search for dark matter in proton-proton collisions at 8 TeV with missing transverse momentum and vector boson tagged jets.
Journal of high energy physics, 1708(08):035, and PUBDB-2018-00412, CMS-EXO-12-055; CERN-EP-2016-178; arXiv:1607.05764.
doi: 10.1007/JHEP08(2017)035.

CMS Collaboration.
Evidence for collectivity in pp collisions at the LHC.
Physics letters / B, 765:193, and PUBDB-2016-06639, CMS-HIN-16-010; CERN-EP-2016-147; arXiv:1606.06198.
doi: 10.1016/j.physletb.2016.12.009.

CMS Collaboration.
Inclusive search for supersymmetry using razor variables in pp collisions at $\sqrt{s} = 13$ TeV.
Physical review / D, 95(1):012003, and PUBDB-2017-01327, CMS-SUS-15-004; CERN-EP-2016-214; arXiv:1609.07658.
doi: 10.1103/PhysRevD.95.012003.

CMS Collaboration.
Jet energy scale and resolution in the CMS experiment in pp collisions at 8 TeV.
Journal of Instrumentation, 12(02):P02014, and PUBDB-2017-01318, CMS-JME-13-004; CERN-PH-EP-2015-305; arXiv:1607.03663.
doi: 10.1088/1748-0221/12/02/P02014.

CMS Collaboration.
Managing the CMS Data and Monte Carlo Processing during LHC Run 2.
Journal of physics / Conference Series, 898:052012, and PUBDB-2017-13487.
doi: 10.1088/1742-6596/898/5/052012.

CMS Collaboration.
Measurement and QCD analysis of double-differential inclusive jet cross sections in pp collisions at $\sqrt{s} = 8$ TeV and cross section ratios to 2.76 and 7 TeV.
Journal of high energy physics, 1703(03):156, and PUBDB-2017-02259, CMS-SMP-14-001; CERN-EP-2016-196; arXiv:1609.05331.
doi: 10.1007/JHEP03(2017)156.

CMS Collaboration.
Measurement of charged pion, kaon, and proton production in proton-proton collisions at $\sqrt{s} = 13$ TeV.
Physical review / D, 96(11):112003, and PUBDB-2017-13850, CMS-FSQ-16-004; CERN-EP-2017-091; arXiv:1706.10194.
doi: 10.1103/PhysRevD.96.112003.

CMS Collaboration.
Measurement of electroweak-induced production of Wγ with two jets in pp collisions at $\sqrt{s} = 8$ TeV and constraints on anomalous quartic gauge couplings.
Journal of high energy physics, 1706(06):106, and PUBDB-2017-10125, CMS-SMP-14-011; CERN-EP-2016-289; arXiv:1612.09256.
doi: 10.1007/JHEP06(2017)106.

CMS Collaboration.
Measurement of inclusive jet cross sections in pp and PbPb collisions at $\sqrt{s_{NN}} = 2.76$ TeV.
Physical review / C, 96(1):015202, and PUBDB-2017-10110, CMS-HIN-13-005; CERN-EP-2016-217; arXiv:1609.05383.
doi: 10.1103/PhysRevC.96.015202.

CMS Collaboration.
Measurement of prompt and nonprompt J/ψ production in pp and pPb collisions at $\sqrt{s_{NN}} = 5.02$ TeV.
The European physical journal / C, 77(4):269, and PUBDB-2017-02342, CMS-HIN-14-009; CERN-EP-2017-009; arXiv:1702.01462.
doi: 10.1140/epjc/s10052-017-4828-3.

CMS Collaboration.
Measurement of the $B^{\pm}$ Meson Nuclear Modification Factor in Pb-Pb Collisions at $\sqrt{s_{NN}} = 5.02$ TeV.
Physical review letters, 119(15):152301, and PUBDB-2017-11825, CMS-HIN-16-011; CERN-EP-2017-076; arXiv:1705.04727.
doi: 10.1103/PhysRevLett.119.152301.

CMS Collaboration.
Measurement of the cross section for electroweak production of Zγ in association with two jets and constraints on anomalous quartic gauge couplings in proton–proton collisions at $\sqrt{s} = 8$ TeV.
Physics letters / B, 770:380, and PUBDB-2017-10162, CMS-SMP-14-018; CERN-EP-2016-308; arXiv:1702.03025.
doi: 10.1016/j.physletb.2017.04.071.

CMS Collaboration.
Measurement of the differential cross sections for the associated production of a W boson and jets in proton-proton collisions at $\sqrt{s} = 13$ TeV.
Physical review / D, 96(7):072005, and PUBDB-2017-11816, CMS-SMP-16-005; CERN-EP-2017-142; arXiv:1707.05979.
doi: 10.1103/PhysRevD.96.072005.

CMS Collaboration.
Measurement of the differential inclusive B^{+} hadron cross sections in pp collisions at $\sqrt{s} = 13$ TeV.
Physics letters / B, 771:435, and PUBDB-2017-10109, CMS-BPH-15-004; CERN-EP-2016-198; arXiv:1609.00873.
doi: 10.1016/j.physletb.2017.05.074.

CMS Collaboration.
Measurement of the inclusive energy spectrum in the very forward direction in proton-proton collisions at $\sqrt{s} = 13$ TeV.
Journal of high energy physics, 1708(08):046, and PUBDB-2017-10143, CMS-FSQ-16-002; CERN-EP-2016-313; arXiv:1701.08695.
doi: 10.1007/JHEP08(2017)046.

CMS Collaboration.
Measurement of the mass difference between top quark and antiquark in pp collisions at $\sqrt{s} = 8$ TeV.
Physics letters / B, 770:50, and PUBDB-2017-02291, CMS-TOP-12-031; CERN-EP-2016-249; arXiv:1610.09551.
doi: 10.1016/j.physletb.2017.04.028.

CMS Collaboration.
Measurement of the production cross section of a W boson in association with two b jets in pp collisions at $\sqrt{s} = 8$ TeV.
The European physical journal / C, 77(2):92, and PUBDB-2017-02263, CMS-SMP-14-020; CERN-EP-2016-190; arXiv:1608.07561.
doi: 10.1140/epjc/s10052-016-4573-z.

CMS Collaboration.
Measurement of the semileptonic $\mathrm{t\bar{t}}+\gamma$ production cross section in pp collisions at $\sqrt{s}=8$ TeV.
Journal of high energy physics, 1710(10):006, and PUBDB-2017-11847, CMS-TOP-14-008; CERN-EP-2017-112; arXiv:1706.08128.
doi: 10.1007/JHEP10(2017)006.

CMS Collaboration.
Measurement of the top quark mass in the dileptonic $t\bar{t}$ decay channel using the mass observables $M_{b\ell}$, M_{T2}, and $M_{b\ell\nu}$ in pp collisions at $\sqrt{s}=8$ TeV.
Physical review / D, 96(3):032002, and PUBDB-2017-10164, CMS-TOP-15-008; CERN-EP-2017-050; arXiv:1704.06142.
doi: 10.1103/PhysRevD.96.032002.

CMS Collaboration.
Measurement of the top quark mass using single top quark events in proton-proton collisions at $\sqrt{s}=8$ TeV.
The European physical journal / C, 77(5):354, and PUBDB-2017-10159, CMS-TOP-15-001; CERN-EP-2017-012; arXiv:1703.02530.
doi: 10.1140/epjc/s10052-017-4912-8.

CMS Collaboration.
Measurement of the transverse momentum spectra of weak vector bosons produced in proton-proton collisions at $\sqrt{s}=8$ TeV.
Journal of high energy physics, 1702(02):096, and PUBDB-2017-01310, CMS-SMP-14-012; CERN-EP-2016-152; arXiv:1606.05864.
doi: 10.1007/JHEP02(2017)096.

CMS Collaboration.
Measurement of the transverse momentum spectrum of the Higgs boson produced in pp collisions at $\sqrt{s}=8$ TeV using $H\rightarrow WW$ decays.
Journal of high energy physics, 1703(03):032, and PUBDB-2017-02251, CMS-HIG-15-010; CERN-EP-2016-125; arXiv:1606.01522.
doi: 10.1007/JHEP03(2017)032.

CMS Collaboration.
Measurement of the triple-differential dijet cross section in proton-proton collisions at $\sqrt{s}=8$ TeV and constraints on parton distribution functions.
The European physical journal / C, 77(11):746, and PUBDB-2017-13837, CMS-SMP-16-011; CERN-EP-2017-061; arXiv:1705.02628.
doi: 10.1140/epjc/s10052-017-5286-7.

CMS Collaboration.
Measurement of the $t\bar{t}$ production cross section using events in the eμ final state in pp collisions at $\sqrt{s}=13$ TeV.
The European physical journal / C, 77(3):172, and PUBDB-2017-02308, CMS-TOP-16-005; CERN-EP-2016-265; arXiv:1611.04040.
doi: 10.1140/epjc/s10052-017-4718-8.

CMS Collaboration.
Measurement of the $t\bar{t}$ production cross section using events with one lepton and at least one jet in pp collisions at $\sqrt{s}=13$ TeV.
Journal of high energy physics, 1709(09):051, and PUBDB-2017-11810, CMS-TOP-16-006; CERN-EP-2016-321; arXiv:1701.06228.
doi: 10.1007/JHEP09(2017)051.

CMS Collaboration.
Measurement of the WZ production cross section in pp collisions at $\sqrt{s}=13$ TeV.
Physics letters / B, 766:268, and PUBDB-2017-01316, CMS-SMP-16-002; CERN-EP-2016-169; arXiv:1607.06943.
doi: 10.1016/j.physletb.2017.01.011.

CMS Collaboration.
Measurements of differential cross sections for associated production of a W boson and jets in proton-proton collisions at $\sqrt{s}=8$ TeV.
Physical review / D, 95(5):052002, and PUBDB-2017-02297, CMS-SMP-14-023; CERN-EP-2016-231; CERN-PH-EP-2016-231; arXiv:1610.04222.
doi: 10.1103/PhysRevD.95.052002.

CMS Collaboration.
Measurements of differential production cross sections for a Z boson in association with jets in pp collisions at $\sqrt{s}=8$ TeV.
Journal of high energy physics, 1704(04):022, and PUBDB-2017-02335, CMS-SMP-14-013; CERN-EP-2016-256; arXiv:1611.03844.
doi: 10.1007/JHEP04(2017)022.

CMS Collaboration.
Measurements of jet charge with dijet events in pp collisions at $\sqrt{s}=8$ TeV.
Journal of high energy physics, 1710(10):131, and PUBDB-2017-11848, CMS-SMP-15-003; CERN-EP-2017-085; arXiv:1706.05868.
doi: 10.1007/JHEP10(2017)131.

CMS Collaboration.
Measurements of properties of the Higgs boson decaying into the four-lepton final state in pp collisions at $\sqrt{s}=13$ TeV.
Journal of high energy physics, 1711(11):047, and PUBDB-2017-13853, CMS-HIG-16-041; CERN-EP-2017-123; arXiv:1706.09936.
doi: 10.1007/JHEP11(2017)047.

CMS Collaboration.
Measurements of the associated production of a Z boson and b jets in pp collisions at $\sqrt{s}=8$ TeV.
The European physical journal / C, 77(11):751, and PUBDB-2017-13832, CMS-SMP-14-010; CERN-EP-2016-254; arXiv:1611.06507.
doi: 10.1140/epjc/s10052-017-5140-y.

CMS Collaboration.
Measurements of the charm jet cross section and nuclear modification factor in pPb collisions at $\sqrt{s_{NN}}=5.02$ TeV.
Physics letters / B, 772:306, and PUBDB-2017-10129, CMS-

HIN-15-012; CERN-EP-2016-274; arXiv:1612.08972.
doi: 10.1016/j.physletb.2017.06.053.

CMS Collaboration.
Measurements of the $pp \to W\gamma\gamma$ and $pp \to Z\gamma\gamma$ cross sections and limits on anomalous quartic gauge couplings at $\sqrt{s} = 8$ TeV.
Journal of high energy physics, 1710(10):072, and PUBDB-2017-11814, CMS-SMP-15-008; CERN-EP-2017-039; arXiv:1704.00366.
doi: 10.1007/JHEP10(2017)072.

CMS Collaboration.
Measurements of the $\mathrm{t\bar{t}}$ production cross section in lepton+jets final states in pp collisions at 8 TeV and ratio of 8 to 7 TeV cross sections.
The European physical journal / C, 77(1):15, and PUBDB-2017-01306, CMS-TOP-12-006; CERN-EP-2016-016; arXiv:1602.09024.
doi: 10.1140/epjc/s10052-016-4504-z.

CMS Collaboration.
Mechanical stability of the CMS strip tracker measured with a laser alignment system.
Journal of Instrumentation, 12(04):P04023, and PUBDB-2017-10132, CMS-TRK-15-002; CERN-EP-2016-320; arXiv:1701.02022.
doi: 10.1088/1748-0221/12/04/P04023.

CMS Collaboration.
Multiplicity and rapidity dependence of strange hadron production in pp, pPb, and PbPb collisions at the LHC.
Physics letters / B, 768:103, and PUBDB-2017-01313, CMS-HIN-15-006; CERN-EP-2016-105; arXiv:1605.06699.
doi: 10.1016/j.physletb.2017.01.075.

CMS Collaboration.
Observation of Υ(1S) pair production in proton-proton collisions at $\sqrt{s} = 8$ TeV.
Journal of high energy physics, 1705(05):013, and PUBDB-2017-10118, CMS-BPH-14-008; CERN-EP-2016-237; arXiv:1610.07095.
doi: 10.1007/JHEP05(2017)013.

CMS Collaboration.
Observation of charge-dependent azimuthal correlations in pPb collisions and its implication for the search for the chiral magnetic effect.
Physical review letters, 118(12):122301, and PUBDB-2017-02269, CMS-HIN-16-009; CERN-EP-2016-236; arXiv:1610.00263.
doi: 10.1103/PhysRevLett.118.122301.

CMS Collaboration.
Observation of the decay $B^+ \to \psi(2S)\phi(1020)K^+$ in pp collisions at $\sqrt{s} = 8$ TeV.
Physics letters / B, 764:66, and PUBDB-2016-06647, CMS-BPH-13-009; CERN-EP-2016-161; arXiv:1607.02638.
doi: 10.1016/j.physletb.2016.11.001.

CMS Collaboration.
Observation of top quark production in proton-nucleus collisions.
Physical review letters, 119(24):242001, and PUBDB-2017-13929, CMS-HIN-17-002; CERN-EP-2017-239; arXiv:1709.07411.
doi: 10.1103/PhysRevLett.119.242001.

CMS Collaboration.
Particle-flow reconstruction and global event description with the CMS detector.
Journal of Instrumentation, 12(10):P10003, and PUBDB-2017-11850, CMS-PRF-14-001; CERN-EP-2017-110; arXiv:1706.04965.
doi: 10.1088/1748-0221/12/10/P10003.

CMS Collaboration.
Principal-component analysis of two-particle azimuthal correlations in PbPb and pPb collisions at CMS.
Physical review / C, 96(6):064902, and PUBDB-2017-13861, CMS-HIN-15-010; CERN-EP-2017-133; arXiv:1708.07113.
doi: 10.1103/PhysRevC.96.064902.

CMS Collaboration.
Pseudorapidity dependence of long-range two-particle correlations in pPb collisions at $\sqrt{s_{NN}}$ = 5.02 TeV.
Physical review / C, 96(1):014915, and PUBDB-2018-00560, CMS-HIN-14-008; CERN-EP-2016-042; arXiv:1604.05347.
doi: 10.1103/PhysRevC.96.014915.

CMS Collaboration.
P-Type Silicon Strip Sensors for the new CMS Tracker at HL-LHC.
Journal of Instrumentation, 12(06):P06018, and PUBDB-2018-00521.
doi: 10.1088/1748-0221/12/06/P06018.

CMS Collaboration.
Search for a heavy composite Majorana neutrino in the final state with two leptons and two quarks at $\sqrt{s} = 13$ TeV.
Physics letters / B, B775:315, and PUBDB-2017-13854, CMS-EXO-16-026; CERN-EP-2017-125; arXiv:1706.08578.
doi: 10.1016/j.physletb.2017.11.001.

CMS Collaboration.
Search for a heavy resonance decaying to a top quark and a vector-like top quark at $\sqrt{s}$ = 13 TeV.
Journal of high energy physics, 1709(09):053, and PUBDB-2017-11798, CMS-B2G-16-013; CERN-EP-2017-035; arXiv:1703.06352.
doi: 10.1007/JHEP09(2017)053.

CMS Collaboration.
Search for a light pseudoscalar Higgs boson produced in association with bottom quarks in pp collisions at $\sqrt{s} = 8$ TeV.
Journal of high energy physics, 1711(11):010, and PUBDB-2017-13864, CMS-HIG-15-009; CERN-EP-2017-159; arXiv:1707.07283.
doi: 10.1007/JHEP11(2017)010.

CMS Collaboration.
Search for anomalous couplings in boosted $\mathrm{WW/WZ} \rightarrow \ell\nu\mathrm{q\bar{q}}$ production in proton-proton collisions at $\sqrt{s} = 8$ TeV.
Physics letters / B, 772:21, and PUBDB-2017-10146, CMS-SMP-13-008; CERN-EP-2017-029; arXiv:1703.06095.
doi: 10.1016/j.physletb.2017.06.009.

CMS Collaboration.
Search for anomalous Wtb couplings and flavour-changing neutral currents in t-channel single top quark production in pp collisions at $\sqrt{s} = 7$ and 8 TeV.
Journal of high energy physics, 1702(02):028, and PUBDB-2017-01332, CMS-TOP-14-007; CERN-EP-2016-207; arXiv:1610.03545.
doi: 10.1007/JHEP02(2017)028.

CMS Collaboration.
Search for associated production of dark matter with a Higgs boson decaying to $\mathrm{b\bar{b}}$ or $\gamma\gamma$ at $\sqrt{s} = 13$ TeV.
Journal of high energy physics, 1710(10):180, and PUBDB-2017-13834, CMS-EXO-16-012; CERN-EP-2017-027; arXiv:1703.05236.
doi: 10.1007/JHEP10(2017)180.

CMS Collaboration.
Search for black holes in high-multiplicity final states in proton-proton collisions at $\sqrt{s}$ =13 TeV.
Physics letters / B, 774:279, and PUBDB-2017-11846, CMS-EXO-15-007; CERN-EP-2017-074; arXiv:1705.01403.
doi: 10.1016/j.physletb.2017.09.053.

CMS Collaboration.
Search for Charged Higgs Bosons Produced via Vector Boson Fusion and Decaying into a Pair of W and Z Bosons Using pp Collisions at $\sqrt{s} = 13$ TeV.
Physical review letters, 119(14):141802, and PUBDB-2017-11829, CMS-HIG-16-027; CERN-EP-2017-068; arXiv:1705.02942.
doi: 10.1103/PhysRevLett.119.141802.

CMS Collaboration.
Search for CP violation in $t\bar{t}$ production and decay in proton-proton collisions at $\sqrt{s} = 8$ TeV.
Journal of high energy physics, 1703(03):101, and PUBDB-2017-02338, CMS-TOP-16-001; CERN-EP-2016-266; CMS-TO-16-001; arXiv:1611.08931.
doi: 10.1007/JHEP03(2017)101.

CMS Collaboration.
Search for Dark Matter and Supersymmetry with a Compressed Mass Spectrum in the Vector Boson Fusion Topology in Proton-Proton Collisions at $\sqrt{s} = 8$ TeV.
Physical review letters, 118(2):021802, and PUBDB-2017-01311, CMS-SUS-14-019; CERN-EP-2016-096; arXiv:1605.09305.
doi: 10.1103/PhysRevLett.118.021802.

CMS Collaboration.
Search for dark matter and unparticles in events with a Z boson and missing transverse momentum in proton-proton collisions at $\sqrt{s} = 13$ TeV.
Journal of high energy physics, 1703(03):061, and PUBDB-2017-02341, CMS-EXO-16-010; CERN-EP-2016-309; FERMILAB-PUB-17-011-CMS; arXiv:1701.02042.
doi: 10.1007/JHEP03(2017)061.

CMS Collaboration.
Search for dark matter produced in association with heavy-flavor quark pairs in proton-proton collisions at $\sqrt{s} = 13$ TeV.
The European physical journal / C, C77(12):845, and PUBDB-2018-00251, CMS-EXO-16-005; CERN-EP-2017-087; arXiv:1706.02581.
doi: 10.1140/epjc/s10052-017-5317-4.

CMS Collaboration.
Search for dark matter produced with an energetic jet or a hadronically decaying W or Z boson at $\sqrt{s} = 13$ TeV.
Journal of high energy physics, 1707(07):014, and PUBDB-2017-10160, CMS-EXO-16-037; CERN-EP-2017-031; arXiv:1703.01651.
doi: 10.1007/JHEP07(2017)014.

CMS Collaboration.
Search for dijet resonances in proton-proton collisions at $\sqrt{s} =$ 13 TeV and constraints on dark matter and other models.
Physics letters / B, 769:520, and PUBDB-2017-01335, CMS-EXO-16-032; CERN-EP-2016-277; arXiv:1611.03568.
doi: 10.1016/j.physletb.2017.02.012.

CMS Collaboration.
Search for direct production of supersymmetric partners of the top quark in the all-jets final state in proton-proton collisions at $\sqrt{s} = 13$ TeV.
Journal of high energy physics, 1710(10):005, and PUBDB-2017-11801, CMS-SUS-16-049; CERN-EP-2017-129; arXiv:1707.03316.
doi: 10.1007/JHEP10(2017)005.

CMS Collaboration.
Search for electroweak production of a vector-like quark decaying to a top quark and a Higgs boson using boosted topologies in fully hadronic final states.
Journal of high energy physics, 1704(04):136, and PUBDB-2017-02340, CMS-B2G-16-005; CERN-EP-2016-290; arXiv:1612.05336.
doi: 10.1007/JHEP04(2017)136.

CMS Collaboration.
Search for electroweak production of charginos in final states with two τ leptons in pp collisions at $\sqrt{s} = 8$ TeV.
Journal of high energy physics, 1704(04):018, and PUBDB-2017-02294, CMS-SUS-14-022; CERN-EP-2016-225; arXiv:1610.04870.
doi: 10.1007/JHEP04(2017)018.

CMS Collaboration.
Search for Evidence of the Type-III Seesaw Mechanism in Multilepton Final States in Proton-Proton Collisions at $\sqrt{s} = 13$ TeV.
Physical review letters, 119(22):221802, and PUBDB-2017-13858, CMS-EXO-17-006; CERN-EP-2017-194; arXiv:1708.07962.
doi: 10.1103/PhysRevLett.119.221802.

CMS Collaboration.
Search for heavy gauge W' boson in events with an energetic lepton and large missing transverse momentum at $\sqrt{s} = 13$ TeV.
Physics letters / B, 770:278, and PUBDB-2017-10127, CMS-EXO-15-006; CERN-EP-2016-281; arXiv:1612.09274.
doi: 10.1016/j.physletb.2017.04.043.

CMS Collaboration.
Search for heavy neutrinos or third-generation leptoquarks in final states with two hadronically decaying τ leptons and two jets in proton-proton collisions at $\sqrt{s} = 13$ TeV.
Journal of high energy physics, 1703(03):077, and PUBDB-2017-02337, CMS-EXO-16-016; CERN-EP-2016-286; arXiv:1612.01190.
doi: 10.1007/JHEP03(2017)077.

CMS Collaboration.
Search for heavy resonances decaying into a vector boson and a Higgs boson in final states with charged leptons, neutrinos, and b quarks.
Physics letters / B, 768:137, and PUBDB-2017-01329, CMS-B2G-16-003; CERN-EP-2016-226; arXiv:1610.08066.
doi: 10.1016/j.physletb.2017.02.040.

CMS Collaboration.
Search for heavy resonances decaying to tau lepton pairs in proton-proton collisions at $\sqrt{s} = 13$ TeV.
Journal of high energy physics, 1702(02):048, and PUBDB-2017-01334, CMS-EXO-16-008; CERN-EP-2016-273; arXiv:1611.06594.
doi: 10.1007/JHEP02(2017)048.

CMS Collaboration.
Search for heavy resonances that decay into a vector boson and a Higgs boson in hadronic final states at $\sqrt{s} = 13$ TeV.
The European physical journal / C, 77(9):636, and PUBDB-2017-11804, CMS-B2G-17-002; CERN-EP-2017-128; arXiv:1707.01303.
doi: 10.1140/epjc/s10052-017-5192-z.

CMS Collaboration.
Search for Higgs boson pair production in the $bb\tau\tau$ final state in proton-proton collisions at $\sqrt{(s)} = 8$ TeV.
Physical review / D, 96(7):072004, and PUBDB-2017-11812, CMS-HIG-215-013; CERN-EP-2017-104; arXiv:1707.00350.
doi: 10.1103/PhysRevD.96.072004.

CMS Collaboration.
Search for high-mass diphoton resonances in proton–proton collisions at 13 TeV and combination with 8 TeV search.
Physics letters / B, 767:147, and PUBDB-2017-01325, CMS-EXO-16-027; CERN-EP-2016-216; CMS-EXO-16-02; arXiv:1609.02507.
doi: 10.1016/j.physletb.2017.01.027.

CMS Collaboration.
Search for high-mass Zγ resonances in $\mathrm{e^+e^-}\gamma$ and $\mu^+\mu^-\gamma$ final states in proton-proton collisions at $\sqrt{s} = 8$ and 13 TeV.
Journal of high energy physics, 1701(01):076, and PUBDB-2017-01333, CMS-EXO-16-021; CERN-EP-2016-230; arXiv:1610.02960.
doi: 10.1007/JHEP01(2017)076.

CMS Collaboration.
Search for high-mass $\mathrm{Z}\gamma$ resonances in proton-proton collisions at $\sqrt{s} = 8$ and 13 TeV using jet substructure techniques.
Physics letters / B, 772:363, and PUBDB-2017-10139, CMS-EXO-16-025; CERN-EP-2016-300; arXiv:1612.09516.
doi: 10.1016/j.physletb.2017.06.062.

CMS Collaboration.
Search for leptophobic Z′ bosons decaying into four-lepton final states in proton–proton collisions at $\sqrt{s} = 8$ TeV.
Physics letters / B, 773:563, and PUBDB-2017-11805, CMS-EXO-14-006; CERN-EP-2016-295; arXiv:1701.01345.
doi: 10.1016/j.physletb.2017.08.069.

CMS Collaboration.
Search for light bosons in decays of the 125 GeV Higgs boson in proton-proton collisions at $\sqrt{s} = 8$ TeV.
Journal of high energy physics, 1710(10):076, and PUBDB-2017-11803, CMS-HIG-16-015; CERN-EP-2016-292; arXiv:1701.02032.
doi: 10.1007/JHEP10(2017)076.

CMS Collaboration.
Search for Low Mass Vector Resonances Decaying to Quark-Antiquark Pairs in Proton-Proton Collisions at $\sqrt{s} = 13$ TeV.
Physical review letters, 119(11):111802, and PUBDB-2017-11819, CMS-EXO-16-030; CERN-EP-2017-098; arXiv:1705.10532.
doi: 10.1103/PhysRevLett.119.111802.

CMS Collaboration.
Search for massive resonances decaying into WW, WZ or ZZ bosons in proton-proton collisions at $\sqrt{s} = 13$ TeV.
Journal of high energy physics, 1703(03):162, and PUBDB-2017-02339, CMS-B2G-16-004; CERN-EP-2016-296; arXiv:1612.09159.
doi: 10.1007/JHEP03(2017)162.

CMS Collaboration.
Search for narrow resonances in dilepton mass spectra in proton-proton collisions at $\sqrt{s} = 13$ TeV and combination with 8 TeV data.
Physics letters / B, 768:57, and PUBDB-2017-01324, CMS-EXO-15-005; CERN-EP-2016-209; arXiv:1609.05391.
doi: 10.1016/j.physletb.2017.02.010.

CMS Collaboration.
Search for new phenomena with multiple charged leptons in proton-proton collisions at $\sqrt{s} = 13$ TeV.
The European physical journal / C, 77(9):635, and PUBDB-2017-11807, CMS-SUS-16-003; CERN-EP-2016-306; arXiv:1701.06940.
doi: 10.1140/epjc/s10052-017-5182-1.

CMS Collaboration.
Search for new phenomena with the M_{T2} variable in the all-hadronic final state produced in proton–proton collisions at $\sqrt{s} = 13$ TeV.
The European physical journal / C, 77(10):710, and PUBDB-2017-11828, CMS-SUS-16-036; CERN-EP-2017-084; arXiv:1705.04650.
doi: 10.1140/epjc/s10052-017-5267-x.

CMS Collaboration.
Search for new physics in the monophoton final state in proton-proton collisions at $\sqrt{s} = 13$ TeV.
Journal of high energy physics, 1710(10):073, and PUBDB-2017-11854, CMS-EXO-16-039; CERN-EP-2017-097; arXiv:1706.03794.
doi: 10.1007/JHEP10(2017)073.

CMS Collaboration.
Search for new physics with dijet angular distributions in proton-proton collisions at $\sqrt{s} = 13$ TeV.
Journal of high energy physics, 1707(07):013, and PUBDB-2017-10168, CMS-EXO-15-009; CERN-EP-2017-047; arXiv:1703.09986.
doi: 10.1007/JHEP07(2017)013.

CMS Collaboration.
Search for pair production of vector-like T and B quarks in single-lepton final states using boosted jet substructure in proton-proton collisions at $\sqrt{s} = 13$ TeV.
Journal of high energy physics, 1711(11):085, and PUBDB-2017-13848, CMS-B2G-16-024; CERN-EP-2017-107; arXiv:1706.03408.
doi: 10.1007/JHEP11(2017)085.

CMS Collaboration.
Search for physics beyond the standard model in events with two leptons of same sign, missing transverse momentum, and jets in proton–proton collisions at $\sqrt{s} = 13$ TeV.
The European physical journal / C, 77(9):578, and PUBDB-2017-11817, CMS-SUS-16-035; CERN-EP-2017-071; arXiv:1704.07323.
doi: 10.1140/epjc/s10052-017-5079-z.

CMS Collaboration.
Search for R-parity violating supersymmetry with displaced vertices in proton-proton collisions at $\sqrt{s} = 8$ TeV.
Physical review / D, 95(1):012009, and PUBDB-2017-01330, CMS-SUS-14-020; CERN-EP-2016-224; arXiv:1610.05133.
doi: 10.1103/PhysRevD.95.012009.

CMS Collaboration.
Search for single production of a heavy vector-like T quark decaying to a Higgs boson and a top quark with a lepton and jets in the final state.
Physics letters / B, 771:80, and PUBDB-2017-10123, CMS-B2G-15-008; CERN-EP-2016-279; arXiv:1612.00999.
doi: 10.1016/j.physletb.2017.05.019.

CMS Collaboration.
Search for single production of vector-like quarks decaying into a b quark and a W boson in proton-proton collisions at $\sqrt{s} =$ 13 TeV.
Physics letters / B, 772:634, and PUBDB-2017-10144, CMS-B2G-16-006; CERN-EP-2016-319; arXiv:1701.08328.
doi: 10.1016/j.physletb.2017.07.022.

CMS Collaboration.
Search for single production of vector-like quarks decaying to a Z boson and a top or a bottom quark in proton-proton collisions at $\sqrt{s} = 13$ TeV.
Journal of high energy physics, 1705(05):029, and PUBDB-2017-10145, CMS-B2G-16-001; CERN-EP-2016-326; arXiv:1701.07409.
doi: 10.1007/JHEP05(2017)029.

CMS Collaboration.
Search for standard model production of four top quarks in proton-proton collisions at $\sqrt{s}$ = 13 TeV.
Physics letters / B, 772:336, and PUBDB-2017-10161, CMS-TOP-16-016; CERN-EP-2017-023; arXiv:1702.06164.
doi: 10.1016/j.physletb.2017.06.064.

CMS Collaboration.
Search for supersymmetry in events with one lepton and multiple jets in proton-proton collisions at $\sqrt{s}$ = 13TeV.
Physical review / D, 95(1):012011, and PUBDB-2017-01305, CMS-SUS-15-006; CERN-EP-2016-239; arXiv:1609.09386.
doi: 10.1103/PhysRevD.95.012011.

CMS Collaboration.
Search for supersymmetry in events with photons and missing transverse energy in pp collisions at 13 TeV.
Physics letters / B, 769:391, and PUBDB-2017-02304, CMS-SUS-15-012; CERN-EP-2016-269; arXiv:1611.06604.
doi: 10.1016/j.physletb.2017.04.005.

CMS Collaboration.
Search for supersymmetry in multijet events with missing transverse momentum in proton-proton collisions at 13 TeV.
Physical review / D, 96(3):032003, and PUBDB-2017-10163, CMS-SUS-16-033; CERN-EP-2017-072; arXiv:1704.07781.
doi: 10.1103/PhysRevD.96.032003.

CMS Collaboration.
Search for Supersymmetry in pp Collisions at $\sqrt{s} = 13$ TeV in the Single-Lepton Final State Using the Sum of Masses of Large-Radius Jets.
Physical review letters, 119(15):151802, and PUBDB-2017-11826, CMS-SUS-16-037; CERN-EP-2017-088; arXiv:1705.04673.
doi: 10.1103/PhysRevLett.119.151802.

CMS Collaboration.
Search for supersymmetry in the all-hadronic final state using top quark tagging in pp collisions at $\sqrt{s} = 13$ TeV.
Physical review / D, 96(1):012004, and PUBDB-2017-10135, CMS-SUS-16-009; CERN-EP-2016-293; arXiv:1701.01954.
doi: 10.1103/PhysRevD.96.012004.

CMS Collaboration.
Search for third-generation scalar leptoquarks and heavy right-handed neutrinos in final states with two tau leptons and two jets in proton-proton collisions at $\sqrt{s} = 13$ TeV.
Journal of high energy physics, 1707(07):121, and PUBDB-2017-10148, CMS-EXO-16-023; CERN-EP-2017-025; arXiv:1703.03995.
doi: 10.1007/JHEP07(2017)121.

CMS Collaboration.
Search for top quark decays via Higgs-boson-mediated flavor-changing neutral currents in pp collisions at $\sqrt{s} = 8$ TeV.
Journal of high energy physics, 1702(02):079, and PUBDB-2017-01331, CMS-TOP-13-017; CERN-EP-2016-208;

arXiv:1610.04857.
doi: 10.1007/JHEP02(2017)079.

CMS Collaboration.
Search for top quark partners with charge 5/3 in proton-proton collisions at $\sqrt{s} = 13$ TeV.
Journal of high energy physics, 1708(08):073, and PUBDB-2017-10170, CMS-B2G-15-006; CERN-EP-2017-102; arXiv:1705.10967.
doi: 10.1007/JHEP08(2017)073.

CMS Collaboration.
Search for top squark pair production in compressed-mass-spectrum scenarios in proton-proton collisions at $\sqrt{s} = 8$ TeV using the α_T variable.
Physics letters / B, 767:403, and PUBDB-2017-01312, CMS-SUS-14-006; CERN-EP-2016-103; arXiv:1605.08993.
doi: 10.1016/j.physletb.2017.02.007.

CMS Collaboration.
Search for top squark pair production in pp collisions at $\sqrt{s} = 13$ TeV using single lepton events.
Journal of high energy physics, 1710(10):019, and PUBDB-2017-11852, CMS-SUS-16-051; CERN-EP-2017-109; arXiv:1706.04402.
doi: 10.1007/JHEP10(2017)019.

CMS Collaboration.
Search for $\mathrm{t\bar{t}}$ resonances in highly boosted lepton+jets and fully hadronic final states in proton-proton collisions at $\sqrt{s} = 13$ TeV.
Journal of high energy physics, 1707(07):001, and PUBDB-2017-10166, CMS-B2G-16-015; CERN-EP-2017-049; arXiv:1704.03366.
doi: 10.1007/JHEP07(2017)001.

CMS Collaboration.
Searches for invisible decays of the Higgs boson in pp collisions at $\sqrt{s} = 7$, 8, and 13 TeV.
Journal of high energy physics, 1702(02):135, and PUBDB-2017-01328, CMS-HIG-16-016; CERN-EP-2016-240; arXiv:1610.09218.
doi: 10.1007/JHEP02(2017)135.

CMS Collaboration.
Searches for pair production of third-generation squarks in $\sqrt{s} = 13$ TeV pp collisions.
The European physical journal / C, 77(5):327, and PUBDB-2017-10121, CMS-SUS-16-008; CERN-EP-2016-284; arXiv:1612.03877.
doi: 10.1140/epjc/s10052-017-4853-2.

CMS Collaboration.
Searches for W′ bosons decaying to a top quark and a bottom quark in proton-proton collisions at 13 TeV.
Journal of high energy physics, 1708(08):029, and PUBDB-2017-11853, CMS-B2G-16-016; CERN-EP-2017-090; arXiv:1706.04260.
doi: 10.1007/JHEP08(2017)029.

CMS Collaboration.
Study of jet quenching with Z+jet correlations in PbPb and pp collisions at $\sqrt{s_{NN}} = 5.02$ TeV.
Physical review letters, 119(8):082301, and PUBDB-2017-10142, CMS-HIN-15-013; CERN-EP-2017-002; arXiv:1702.01060.
doi: 10.1103/PhysRevLett.119.082301.

CMS Collaboration.
Suppression and azimuthal anisotropy of prompt and non-prompt J/ψ production in PbPb collisions at $\sqrt{s_{\mathrm{NN}}} = 2.76$ TeV.
The European physical journal / C, 77(4):252, and PUBDB-2017-02301, CMS-HIN-14-005; CERN-EP-2016-243; arXiv:1610.00613.
doi: 10.1140/epjc/s10052-017-4781-1.

CMS Collaboration.
Test beam results of the first CMS double-sided strip module prototypes using the CBC2 read-out chip.
Nuclear instruments & methods in physics research / A, 845:93, and PUBDB-2017-10796.
doi: 10.1016/j.nima.2016.06.027.

CMS Collaboration.
The CMS trigger system.
Journal of Instrumentation, 12(01):P01020, and PUBDB-2017-01326, CMS-TRG-12-001; CERN-EP-2016-160; arXiv:1609.02366.
doi: 10.1088/1748-0221/12/01/P01020.

F. Costanza et al.
The next generation Front-End Controller for the Phase-I Upgrade of the CMS Hadron Calorimeters.
Journal of Instrumentation, 12(03):C03003, and PUBDB-2017-02446.
doi: 10.1088/1748-0221/12/03/C03003.

D0 Collaboration.
Combination of D0 measurements of the top quark mass.
Physical review / D, 95(11):112004, and PUBDB-2017-13960, FERMILAB-PUB-17-079-E; arXiv:1703.06994.
doi: 10.1103/PhysRevD.95.112004.

D0 Collaboration.
Measurement of the direct CP violating charge asymmetry in $B^{\pm} \to \mu^{\pm}\nu_{\mu}D^{0}$ decays.
Physical review / D, 95(3):031101, and PUBDB-2017-13961, FERMILAB-PUB-16-300-E; arXiv:1608.00863.
doi: 10.1103/PhysRevD.95.031101.

D0 Collaboration.
Measurement of top quark polarization in $t\bar{t}$ lepton+jets final states.
Physical review / D, 95(1):011101, and PUBDB-2017-13962, FERMILAB-PUB-16-284-E; arXiv:1607.07627.
doi: 10.1103/PhysRevD.95.011101.

M. Dragicevic et al.
Test beam performance measurements for the Phase I upgrade of the CMS pixel detector.
Journal of Instrumentation, 12(05):P05022, and PUBDB-2018-00549, CMS-NOTE-2017-002; arXiv:1706.00222.
doi: 10.1088/1748-0221/12/05/P05022.

M. Duerr et al.
Hunting the dark Higgs.
Journal of high energy physics, 1704(04):143, and PUBDB-2017-02497, DESY-17-016; arXiv:1701.08780.
doi: 10.1007/JHEP04(2017)143.

K. Hansen et al.
Fluxless flip-chip bonding using a lead-free solder bumping technique.
Journal of Instrumentation, 12(09):T09006, and PUBDB-2017-13205.
doi: 10.1088/1748-0221/12/09/T09006.

T. Harenberg et al.
Online production validation in a HEP environment.
The European physical journal / C, 77(3):188, and PUBDB-2018-00497, arXiv:1611.10112.
doi: 10.1140/epjc/s10052-017-4755-3.

F. Hautmann et al.
Soft-gluon resolution scale in QCD evolution equations.
Physics letters / B, 772:446, and PUBDB-2017-09225, DESY-16-174; arXiv:1704.01757.
doi: 10.1016/j.physletb.2017.07.005.

V. Khachatryan et al.
Measurement of the WZ production cross section in pp collisions at $\sqrt{s} = 7$ and $8\,$TeV and search for anomalous triple gauge couplings at $\sqrt{s} = 8\,$TeV.
The European physical journal / C, 77(4):236, and PUBDB-2017-02256, CMS-SMP-14-014; CERN-EP-2016-205; arXiv:1609.05721.
doi: 10.1140/epjc/s10052-017-4730-z.

V. Khachatryan et al.
A search for new phenomena in pp collisions at $\sqrt{s} = 13\,$TeV in final states with missing transverse momentum and at least one jet using the α_T variable.
The European physical journal / C, 77(5):294, and PUBDB-2017-10115, CMS-SUS-15-005; CERN-EP-2016-246; arXiv:1611.00338.
doi: 10.1140/epjc/s10052-017-4787-8.

A. Luszczak and H. Kowalski.
Dipole model analysis of highest precision HERA data, including very low Q^2.
Physical review / D, D95(1):014030, and PUBDB-2017-00952, DESY-16-231; DESY-REPORT-16-231; arXiv:1611.10100.
doi: 10.1103/PhysRevD.95.014030.

PROSA Collaboration.
Prompt neutrino fluxes in the atmosphere with PROSA parton distribution functions.
Journal of high energy physics, 1705(05):004, and PUBDB-2017-03330, DESY-16-152; arXiv:1611.03815.
doi: 10.1007/JHEP05(2017)004.

A. M. Sirunyan et al.
Combination of searches for heavy resonances decaying to WW, WZ, ZZ, WH, and ZH boson pairs in proton–proton collisions at $\sqrt{s} = 8$ and 13 TeV.
Physics letters / B, 774:533, and PUBDB-2017-11820, CMS-B2G-16-007; CERN-EP-2017-077; arXiv:1705.09171.
doi: 10.1016/j.physletb.2017.09.083.

A. M. Sirunyan et al.
Measurement of double-differential cross sections for top quark pair production in pp collisions at $\sqrt{s} = 8$ TeV and impact on parton distribution functions.
The European physical journal / C, 77(7):459, and PUBDB-2017-08042, CMS-TOP-14-013; CERN-EP-2017-030; arXiv:1703.01630.
doi: 10.1140/epjc/s10052-017-4984-5.

A. M. Sirunyan et al.
Search for associated production of a Z boson with a single top quark and for tZ flavour-changing interactions in pp collisions at $\sqrt{s} = 8$ TeV.
Journal of high energy physics, 1707(7):3, and PUBDB-2017-10140, CMS-TOP-12-039; CERN-EP-2016-324; arXiv:1702.01404.
doi: 10.1007/JHEP07(2017)003.

O. Zenaiev.
Charm Production and QCD Analysis at HERA and LHC.
The European physical journal / C, C77(3):151, and PUBDB-2018-00494, DESY-17-025; arXiv:1612.02371;
doi: 10.1140/epjc/s10052-017-4620-4.

Ph.D. Thesis

A. Harb.
Novel Trigger-Capable Modules for the Future CMS Tracking Detector and Inclusive Top Quark Pair Production Cross Section at $\sqrt{s} = 13$TeV.
Universität Hamburg, Hamburg, 2017.

M. Hempel.
Development of a Novel Diamond Based Detector for Machine Induced Background and Luminosity Measurements.
Brandenburg University of Technology Cottbus-Senftenberg, Hamburg, 2017.

O. Karacheban.
Luminosity measurement at CMS.
Brandenburg University of Technology Cottbus-Senftenberg, 2017.

D. Nowatschin.
Search for vector-like quarks using jet substructure techniques with the CMS experiment.
Universität Hamburg, Hamburg, 2017.

M. O. Sahin.
Search for Supersymmetric Top-Quark Partners Using Support Vector Machines and Upgrade of the Hadron Calorimeter Front-End Readout Control System at CMS.
Universität Hamburg, Hamburg, 2017.

N. Stefaniuk.
Measurement of the total and differential b cross sections at HERA and CMS tracker alignment at LHC.
Universität Hamburg, Hamburg, 2017.

N. Stefaniuk and E. Gallo-Voss.
Measurement of the total and differential b cross sections at HERA and CMS tracker alignment at LHC.
Universität Hamburg, 2017.

Electronics Development

Published

M. Donato et al.
First functionality tests of a 64 × 64 pixel DSSC sensor module connected to the complete ladder readout.
Journal of Instrumentation, 12(03):C03025, and PUBDB-2017-10155, arXiv:1701.03613.
doi: 10.1088/1748-0221/12/03/C03025.

K. Hansen et al.
Fluxless flip-chip bonding using a lead-free solder bumping technique.
Journal of Instrumentation, 12(09):T09006, and PUBDB-2017-13205.
doi: 10.1088/1748-0221/12/09/T09006.

H1

Published

H1 Collaboration.
Determination of the strong coupling constant $\alpha_s(m_Z)$ in next-to-next-to-leading order QCD using H1 jet cross section measurements.
The European physical journal / C, 77(11):791, and PUBDB-2017-14035, DESY-17-137; arXiv:1709.07251.
doi: 10.1140/epjc/s10052-017-5314-7.

H1 Collaboration.
Measurement of D^* production in diffractive deep inelastic scattering at HERA.
The European physical journal / C, 77(5):340, and PUBDB-2017-04157, DESY-17-043; arXiv:1703.09476.
doi: 10.1140/epjc/s10052-017-4875-9.

H1 Collaboration.
Measurement of jet production cross sections in deep-inelastic ep scattering at HERA.
The European physical journal / C, 77(4):215, and PUBDB-2017-02353.
doi: 10.1140/epjc/s10052-017-4717-9.

A. Verbytskyi.
HERA results on jets and hadronic final states.
19th High-Energy Physics International Conference in Quantum Chromodynamics, Montpellier (France), 4 Jul 2016 - 8 Jul 2016.
Elsevier, Amsterdam [u.a.]
doi: 10.1016/j.nuclphysbps.2016.12.009.

HERMES

Published

HERMES Collaboration.
Ratios of helicity amplitudes for exclusive ρ^0 electroproduction on transversely polarized protons.
The European physical journal / C, 77(6):378, and PUBDB-2017-04871, DESY-17-017; arXiv:1702.00345.
doi: 10.1140/epjc/s10052-017-4899-1.

IPP

Master Thesis

T. Rzepka.
Development of a Prototype Inventory Management Module for the Computer-Aided Facility Management System (CAFM) at DESY.
Silesian University of Technology, 2017.

IT

Published

M. Babik et al.
Deployment of IPv6-only CPU resources at WLCG sites.
8. 22nd International Conference on Computing in High Energy and Nuclear Physics (CHEP 2016), San Francisco (United States of America), 10 Oct 2016 - 14 Oct 2016.
IOP Publ., Bristol.
doi: 10.1088/1742-6596/898/8/082033.

M. Babik et al.
IPv6 Security.
10. 22nd International Conference on Computing in High Energy and Nuclear Physics, San Francisco (United States), 10 Oct 2016 - 14 Oct 2016.
IOP Publ., Bristol.
doi: 10.1088/1742-6596/898/10/102008.

C. Beyer et al.
Integration of Grid and Local Batch Resources at DESY.
22nd International Conference on Computing in High Energy and Nuclear Physics, San Francisco (USA), 10 Oct 2016 - 14 Oct 2016.
IOP Publ., Bristol.
doi: 10.1088/1742-6596/898/8/082020.

N. Braun et al.
Migrating the Belle II collaborative services and tools.
22nd International Conference on Computing in High Energy and Nuclear Physics, San Francisco (U.S.A.), 10 Oct 2016 - 14 Oct 2016.
IOP Publ., Bristol.
doi: 10.1088/1742-6596/898/10/102014.

T. Mkrtchyan et al.
dCache on Steroids - Delegated Storage Solutions.
22nd International Conference on Computing in High Energy and Nuclear Physics, San Francisco (USA), 10 Oct 2016 - 14 Oct 2016.
IOP Publ., Bristol.
doi: 10.1088/1742-6596/898/6/062021.

Linear Collider

Published

I. Abt et al.
Investigation into the limits of perturbation theory at low Q^2 using HERA deep inelastic scattering data.
Physical review / D, 96(1):014001, and PUBDB-2017-10569, DESY-17-051; arXiv:1704.03187.
doi: 10.1103/PhysRevD.96.014001.

D. Attié et al.
A time projection chamber with GEM-based readout.
Nuclear instruments & methods in physics research / A, 856:109, and PUBDB-2017-01745.
doi: 10.1016/j.nima.2016.11.002.

R. Brinkmann et al.
Chirp Mitigation of Plasma-Accelerated Beams by a Modulated Plasma Density.
Physical review letters, 118(21):214801, and PUBDB-2017-03953, arXiv:1603.08489.
doi: 10.1103/PhysRevLett.118.214801.

CALICE Collaboration.
Tracking within Hadronic Showers in the CALICE SDHCAL prototype using a Hough Transform Technique.
Journal of Instrumentation, 12(05):P05009, and PUBDB-2017-14102, arXiv:1702.08082.
doi: 10.1088/1748-0221/12/05/P05009.

A. Ferran Pousa et al.
External injection into a laser-driven plasma accelerator with sub-femtosecond timing jitter.
8th International Particle Accelerator Conference, Copenhagen (Denmark), 14 May 2017 - 19 May 2017.
IOP Publ., Bristol.
doi: 10.1088/1742-6596/874/1/012032.

J. Fuster et al.
Extracting the top-quark running mass using $t\bar{t}+1$-jet events produced at the Large Hadron Collider.
The European physical journal / C, 77(11):794, and PUBDB-2018-00554, HU-EP-17-05; LAL-17-034; DESY-17-053; arXiv:1704.00540.
doi: 10.1140/epjc/s10052-017-5354-z.

F. Gaede, B. Hegner and P. Mato.
PODIO: An Event-Data-Model Toolkit for High Energy Physics Experiments.
22nd International Conference on Computing in High Energy and Nuclear Physics (CHEP2016), San Francisco (USA), 10 Oct 2016 - 14 Oct 2016.
IOP Publ., Bristol.
doi: 10.1088/1742-6596/898/7/072039.

M. Kobayashi et al.
A novel technique for the measurement of the avalanche fluctuation of gaseous detectors.
Nuclear instruments & methods in physics research / A, 845:236, and PUBDB-2017-13841.
doi: 10.1016/j.nima.2016.06.073.

LCTPC Collaboration.
Studies on GEM modules for a Large Prototype TPC for the ILC.
Nuclear instruments & methods in physics research / A, 845:309, and PUBDB-2017-10471, DESY-16-058.
doi: 10.1016/j.nima.2016.05.011.

A. Martinez de la Ossa et al.
Optimizing density down-ramp injection for beam-driven plasma wakefield accelerators.
Physical review accelerators and beams, 20(9):091301, and PUBDB-2017-11818.
doi: 10.1103/PhysRevAccelBeams.20.091301.

S. Petrovics et al.
A novel Silicon Photomultiplier with bulk integrated quench resistors: utilization in optical detection and tracking applications for particle physics.
Nuclear instruments & methods in physics research / A, 845:150, and PUBDB-2017-14100.
doi: 10.1016/j.nima.2016.06.098.

D. Reschke et al.
Performance in the vertical test of the 832 nine-cell 1.3 GHz cavities for the European X-ray Free Electron Laser.
Physical review accelerators and beams, 20(4):042004, and PUBDB-2017-01882.
doi: 10.1103/PhysRevAccelBeams.20.042004.

R. E. Robson, T. J. Mehrling and J. Osterhoff.
Great moments in kinetic theory: 150 years of Maxwell's (other) equations.
European journal of physics, 38(6):065103, and PUBDB-2017-11640.
doi: 10.1088/1361-6404/aa87d4.

H. L. Tran et al.
Software compensation in particle flow reconstruction.
The European physical journal / C, 77(10):698, and PUBDB-2017-14101.
doi: 10.1140/epjc/s10052-017-5298-3.

P. A. Walker et al.
Horizon 2020 EuPRAXIA design study.
8th International Particle Accelerator Conference, Copenhagen (Denmark), 14 May 2017 - 19 May 2017.
IOP Publ., Bristol.
doi: 10.1088/1742-6596/874/1/012029.

M. Wenskat.
Automated Optical Inspection and Image Analysis of Superconducting Radio-Frequency Cavities.
Journal of Instrumentation, 12(05):P05016, and PUBDB-2017-04531, DESY-17-061; arXiv:1704.06081.
doi: 10.1088/1748-0221/12/05/P05016.

M. Wenskat.
Optical surface properties and their RF limitations of European XFEL cavities.
Superconductor science and technology, 30(10):105007, and PUBDB-2018-00359.
doi: 10.1088/1361-6668/aa828b.

M. Wenskat and J. Schaffran.
Analysis of the Cool Down Related Cavity Performance of the European XFEL Vertical Acceptance Tests.
AIP Advances, 7(11):14, and PUBDB-2017-11797, DESY-17-135; arXiv:1609.06503.
doi: 10.1063/1.5004482.

Master Thesis

S. Weichert.
Spectral Broadening of 25 fs Laser Pulses via Self-Phase Modulation in a Neon filled Hollow Core Fibre.
University of Hamburg, Hamburg, 2017.

Ph.D. Thesis

A. Ebrahimi.
Jet Energy Measurements at ILC:Calorimeter DAQ Requirements and Application in Higgs Boson Mass Measurements.
Universität Hamburg, Hamburg, 2017.

V. Myronenko.
Combination of the inclusive DIS $e^{\pm}p$ cross sections from HERA, QCD and EW analyses and the need for low-Q^2 higher-twist corrections.
Universität Hamburg, Hamburg, 2017.

O. Turkot.
Search for contact interactions and finite quark radius using combined $e^{\pm}p$ data at HERA.
Universität Hamburg, Hamburg, 2017.

M. Zvolsky.
Simulation, Image Reconstruction and SiPM Characterisation for a Novel Endoscopic Positron Emission Tomography Detector.
Universität Hamburg, Hamburg, 2017.

OLYMPUS

Published

OLYMPUS Collaboration.
Hard Two-Photon Contribution to Elastic Lepton-Proton Scattering Determined by the OLYMPUS Experiment.
Physical review letters, 118(9):092501, and PUBDB-2016-05579, DESY-16-217; arXiv:1611.04685.
doi: 10.1103/PhysRevLett.118.092501.

Theory

Published

A. Abada et al.
Neutrino masses, leptogenesis and dark matter from small lepton number violation?
Journal of cosmology and astroparticle physics, 2017(12):024, and PUBDB-2017-13978, DESY-17-124.
doi: 10.1088/1475-7516/2017/12/024.

A. Abdel-Rehim et al.
First physics results at the physical pion mass from $N_f = 2$ Wilson twisted mass fermions at maximal twist.
Physical review / D, 95(9):094515, and PUBDB-2017-04977.
doi: 10.1103/PhysRevD.95.094515.

J. Ablinger et al.
Heavy quark form factors at two loops in perturbative QCD.
12. XLI International Conference of Theoretical Physics "Matter to the Deepest", Podlesice (Poland), 3 Sep 2017 - 8 Sep 2017.
Inst. of Physics, Jagellonian Univ., Cracow.
doi: 10.5506/APhysPolB.48.2155.

J. Ablinger et al.
The three-loop splitting functions $P_{qg}^{(2)}$ and $P_{gg}^{(2,N_F)}$.
Nuclear physics / B, 922:1, and PUBDB-2017-07732.
doi: 10.1016/j.nuclphysb.2017.06.004.

J. Ablinger et al.
Three Loop Massive Operator Matrix Elements and Asymptotic Wilson Coefficients with Two Different Masses.
Nuclear physics / B, 921:585, and PUBDB-2018-00428, DESY-14-019; DO-TH-15-08; arXiv:1705.07030.
doi: 10.1016/j.nuclphysb.2017.05.017.

N. Aghaei, M. Pawelkiewicz and J. Teschner.
Quantisation of Super Teichmüller Theory.
Communications in mathematical physics, 353(2):597, and PUBDB-2017-07769, arXiv:1512.02617; DESY-15-249.
doi: 10.1007/s00220-017-2883-0.

I. Akal and G. Moortgat-Pick.
Quantum tunnelling from vacuum in multidimensions.
Physical review / D, 96(9):096027, and PUBDB-2017-13980, DESY-17-159.
doi: 10.1103/PhysRevD.96.096027.

S. Alekhin et al.
Parton distribution functions, α_s, and heavy-quark masses for LHC Run II.
Physical review / D, 96(1):014011, and PUBDB-2017-08782, DESY-16-179, DO-TH-16-13, arXiv:1701.05838.
doi: 10.1103/PhysRevD.96.014011.

C. Alexandrou et al.
A complete non-perturbative renormalization prescription for quasi-PDFs.
Nuclear physics / B, 923:394, and PUBDB-2017-11468, DESY-17-092; arXiv:1706.00265.
doi: 10.1016/j.nuclphysb.2017.08.012.

C. Alexandrou et al.
Gluon momentum fraction of the nucleon from lattice QCD.
Physical review / D, 96(5):054503, and PUBDB-2017-11705, arXiv:1611.06901; DESY-16-223.
doi: 10.1103/PhysRevD.96.054503.

C. Alexandrou et al.
Updated lattice results for parton distributions.
Physical review / D, 96(1):014513, and PUBDB-2017-09401, DESY-16-192; arXiv:1610.03689.
doi: 10.1103/PhysRevD.96.014513.

C. Alexandrou et al.
Erratum: Nucleon scalar and tensor charges using lattice QCD simulations at the physical value of the pion mass [Phys. Rev. D 95 , 114514 (2017)].
Physical review / D, 96(9):099906, and PUBDB-2018-00253.
doi: 10.1103/PhysRevD.96.099906.

C. Alexandrou et al.
Nucleon Axial Form Factors Using $N_f = 2$ twisted mass fermions with a physical value of the pion mass.
Physical review / D, 96(5):054507, and PUBDB-2017-11469, arXiv:1705.03399.
doi: 10.1103/PhysRevD.96.054507.

C. Alexandrou et al.
Nucleon electromagnetic form factors using lattice simulations at the physical point.
Physical review / D, 96(3):034503, and PUBDB-2017-10004, DESY-17-085; arXiv:1706.00469.
doi: 10.1103/PhysRevD.96.034503.

C. Alexandrou et al.
Nucleon scalar and tensor charges using lattice QCD simulations at the physical value of the pion mass.
Physical review / D, 95(11):114514, and PUBDB-2017-06705, arXiv:1703.08788.
doi: 10.1103/PhysRevD.95.114514.

C. Alexandrou et al.
Nucleon Spin and Momentum Decomposition Using Lattice QCD Simulations.
Physical review letters, 119(14):142002, and PUBDB-2017-11576, arXiv:1706.02973.
doi: 10.1103/PhysRevLett.119.142002.

A. Ali.
Precision tests of the Standard Model: Rare B -meson decays.
International journal of modern physics / A, 32(9):1741015, and PUBDB-2018-00524.
doi: 10.1142/S0217751X17410159.

A. Ali, J. S. Lange and S. Stone.
Exotics: Heavy pentaquarks and tetraquarks.
Progress in particle and nuclear physics, 97:123, and PUBDB-2017-11774, DESY-17-071.
doi: 10.1016/j.ppnp.2017.08.003.

M. Bruno et al.
The determination of α_s by the ALPHA collaboration.
Sixth Workshop on Theory, Phenomenology and Experiments in Flavour Physics Interplay of Flavour Physics with Electroweak symmetry breaking, Anacapri (Italy), 11 Jun 2016 - 13 Jun 2016.
Elsevier, Amsterdam [u.a.]
doi: 10.1016/j.nuclphysbps.2017.03.024.

H. An, J. Gu and L.-T. Wang.
Exploring the nearly degenerate stop region with sbottom decays.
Journal of high energy physics, 1704(04):084, and PUBDB-2017-01833, DESY-16-101; arXiv:1611.09868; CALT-TH-2016-036.
doi: 10.1007/JHEP04(2017)084.

M. Artymowski, M. Lewicki and J. Wells.
Gravitational wave and collider implications of electroweak baryogenesis aided by non-standard cosmology.
Journal of high energy physics, 1703(03):066, and PUBDB-2017-01601, arXiv:1609.07143.
doi: 10.1007/JHEP03(2017)066.

E.-C. Aschenauer et al.
Pre-Town Meeting on spin physics at an Electron-Ion Collider.
The European physical journal / A, 53(4):71, and PUBDB-2018-00526.
doi: 10.1140/epja/i2017-12251-4.

P. Athron et al.
GAMBIT: the global and modular beyond-the-standard-model inference tool.
The European physical journal / C, 77(11):784, and PUBDB-2018-00527, DESY-17-236; COEPP-MN-17-6; CERN-TH-2017-166; NORDITA-2017-074; arXiv:1705.07908.
doi: 10.1140/epjc/s10052-017-5321-8.

P. Athron et al.
Precise Higgs mass calculations in (non-)minimal supersymmetry at both high and low scales.
Journal of high energy physics, 1701(01):079, and PUBDB-2017-00885, COEPP-MN-16-20; DESY-16-057; KIAS-Q16008; arXiv:1609.00371.
doi: 10.1007/JHEP01(2017)079.

E. Bagnaschi, J. P. Vega and P. Slavich.
Improved determination of the Higgs mass in the MSSM with heavy superpartners.
The European physical journal / C, 77(5):334, and PUBDB-2017-05992, DESY-17-033; arXiv:1703.08166.
doi: 10.1140/epjc/s10052-017-4885-7.

E. Bagnaschi et al.
Likelihood analysis of supersymmetric SU(5) GUTs.
The European physical journal / C, 77(2):104, and PUBDB-2017-01137, DESY-16-156.
doi: 10.1140/epjc/s10052-017-4639-6.

E. Bagnaschi et al.
Likelihood analysis of the minimal AMSB model.
The European physical journal / C, 77(4):268, and PUBDB-2017-02669, DESY-16-155; KCL-PH-TH-2016-58; CERN-PH-TH-2016-220; IFT-UAM-CSIC-16-112; IPMU16-0157; FTPI-MINN-16-30; UMN-TH-3610-16; FERMILAB-PUB-16-502-CMS; IPPP-16-104; arXiv:1612.05210.
doi: 10.1140/epjc/s10052-017-4810-0.

I. Baldes.
Gravitational waves from the asymmetric-dark-matter generating phase transition.
Journal of cosmology and astroparticle physics, 1705(05):028, and PUBDB-2017-05987, DESY-17-021; arXiv:1702.02117.
doi: 10.1088/1475-7516/2017/05/028.

I. Baldes and K. Petraki.
Asymmetric thermal-relic dark matter: Sommerfeld-enhanced freeze-out, annihilation signals and unitarity bounds.
Journal of cosmology and astroparticle physics, 1709(09):028, and PUBDB-2017-11764, DESY-17-034; Nikhef 2017-009; arXiv:1703.00478.
doi: 10.1088/1475-7516/2017/09/028.

G. Ballesteros et al.
Standard Model—axion—seesaw—Higgs portal inflation. Five problems of particle physics and cosmology solved in one stroke.
Journal of cosmology and astroparticle physics, 1708(08):001, and PUBDB-2017-08981, DESY-16-184; arXiv:1610.01639.
doi: 10.1088/1475-7516/2017/08/001.

G. Ballesteros et al.
Unifying Inflation with the Axion, Dark Matter, Baryogenesis, and the Seesaw Mechanism.
Physical review letters, 118(7):071802, and PUBDB-2017-00981, DESY 16-049.
doi: 10.1103/PhysRevLett.118.071802.

M. C. Bañuls et al.
Density Induced Phase Transitions in the Schwinger Model: A Study with Matrix Product States.
Physical review letters, 118(7):071601, and PUBDB-2018-00255.
doi: 10.1103/PhysRevLett.118.071601.

M. C. Bañuls et al.
Efficient Basis Formulation for (1 + 1)-Dimensional SU(2) Lattice Gauge Theory: Spectral Calculations with Matrix Product States.
Physical review / X, 7(4):041046, and PUBDB-2018-00238.
doi: 10.1103/PhysRevX.7.041046.

T. Bargheer.
Four-point functions with a twist.
Journal of physics / A, 51(3):035401, and PUBDB-2017-12765, DESY-16-248.
doi: 10.1088/1751-8121/aa9cc0.

T. Bargheer.
Systematics of the multi-Regge three-loop symbol.
Journal of high energy physics, 2017(11):77, and PUBDB-2017-12764, DESY-16-115.
doi: 10.1007/JHEP11(2017)077.

P. Baseilhac, A. Gainutdinov and T. T. Vu.
Cyclic tridiagonal pairs, higher order Onsager algebras and orthogonal polynomials.
Linear algebra and its applications, 522:71, and PUBDB-2018-00632.
doi: 10.1016/j.laa.2017.02.009.

P. Basler et al.
Strong first order electroweak phase transition in the CP-conserving 2HDM revisited.
Journal of high energy physics, 1702(02):121, and PUBDB-2017-01371, arXiv:1612.04086.
doi: 10.1007/JHEP02(2017)121.

M. Bauer, U. Haisch and F. Kahlhoefer.
Simplified dark matter models with two Higgs doublets: I. Pseudoscalar mediators.
Journal of high energy physics, 1705(05):138, and PUBDB-2017-05984, CERN-TH-2017-011; DESY-17-010; arXiv:1701.07427.
doi: 10.1007/JHEP05(2017)138.

T. Becher et al.
Erratum to: Factorization and resummation for jet processes.
Journal of high energy physics, 1705(05):154, and PUBDB-2018-00529, arXiv:1605.02737.
doi: 10.1007/JHEP05(2017)154.

P. Bechtle et al.
The light and heavy Higgs interpretation of the MSSM.
The European physical journal / C, 77(2):67, and PUBDB-2017-00886, BONN-TH-2016-06; DESY-16-151; IFT-UAM-CSIC-16-068; NIKHEF-2016-033; SCIPP-16-10; arXiv:1608.00638.
doi: 10.1140/epjc/s10052-016-4584-9.

A. Behring et al.
Asymptotic 3-loop heavy flavor corrections to the charged current structure functions $F_L^{W^+-W^-}(x,Q^2)$ and $F_2^{W^+-W^-}(x,Q^2)$.
Physical review / D, 94(11):114006, and PUBDB-2017-04944, DESY-16-148; DO-TH-16-15; arXiv:1609.06255.
doi: 10.1103/PhysRevD.94.114006.

R. Bellwied et al.
Lattice QCD thermodynamics up to the perturbative regime.
The 26th International Conference on Ultra-relativistic Nucleus-Nucleus Collisions: Quark Matter 2017, Chicago (USA), 5 Feb 2017 - 11 Feb 2017.
Elsevier, Amsterdam.
doi: 10.1016/j.nuclphysa.2017.06.017.

M. Beneke et al.
On the ultimate uncertainty of the top quark pole mass.
Physics letters / B, 775:63, and PUBDB-2017-12402.
doi: 10.1016/j.physletb.2017.10.054.

A. Beniwal et al.
Gravitational wave, collider and dark matter signals from a scalar singlet electroweak baryogenesis.
Journal of high energy physics, 1708(08):108, and PUBDB-2018-00631, arXiv:1702.06124.
doi: 10.1007/JHEP08(2017)108.

G. Bergner et al.
Spectrum and mass anomalous dimension of SU(2) adjoint QCD with two Dirac flavors.
Physical review / D, 96(3):034504, and PUBDB-2017-09602, MS-TP-16-26; DESY-16-135; arXiv:1610.01576.
doi: 10.1103/PhysRevD.96.034504.

D. Bertolini et al.
Soft functions for generic jet algorithms and observables at hadron colliders.
Journal of high energy physics, 1707(07):099, and PUBDB-2017-12467, DESY-16-137; NIKHEF 2016-035; MIT-CTP 4823; arXiv:1704.08262.
doi: 10.1007/JHEP07(2017)099.

L. Bianchi et al.
Wilson lines as superconformal defects in ABJM theory: a formula for the emitted radiation.
Journal of high energy physics, 2017(10):50, and PUBDB-2018-00531.
doi: 10.1007/JHEP10(2017)050.

J. Blümlein, K. H. Phan and T. Riemann.
Scalar one-loop vertex integrals as meromorphic functions of space-time dimension d.
12. XLI International Conference of Theoretical Physics “Matter to the Deepest”„ Podlesice (Poland), 3 Sep 2017 - 8 Sep 2017.
Inst. of Physics, Jagellonian Univ., Cracow.
doi: 10.5506/APhysPolB.48.2313.

J. Blümlein and C. Schneider.
The method of arbitrarily large moments to calculate single scale processes in quantum field theory.
Physics letters / B, 771:31, and PUBDB-2017-04322, DESY-17-009; DO-TH 17-01; arXiv:1701.04614.
doi: 10.1016/j.physletb.2017.05.001.

V. G. Bornyakov et al.
Flavour breaking effects in the pseudoscalar meson decay constants.
Physics letters / B, 767:366, and PUBDB-2017-01139, DESY-16-241; ADP-16-46-T1002; DESY-16-241; EDINBURGH-2016-19; LIVERPOOL-LTH-1116; arXiv:1612.04798.
doi: 10.1016/j.physletb.2017.02.018.

T. Bringmann et al.
DarkBit: A GAMBIT module for computing dark matter observables and likelihoods.
The European physical journal / C, 77(12):831, and PUBDB-2018-00534, DESY-17-235; NORDITA-2017-076; arXiv:1705.07920.
doi: 10.1140/epjc/s10052-017-5155-4.

T. Bringmann et al.
Strong Constraints on Self-Interacting Dark Matter with Light Mediators.
Physical review letters, 118(14):141802, and PUBDB-2017-01600, DESY-16-226.
doi: 10.1103/PhysRevLett.118.141802.

S. Bruggisser, T. Konstandin and G. Servant.
CP-violation for electroweak baryogenesis from dynamical CKM matrix.
Journal of cosmology and astroparticle physics, 2017(11):034, and PUBDB-2017-12767, DESY-17-094.
doi: 10.1088/1475-7516/2017/11/034.

M. Bruno, T. Korzec and S. Schaefer.
Setting the scale for the CLS 2 + 1 flavor ensembles.
Physical review / D, 95(7):074504, and PUBDB-2017-02420.
doi: 10.1103/PhysRevD.95.074504.

M. Bruno et al.
QCD Coupling from a Nonperturbative Determination of the Three-Flavor Λ Parameter.
Physical review letters, 119(10):102001, and PUBDB-2017-11580, CERN-TH-2017-129; DESY-17-088; WUB-17-03; arXiv:1706.03821.
doi: 10.1103/PhysRevLett.119.102001.

W. Buchmuller and J. Schweizer.
Flavor mixings in flux compactifications.
Physical review / D, 95(7):075024, and PUBDB-2017-01838, DESY-16-238; arXiv:1701.06935.
doi: 10.1103/PhysRevD.95.075024.

W. Buchmuller et al.
Effective field theory for magnetic compactifications.
Journal of high energy physics, 1704(04):052, and PUBDB-2017-01835, CPHT-RR047.112016; DESY-16-206; arXiv:1611.03798.
doi: 10.1007/JHEP04(2017)052.

W. Buchmüller et al.
The toric SO(10) F-theory landscape.
Journal of high energy physics, 2017(12):35, and PUBDB-2017-13977, DESY-17-091.
doi: 10.1007/JHEP12(2017)035.

G. Carvalho Dorsch et al.
A second Higgs doublet in the early universe: baryogenesis and gravitational waves.
Journal of cosmology and astroparticle physics, 1705(05):052, and PUBDB-2017-05847, DESY-16-213; arXiv:1611.05874.
doi: 10.1088/1475-7516/2017/05/052.

G. Carvalho Dorsch et al.
The Higgs vacuum uplifted: revisiting the electroweak phase transition with a second Higgs doublet.
Journal of high energy physics, 2017(12):86, and PUBDB-2017-13974, DESY-17-076.
doi: 10.1007/JHEP12(2017)086.

M. Cè, L. Giusti and S. Schaefer.
Local factorization of the fermion determinant in lattice QCD.
Physical review / D, 95(3):034503, and PUBDB-2017-01277.
doi: 10.1103/PhysRevD.95.034503.

M. Chala et al.
Minimally extended SILH.
Journal of high energy physics, 1706(06):088, and PUBDB-2017-06632, DESY-17-049; IFIC-17-15; FTUV-17-0322.9647; arXiv:1703.10624.
doi: 10.1007/JHEP06(2017)088.

A. J. Chambers et al.
Electromagnetic form factors at large momenta from lattice QCD.
Physical review / D, 96(11):114509, and PUBDB-2018-00567, DESY-17-019.
doi: 10.1103/PhysRevD.96.114509.

A. J. Chambers et al.
Nucleon Structure Functions from Operator Product Expansion on the Lattice.
Physical review letters, 118(24):242001, and PUBDB-2017-05989, ADP-17-09-T1015; DESY-17-027; EDINBURGH-2017-04; LIVERPOOL-LTH-1122; arXiv:1703.01153.
doi: 10.1103/PhysRevLett.118.242001.

K. G. Chetyrkin et al.
Addendum to "Charm and bottom quark masses: An update".
Physical review / D, 96(11):116007, and PUBDB-2018-00474, DESY-17-152; FR-PHENO-2017-018; IPPP-17-72; TTP17-039; arXiv:1710.04249.
doi: 10.1103/PhysRevD.96.116007.

I. Coman et al.
Spectral curves of $\mathcal{N} = 1$ theories of class $\mathcal{S}_k$.
Journal of high energy physics, 1706(06):136, and PUBDB-2017-06589, DESY-15-248; arXiv:1512.06079.
doi: 10.1007/JHEP06(2017)136.

M. Cornagliotto, M. Lemos and V. Schomerus.
Long multiplet bootstrap.
Journal of high energy physics, 1710(10):119, and PUBDB-2017-11762, DESY-17-026; arXiv:1702.05101.
doi: 10.1007/JHEP10(2017)119.

R. Couso-Santamaría, R. Schiappa and R. Vaz.
On asymptotics and resurgent structures of enumerative Gromov–Witten invariants.
Communications in number theory and physics, 11(4):707, and PUBDB-2017-13997, DESY-16-089.
doi: 10.4310/CNTP.2017.v11.n4.a1.

M. Dalla Brida et al.
Slow running of the gradient flow coupling from 200 MeV to 4 GeV in $N_f = 3$ QCD.
Physical review / D, 95(1):014507, and PUBDB-2017-01039.
doi: 10.1103/PhysRevD.95.014507.

G. D'Amico et al.
An étude on global vacuum energy sequester.
Journal of high energy physics, 1709(09):074, and PUBDB-2017-11830, CERN-TH-2017-115; DESY-17-080; arXiv:1705.08950.
doi: 10.1007/JHEP09(2017)074.

S. Di Vita et al.
Two-loop master integrals for the leading QCD corrections to the Higgs coupling to a W pair and to the triple gauge couplings ZWW and $\gamma^* WW$.
Journal of high energy physics, 1704(04):008, and PUBDB-2017-01608, DESY-17-032; arXiv:1702.07331.
doi: 10.1007/JHEP04(2017)008.

S. Di Vita et al.
A global view on the Higgs self-coupling.
Journal of high energy physics, 1709(09):069, and PUBDB-2017-11765, DESY-17-044; arXiv:1704.01953.
doi: 10.1007/JHEP09(2017)069.

C. O. Dib, C. S. Kim and K. Wang.
Search for heavy sterile neutrinos in trileptons at the LHC.
Chinese physics / C, 41(10):103103, and PUBDB-2017-11759, DESY-16-202.
doi: 10.1088/1674-1137/41/10/103103.

C. O. Dib, C. S. Kim and K. Wang.
Signatures of Dirac and Majorana sterile neutrinos in trilepton events at the LHC.
Physical review / D, 95(11):115020, and PUBDB-2017-05993.
doi: 10.1103/PhysRevD.95.115020.

M. Diehl, J. R. Gaunt and K. Schoenwald.
Double hard scattering without double counting.
Journal of high energy physics, 1706(06):083, and PUBDB-2017-05986, DESY-17-013; NIKHEF-2017-007; arXiv:1702.06486.
doi: 10.1007/JHEP06(2017)083.

P. Diessner et al.
Squark production in R-symmetric SUSY with Dirac gluinos: NLO corrections.
Journal of high energy physics, 1710(10):142, and PUBDB-2017-12787, DESY-17-100; arXiv:1707.04557.
doi: 10.1007/JHEP10(2017)142.

L. J. Dixon et al.
Heptagons from the Steinmann cluster bootstrap.
Journal of high energy physics, 1702(02):137, and PUBDB-2017-01485, DESY-16-242; arXiv:1612.08976; Brown-HET-1705; SLAC-PUB-16894.
doi: 10.1007/JHEP02(2017)137.

M. J. Dolan et al.
Revised constraints and Belle II sensitivity for visible and invisible axion-like particles.
Journal of high energy physics, 1712(12):094, and PUBDB-2018-00299, DESY-17-127; arXiv:1709.00009.
doi: 10.1007/JHEP12(2017)094.

P. Drechsel et al.
Precise predictions for the Higgs-boson masses in the NMSSM.
The European physical journal / C, 77(1):42, and PUBDB-2018-00318, DESY-15-069; arXiv:1601.08100.
doi: 10.1140/epjc/s10052-017-4595-1.

P. Drechsel et al.
Higgs-boson masses and mixing matrices in the NMSSM: analysis of on-shell calculations.
The European physical journal / C, 77(6):366, and PUBDB-2017-05981, DESY-16-244.
doi: 10.1140/epjc/s10052-017-4932-4.

I. Dubovyk et al.
New Prospects for the Numerical Calculation of Mellin–Barnes Integrals in Minkowskian Kinematics.
Acta physica Polonica / B, 48(6):995, and PUBDB-2017-12453, arXiv:1704.02288.
doi: 10.5506/APhysPolB.48.995.

M. Duerr, P. F. Pérez and J. Smirnov.
Baryonic Higgs at the LHC.
Journal of high energy physics, 1709(09):093, and PUBDB-2017-11773, DESY-17-050; arXiv:1704.03811.
doi: 10.1007/JHEP09(2017)093.

M. Duerr et al.
Hunting the dark Higgs.
Journal of high energy physics, 1704(04):143, and PUBDB-2017-02497, DESY-17-016; arXiv:1701.08780.
doi: 10.1007/JHEP04(2017)143.

G. Durieux and Y. Grossman.
CP violation: Another piece of the puzzle.
Nature physics, 13(4):322, and PUBDB-2017-05684.
doi: 10.1038/nphys4068.

G. Durieux et al.
The leptonic future of the Higgs.
Journal of high energy physics, 1709(09):014, and PUBDB-2017-11755.
doi: 10.1007/JHEP09(2017)014.

M. A. Ebert and F. J. Tackmann.
Resummation of transverse momentum distributions in distribution space.
Journal of high energy physics, 1702(02):110, and PUBDB-2017-01138, DESY-16-215; arXiv:1611.08610.
doi: 10.1007/JHEP02(2017)110.

M. Ebert, J. K. L. Michel and F. J. Tackmann.
Resummation improved rapidity spectrum for gluon fusion Higgs production.
Journal of high energy physics, 1705(05):088, and PUBDB-2017-05978, DESY-16-216; MS-TP-16-30; arXiv:1702.00794.
doi: 10.1007/JHEP05(2017)088.

S. Ellis and J. Wells.
High-scale supersymmetry, the Higgs boson mass, and gauge unification.
Physical review / D, 96(5):055024, and PUBDB-2018-00625.
doi: 10.1103/PhysRevD.96.055024.

J. R. Espinosa et al.
Gauge-independent scales related to the standard model vacuum instability.
Physical review / D, 95(5):056004, and PUBDB-2017-01479, DESY-16-161; arXiv:1608.06765; CERN-TH-2016-187.
doi: 10.1103/PhysRevD.95.056004.

FLAG Collaboration.
Review of lattice results concerning low-energy particle physics.
The European physical journal / C, 77(2):112, and PUBDB-2017-01363.
doi: 10.1140/epjc/s10052-016-4509-7.

R. Flauger et al.
Drifting oscillations in axion monodromy.
Journal of cosmology and astroparticle physics, 1710(10):055, and PUBDB-2017-13763, SU/ITP-14/29; SLAC-PUB-16165; DESY-14-225; arXiv:1412.1814.
doi: 10.1088/1475-7516/2017/10/055.

C. Fleper et al.
Scattering of W and Z bosons at high-energy lepton colliders.
The European physical journal / C, 77(2):120, and PUBDB-2017-01451, DESY-16-098; arXiv:1607.03030.
doi: 10.1140/epjc/s10052-017-4656-5.

E. Fuchs and G. Weiglein.
Breit-Wigner approximation for propagators of mixed unstable states.
Journal of high energy physics, 1709(09):079, and PUBDB-2017-11757, DESY-16-182; arXiv:1610.06193.
doi: 10.1007/JHEP09(2017)079.

J. Fuster et al.
Extracting the top-quark running mass using $t\bar{t}+1$-jet events produced at the Large Hadron Collider.
The European physical journal / C, 77(11):794, and PUBDB-2018-00554, HU-EP-17-05; LAL-17-034; DESY-17-053; arXiv:1704.00540.
doi: 10.1140/epjc/s10052-017-5354-z.

A. Gainutdinov and I. Runkel.
Symplectic fermions and a quasi-Hopf algebra structure on $\bar{U}_{\mathrm{i}} s\ell(2)$.
Journal of algebra, 476:415, and PUBDB-2018-00624.
doi: 10.1016/j.jalgebra.2016.11.026.

GAMBIT Collaboration.
Status of the scalar singlet dark matter model.
The European physical journal / C, 77(8):568, and PUBDB-2018-00528, COEPP-MN-17-10; arXiv:1705.07931; CERN-TH-2017-170; CoEPP-MN-17-10; NORDITA 2017-079.
doi: 10.1140/epjc/s10052-017-5113-1.

S. Gangal et al.
Two-loop beam and soft functions for rapidity-dependent jet vetoes.
Journal of high energy physics, 0217(02):026, and PUBDB-2017-01136, DESY-16-154; MITP-16-078; NIKHEF-2016-032; arXiv:1608.01999.
doi: 10.1007/JHEP02(2017)026.

M. Giannotti et al.
Stellar recipes for axion hunters.
Journal of cosmology and astroparticle physics, 1710(10):010, and PUBDB-2017-11543, DESY-17-116; arXiv:1708.02111.
doi: 10.1088/1475-7516/2017/10/010.

A. Gizhko et al.
Running of the charm-quark mass from HERA deep-inelastic scattering data.
Physics letters / B, 775:233, and PUBDB-2017-12115.
doi: 10.1016/j.physletb.2017.11.002.

M. D. Goodsell, S. Liebler and F. Staub.
Generic calculation of two-body partial decay widths at the full one-loop level.
The European physical journal / C, 77(11):758, and PUBDB-2017-12766, DESY-17-042KA-TP-11-2017; arXiv:1703.09237.
doi: 10.1140/epjc/s10052-017-5259-x.

J. Green et al.
Up, down, and strange nucleon axial form factors from lattice QCD.
Physical review / D, 95(11):114502, and PUBDB-2017-05459.
doi: 10.1103/PhysRevD.95.114502.

J. Gu et al.
Learning from Higgs Physics at Future Higgs Factories.
Journal of high energy physics, 1712(12):153, and PUBDB-2018-00571, FERMILAB-PUB-17-348-T; DESY-17-130; arXiv:1709.06103.
doi: 10.1007/JHEP12(2017)153.

T. Hahn and S. Paßehr.
Implementation of the $\mathcal{O}\left(\alpha_t^2\right)$ MSSM Higgs-mass corrections in FeynHiggs.
Computer physics communications, 214:91, and PUBDB-2017-01480, DESY-15-127; arXiv:1508.00562.
doi: 10.1016/j.cpc.2017.01.026.

J. Halverson, B. D. Nelson and F. Ruehle.
String theory and the dark glueball problem.
Physical review / D, 95(4):043527, and PUBDB-2017-01481, DESY-16-170; arXiv:1609.02151.
doi: 10.1103/PhysRevD.95.043527.

R. V. Harlander, S. Liebler and H. Mantler.
SusHi Bento: Beyond NNLO and the heavy- top limit.
Computer physics communications, 212:239, and PUBDB-2016-06544, DESY-16-061.
doi: 10.1016/j.cpc.2016.10.015.

B. von Harling and G. Servant.
Cosmological evolution of Yukawa couplings: the 5D perspective.
Journal of high energy physics, 1705(05):077, and PUBDB-2017-05979, DESY-16-221; arXiv:1612.02447.
doi: 10.1007/JHEP05(2017)077.

J. Hayling et al.
Exact deconstruction of the 6D (2,0) theory.
Journal of high energy physics, 1706(06):072, and PUBDB-2017-05991, DESY-17-030; arXiv:1704.02986.
doi: 10.1007/JHEP06(2017)072.

M. Hoffman.
On multiple zeta values of even arguments.
International journal of number theory, 13(03):705, and PUBDB-2018-00306.
doi: 10.1142/S179304211750035X.

F. Jegerlehner and K. Kołodziej.
Photon radiation in $e^+e^- \rightarrow$ hadrons at low energies with carlomat$_3$.1.
The European physical journal / C, 77(4):254, and PUBDB-2017-06699, DESY-17-001; HU-EP-17-01; arXiv:1701.01837.
doi: 10.1140/epjc/s10052-017-4816-7.

F. Kahlhoefer.
Review of LHC dark matter searches.
International journal of modern physics / A, 32:1730006, and PUBDB-2017-01489, DESY-17-024; arXiv:1702.02430.
doi: 10.1142/S0217751X1730006X.

F. Kahlhoefer, S. Kulkarni and S. Wild.
Exploring Light Mediators with Low-Threshold Direct Detection Experiments.
Journal of cosmology and astroparticle physics, 2017(11):016, and PUBDB-2017-12773, DESY-17-113.
doi: 10.1088/1475-7516/2017/11/016.

F. Kahlhoefer, K. Schmidt-Hoberg and S. Wild.
Dark matter self-interactions from a general spin-0 mediator.
Journal of cosmology and astroparticle physics, 1708(08):003, and PUBDB-2017-09578, DESY-17-052; arXiv:1704.02149.
doi: 10.1088/1475-7516/2017/08/003.

H. Kastrup.
Wigner functions for angle and orbital angular momentum: Operators and dynamics.
Physical review / A, 95(5):052111, and PUBDB-2017-07444.
doi: 10.1103/PhysRevA.95.052111.

KLOE-2 Collaboration.
Measurement of the running of the fine structure constant below 1 GeV with the KLOE detector-2.
Physics letters / B, 767:485, and PUBDB-2017-12398, arXiv:1609.06631.
doi: 10.1016/j.physletb.2016.12.016.

M. Lemos et al.
Bootstrapping $\mathcal{N} = 3$ superconformal theories.
Journal of high energy physics, 1704(04):032, and PUBDB-2017-01837, DESY-16-237.
doi: 10.1007/JHEP04(2017)032.

S. Liebler, S. Patel and G. Weiglein.
Phenomenology of on-shell Higgs production in the MSSM with complex parameters.
The European physical journal / C, 77(5):305, and PUBDB-2017-05972, DESY-16-190; arXiv:1611.09308.
doi: 10.1140/epjc/s10052-017-4849-y.

P. Liendo.
Revisiting the dilatation operator of the Wilson-Fisher fixed point.
Nuclear physics / B, 920:368, and PUBDB-2017-05983, DESY-17-002; arXiv:1701.04830.
doi: 10.1016/j.nuclphysb.2017.04.020.

T. Luthe et al.
Complete renormalization of QCD at five loops.
Journal of high energy physics, 1703(03):020, and PUBDB-2017-03382, BI-TP-2017-01; DESY-17-011; IPPP-17-7; arXiv:1701.07068.
doi: 10.1007/JHEP03(2017)020.

T. Luthe et al.
Five-loop quark mass and field anomalous dimensions for a general gauge group.
Journal of high energy physics, 1701(01):081, and PUBDB-2017-00790.
doi: 10.1007/JHEP01(2017)081.

T. Luthe et al.
The five-loop Beta function for a general gauge group and anomalous dimensions beyond Feynman gauge.
Journal of high energy physics, 1710(10):166, and PUBDB-2017-12456, DESY-17-142; BI-TP-2017-13; IPPP-17-68; arXiv:1709.07718;
doi: 10.1007/JHEP10(2017)166.

V. Mitev and E. Pomoni.
2D CFT blocks for the 4D class $\mathcal{S}_k$ theories.
Journal of high energy physics, 1708(08):009, and PUBDB-2017-09606, DESY-17-029; MITP-17-012; arXiv:1703.00736.
doi: 10.1007/JHEP08(2017)009.

J. Mo, F. J. Tackmann and W. J. Waalewijn.
A Case Study of Quark-Gluon Discrimination at NNLL$'$ in Comparison to Parton Showers.
The European physical journal / C, 77(11):770, and PUBDB-2017-12772, DESY-17-111.
doi: 10.1140/epjc/s10052-017-5365-9.

I. Moult et al.
Subleading power corrections for N-jettiness subtractions.
Physical review / D, 95(7):074023, and PUBDB-2017-01801, MIT-CTP-4855; DESY-16-229; arXiv:1612.00450.
doi: 10.1103/PhysRevD.95.074023.

M. Mühlleitner et al.
Phenomenological comparison of models with extended Higgs sectors.
Journal of high energy physics, 1708(08):132, and PUBDB-2017-11767, DESY-17-046; KA-TP-10-2017; arXiv:1703.07750.
doi: 10.1007/JHEP08(2017)132.

M. Mühlleitner et al.
The N2HDM under theoretical and experimental scrutiny.
Journal of high energy physics, 1703(03):094, and PUBDB-2017-01612, arXiv:1612.01309; KA-TP-39-2016.
doi: 10.1007/JHEP03(2017)094.

N. Orlofsky, A. Pierce and J. Wells.
Inflationary theory and pulsar timing investigations of primordial black holes and gravitational waves.
Physical review / D, 95(6):063518, and PUBDB-2017-01602.
doi: 10.1103/PhysRevD.95.063518.

F. G. Pedro and A. Westphal.
Nonequilibrium random matrix theory: Transition probabilities.
Physical review / E, 95(3):032144, and PUBDB-2017-01596.
doi: 10.1103/PhysRevE.95.032144.

F. Pedro and A. Westphal.
Inflation with a Graceful Exit in a Random Landscape.
Journal of high energy physics, 2017(3):163, and PUBDB-2017-01557, IFT-UAM-CSIC-16-128 DESY-16-224; arXiv:1611.07059.
doi: 10.1007/JHEP03(2017)163.

P. Pietrulewicz et al.
Factorization and Resummation for Massive Quark Effects in Exclusive Drell-Yan.
Journal of high energy physics, 1708(08):114, and PUBDB-2017-11858, DESY-16-199; UWTHPH-2017-3; HU-EP-16-42; arXiv:1703.09702.
doi: 10.1007/JHEP08(2017)114.

M. Preti, D. Trancanelli and E. Vescovi.
Quark-antiquark potential in defect conformal field theory.
Journal of high energy physics, 2017(10):79, and PUBDB-2017-13998.
doi: 10.1007/JHEP10(2017)079.

G. G. Ross, K. Schmidt-Hoberg and F. Staub.
Revisiting fine-tuning in the MSSM.
Journal of high energy physics, 1703(03):021, and PUBDB-2017-01488, OUTP-17-01P; DESY-17-008; KA-TP-01-2017; arXiv:1701.03480.
doi: 10.1007/JHEP03(2017)021.

J. Ruiz de Elvira et al.
Feynman–Hellmann theorem for resonances and the quest for QCD exotica.
The European physical journal / C, 77(10):659, and PUBDB-2018-00479.
doi: 10.1140/epjc/s10052-017-5237-3.

V. Schomerus, E. Sobko and M. Isachenkov.
Harmony of spinning conformal blocks.
Journal of high energy physics, 1703(03):085, and PUBDB-2017-01603.
doi: 10.1007/JHEP03(2017)085.

J. Wells, Z. Zhang and Y. Zhao.
Establishing the isolated standard model.
Physical review / D, 96(1):015005, and PUBDB-2017-07777, MCTP-17-02; DESY-17-031; arXiv:1702.06954.
doi: 10.1103/PhysRevD.96.015005.

B. Yoon et al.
Isovector charges of the nucleon from 2 + 1 -flavor QCD with clover fermions.
Physical review / D, 95(7):074508, and PUBDB-2018-00263.
doi: 10.1103/PhysRevD.95.074508.

B. Yoon et al.
Nucleon transverse momentum-dependent parton distributions in lattice QCD: Renormalization patterns and discretization effects.
Physical review / D, 96(9):094508, and PUBDB-2017-12818,

arXiv:1706.03406; LA-UR-17-24472.
doi: 10.1103/PhysRevD.96.094508.

N. Zerf et al.
Four-loop critical exponents for the Gross-Neveu-Yukawa models.
Physical review / D, 96(9):096010, and PUBDB-2017-12477, DESY-17-133; arXiv:1709.05057.
doi: 10.1103/PhysRevD.96.096010.

Z. Zhang.
Covariant diagrams for one-loop matching.
Journal of high energy physics, 1705(05):152, and PUBDB-2017-05969, MCTP-16-23; DESY-16-188; arXiv:1610.00710.
doi: 10.1007/JHEP05(2017)152.

Z. Zhang.
Time to Go Beyond Triple-Gauge-Boson-Coupling Interpretation of W Pair Production.
Physical review letters, 118(1):011803, and PUBDB-2017-00562.
doi: 10.1103/PhysRevLett.118.011803.

Master Thesis

J. Michel.
Transverse Momentum Resummation at Forward Rapidities and Its Applications to LHC Physics.
WWU Muenster, 2017.

Ph.D. Thesis

B. Chokoufe.
Scrutinizing the Top Quark at Lepton Colliders with Higher Orders.
Universität Hamburg, Hamburg, 2017.

M. Dierigl.
Aspects of Six-Dimensional Flux Compactifications.
Universität Hamburg, Hamburg, 2017.

M. Ebert.
Precision Predictions for Higgs Differential Distributions at the LHC.
Universität Hamburg, Hamburg, 2017.

S. Patel.
Interplay of Higgs Phenomenology and New Physics in Supersymmetric Theories.
Universität Hamburg, Hamburg, 2017.

C. Weiss.
Top quark physics as a prime application of automated higher-order corrections.
Universität Hamburg, Hamburg, 2017.

ZEUS

Published

I. Abt et al.
Investigation into the limits of perturbation theory at low Q^2 using HERA deep inelastic scattering data.
Physical review / D, 96(1):014001, and PUBDB-2017-10569, DESY-17-051; arXiv:1704.03187.
doi: 10.1103/PhysRevD.96.014001.

A. Verbytskyi.
HERA results on jets and hadronic final states.
19th High-Energy Physics International Conference in Quantum Chromodynamics, Montpellier (France), 4 Jul 2016 - 8 Jul 2016.
Elsevier, Amsterdam [u.a.]
doi: 10.1016/j.nuclphysbps.2016.12.009.

H. Kowalski et al.
Decoupling of the leading contribution in the discrete BFKL Analysis of High-Precision HERA Data.
The European physical journal / C, C77(11):777, and PUBDB-2018-00117, DESY-17-090; arXiv:1707.01460.
doi: 10.1140/epjc/s10052-017-5359-7.

A. Luszczak and H. Kowalski.
Dipole model analysis of highest precision HERA data, including very low Q^2.
Physical review / D, D95(1):014030, and PUBDB-2017-00952, DESY-16-231; DESY-REPORT-16-231; arXiv:1611.10100.
doi: 10.1103/PhysRevD.95.014030.

O. Zenaiev.
Charm Production and QCD Analysis at HERA and LHC.
The European physical journal / C, C77(3):151, and PUBDB-2018-00494, DESY-17-025; arXiv:1612.02371;
doi: 10.1140/epjc/s10052-017-4620-4.

ZEUS Collaboration.
Studies of the diffractive photoproduction of isolated photons at HERA.
Physical review / D, 96(3):032006, and PUBDB-2017-11252, DESY-17-077; arXiv:1705.10251.
doi: 10.1103/PhysRevD.96.032006.

Ph.D. Thesis

V. Myronenko.
Combination of the inclusive DIS $e^{\pm}p$ cross sections from HERA, QCD and EW analyses and the need for low-Q^2 higher-twist corrections.
Universität Hamburg, Hamburg, 2017.

N. Stefaniuk.
Measurement of the total and differential b cross sections at HERA and CMS tracker alignment at LHC.
Universität Hamburg, Hamburg, 2017.

N. Stefaniuk and E. Gallo-Voss.
Measurement of the total and differential b cross sections at HERA and CMS tracker alignment at LHC.
Universität Hamburg, 2017.

O. Turkot.
Search for contact interactions and finite quark radius using combined $e^{\pm}p$ data at HERA.
Universität Hamburg, Hamburg, 2017.

Photographs and graphics

Belle II experiment @ KEK
Brookhaven National Laboratory
Caltech Optical Observatories
H.E.S.S
Fermi All-Sky Variability Analysis
KEK
Milde Science Communication / DESY
NASA / CXC / SAO
Wikipedia

Lars Berg / DESY
Gesine Born / DESY
Michael Grefe, University of Hamburg
Stefan Klepser
Ralf Kähler, KIPAC / SLAC
Marta Mayer / DESY
Heiner Müller-Elsner / DESY
Dirk Nölle / DESY
Bente Stachowske / DESY

The figures were reproduced by permission of authors or journals.

Acknowledgement

We would like to thank all authors and everyone who helped in the creation of this annual report.

Imprint

Publishing and contact
Deutsches Elektronen-Synchrotron DESY
A Research Centre of the Helmholtz Association

Hamburg location:
Notkestr. 85, 22607 Hamburg, Germany
Tel.: +49 40 8998-0, Fax: +49 40 8998-3282
desyinfo@desy.de

Zeuthen location:
Platanenallee 6, 15738 Zeuthen, Germany
Tel.: +49 33762 7-70, Fax: +49 33762 7-7413
desyinfo.zeuthen@desy.de

www.desy.de
ISBN 978-3-945931-19-6
doi: 10.3204/PUBDB-2018-01854

Editing
Ilka Flegel, Manfred Fleischer, Thomas Konstandin

Layout
Sabine Kuhls-Dawideit

Production
Britta Liebaug

Printing
EHS druck GmbH, Schenefeld

Editorial deadline
1 March 2018

Editorial note
The authors of the individual scientific contributions published in this report are fully responsible for the contents.

Reproduction including extracts is permitted subject to crediting the source.
This report is neither for sale nor may be resold.

HELMHOLTZ
RESEARCH FOR GRAND CHALLENGES

Deutsches Elektronen-Synchrotron
A Research Centre of the Helmholtz Association

The Helmholtz Association pursues the long-term research goals of the state and society, including basic research, in scientific autonomy. To do this, the Helmholtz Association conducts top-level research to identify and explore the major challenges facing society, science and the economy. Its work is divided into six research fields.

The Helmholtz Association brings together 18 scientific-technical and biological-medical research centres. With more than 38 700 employees and an annual budget of over 4.5 billion euros, the Helmholtz Association is Germany's largest scientific organisation.

www.helmholtz.de